Novel Therapeutic Approaches to Paediatric Cancer

Dr. Paul J. Wood

B.Pharm, MSc, MB.BS, FRACP

ORCID; 0000-0003-1383-3450

Submitted in total fulfilment of the requirements

of the degree of Doctor of Philosophy

December 2020

The University of Melbourne, Department of Paediatrics

Peter MacCallum Cancer Centre

For Elisa, Emily and Lachlan.

Abstract

The overall cure rates for paediatric cancer have improved dramatically over the last 60 years. There is, however, a subset of paediatric embryonal tumours that carry a poor prognosis. In particular, metastatic neuroblastoma, in association with *MYCN* amplification, remains difficult to cure. The phosphatidylinositol-3-kinase (PI3K)/Protein Kinase B (AKT)/mammalian target of rapamycin (mTOR) cell signalling pathway, as well as epigenetic factors, play a key role in numerous cellular functions including cell growth, survival and angiogenesis. Activation of the PI3K/AKT/mTOR pathway is common in a variety of tumours including those associated with the MYC family of proto-oncogenes. As a result of its multiple cellular functions it is not surprising that deregulation of this pathway is frequently observed in cancer. The importance of *MYCN* as a therapeutic target, and the impact of PI3K inhibitors in *MYCN* amplified neuroblastoma has been well documented. Rapamycin and its analogues everolimus (RAD001) and temsirolimus (CCI-779) exert selective cytostatic/cytotoxic effects on by targeting mTORC1. PF-502 is a combined PI3K/mTOR inhibitor that serially inhibits multiple targets within this pathway. Accordingly, interest in both mTOR inhibitors and combined PI3K/mTOR inhibitors as anticancer drugs, with particular applications to neuroblastoma, has recently surged. When used in the aggressive TH-*MYCN* murine model of neuroblastoma, PF-502 produced a significant survival benefit by both apoptotic and anti-angiogenesis effects whereas temsirolimus worked primarily by an anti-angiogenic effect. Epigenetic modulation of tumours has recently received increasing attention recently. Histone deacetylase inhibitors have shown pre-clinical promise in a variety of paediatric tumours. Specifically, they have been shown to promote both tumour apoptosis and terminal differentiation in other paediatric embryonal tumour pre-clinical models. Accordingly, the role of agents targeting these pathways was studied in the aggressive TH-*MYCN* mouse model of neuroblastoma. Panobinostat, when given as a continuous, low dose, resulted in a significant survival benefit as a result of both apoptosis and differentiation, with terminal differentiation achieved by

prolonged exposure to the drug. Following on from these pre-clinical studies, an open label, Phase I (3+3 design), multi-centre study evaluating panobinostat in pediatric patients with refractory solid tumours, including neuroblastoma, was conducted. Primary endpoints were to establish MTD, define and describe associated toxicities, including dose limiting toxicities (DLT) and to characterise its pharmacokinetics (PK). Secondary endpoints included assessing the anti-tumour activity of panobinostat, and its biologic activity, by measuring acetylation of histones in peripheral blood mononuclear cells (PBMNC). Panobinostat significantly induced acetylation of histone H3 and H4 at all time points measured when compared to pre-treatment samples. A significant biological effect of panobinostat, measured by acetylation status of histone H3 and H4, was achieved at a dose of 15mg/m^2 and was well tolerated. PK data and drug tolerability at 15mg/m^2 was similar to that previously published. In summary, pre-clinical experiments support serial inhibition of the PI3K/AKT/mTOR pathway and the use of histone deacetylase inhibitors as treatment approaches in neuroblastoma.

Declaration

This is to certify that:

(i) this thesis comprises only my original work towards the PhD except where indicated in the Preface. My original work accounts for 95% of work presented in this thesis

(ii) due acknowledgement has been made in the text to all other material used,

(iii) the thesis is fewer than 100,000 words in length, exclusive of tables, maps, bibliographies and appendices.

Paul J. Wood

Preface

The work presented in this thesis represents my original work with the exception of the following experiments that were assisted by the following collaborators of this project:

1, Chapter 4: Dr. Kelly Waldeck. Assistance with Figure 52.

2, Chapter 4: Dr. Kelly Waldeck. Assistance with Figure 53.

3, Chapter 4: Dr. Kelly Waldeck. Assistance with Figure 54.

4, Chapter 4: Dr. Kelly Waldeck. Assistance with Figure 55.

5, Chapter 4: Dr.Kelly Waldeck. Assistance with Figure 56.

6, Chapter 5: Dr. Michael Michael. Assistance with Table 12.

7, Chapter 5: Dr. Andrea Muscat. Assistance with Figure 57.

8, Chapter 5: Dr. Andrea Muscat. Assistance with Figure 58.

9, Chapter 5: Dr. Andrea Muscat. Assistance with Figure 59.

Chapter 3: I was responsible for all experiments and data analysis undertaken in this chapter.

Chapter 4: I have included only the work that was included in the manuscript that I was responsible for performing. I was responsible for most of the TH-MYCN mouse derived data: dosing mice (with assistance from animal techs), inspecting mice (with assistance from animal techs), performing ultrasounds, harvesting mice and preparing mouse tissue for interrogation, analysing data and preparing for manuscript. I was responsible for writing the introduction and discussion sections of

the manuscript, and shared writing the results and methods sections with Dr. Kelly Waldeck (first author).

Chapter 5: I was responsible for trial design, writing the entire protocol from scratch, making any changes or amendments, overall trial site co-ordination with site CRA's, the principal study contact throughout the trial, co-ordination of tissue samples, data collection (with Centre for Biostatistics and Clinical Trials (BaCT) at Peter MacCallum), data analysis and preparation of entire manuscript.

This PhD was supported by:

The You Are My Sunshine (YAMS) foundation.

An Australian Postgraduate Award, University of Melbourne, Australia.

The Basser Research Entry Scholarship, Royal Australasian College of Physicians (RACP).

The Haematology and Oncology Targeted Therapy (HOTT) Fellowship, Clinical Oncology Society of Australia (COSA).

Acknowledgements

I am very grateful to my supervisors Professor Grant McArthur, Professor David Ashley and Associate Professor Paul Ekert.

To **Associate Professor Paul Ekert,** thank you for your guidance and encouragement during my PhD.

To **Professor David Ashley**, thank you for encouraging and supporting me in undertaking this journey. Your support and confidence in my abilities was essential to my success. Both clinically and from a research perspective you have been an enormous inspiration to me.

To **Professor Grant McArthur**, twelve years ago you accepted an oncology trainee with limited experience in the lab to join your team. I had no idea what a steep learning curve it would be. I have immensely enjoyed my time as part of the Molecular Oncology laboratory, and I have learnt so much from you. Thank you for your patience, your support, and your guidance.

To the members of the Molecular Oncology, Translational Research Laboratory and Gene Regulation Laboratory, **Prof. Rod Hicks, Prof. Rick Pearson**, **Prof. Ross Hannan**, **Dr. Carleen Cullinane, Dr. Gretchen Poortinga, Dr. Meghan Bywater, Dr. Petranel Ferrao, Dr. Kathryn Kinross, Dr. Kelly Waldeck, Ms. Kerry Ardley, Ms. Susan Mitchell, Dr. Richard Young, Ms Rachel Ramsdale, Dr. Elaine Sanji, Dr. Karen Sheppard, Ms. Kym Stanley, A. Prof. Jake Shortt, and Dr. Richard Tothill**, thank you for accepting me into the lab and for all that you have taught me.

To my collaborators during the project, **Prof. Ricky Johnstone, Prof. Michelle Haber, Dr. Elizabeth Algar, A/Prof. Michael Michael, Dr Andrea Muscat,** thank you for your expertise and time.

To all in the members of the ANZCHOG office, **Ms. Robyn Strong** and **Ms Janelle Jones** thank you for all of your hard work in coordinating a nationwide Phase I clinical trial.

To my PhD Committee members, **Prof. Rob Ramsay, Dr. Keiran Harvey, Prof. Ricky Johnstone and Dr. Sarah Russell** thank you for your valuable guidance.

To all in the Children's Cancer Centres at Monash Health and Royal Children's Hospital, thank you for your friendship and encouragement. A special thank you to **Dr. Peter Downie** for your mentorship and **A/Prof. Pratiti Bandopadhayhay** for your friendship throughout our training.

Finally, to **my family**, thank you for all of the love and support you always give me.

Publications and presentations of data related to PhD during candidature.

Publications

Waldeck K, Cullinane C, Ardley K, Shorrt J, Martin B, Tothill RW, Li J, Johnstone RW, McArthur GA, Hicks RJ, **Wood PJ**. Long term, continuous exposure to panobinostat induces terminal differentiation and long-term survival in the TH-*MYCN* neuroblastoma mouse model. Int. J. Cancer: 2016 Jul 1;139(1):194-204. doi: 10.1002/ijc.30056. Epub 2016 Mar 10.

Kong G, Hofman MS, Murray WK, Wilson S, **Wood P**, Downie P, Super L, Hogg A, Eu P, Hicks RJ. Initial Experience with Gallium-68 DOTA-Octreotate PET/CT and Peptide Receptor Radionuclide Therapy for Pediatric Patients with Refractory Metastatic Neuroblastoma. J. Pediatr Hematol Oncol. 2016 Mar; 38(2):87-96. doi: 10.1097/MPH.0000000000000411.

Wood PJ, Strong R, McArthur GA, Michael M, Algar E, Muscat A, Rigby L, Ferguson M, Ashley DM. A phase I study of panobinostat in pediatric patients with refractory solid tumors, including CNS tumors. Cancer Chemother Pharmacol. 2018 Sep;82(3):493-503. doi: 10.1007/s00280-018-3634-4

International Oral Presentations

Wood PJ, Ashley DA, Cullinane C, Kinross K, Poortinga G, Ardley K, McArthur GA. Molecular analysis and therapeutic targeting of the PI3K/AKT/mTOR pathway in paediatric neuroblastoma. Advances in Neuroblastoma Research, Sweden, June 2010.

Wood PJ, Ashley DA, Cullinane C, Kinross K, Poortinga G, Ardley K, McArthur GA. Molecular analysis and therapeutic targeting of the PI3K/AKT/mTOR pathway in paediatric neuroblastoma. Best of the Best. Basic and Translational Research. COSA ASM, Melbourne, November 2010. **Awarded first prize for this presentation.**

Waldeck K, Cullinane C, Ardley K, Shortt J, Martin B, Tothill RW, Li J, Johnstone RW, McArthur GA, Hicks RJ, **Wood PJ**. Long term, continuous exposure to panobinostat induces terminal differentiation and long-term survival in the TH-NMYC neuroblastoma mouse model. Advances in Neuroblastoma Research, Cairns, June 2016. **In final six contestants for translational research prize.**

Poster Presentations

P. J. Wood, R. Strong, G.A. McArthur, M. Michael, E. Algar, A. Muscat, A. Rigby, D. M. Ashley. A Phase I Study of Panobinostat in Pediatric Patients with Refractory Solid Tumors, including CNS tumors. J Clin Oncol 2014: 35(5s): abstract 10061.

K. Waldeck, C. Cullinane, J. Shortt, K. Ardley, G.A. McArthur, **P. J. Wood**. The histone deacetylase inhibitor, Panobinostat, induces apoptosis and prolongs survival in the TH-*MYCN* murine model of high-risk neuroblastoma. Advances in Neuroblastoma Research, Cologne, May 2014.

Table of Contents

List of Tables

Table of Figures

Abbreviations

ABMT	Autologous Bone Marrow Transplant
ACCT	Australian Children's Cancer Trials
AE	Adverse Event
AKT	Protein Kinase B
ALK	Anaplastic Lymphoma Kinase
ALL	Acute Lymphoblastic Leukaemia
ALT	Alanine aminotransferase
AML	Acute Myeloid Leukaemia
AST	Aspartate aminotransferase
ATM	Ataxia-telangiectasia mutated
ATRA	All Trans Retinoic Acid
AT/RT	Atypical Teratoid Rhabdoid Tumour
AYA	Adolescent and Young Adult
BRCA	Breast Cancer Gene
BSA	Bovine Serum Albumin
b.i.d.	bis in diem/twice a day
CCIA	Children's Cancer Institute Australia
CDK	Cyclin-dependent kinase
CDKI	Cyclin-dependent kinase inhibitors
CHiP	Chromatin Immunoprecipitation
CNS	Central Nervous System
CM	Chronic Myelogenous Leukaemia
CML	Centimeter
CRF	Case Report/Record Form

CRP	CREB-binding Protein
CSC	Cancer Stem Cells
CS&E	Clinical Safety and Epidemiology
CR	Clinical Research
CRO	Contract Research Organization
CSF	Cerebrospinal Fluid
CT	Computed tomography
DAPI	4',6'-Diamidino-2-Phenylindole Dihydrochloride
DDR	DNA damage response
DLT	Dose Limiting Toxicities
DMEM	Dulbeccos Modified Eagle Medium
DMF	Dimethylformamide
DMSO	Dimethyl Sulphoxide
DNA	Deoxyribonucleic Acid
DQF	Data Query Form
DS&E	Drug Safety & Epidemiology
EBV	Epstein-Barr Virus
EDTA	Ethylenediaminetetraacetic acid
EFS	Event Free Survival
F/U form	Follow-up to original SAE report
FACS	Flourescence-Activated Cell Sorting
FAK	Focal Adhesion Kinase
FBP	FUSE-Binding Proteins
FCS	Fetal Calf Serum
FDA	Food and Drug Administration
FFT	Fresh frozen tissue

FIR	FBP-Interacting Receptor
FOXO	Forkhead Box
Ga-Tate	Ga-68 DOTATATE
GBM	Glioblastoma Multiforme
GFP	Green Fluorescent Protein
GPCR	G Protein Coupled Receptors
H&E	Haemotoxylin and Eosin
HHV	Human-Herpes Virus
IC	Inhibitory Concentration
IDRF	Image Defined Risk Factors
IEC	Independent Ethics Committee
IL	Interleukin
ILLN	Institutional Lower Limit of Normal
IR	Intermediate Risk
IND	Investigational New Drug
INI1	Integrase Interactor 1
INRC	International Neuroblastoma Response Criteria
IDRF	Image Defined Risk Factors
INSS	International Neuroblastoma Staging System
INRG	International Neuroblastoma Risk Group
IP	Intra-peritoneal
IR	Intermediate Risk
IULN	Institutional Upper Limit of Normal
LR	Low Risk
I.V	Intravenous(ly)
HATs	Histone acetyltransferase

HCL	Hydrochloride
HDAC	Histone deacetylases
HDACi	Histone deacetylase inhibitors
Hemi	Hemizygotic
Homo	Homozygotic
HR	High Risk
HREC	Human Research Ethics Committee
IHC	Immunohistochemistry
IR	Intermediate Risk
IRB	Institutional Review Board
KCL	Potassium Chloride
LR	Low Risk
M	Molar
MAPK	Mitogen Activated Protein Kinase
MCRI	Murdoch Children's Research Institute
$MgCL_2$	Magnesium Chloride
MIBG	$Iodine^{123}$ Metaiodobenzylguanidine
Min	Minutes
ML	Millilitre
mM	Millimolar
MRI	Magnetic Resonance Imaging
MRT	Malignant Rhabdoid Tumour
MTD	Maximum Tolerated Dose
MYD	Myeloid differentiating
mTOR	Mammalian target of rapamycin
Na F	Sodium Fluoride

NaOAc	Sodium Acetate
NBF	Neutral Buffered Formalin
NBL	Neuroblastoma
NSCLC	Non-small cell lung cancer
nM	Nanomolar
NSE	Enolase 2
o.d	omnia die/once a day
OCT.	Optimal Cutting Temperature
OS	Overall Survival
PBS	Phosphate Buffered Saline
PCR	Polymerase Chain Reaction
PDX	Patient Derived Xenograft
PEI	Polyethylenimine
PET	Positron Emission Tomography
PFA	Paraformaldehyde
PFS	Progression Free Survival
PI	Propidium Iodide
PI3K	Phosphatidylinositol-3-kinase
PMCC	Peter MacCallum Cancer Centre
PMNC	Peripheral Mononuclear Cells
POL	RNA Polymerase
PROS	PIK3CA-Related Overgrowth Spectrum
PTEN	Phosphatase and Tensin Homolog
p.o.	per os/ by mouth/orally
RCH	Royal Children's Hospital
RNA	Ribose nucleic acid

RCC	Renal Cell Carcinoma
RCT	Randomised Controlled Trial
ROS	Reactive Oxygen Species
RPM	Revolutions per minute
RT	Rhabdoid Tumour
RTK	Receptor Tyrosine Kinases
RT-PCR	Real Time Polymerase Chain Reaction
SAE	Serious Adverse Event
SASP	Secretory Associated Senescence Phenotype
SCID	Severe Combined Immune Deficiency
SD	Standard Deviation
SDS	Sodium Dodecyl Sulphate
SHH	Sonic Hedgehog
SLB	Sample Loading Buffer
SOP	Standard Operating Procedure
SRB	Sulforhodamine B
SSTR2	Somatostatin Receptor 2
SUSAR	Suspected Unexpected Serious Adverse Reaction
SUV	Standard Uptake Value
TAD	Trans Activation Domain
TCA	Trichloroacetic Acid
TK	Tyrosine Kinase
TME	Tumour microenvironmant
TTP	Time To Progression
uM/μM	Micromolar
μm	Micron

uL/μL	Microlitre
UBF	Upstream Binding Factor
UHR	Ultra-High Risk
US	Ultrasound
USA	United States of America
V	Volt
VEGF	Vascular Endothelial Growth Factor
VEGFR	Vascular Endothelial Growth Factor Receptor
WB	Western Blot
WES	Whole Exome Sequencing
WGS	Whole Genome Sequencing
WNT	Wingless sub-group
WT	Wild-type
XRT	Radiation Therapy

1 Novel therapeutic approaches to paediatric solid tumours

1.1.**Paediatric cancer**

Each year over 950 children and adolescents in Australia are diagnosed with cancer making it the second most common cause of death in children aged 0-14 years, behind accidents. This is similar to rates seen in other developed countries (Baade et al., 2010; Isaevska et al., 2017; Pesola, Ferlay, & Sasieni, 2017). One third of these are diagnosed in children aged 0-4 years. At present at least 80% of children diagnosed with cancer will be cured (Isaevska et al., 2017; Saletta, Seng, & Lau, 2014), with more recent statistics from The Australian Cancer Council documenting the 5-year relative survival as being 84.7% (Australian Childhood Cancer Statistics Online).

Despite the advances in treatment protocols that have dramatically improved the cure rates of many childhood tumours since the 1960's, certain tumours, in particular embryonal solid tumours, continue to have poor outcomes (Tulla et al., 2015). For instance atypical teratoid rhabdoid tumours (ATRT) have a 3 year OS of 20-30% (Ginn & Gajjar, 2012; Tulla et al., 2015), metastatic medulloblastoma has a 5 year OS of 60% (Ramaswamy et al., 2016) and high-risk (HR) neuroblastoma (NBL) has a 3 year OS of approximately 50% (Katherine K. Matthay et al., 2016; A. L. Yu et al., 2010). Risk classification, often represented by cancer staging, can have an enormous impact on outcomes. The overall 5-year survival of patients with osteosarcoma is close to 70%; however, those that present with metastatic disease have a 3-year survival closer to 30% (Aljubran, Griffin, Pintilie, & Blackstein, 2009). This is very similar to the outcome patterns seen in neuroblastoma (Coughlan, Gianferante, Lynch, Stevens, & Harlan, 2017; Tulla et al., 2015).

Despite the treatment advances that have been made with current multi-agent chemotherapy regimens they carry with them significant acute and long-term toxicities. It is unlikely that any further changes to these treatment protocols will produce better outcomes (Macy, Sawczyn, Garrington, Graham, & Gore, 2008). Therefore, new approaches are needed. Recent advances in technology have allowed researchers to interrogate the genomic landscape of paediatric solid tumours with

the hope of finding new and promising therapeutic targets and strategies (X. Chen, Pappo, & Dyer, 2015).

An example of this is the paediatric brain tumour medulloblastoma. Previously medulloblastoma treatment was based on morphology, age, metastatic status and extent of tumour resection. Current protocols base treatment on the four distinct molecular sub-groups of medulloblastoma that have been identified and furthermore incorporate treatment approaches specific to the molecular signature, and associated clinical outcomes, of each sub-group (Northcott, Dubuc, Pfister, & Taylor, 2012). It is hoped that this new approach, that will tailor treatment according to molecular sub-type, will improve patient outcomes and reduce immediate and long-term toxicities.

1.1.1. **Paediatric solid tumours**

Solid tumours make up 30% of paediatric cancers with the most common types including brain tumours, NBL, Wilms' tumour and sarcomas (Kline & Sevier, 2003). The overall survival outcomes of solid tumours, compared with their liquid counterparts, is poor (Friedman & Gillespie, 2011). Interestingly out of the current 82 U.S Food and Drug Administration (FDA) approved guided therapies for adults, only three of those are approved for children, regardless of their genomic status (Tsui et al., 2017).

Paediatric tumours differ from their adult counterparts in many ways; incidence, pathogenesis, biology, response rates and outcomes. The most important of these factors appears to be tumour biology (Friedman & Gillespie, 2011). Most adult tumours are carcinomas which are derived from highly differentiated epithelial tissues. Carcinomas are inherently resistant to current cancer therapies including chemotherapy and radiation therapy most often due to alterations in DNA repair pathways (Gottesman, 2002; Willers, Azzoli, Santivasi, & Xia, 2013). Carcinomas are almost never seen in the paediatric population which are instead tumours of primarily embryonal origin (Murphy, Bithell, Stiller, Kendall, & O'Neill, 2013).

Interestingly the tumours seen in adolescent and young adult (AYA) patients often have an overlap between the two biologies which might contribute to the poor outcomes seen in this age group (Murphy et al., 2013).

With the advent of newer and more sophisticated sequencing technologies it has now become clear that the spectra of genomic based alterations and tumour initiating mechanisms in paediatric malignancies are very different from those observed in adult malignancies. Adult solid tumours, on average, harbour substantially higher mutational burdens compared to paediatric solid tumours (Rahal, Abdulhai, Kadara, & Saab, 2018). This, in part, contributes to the differences in outcomes seen between paediatric and adult cancers. It is postulated that paediatric cancers manifest in precursor cells of non-renewing tissues and have therefore accumulated lower mutational burdens prior to tumour initiation (Vogelstein et al., 2013). Whereas the majority of adult epithelial tumours, for instance, are the result of accumulated environmental impacts (Vogelstein et al., 2013), the peak incidence of many paediatric solid tumours often corresponds to the maturation stage of the underlying tissue of origin, thus favouring a developmental model for cancer initiation (Baker, Ellison, & Gutmann, 2016; Pierce, Frazier, & Amatruda, 2018). Therefore, the origin of adult and paediatric solid tumours, are likely to be very different.

Recently a population of cells within tumours have been identified and referred to as cancer stem cells (CSC). These CSC have been identified in many common adult cancers including brain tumours, lung cancer, prostate cancer and melanomas (Collins, Berry, Hyde, Stower, & Maitland, 2005; Dirks, 2010; D. Fang et al., 2005; S. K. Singh et al., 2003). A similar population of cells has also been identified in paediatric tumours, including sarcomas, brain tumours and neuroblastoma (Dela Cruz, 2013; Friedman & Gillespie, 2011; Lasky, Choe, & Nakano, 2009). These cells appear to be crucial in the inherent tumour resistance observed in both adult and paediatric tumours. They have the ability for self-renewal and regeneration which allows them to maintain a neoplastic clone. Identifying and treating these CSC's has become somewhat of a challenge. Candidate surface cell markers including CD133, CD17 and

Stro-1 have been identified as potential targets (Dela Cruz, 2013). CD133 + cells have certainly been identified in human neuroblastoma cell lines and the degree of CD133 expression is negatively associated with the degree of malignancy. CD133 expression is seen less in patients with the more benign ganglioneuroblastoma than in neuroblastoma and has a higher association with unfavourable histology than favourable histology and therefore prognosis (Tong et al., 2008). Once there is a better understanding about the role CSC play in tumour resistance, and how they achieve this, targeted therapies may become possible in the future.

New therapeutic approaches are required for certain paediatric malignancies, especially in solid tumours associated with a poor outcome such as paediatric embryonal tumours, which represent 20% of all paediatric cancers (Tulla et al., 2015). The PI3K/AKT/mTOR pathway has been identified as a promising target in paediatric solid tumours (Loh et al., 2013; Hazel A. Rogers, Estranero, Gudka, & Grundy, 2017), as has epigenetic modulation via histone deacetylase inhibition (Cain et al., 2013; Muscat et al., 2016; Waldeck et al., 2016).

This thesis explores the relationship between the PI3K/AKT/mTOR pathway and MYC, specifically in the setting of paediatric NBL. It explores the role of targeted inhibitors of the PI3K/AKT/mTOR pathway in the treatment of NBL. It also evaluates the use of the histone deacetylase inhibitor (HDACi) panobinostat as a differentiating agent in pre-clinical models of neuroblastoma. In the final results chapter this pre-clinical work is translated into paediatric patients with refractory solid tumours, including central nervous system (CNS) tumours, in the setting of an early Phase I clinical trial. Although this early Phase clinical trial did not focus specifically on the use of Panobinostat as a differentiating agent, due to its weekly and therefore intermittent IV dosing schedule, it did provide some of the earliest tolerability and pharmacokinetic (PK) data on the use of panobinostat in the paediatric population. In particular, it provided essential PK data, that allowed us to model the projected dosing of the oral formulation in the currently recruiting Phase II study.

1.1.2. **Personalised medicine**

In an attempt to further improve patient outcomes in cancer therapy the era of personalised medicine has arrived. This process involves detailed analysis of the cancer genome in order to identify and incorporate targeted therapies based on an individual's results (Forrest, Geoerger, & Janeway, 2018). The largest study assessing the feasibility of incorporating this approach into all Australian paediatric cancer patients is the PRecISion Medicine for children with cancer (PRISM) project being run out of the Children's Cancer Institute Australia (CCIA) (NCT03336931). Two of the biggest concerns about such an approach are the costs involved and the time taken to produce the final individualised recommendation.

The costs involved encompass both the detailed genomic analysis and the subsequent therapeutic recommendations which include many newer, more expensive therapies (Gavan, Thompson, & Payne, 2018). The improvement of the overall health of a society is the prime objective of any healthcare system and the economic benefits of a healthy population have been well described (Martin, Grant, & D'Agostino, 2012; Onarheim, Iversen, & Bloom, 2016). There is much debate about whether the research money being spent on personalised medicine approaches may instead be better spent on general population healthcare measures, such as addressing obesity (Feiler, Gaitskell, Maughan, & Hordern, 2017). As with any healthcare system with finite resources, an increased expenditure in one area results in reduced expenditure in other areas. This resource re-allocation may result in poorer health outcomes in other patient groups (Gavan et al., 2018). It is potentially too early to definitively quantify the cost to benefit of personalised medicine in paediatric cancer, the general concept of pharmacogenetic and pharmacogenomic screening has been shown to be cost-effective (Berm et al., 2016; Hatz, Schremser, & Rogowski, 2014). The final point regarding cost is the potential for a more expensive personalised medicine approach to lead to health care inequity in countries that do not, or cannot afford, to provide universal access to healthcare (McClellan, Avard, Simard, & Knoppers, 2013).

The comprehensive panel of testing that is required to be performed on a patient's tumour takes time. This can potentially become more time consuming if approaches such as generating patient derived xenograft (PDX) models is factored into the equation (Yada, Wada, Yoshida, & Sasada, 2018). Despite the cost and time involved in producing PDX models, in even aggressive tumour models such as glioblastoma multiforme (GBM) the success rate of developing a useful model ranges between 20-40% (William et al., 2017). Perhaps the largest study published in the use of personalised medicine in paediatrics to date is the Individualized Therapy for Relapsed Malignancies in Childhood (INFORM) project. In this study, which involved 20 paediatric cancer centres, a meaningful druggable target was identified in 50% of patients tested with a mean turnaround time of 28 days for results to become available to clinicians (Worst et al., 2016). However, in only 10 of the 26 patients identified with a druggable target was the therapeutic recommendation adopted by the treating physician, meaning that precision medicine approach in this study impacted the treatment in less than 20% of patients. The economic impact of this approach was not addressed by the authors (Worst et al., 2016).

Personalised medicine has the prospect of improving patient outcomes in paediatric NBL (Couzin-Frankel, 2011; Esposito, Aveic, Seydel, & Tonini, 2017). Possible targets include anaplastic lymphoma kinase (ALK), *MYCN* (1.6.1), aurora kinases (1.6.3.10) and p53/MDM2/ARF (1.10.1.6). Interestingly, the most recent Children's Oncology Group (COG) high risk NBL trial has incorporated crizotinib as a therapy for those patients with an identified ALK mutation. As more therapies, such as small molecule inhibitors that target *MYCN* become available, such treatment approaches will only expand in the future (Fletcher & Prochownik, 2015).

1.2.**Neuroblastoma**

NBL is the most common extra-cranial solid tumour in paediatrics (Katherine K. Matthay et al., 2016) with 90% of patients below five years of age and a median age of diagnosis of 19 months (Whittle et al., 2017). It was first described in 1910 by James Wright who recognised the tumour was of primitive neural cell origin (Wright, 1910). Half of the children that present are considered to have high risk disease (J. M. Maris, Hogarty, Bagatell, & Cohn, 2007). NBL is responsible for approximately 15% of cancer-related deaths in this population (Mlakar et al., 2017).

In 1974 the overall survival of 487 NBL cases, notified to the British Cancer Registry between 1962-67 was reported (Wilson & Draper, 1974). At that time the three-year overall survival (OS) was 23% and a five-year OS was 13%. Factors that were identified to influence survival at that time were age at diagnosis, site, histology and gender. Not surprisingly Stage I patients (17% of total cases) had a three-year OS of 59% and Stage IV patients (33% of total cases) had a dismal three-year OS of 5% (Wilson & Draper, 1974). In contrast a more recent institutional review looking at Stage I and Stage II NBL patients over a 20-year period, had a five-year OS of 100% in both groups and a five-year event free survival (EFS) of 91.7% and 81.8%, respectively (P. C. Y. Chang et al., 2018). Stage III, International Neuroblastoma Staging System (INSS) classified as HR NBL have a five-year EFS and OS of 55% and 59%, respectively (J. R. Park et al., 2009). Prior to the immunotherapy era Stage IV HR NBL patients had a five-year OS of between 30-40% despite aggressive therapy including stem cell supported chemotherapy (Berthold et al., 2018; Sung, 2012). The advent of immunotherapy using anti-GD2 antibodies in combination with surgery, chemotherapy and radiation therapy, has increased the five-year OS in this group of HR patients to close to 50% (Katherine K. Matthay et al., 2016; Sait & Modak, 2017; A. L. Yu et al., 2010). Sadly the survival of HR NBL patients is significantly worse in developing countries due to lack of access to agents such as immunotherapy and differences in supportive care (Easton et al., 2016).

For those HR NBL patients that are either refractory to front line therapy, or who relapse after completing therapy the outcomes are dismal. A metanalysis of the ITCC/SIOPEN Phase II clinical trial data showed an OS of 16% in this patient group (Moreno et al., 2017). *MYCN* amplified disease and bone marrow metastasis at relapse have been identified as predictors of poor prognosis in this patient group (Basta et al., 2016; Marrano, Irwin, & Thorner, 2017).

1.2.1. **Epidemiology**

As stated above, NBL is the most common extra-cranial solid tumour in young children (1.2). Although there have been many attempts to identify possible causes, including environmental causes, there have been no clearly established links. One systematic review identified risk factors such as alcohol or diuretic intake during pregnancy, whilst identified protective factors were vitamin intake during pregnancy or a decreased risk in children with allergic disease (Heck, Ritz, Hung, Hashibe, & Boffetta, 2009). The authors acknowledge that the rarity of the tumour makes definitive associations difficult.

The majority of NBL cases in families are sporadic. Familial NBL is only seen in 1-2% of cases and that these are associated with germline mutations in the ALK gene in approximately 23% of cases (Mossë et al., 2008). Germline mutations in PHOX2B have also been identified in family pedigrees of familial NBL (Mosse et al., 2004).

Large scale screening effort, using urinary catecholamines as a marker of NBL have been attempted in some countries, particularly Germany, Canada and Japan (Chamberlain, 1994). Urinary catecholamines are excreted in over 90% of patients with NBL. In theory, if the 50% of patients that present with metastatic disease could be identified earlier, then perhaps cure rates could be improved. Unfortunately, these screening programs only detected those patients with low risk (LR) disease with an OS of greater than 90% and did not reduce the incidence or OS of HR NBL patients. In

2003, the Japanese Ministry of Health officially ended these screening programs, the last of the three countries to do so (Tsubono & Hisamichi, 2004).

1.3.**Symptoms and diagnosis**

The symptoms that children present with depend on tumour size, location and whether there is metastatic disease present. Most tumours arise in the abdomen with the adrenal gland being the most common primary site. Depending on the size of the tumour there may be abdominal distension, pain, constipation or bowel obstruction. Constitutional symptoms include weight loss, irritability, night sweating and diarrhoea. Intra-spinal extension of NBL is present in approximately 10% of patients (Fawzy et al., 2015). This can manifest as lower limb weakness or even paralysis and is considered an oncological emergency. With appropriate recognition and quick treatment complete recovery can be seen in 47% of patients (Fawzy et al., 2015). When NBL has metastasised to either cortical bone or bone marrow, pain can be a presenting symptom. This can often manifest as a limp (Parmar, Wadia, Yassa, & Zenios, 2013). Additional signs of bony involvement include periorbital ecchymoses (racoon eyes) or palpable lumps. Thoracic NBL, seen more frequently in infants, can present as a Horner syndrome (Smith, Diehl, Leavitt, & Mohney, 2010) due to an interruption in the oculo-sympathetic tracts. Paraneoplastic syndromes can include opsoclonus-myoclonus-ataxia (OMA) syndrome which is often associated with younger children with LR disease and seen in 2-3% of patients (Rudnick et al., 2001). Interestingly in infants, the OMA can present after the primary tumour has spontaneously resolved.

1.4.**Risk groups**

1.4.1. **International neuroblastoma risk group (INRG) risk classification**

In 2009, the International Neuroblastoma Risk Group (INRG) risk classification system was published (Cohn et al., 2009). This was an attempt to standardise the way risk is assigned in NBL patients in international trials (Monclair et al., 2009). Essentially, the previously used INSS was a post-surgical staging system, whereas the INRG is a pre-treatment staging system based on tumour locality and Image Defined Risk Factors (IDRF's) (Cohn et al., 2009; Monclair et al., 2009) (Table 1). The current prognosis of each risk group is: very low risk (5-year EFS > 85%); low risk (5-year EFS > 75% to ≤ 85%); intermediate risk (5-year EFS ≥ 50% to ≤ 75%); high risk (5-year EFS < 50%) (Cohn et al., 2009)

INRG Stage	**Age (months)**	**Histologic Category**	**Grade or Tumour Differentiation**	***MYCN***	**11q Aberration**	**Ploidy**	**Risk Group**
L1/L2		GN maturing; GNB intermixed					Very low
L1		Any except; GN maturing; GNB intermixed		NA			Very low
				Amp			High
L2	< 18	Any except; GN maturing; GNB intermixed		NA	No		Low
					Yes		Intermediate
	≥ 18	GNB nodular; neuroblastoma	Differentiating	NA	No		Low
					Yes		Intermediate
			Poorly differentiated or undifferentiated	NA			
				Amp			High
M	< 18			NA		Hyperdiploid	Low
	< 12			NA		Diploid	Intermediate
	12 to < 18			NA		Diploid	Intermediate
	< 18			Amp			High
	≥ 18						High
MS	< 18				No		Very low
				NA	Yes		High
				Amp			High

Table 1 INRG Consensus Pre-treatment Classification schema

GN, ganglioneuroma; GNB, ganglioneuroblastoma; Amp, amplified; NA, not amplified; L1, localised tumour confined to one body compartment and with absence of image-defined risk factors IDRFs; L2, loco-regional tumour with presence of one or more IDRFs; M, distant metastatic disease (except stage MS); MS, metastatic disease confined to skin, liver and/or bone marrow in children < 18 months of age (Monclair et al., 2009); EFS, event-free survival, 12 months = 365 days; 18 months = 547 days; blank field = "any"; diploid (DNA index ≤ 1.0); hyperdiploid (DNA index > 1.0 and includes near-triploid and near-tetraploid tumors)(Cohn et al., 2009).

1.5. **Treatment**

The aim of NBL therapy is to achieve cytoreduction to improve the chances of surgical resection and local control. It also aims to achieve a significant reduction in metastatic tumour burden to make aggressive surgical resection warranted, prior to consolidation therapy. Radiation therapy typically 21.6Gy is delivered in 12 1.8Gy fractions to the primary tumour bed and any metastatic sites still present at the end of induction (De Ioris et al., 2015) is used to consolidate local control. Consolidation therapy involves stem cell supported chemotherapy, whether it be a single or tandem autologous transplant. Maintenance therapy includes immunotherapy combined with cis-retinoic acid (cis-RA) as a differentiating agent (Ganeshan & Schor, 2011).

1.5.1. **Maintenance**

Traditional maintenance therapy has consisted of differentiating agents including Cis-RA (Reynolds, Matthay, Villablanca, & Maurer, 2003). GD2 is the first ganglioside to be targeted as an anti-cancer therapy (Fleurence et al., 2017). GD2 has been shown to be preferentially expressed in many aggressive tumours, including NBL, melanomas and soft tissue sarcomas when compared to normal body cells (Navid, Santana, & Barfield, 2010). More recently anti-GD2 immunotherapy, in combination with IL-2, GM-CSF and Cis-RA has been shown to improve outcomes in HR NBL patients (Sait & Modak, 2017; A. L. Yu et al., 2010). Immunotherapy was shown to be superior to standard therapy in both 2-year EFS (66% v 46%, respectively) and 2-year OS (86% v 75%, respectively) (A. L. Yu et al., 2010). Subsequently dinutuximab (Unituxin™) has been FDA approved for the treatment of HR NBL.

Until now Unituxin™ has been combined with Cis-RA as the differentiating agent of choice (A. L. Yu et al., 2010). Cis-RA has been shown to be beneficial in high risk NBL patients that have received prior high dose therapy without evidence of progressive disease (K. K. Matthay et al., 1999). However Cis-RA has many undesirable side-effects including skin and mucous membrane inflammation that often make them

very difficult for children to tolerate (David, Hodak, & Lowe, 1988). Given the importance of targeting both microscopic and macroscopic residual disease, in both primary and metastatic sites, an alternative, more effective and more tolerable differentiating agent may be the next step in improving survival in this patient group. This thesis explores the use of epigenetic modifiers, such as HDACi, as a potential replacement therapy for Cis-RA in the maintenance phase of HR NBL.

1.6. Tumour histology and molecular genetics of neuroblastoma

Neuroblastoma encompasses a spectrum of diseases that are classified according to their degree of differentiation. NBL is typically poorly differentiated whilst ganglioneuroma represents the most differentiated form of the disease. Tumours that contain elements of both are classified as ganglioneuroblastomas and represent and intermediate histology (Van Arendonk & Chung, 2019). The impact that histology has on treatment and prognosis was initially classified by The Shimada System (Shimada et al., 1999) and has subsequently been incorporated into the INRG risk classification system (Cohn et al., 2009).

Perhaps the most comprehensive analysis of the genetic landscape of HR neuroblastoma was performed as part of the Therapeutically Applicable Research to Generate Effective Treatments (TARGET) initiative (Pugh et al., 2013). Two hundred and forty samples of HR NBL, paired with blood for germline analysis, were interrogated with a combination of whole genome sequencing (WGS) and whole exome sequencing (WES). An interesting finding was the low mutational burden identified in this study, with an median of 0.6 mutations per mega-base, which is significantly less than that seen in adult cancers (Chalmers et al., 2017). However, the mutational burden was consistent with data acquired in 24 common paediatric cancer types, once again as compared to adults (Gröbner et al., 2018). This study also confirmed that NBL had a low germline mutation rate in cancer predisposition genes (Gröbner et al., 2018). Somatically acquired amplification of *MYCN*, and hemizygous deletions of 1p and 11q have previously been identified as frequently detected

mutations and are associated with poor prognosis (Deyell & Attiyeh, 2011; Mlakar et al., 2017). In the TARGET initiative significant somatic mutation frequencies in HR NBL included ALK (9.2% of cases), PTPN11 (2.9% of cases), ATRX (2.5% of cases), *MYCN* (1.7% of cases) and NRAS (0.83% of cases) (Pugh et al., 2013).

1.6.1. **Myc in neuroblastoma**

The *MYCN* gene was first reported in the 1980's when researchers observed that NBL cell lines harboured DNA sequences related to c-MYC. N-Myc is coded by the *MYCN* gene on chromosome 2 (2p24) (Beltran, 2014). Subsequently amplification of N-Myc was reported to contribute to cancer cell formation in non-NBL cell lines (Kohl et al., 1983; Schwab et al., 1983). N-Myc has also been reported to be essential in normal mammalian embryogenesis with embryonic lethality and failure of the epithelial component of the embryo to develop with loss of N-Myc (Jakobovits, Schwab, Bishop, & Martin, 1985; Stanton, Perkins, Tessarollo, Sassoon, & Parada, 1992). Germline mutations that inactivate *MYCN* cause Feingold syndrome with phenotypic features including microcephaly, gut atresia, limb abnormalities and learning disability (van Bokhoven et al., 2005). Enforced expression of N-Myc in neural crest cells resulted in NBL with similar copy number gains that are seen in human NBL and similar clinical characteristics (Olsen et al., 2017). In the 1980's it was established that N-Myc amplification was linked to advanced disease in NBL, typically with a poor prognosis (Brodeur, Seeger, Schwab, Varmus, & Bishop, 1984; Gamble, Kees, Tweddle, & Lunec, 2012), and even to this day it is used to stratify NBL risk (Table 1). Although N-Myc has been the most studied oncogene involved in HR NBL, there is a subset of NBL patients with tumours primarily driven by c-Myc that have equally poor outcomes (Jung et al., 2017; Zimmerman et al., 2018).

1.6.2. **N-Myc and metastatic disease**

Evidence also suggests that N-Myc plays a pivotal role in the ability of NBL to metastasise, as is common in 50% of patients on presentation, and contributes to poor prognosis (Goodman et al., 1997). Over-expression of focal adhesion kinase

(FAK) by N-Myc has been implicated in the ability of NBL to metastasise (Lee et al., 2012). This association has been observed in other human tumours, such as oesophageal carcinoma (Miyazaki et al., 2003). FAK is frequently over-expressed in N-Myc amplified NBL cell lines. Inhibition of FAK, via siRNA knockdown, correspondingly reduced the metastatic tumour burden in modified NBL cells implanted in nude mice (Lee et al., 2012; M. L. Megison, Stewart, Nabers, Gillory, & Beierle, 2013).

1.6.3. **MYC**

MYC was first discovered and identified in studies of oncogenic retroviruses in the 1970's (Sheiness, Fanshier, & Bishop, 1978) and then c-Myc was formally identified, and isolated to chromosome 8, in Burkitt's lymphoma cells (Dalla-Favera et al., 1982) in the early eighties. In 1985 it was established that deregulated expression of Myc was enough to drive the formation of lethal lymphomas in mice (J. M. Adams et al., 1985). The MYC family of proto-oncogenes comprises c-MYC, N-MYC and L-MYC that act as transcriptional factors, regulating many essential genes responsible for cell growth and differentiation (Mukherjee, Morgenbesser, & DePinho, 1992). The Myc/Max/Mad group of transcriptional factors, members of the basic-helix-loop-basic-helix-zipper (bHLHZ) class (Figure 1) interact in a way that promotes either transcriptional gene activation or repression (Grandori, Cowley, James, & Eisenman, 2000; Grinberg, Hu, & Kerppola, 2004). MYC and Mad family proteins form dimers with Max and play opposing roles which is essential for the regulatory function of these proteins (Grinberg et al., 2004). Heterodimerisation with Max is required before MYC can activate gene targets via RNA Pol II (Figure 1B). N-Myc tends to have a closer association with the CATGCG E-box motif rather than the classic CACGTG E-box motif (Cotterman et al., 2008).

Correspondingly MYC can induce transcriptional repression via its interaction with MIZ1, impacting on many cellular functions including autocrine signalling (Shostak et al., 2016; van Riggelen et al., 2010) (Figure 1C). The co-operation between MYC and

MIZ1 has been implicated tumourigenesis via its down-regulation of anti-mitogenic signals such as TGF-β or DNA damage (van Riggelen et al., 2010; Wiese et al., 2013).

The MYC family of oncogenes are implicated in at least 50-70% of human cancers (Kalkat et al., 2017; Klapproth & Wirth, 2010). Although c-Myc and N-Myc are known to share targets and can functionally replace one another, they tend to be associated with specific cancers with no crossover. As stated earlier, c-Myc is associated with Burkitt's lymphoma whereas N-Myc is associated with NBL (Beltran, 2014). Interestingly, the expression of MYC in medulloblastoma is dependent on sub-group (Roussel & Robinson, 2013). Unlike other sub-groups, c-MYC, N-Myc are never expressed in the WNT sub-group which has the best overall cure rates which are close to 90% (D. T. Jones et al., 2012). The SHH sub-group, which has an intermediate prognosis, can occasionally express both N-Myc and c-Myc, which is associated with a poorer prognosis in this group (Ellison et al., 2011). Group 3 medulloblastomas have the worst overall survival and account for 30% of medulloblastomas (Roussel & Robinson, 2013), with high expression of Myc (D. T. Jones et al., 2012). Group 4 medulloblastomas have similar outcomes to the SHH sub-group and tend to have low expression of both N-Myc and c-Myc (Roussel & Robinson, 2013).

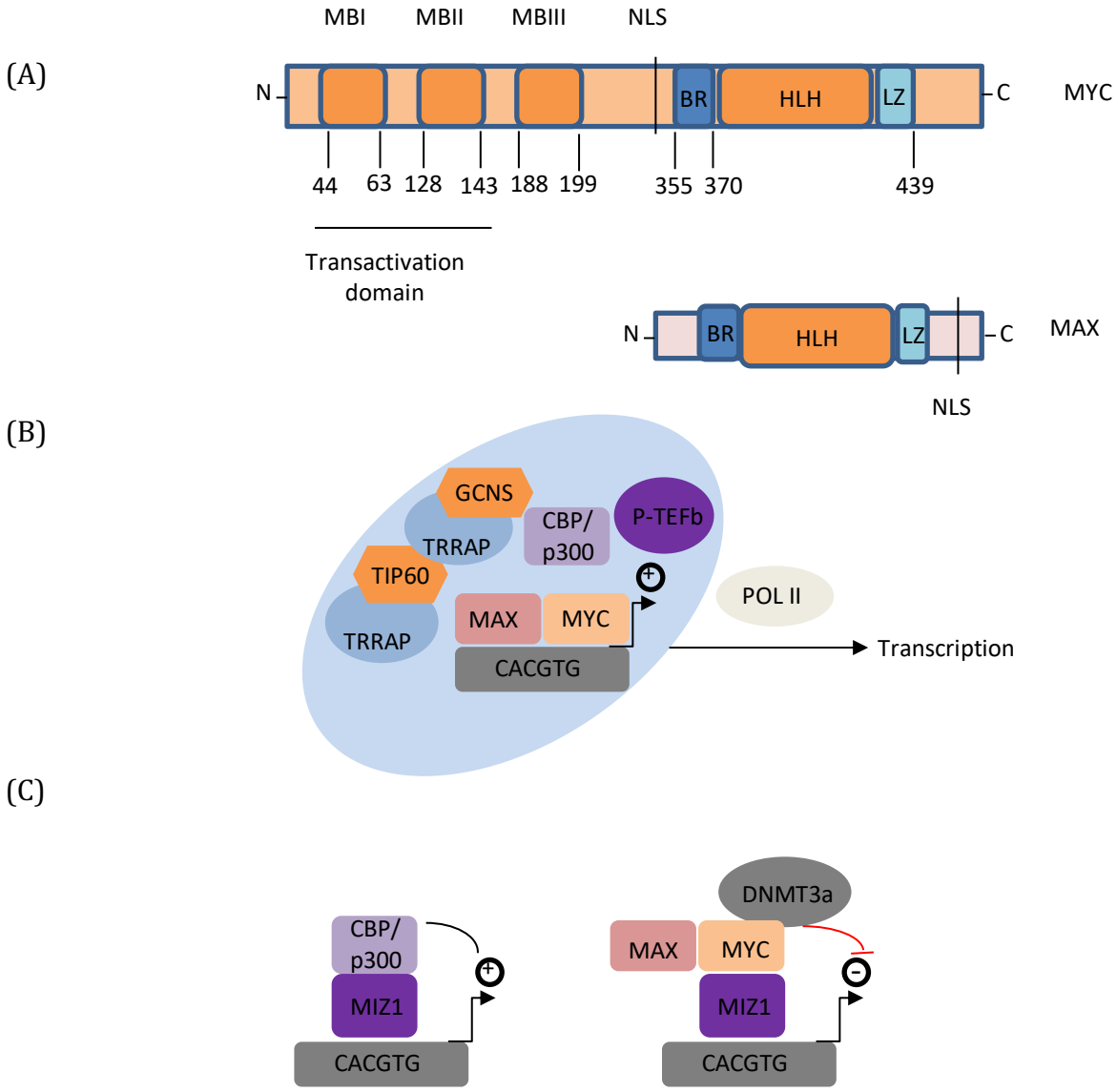

Figure 1. MYC structure and transcriptional activation and suppression

(A) MYC and its heterodimeric binding partner MAX (B) Transcriptional activation by MYC, via RNA Pol II, and its co-operative binding partners; multiprotein mammalian TRRAP-TIP60 & TRRAP-GCNS, transcriptional elongation factors (P-TEFb) and histone acetyl transferases (p300) (C) MYC/MAX heterodimers prevent transcription of MIZ1 by preventing its association with p300 (Klapproth & Wirth, 2010). MB; Myc Box, NLS; Nuclear localisation signal, BR; Basic region, HLH;Helix-loop-helix; LZ leucine zipper.

1.6.3.1. *MYC transcription and targets*

MYC has been implicated in the translational regulation of approximately 15% of human genes (Klapproth & Wirth, 2010) representing up to 25,000 MYC binding sites (Adhikary & Eilers, 2005). The target genes include examples of known oncogenes, genes associated with neuronal differentiation and genes related to cell proliferation (Alaminos et al., 2003).

Transcription is primarily via RNA polymerase II (POL II) (Price, 2010; Raha et al., 2010) but POL I, POL II and POL III have all been identified as being important in transcription (Gomez-Roman et al., 2006). Interestingly, MAD1 and c-Myc reciprocally regulate rDNA transcription via down-regulation of upstream binding factor (UBF) during periods of cell growth to ensure cellular factors required for cell growth are present (Gretchen Poortinga et al., 2004). This phenomenon has also been observed in B-cell lymphomagenesis in mice via activation and repression of discrete gene sets (Sabò et al., 2014). It is this reliance on the RNA polymerases (POL) that has postulated use of POL inhibitors as an indirect way of treating MYC driven tumours (G. Poortinga, Quinn, & Hannan, 2015).

1.6.3.2. *Transcriptional regulation of MYC*

Different members of the MYC family of genes have been shown to be differentially expressed relative to tissue type and developmental stage (L. Xu, Morgenbesser, & DePinho, 1991). The process of transcription involves at least three steps; initiation, elongation and termination (Rahl & Young, 2014). Recent evidence suggests that MYC is regulated by several factors: POL II, FUSE-binding proteins (FBP) and FBP-interacting receptor (FIR) (Levens, 2008). The earliest evidence of a factor that influences MYC initiation was TFII-I, a transcription initiation factor that initiates core promoters (Roy, Carruthers, Gutjahr, & Roeder, 1993). MYC itself has been shown to regulate POL II, which in turn regulates MYC (de Pretis et al., 2017). c-Myc regulates pause release by recruiting P-TEFb to its target genes which is the final step in the transcriptional activation of the carbamoylphosphate synthetase-2, aspartate

transcarbamylase, dihydroorotase (CAD) promoter (Cole & Cowling, 2008; Eberhardy & Farnham, 2002; Rahl et al., 2010). Inhibitors of CHK9 have been shown to suppress CDK9 phosphorylation and causing POL II pausing and increased MYC expression (H. Lu et al., 2015). Wnt/β-catenin signalling has also been shown to up-regulate MYC via Gsk3β (S. Zhang et al., 2012). This pathway has also been implicated in the tumourigenesis of a specific myeloid differentiating (MYD) primary response regulated sub-group of paediatric medulloblastoma (H. A. Rogers et al., 2012).

1.6.3.3. ***Post-transcriptional regulation of MYC***

Post-transcriptional regulation is the control of gene expression at the RNA level. It occurs once the RNA polymerase has been attached to the gene's promoter and is synthesizing the nucleotide sequence (Figure 1C). It has been shown that Myc and eIF4F constitute a "feedforward" loop that regulates cell growth. When Myc activity is stimulated, all three subunits of eIF4F are correspondingly increased (Lin, Malina, & Pelletier, 2009). Given that eIF4F formation is modulated by mTOR signalling, and mTOR signalling is essential the cellular growth (Ben-Sahra & Manning, 2017), this then links the MYC transcriptional response to the eIF4F translational response as a means to adapt cells to changes in cellular environment (Lin et al., 2009). It also appears that post-transcriptional regulation of N-Myc, as measured by N-Myc RNA in different cell types, may be tissue dependent (Babiss & Friedman, 1990). Interferon-α has also been shown to strongly shown to post-transcriptionally induce c-Myc at the protein level (Ehninger et al., 2014).

HDACi have been shown to relieve the *MYC* mediated transcriptional repression of apoptosis, in particular by relieving the downregulation of the anti-apoptotic genes Bcl-2 and Bcl-xL, thereby promoting apoptosis (C. M. Adams, Hiebert, & Eischen, 2016). Given the clear role that *MYC* has in inhibiting cellular differentiation (Leon, Ferrandiz, Acosta, & Delgado, 2009), it is not unreasonable to postulate that HDACi can promote cellular differentiation particularly in MYC driven malignancies.

1.6.3.4. ***Post-translational regulation of MYC***

Two sites, Thr-58 and Ser-62, within Myc box (MB) I, the transactivation domain (TAD) of MYC, are targeted by GSK3 and proline-directed kinases, respectively. Ser-62 phosphorylation is required for Thr-58 to become a substrate of GSK3 (Vervoorts, Lüscher-Firzlaff, & Lüscher, 2006). Kinases implicated in phosphorylation of Ser-62 include mitogen active protein kinase (MAPK) (Cargnello & Roux, 2011), c-JUN N-terminal kinase (JNK) (Noguchi et al., 1999) and cyclin-dependent kinases 1 & 5 (CDK1,CDK5) (Seo, Kim, Bae, Soh, & Lee, 2008; Sjostrom, Finn, Hahn, Rowitch, & Kenney, 2005). Interestingly, two of the main pathways in which the RAS protein is activated is the MAPK and the PI3K pathways (Zenonos & Kyprianou, 2013) which are important in cell growth and survival. Phosphorylation of Ser-62 stabilises MYC whereas phosphorylation of Thr-58 primes MYC for degradation via polyubiquitinylation and subsequent proteasomal degradation (Vervoorts et al., 2006).

1.6.3.5. ***MYC and the cell cycle***

Over expression of the cyclin-dependent kinase inhibitor $p21^{(WAF1/CIP1)}$ in normal and tumour cell lines results in cell cycle arrest (Karimian, Ahmadi, & Yousefi, 2016) (A. Chen et al., 2015). MYC can repress p21 transcription and therefore over-riding the p21 cell cycle checkpoint and in turn promoting cell proliferation (Gartel et al., 2001). MYC has also been shown to act through the cyclin-dependent kinase (Cdk) inhibitor $p27^{Kip1}$ to activate Cdk4/6 and promote cell cycle progression (Obaya, Kotenko, Cole, & Sedivy, 2002).

1.6.3.6. ***MYC and microRNA***

MicroRNAs (miRNAs) are important regulators of gene expression that bind complementary target mRNAs and repress their expression (Michlewski & Cáceres, 2019). Evidence suggests that these key MYC driven phenotypes, including cell cycle progression, are under the control of multiple microRNA's and therefore deregulation of these microRNA's by MYC can impact on these phenotypes (Psathas & Thomas-

Tikhonenko, 2014). Various targets of this transcriptional regulation have been identified including Drosha (Xingwu Wang, Zhao, Gao, & Wu, 2013), miR-34 and miR-15a/16-1 and in turn these microRNA's can regulate MYC (Jackstadt & Hermeking, 2015).

1.6.3.7. ***MYC and p53***

N-Myc has been shown to transcriptionally upregulate p53 in NBL and co-operates with p53 to mediate apoptosis (L. Chen et al., 2010; Gamble et al., 2012). In the TH-*MYCN* mouse model of neuroblastoma, chemotherapy induced apoptosis requires p53 induction (Louis Chesler et al., 2008). In N-Myc amplified neuroblastoma cell lines, knockdown of N-Myc reduces p53 expression (L. Chen et al., 2010). This was further evaluated using a Tet21N-regulatable N-Myc expression system. In Tet21N *MYCN*+ cells, higher levels of p53 transcription, mRNA, and protein were observed relative to Tet21N *MYCN*- cells thereby confirming the direct relationship between N-Myc and p53 expression (L. Chen et al., 2010). Correspondingly, when p53 is reactivated by using MDM2 inhibitors, p53 mediated apoptosis is observed preferentially in N-Myc amplified NBL cell lines (Gamble et al., 2012). This is also true of c-Myc and p53 (Phesse et al., 2014) where c-Myc has additionally been shown to co-operate with p53 to induce G_1 cell cycle arrest (Ho, Ma, Mao, & Benchimol, 2005).

1.6.3.8. ***MYC and malignant transformation***

The *MYC* oncogene contributes to many human cancers (Dang, 2012). This makes sense when you consider the multitude of cellular pathways that involve growth, proliferation and metabolism that it modulates (Y. Dong, Tu, Liu, & Qing, 2020; Schmidt, 1999). Evidence has emerged that *MYC* deregulation on its own may not be enough to initiate cancer and it fact requires co-operating pathways, including *Ras* and PI3K/AKT/mTOR to achieve this (Gabay, Li, & Felsher, 2014). This co-operation may be in fact necessary to overcome the cancer protective properties of *MYC,* such as the initiation of the protective DNA damage response (DDR). This DDR has been

shown to activate an ARF-independent process that limits aberrant cell division possibly by the production of reactant oxygen species (ROS) (Campaner & Amati, 2012). Because of this, and the impact that MYC has on maintaining tumour microenvironment (TME), tumours initiated by MYC may in fact become addicted to MYC (von Eyss & Eilers, 2011).

1.6.3.9. ***MYC transformation and oncogene addiction***

Central to the concept of "oncogene addiction" is the theory that tumours have an ongoing and essential reliance on the oncogenic lesion that initiated them (Weinstein, 2002). This concept is supported by evidence that has been derived from murine models with adjustable expression of oncogenes. In an aggressive *MYC* driven mouse model of lymphoma, 90% of mice with established tumours demonstrated tumour regression when MYC expression was suppressed. This tumour regression was characterised by growth arrest, apoptosis and differentiation (Felsher & Bishop, 1999). Interestingly 10% of mice did not demonstrate tumour regression. This suggests that tumours can escape from their addiction to the initiating oncogene by developing compensatory genetic events (Arvanitis & Felsher, 2006).

1.6.3.10. ***MYC proteins as therapeutic targets***

Given the diverse range of cellular functions that the MYC family of proto-oncogenes regulate, with their dysregulation implicated in a number of human cancers (The Cancer Genome Atlas Research et al., 2008), it is not surprising that attempts to target these oncogenes are a focus of current research (H. Chen, Liu, & Qing, 2018; Gustafson & Weiss, 2010). Additionally MYC-induced tumours show signs of "oncogene addiction" making targeting MYC even more crucial in their treatment (Gabay et al., 2014). However, to date, attempts to target MYC directly have been largely unsuccessful (Beltran, 2014).

Targets upstream of *MYCN* include the receptor tyrosine kinases (RTKs) and the PI3K/AKT/mTOR pathway which converge on GS3Kβ which in turn is critical in the

serial phosphorylation and stabilisation of *MYCN*. The stability of *MYCN* is under the control of both GSK3β and mTORC1, the latter controlling ubiquitination of *MYCN* via downregulation of PP2A. CDK1 is also involved in this serial phosphorylation process with many CDK1 inhibitors in development.

Aurora kinases are involved in the stabilisation and degradation of *MYCN* by proteases (Otto et al., 2009) (1.6.3.4) with several Aurora A kinase inhibitors in development at the moment (Brockmann et al., 2013). Translation of *MYCN*, via ribosomal biogenesis, can be inhibited by agents such as POL I inhibitors (Gustafson & Weiss, 2010; Koh, Sabò, & Guccione, 2016; Rickman, Schulte, & Eilers, 2018) (Figure 2). Databases that identify direct genomic targets of MYC will hopefully identify further downstream targets (Zeller, Jegga, Aronow, O'Donnell, & Dang, 2003).

Antisense oligonucleotides have shown early promise as a downstream mechanism of inhibiting MYC expression in breast cancer cell lines, primarily by inhibition of cyclin D1 expression (J. S. Carroll, Swarbrick, Musgrove, & Sutherland, 2002). As an extension of this approach, double stranded decoy oligonucleotides can be used to target specific oncogenic proteins such as N-Myc, and reduce the proliferative capacity of NBL cell lines (El-Andaloussi et al., 2005). More recently antisense peptide nucleic acid therapy has been shown to influence *MYCN* translational inhibition and induce G_1 cell cycle arrest, induce apoptosis and differentiation, in human NBL cell lines (Pession et al., 2004). In melanoma, siRNA's directed against c-Myc expression effectively inhibited tumour growth (Y. Chen, Bathula, Yang, & Huang, 2010). As stated earlier, small molecule inhibitors of MYC are currently in the early stages of development (Fletcher & Prochownik, 2015). One such agent, stauprimide, inhibits nuclear localisation of the MYC transcription factor NME2 which in turn results in down-regulation of MYC transcription (Bouvard et al., 2017).

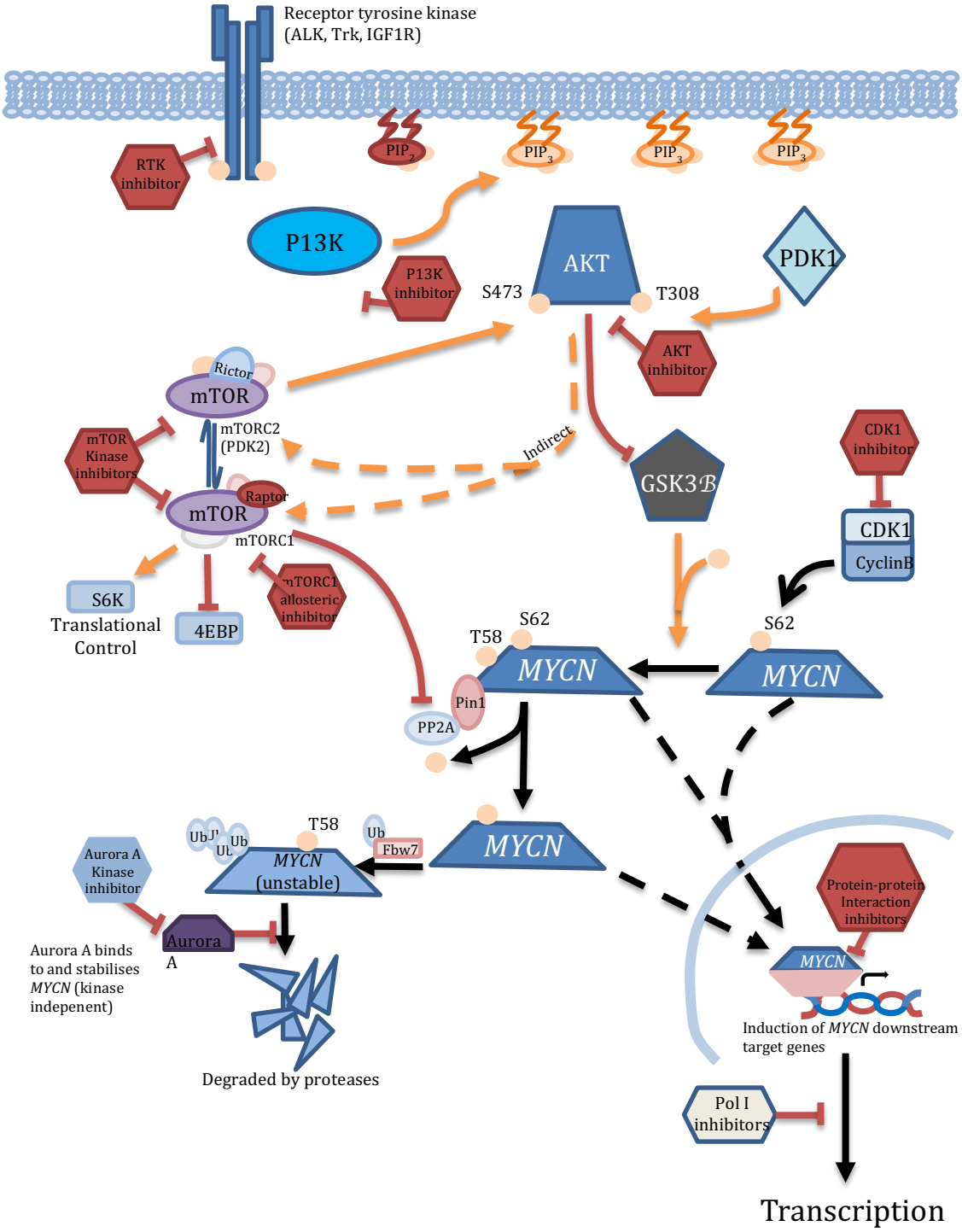
Receptor tyrosine kinase
(ALK, Trk, IGF1R)
RTK inhibitor
PIP2
PIP3
PIP3
PIP3
P13K
P13K inhibitor
AKT
S473
T308
PDK1
AKT inhibitor
Rictor
mTOR
mTORC2
(PDK2)
mTOR Kinase inhibitors
Raptor
mTOR
mTORC1
Indirect
GSK3β
CDK1 inhibitor
CDK1
CyclinB
S6K
Translational Control
4EBP
mTORC1 allosteric inhibitor
T58
S62
S62
MYCN
MYCN
Pin1
PP2A
MYCN
T58
Ub
Ub
Ub
Fbw7
MYCN (unstable)
Aurora A Kinase inhibitor
Aurora A
Aurora A binds to and stabilises MYCN (kinase indepenent)
Degraded by proteases
Protein-protein Interaction inhibitors
MYCN
Induction of MYCN downstream target genes
Pol I inhibitors
Transcription

Figure 2 MYC proteins as therapeutic targets

In actively dividing cells *MYCN* is initially phosphorylated at Ser62 by CDK1. Subsequent to this, active GSK3β phosphorylates *MYCN* at Thr58 which results in stabilised and transcriptionally active *MYCN*. PP2A dephosphorylates Ser62, allowing binding of ubiquitin ligase Fbw7 which primes *MYCN* for proteasomal degradation. Aurora A kinase can bind to and stabilise poly-ubiquinated *MYCN*, which allows it to continue its transcriptional functions. Pathways influencing MYC activity are indicated and are potentially targetable for therapy (Gustafson & Weiss, 2010).

1.7. TH-*MYCN* neuroblastoma mouse model and small animal imaging

The TH-*MYCN* model of neuroblastoma, using targeted N-Myc overexpression in the neural crest as the driver of NBL tumour formation, was first developed in 1997 (Weiss, Aldape, Mohapatra, Feuerstein, & Bishop, 1997). At that time, it was a unique model in that is encapsulated all the syntenic chromosomal gains and losses associated with human NBL, with an intact immune system. Also, the N-Myc dosage impacted on the penetrance of NBL seen in the mouse model (Weiss et al., 1997) with homozygous mice having 100% tumour penetrance compared to the 40% penetrance seen in the hemizygous mice. When 31 tumours from TH-*MYCN* transgenic mice had histological profiles performed, including H&E and Ki67, the similarities between the mouse and human NBL tumours were striking (H. C. Moore et al., 2008). Cell lines derived from this model have also been shown to encapsulate the characteristics of human NBL (A. J. Cheng et al., 2007).

At the time that this thesis started there was very little in the way of available mouse models for NBL. In particular, as is the case with many pre-clinical models for solid tumours, there was little in the way of manipulative systems. In fact, it is this lack of appropriate pre-clinical models that has limited the translation of pre-clinical research into human subjects (Vandamme, 2014). Animal studies are required as proof of principle before any new compound can be tested in humans making appropriate models even more essential. Mouse models are favoured as the mouse genome has a 99% concordance with the human genome, and the animal's small size and reproductive capability allows for cost-effective housing and high throughput studies (Vandamme, 2014). Subcutaneous xenograft models, using immunodeficient mice has long been favoured as they are relatively quick, cheap and reliable. Tumour growth is also easy to monitor with simple techniques such as calipers (Vandamme, 2014). An ideal mouse model, however, mimics the disease being studied genetically and physiologically (Justice & Dhillon, 2016). Subcutaneous xenograft models lack key characteristics in that the tumours do not grow in the organ of origin which removes the important impact of TME and there is no intact immune system. In

addition, there are concerns that cell line derived models lose many of their important genomic characteristics as the implanted cells have often adapted to *in-vitro* tissue culture thereby potentially loosing characteristics important to their original human environment (Braekeveldt & Bexell, 2018). Patient derived xenograft (PDX) models, where human tumour tissue is implanted directly into the mice without cell culture passage, can avoid this problem. This, however, does not alleviate the limitations of an abnormal immune system, lack of TME and tumour heterogeneity (Braekeveldt & Bexell, 2018). Despite these limitations they have been shown to parallel the clinical outcomes seen in human tumours (Hidalgo et al., 2014). Many researchers have been actively developing and validating xenograft models for pre-clinical research, including xenograft models for NBL (Rokita et al., 2019). However, some of the earliest established PDX models for NBL were not published until 2015 and were unavailable for use at the time of this thesis (Braekeveldt & Bexell, 2018).

More recently orthotopic xenograft models have been used, where the tumour cells are injected, or tumour tissue itself implanted into the organ of origin, to mimic local tumour growth, TME and pathways for metastasis (Vandamme, 2014). If such an orthotopic model could be developed, with an intact immune system, this would prove to be a very useful model for translational research. Finally, newer tools such as CRISPR/Cas9 allow for germline manipulation opening the door for relatively quick and inexpensive development of new mouse models (Zuberi & Lutz, 2017).

Similar to the transgenic model, an ideal orthotopic model of NBL would be an intra-abdominal tumour. It would require cells to be injected into/as close to the mouse adrenal gland as possible. Being an intra-abdominal tumour presents unique challenges in terms of tumour monitoring for growth and response to treatment. From a purely ethical standpoint we need to ensure that mice are not exposed to an unreasonable tumour burden. From an experimental standpoint we need to identify tumours at a size when the mice can be safely allocated to experiments and then be able to monitor their response to the intervention being studied. Small animal

imaging techniques allow for this (Cunha et al., 2014; R. Yao, Lecomte, & Crawford, 2012).

There are two aspects when monitoring tumour response: tumour size and activity. Tumour size can be monitored using a variety of non-invasive small animal imaging techniques including ultrasound (US), magnetic resonance imaging (MRI) or computed tomography (CT) scans. All are equally reproducible, can provide three dimensional images and allow for tumour volume calculations. US and MRI have the advantage of not exposing the mice or the technician to radiation. Of these two US has the advantage of being less expensive and quicker, the later allowing for higher volumes of scans (Cunha et al., 2014; Hoyer, Gass, Weber-Fahr, & Sartorius, 2014).

Small animal positron emission tomography (PET) has been previously validated as a form of functional imaging that quantifies metabolic activity within a tumour (Cullinane et al., 2005). Of the murine tracers available fluorodeoxyglucose (FDG-PET) has been repeatedly validated in human NBL patients as being reliable as a means of disease detection and therefore response to therapy. Indeed in some studies it has been shown to be superior to traditional 131I-MIBG scintigraphy for detecting metastatic lesions (Kumar et al., 2013). Newer tracers, that may be more specific for NBL, include 68Ga-DOTA-Octreotate (GaTATE) are now becoming available in murine models. These are yet to be as robustly validated in human NBL patients as a means of tumour detection and response, although the early studies that these tracers too may be superior to traditional 131I-MIBG scintigraphy (Kong et al., 2016). Functional imaging allows for the detection of tumour response, as a quantifiable measure of tumour metabolism, at earlier treatment timepoints, often before there has been any discernible change in tumour volume (R. Yao et al., 2012).

1.7.1. **Targeting PI3K in neuroblastoma**

Significant expression of the PI3K/AKT/mTOR pathway has been demonstrated in both human NBL tissue samples and human NBL cell lines (Johnsen et al., 2008; Spitzenberg et al., 2010) (3.1). N-Myc co-operates with signalling proteins of the PI3K/AKT/mTOR pathway to alter many cellular functions including DNA methylation (Popkie et al., 2010), angiogenesis (J. Kang et al., 2008), apoptosis (Bender et al., 2011) via stimulation of S6K, 4-EBP1 and inactivation of GSK3β and FOXO1 (Spitzenberg et al., 2010). PI3K inhibition has been shown to activate GSK3β, leading to phosphorylation and de-stabilisation on N-Myc (L. Chesler et al., 2006).

Given the importance of the PI3K/AKT/mTOR pathway in most human cancers (J. Yang et al., 2019) including NBL it forms the basis of the first results chapter of this thesis. There are multiple aspects of the pathway that can be targeted with drugs that inhibit the pathway with either single or combined inhibition. Some of these agents have already been rigorously tested in other tumour types (J. Yang et al., 2019).

1.8.**PI3K and MYC deregulation in cancer.**

The PI3K/AKT/mTOR pathway plays a key role in all aspects of cancer including cell cycle, survival, metabolism, motility and genomic instability. It also controls the tumour microenvironment via inflammatory cell recruitment and angiogenesis (David A. Fruman & Rommel, 2014). Aberrant signalling of this pathway has been implicated in a multitude of human cancers (Engelman, Luo, & Cantley, 2006) making it an attractive therapeutic target (Courtney, Corcoran, & Engelman, 2010).

MYC proteins target proliferative and apoptotic pathways essential for the progression of cancer (Gustafson & Weiss, 2010). The MYC family are transcriptional factors that have also been implicated in a multitude of human cancers (Kalkat et al., 2017). In particular paediatric neuroblastoma (NBL) is associated with amplification of MYC and this has been directly implicated in tumour formation. Additionally the

presence of amplified N-Myc in NBL imparts a poor prognosis (J. M. Maris et al., 2007). Targeting MYC directly has to date been challenging and unsuccessful; however, small molecule inhibitors of MYC are currently in development (Fletcher & Prochownik, 2015). Therefore research is focusing on targeting MYC indirectly, via downstream mechanisms (Posternak & Cole, 2016). Given that the PI3K/AKT/mTOR pathway and MYC play such prominent roles in human cancer it is not surprising that they interact and co-operate (J. Kang et al., 2008; Sander et al., 2012).

1.9.**Phosphoinositide signalling**

The phosphoinositides are a family of acidic phospholipids that reside in cell membranes and their principal role is to interact with proteins. Like other phospholipids they have a glycerol backbone esterified to two fatty acid chains and a phosphate, and attached to a polar head group that extends into the cytoplasm (Falkenburger, Jensen, Dickson, Suh, & Hille, 2010). The seven phosphoinositides are structurally and metabolically related. They are formed when phosphatidylinositol (PI) is phosphorylated at three different positions of its inositol ring. The major phosphoinositides, that are of interest in cancer, consist of PI and the three polyphosphoinositides, namely phosphatidylinositol 4-phosphate PI(4)P (PIP_1), phosphatidylinositol 4,5-bisphosphate PI(4,5)P_2 (PIP_2) and phosphatidylinositol 3,4,5-triphosphate PI(3,4,5)P_3 (PIP_3) (Falkenburger et al., 2010). PIP_2 is the major substrate of receptor stimulated phospholipase C (PLC) and PLC is in turn modulated by over 50 hormones receptors. PIP_2 has been implicated in cancer both by its vesicle trafficking and the promotion of cell migration and invasion via recruitment of β1-Integrins (Thapa & Anderson, 2012). Both PIP_2 and PIP_3 have the ability to recruit protein kinases, such as AKT/PKB to the cell membrane (Zlotorynski, 2017) with PIP_3 initiating signals of the growth factor response pathway (Chalhoub & Baker, 2009; Zlotorynski, 2017) (Figure 3).

It has been shown that PI3K signalling can be regulated by non-phosphoinositol substrates such as phosphatidylinositol transfer protein (PITP), and that PITP

mediated axonal extension can be inhibited by PI3K inhibition (Cosker et al., 2008; Hsuan & Cockcroft, 2001). Activation of class I PI3Ks occurs through multiple upstream pathways that couple a broad range of cell surface receptors to specific PI3K isoforms. Generally, PI3Ks are capable of being activated by receptor-coupled tyrosine kinase activities, small Ras-related GTPases, and heterotrimeric G proteins (D. A. Fruman et al., 2017).

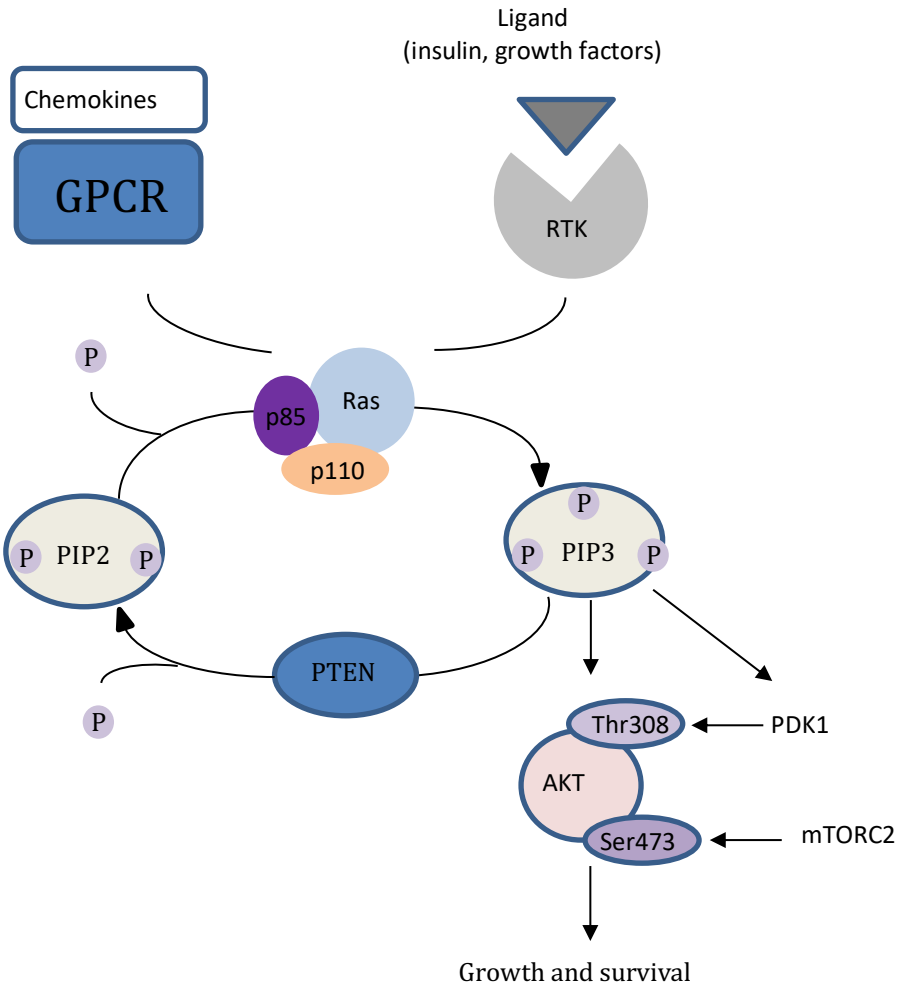

Figure 3 Phosphoinositide signalling

Class I PI3K's signalling is antagonised by PTEN. In response to activation of G-protein couple receptors (GPCR) or activation of receptor tyrosine kinases (RTK) the catalytic subunit of PI3K (p110) is recruited through its regulatory subunit (p85) where it phosphorylates PIP_2 to generate PIP_3. PTEN antagonises this process via de-phosphorylation of PIP_3. Growth factors such as AKT are then recruited where they are subsequently activated by serial phosphorylation. Activated AKT can then enter the cytoplasm and promote growth and other cellular functions.

1.9.1. **Phosphatidylinositol-3-kinase**

There are three classes of phosphatidylinositol 3-kinase (PI3K) grouped according to structure and function. PI3K was first discovered in the 1980's when the reliance of viral oncoproteins on PI3K activity was established (Sugimoto, Whitman, Cantley, & Erikson, 1984; Whitman, Kaplan, Schaffhausen, Cantley, & Roberts, 1985). It has been suggested that almost every ion channel and transporter is affected by phosphoinositide signalling, thereby regulating many cellular functions (Balla, Szentpetery, & Kim, 2009). Many human tumours harbour somatic missense mutations in PIK3CA (The Cancer Genome Atlas Research et al., 2008).

1.9.1.1. ***Class I PI3K***

Class I PI3Ks have been directly implicated in human cancer (T. L. Yuan & Cantley, 2008). Class I PI3Ks consist of a regulatory subunit and a catalytic subunit. The catalytic isoforms p110α, p110β, p110γ and p110δ are the products of four genes, PIK3CA, PIK3CB, PIK3CG and PIK3CD, respectively (Courtney et al., 2010).

Class IA PI3K comprise of p110α, β or δ bound to a p85 regulatory subunit. Three mammalian genes PIK3R1, PIK3R2 and PIK3R3 encode p85α (p85α, p55α and p50α isoforms), p85β and p55γ regulatory subunits respectively, which are referred to collectively as p85 (T. L. Yuan & Cantley, 2008). Both PIK3CA and PIK3R1 can be somatically mutated in cancer with inherent activation of the PI3K pathway (Courtney et al., 2010).

Class IA PI3Ks are activated by growth factor stimulation via receptor tyrosine kinases (RTK) or G-protein couple receptors (GPCR). The relationship between PI3K, phosphatase and tensin homologue on chromosome 10 (PTEN), PIP_2 and PIP_3 is summarised (Figure 3). Additionally, PI3K can be activated by RAS proteins, and both PI3K and MEK have been shown to be essential in RAS driven malignant transformation (Castellano & Downward, 2011; Jokinen & Koivunen, 2015). RAS has also been shown to directly interact with the PI3K p110α to promote tumour induced

angiogenesis (Murillo et al., 2014). Additionally disruption of RAS interaction with p110α decreases cell motility, via promotion of Reelin, and potentially its ability to metastasise (Castellano et al., 2016). Radiation therapy, an integral part of NBL therapy, can potentially be affected by RAS-mediated radio-resistance, by PI3K and RAF dependent pathways (Grana, Rusyn, Zhou, Sartor, & Cox, 2002).

1.9.1.2. ***Class II PI3K***

Class II PI3K comprise PI3KC2α (PIK3C2A), PI3KC2β (PIK3C2B) and PI3KC2γ (PIK3C2G). Class II PI3k have important cellular roles including cell migration, cortical re-modelling, glucose transport, insulin signalling, endocytosis and exocytosis. PI3KC2-induced PtdIns(3)*P* appears to mediate K^+ channel activity, growth factor receptor responses, cell contraction and migration. PI3KC2α-induced PtdIns(3,4)P_2 is associated with insulin induced AKT stimulation (Jean & Kiger, 2014). Class II PI3K's have been linked to diabetes and cancer (Falasca & Maffucci, 2012).

1.9.1.3. ***Class III PI3K***

There is one class III PI3K comprising Vps34 (PIK3C3), PI3KC2β (PIK3C2B) and PI3KC2γ (PIK3C2G). Vps34 forms a heterodimer with the regulatory subunit Vps15 (PIK3R4). Vps34 regulates membrane trafficking with essential roles in autophagy, endocytosis and heart and liver function (Jaber & Zong, 2013). Class III PI3K's have not been directly linked to human cancer (Jean & Kiger, 2014).

1.9.2. **PTEN and Phosphoinositide signalling**

PIP_3 can be dephosphorylated by 3- or 5- phosphatases, the latter producing PIP_2. The PTEN tumour suppressor is primarily thought to act as a PI(3,4,5)P_3 3-phosphatase although it has been shown to function as a PI(3,4)P_2 phosphatase (Malek et al., 2017). Regardless of how it functions, PTEN's role in suppressing aberrant PI3K signalling establishes its role as a tumour suppressor (Goberdhan & Wilson, 2003; Song, Salmena, & Pandolfi, 2012). Mutations in PTEN have been documented in a wide range of human tumours including melanomas, glioblastomas

and prostate cancer. Activated AKT can regulate phosphorylation of PTEN's C-terminal tail and compromise PTEN stability, suggesting a negative feedback loop for PI3K/AKT signalling (Goberdhan & Wilson, 2003). Germline mutations in PTEN result in increased cancer lifetime risks of cancers including colorectal cancer, melanoma and kidney cancer (Tan et al., 2012).

1.9.3. **Phosphoinositide signalling in neuroblastoma**

The expression of PI3K-related phosphoinositide signalling was determined in tumours from 68 NBL patients, revealing an over-expression of PI3K isoforms including PIK3R1(encoding p85) and PIK3CD (encoding p110δ). Similar results were observed in eight commonly used NBL cell lines. In SH-SY5Y cells that display increased PIK3CA and PIK3CD expression, down regulation of p110δ had a significant impact on cell growth. Interestingly the expression of p85 and p110δ was inversely related to N-Myc amplification and primarily found in tumours of patients less than 1 year of age (Boller et al., 2008). Human neuroblastoma samples have also been shown to have increased expression of AKT, which correlates with poor prognosis (Opel, Poremba, Simon, Debatin, & Fulda, 2007), and of other members of the PI3K/AKT/mTOR pathway (Johnsen et al., 2008).

1.9.4. **Activating lesions upstream of PI3K**

PI3K can be activated upstream via a number of mechanisms such as aberrations in RTK's, GRCR's and RAS activation. These events are commonly seen in paediatric cancers.

1.9.4.1. ***Deregulation of receptor tyrosine kinases***

Deregulation of RTK's have traditionally been documented in paediatric haematological malignancies. Mutations in c-Kit and FLT3 are examples of aberrant RTK's contributing to haematological malignancies such as acute myeloid leukaemia (AML) (Matsumura, Mizuki, & Kanakura, 2008). Possibly the most well-known

example is the BCR-ABL, designated Philadelphia chromosome (Ph+), translocation which is the most common mutation seen in adult acute lymphoblastic leukaemia (ALL) and seen in 3-5% of paediatric ALL (Ottmann & Pfeifer, 2009). Reciprocal translocation of ABL (chromosome 9) and BCR (chromosome 22) results in a fusion protein with enhanced ABL-kinase activity. Regardless it imparts a particularly poor prognosis. The advent of targeted tyrosine kinase inhibitors, such as imatinib mesylate, has significantly improved the outcomes of these patients (Leoni & Biondi, 2015). BCR-ABL has been shown to activate the PI3K signalling in CML patients via Nox-4 generated reactive oxygen species (Q. Li et al., 2015; Naughton, Quiney, Turner, & Cotter, 2009).

Deregulation of RTK's are also becoming more significant in paediatric solid tumours (Gröbner et al., 2018) although resistance to RTK inhibitors in paediatric solid tumours is becoming an increasing therapeutic challenge (Aveic & Tonini, 2016). Both sunitinib and the multikinase inhibitor regorafenib have shown pre-clinical activity in NBL cell lines via multiple mechanisms including degradation of N-Myc, induction of apoptosis and via an anti-angiogenic effect (Calero, Morchon, Johnsen, & Serrano, 2014; Zage, Subramonian, Mo, & Huang, 2017).

1.9.4.2. ***RAS activating lesions***

Ras proteins are proto-oncogenes that are frequently mutated in human cancer (Bos, 1989). Analysis of 23 relapsed NBL tumour samples identified that 18 (78%) harboured mutations that would activate the RAS-MAPK pathway (Eleveld et al., 2015). A comprehensive pan-cancer genomic analysis revealed the (RTK)-RAS-RAF-MEK as a key dysregulated pathway in cancer (Imperial, Toor, Hussain, Subramanian, & Masood, 2017).

They are encoded by three ubiquitously expressed genes: HRAS, KRAS and NRAS (Prior, Lewis, & Mattos, 2012) and act as GTPases, although mutant RAS remains resistant to regulation by GTPase activating proteins. KRAS potentially has the

greatest influence with 30% of tumours being associated with KRAS mutations (Fernández-Medarde & Santos, 2011). Mice with mutations in the p110α isoform, that block its ability to interact with RAS, are highly resistant to NRAS and HRAS induced tumourigenesis (Castellano & Downward, 2011) confirming that the interaction with RAS and p110α is essential to tumour formation.

1.9.4.3. ***Abnormal GPCR activity***

GPCR have been implicated in tumourigenesis including paediatric solid tumours (Bar-Shavit et al., 2016). Specifically for NBL, the GPCR gastrin releasing peptide R (GRP-R) has been shown to regulate the metastatic potential of NBL via AKT2 (Qiao et al., 2013). GPCR bind a wide range of ligands to relay extracellular signals through G-protein mediated signalling cascades, and each lymphoma subgroup expresses a unique pattern of GPCR's. Mutation, fusion and copy number alterations occur in B cell malignancies (Nugent & Proia, 2017). Epstein-Barr virus (EBV) encoded GPCR has been implicated in Burkitt's lymphoma (Nijmeijer, Leurs, Smit, & Vischer, 2010) and Human-Herpes virus 8 (HHV-8) encoded GPCR has been implicated in Kaposi's sarcoma (Cannon, Philpott, & Cesarman, 2003). Both EBV and HHV-8 rely on the PI3K/AKT signalling pathway for viral replication (X. Liu & Cohen, 2015).

1.9.5. **Direct activation of PI3K**

As stated earlier many human tumours harbour somatic missense mutations in PIK3CA. Specifically, the PIK3CA genes and PTEN genes are the second and third most commonly mutated genes across 12 cancer types (L. W. T. Cheung & Mills, 2016; The Cancer Genome Atlas Research et al., 2008). This includes the majority of cancers responsible for adult cancer related deaths; breast cancer (Mukohara, 2015), colon cancer, skin cancer, cervical cancer, brain cancers and lung cancers (Samuels & Waldman, 2010). In a diverse cohort of breast cancer patients, PIK3CA mutations were seen in 44% of patients and PIK3R1 mutations were seen in 17% of patients (L. Chen et al., 2018). PIK3R1 and PIK3R2 mutations have been strongly linked to endometrial cancers suggesting the PI3K pathway is important in this tumour (L. W.

T. Cheung et al., 2011). Germline mutations in the PIK3R1 gene have also been linked to immunodeficiencies involving both T and B lymphocytes (Deau et al., 2014).

Cancer associated PIK3CA mutations have been associated with many benign paediatric overgrowth syndromes. These are collectively known as the PIK3CA-related overgrowth spectrum (PROS) (Madsen, Vanhaesebroeck, & Semple, 2018). PIK3CA mutations have also been identified in a number of paediatric CNS tumours, which constitute the most common paediatric solid tumour (Hazel A. Rogers et al., 2017). In fact, there is a similar frequency of PIK3CA mutations in both paediatric and adult glioblastoma multiforme (GBM), an aggressive brain tumour, with identified mutational rates of 21% and 17%, respectively (Gallia et al., 2006). In addition, activation of the PI3K/AKT/mTOR pathway may be essential in metastatic spread of these tumours (Le Rhun et al., 2017). In non-CNS paediatric solid tumours, PIK3CA mutations are less frequent. In a study analyzing four common paediatric solid tumours, including NBL, PIK3CA mutations were seen in 5% of embryonal rhabdomyosarcomas analysed, but not identifed in the NBL samples. These mutations included two within the helical domain of the gene (E542K and E545K) and one in the kinase domain of the gene (H1047R) (Shukla et al., 2012). This is consistent with other literature that has identified a low PI3KCA mutational rate in NBL with PIK3CA mutations were found to be present in only 2.9% of 69 human NBL samples tested (Dam, Morgan, Mazanek, & Hogarty, 2006; Kostopoulou et al., 2019).

1.10. AGC protein kinases

The group of AGC protein kinases includes more than 60 protein kinases in the human genome, classified into 14 families (Arencibia, Pastor-Flores, Bauer, Schulze, & Biondi, 2013). The first PI3K effector discovered was p70 ribosomal S6-kinase (p70S6K); however, serine/threonine protein kinase AKT/PKB is probably the most studied and best understood of the AGC effectors (Toker, 2000). The activity of many AGC protein kinases is regulated allosterically via the PIF-pocket which is a regulatory site within the kinase domain (Najafov, Shpiro, & Alessi, 2012). Alterations of AGC protein kinase

activity has been linked to many human diseases and accordingly drug companies have focused 30% of their drug development programs to this area over the last 15 years (P. Cohen, 2002; Leroux, Schulze, & Biondi, 2018). Specifically to NBL, activation of AKT has been shown to impart a poor prognosis in patients (Opel et al., 2007; Sartelet, Oligny, & Vassal, 2008). Pre-clinical studies confirm that either downregulation of AKT, or the use of small molecule inhibitors significantly impacts on NBL cell survival (Michael L. Megison, Gillory, & Beierle, 2013; Navrátilová et al., 2017).

1.10.1. **AKT**

Stephen Staal first isolated and identified the cloned v-AKT oncogene from the AKT8 transforming retrovirus in 1987 (Staal, 1987). In 1991 protein kinase B (PKB) was identified and named because of its similarities to protein kinase A (PKA) and protein kinase C (PKC) (Coffer & Woodgett, 1991). There are three widely expressed isoforms of PKB/AKT, AKT1 (PKBα), AKT2 (PKBβ) and AKT3 (PKBγ). They are each composed of an N-terminal PIP_3, and PIP_2-binding PH domain and a C-terminal kinase catalytic domain (Lawlor & Alessi, 2001) (Figure 4).

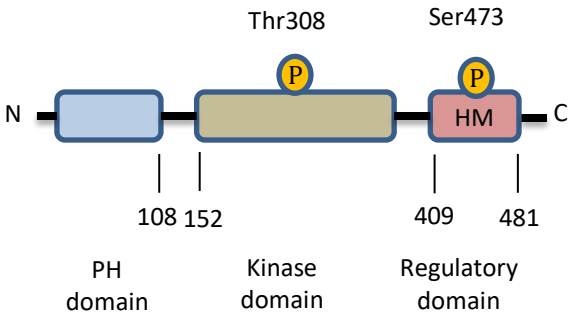

Figure 4 Structure of PKB/AKT

Structure of human PKB/AKT in its phosphorylated state. Phosphorylation of both residues, Thr308 and Ser473, are required for maximal activation. PH; plekstrin homology.

1.10.1.1. ***Activation of AKT***

Stimulation of RTK's or GPCR in the cell membrane leads to PI3K activation and PIP_3 production. Although other mechanisms of PI3K activation have been demonstrated, such as via viral activation, these are traditionally the two main initiators of the pathway (Wei, Zhu, Wang, & Liu, 2012). Inactive AKT engages PIP_3 at the PH binding domain. This results in the serial phosphorylation of two key residues on AKT. Thr308 phosphorylation is mediated by PDK-1 (Calleja et al., 2007) in the catalytic protein kinase core and Ser473 phosphorylation is mediated by mTORC2 (Sarbassov, Guertin, Ali, & Sabatini, 2005), and to a lesser extent during deoxy-ribonucleic acid (DNA) damage, DNA-dependent protein kinase (DNA-PK) (Bozulic & Hemmings, 2009), in the C-terminal hydrophobic motif (Figure 3 & Figure 4). Regulation also occurs on corresponding residues in AKT2 (Thr309 and Ser474) and AKT3 (Thr305 and Ser472) (Manning & Toker, 2017). A third phosphorylation site of AKT1 has been identified at Thr450 which is also phosphorylated by mTORC2 but its significance in AKT signalling is yet to be fully determined (Hart & Vogt, 2011). There are numerous other phosphorylation sites on AKT that have been identified and which may be linked to AKT function. Ser129 is phosphorylated by CK2 to increase catalytic activity. Ser477 and Thr479 can be phosphorylated by the cyclin A-CDk2 complex to enhance AKT activity. GSK-3α-mediated phosphorylation of Thr312 may stimulate AKT activity (Manning & Toker, 2017). To date, the physiological significance of many of these phosphorylation sites remains unknown.

1.10.1.2. ***Negative regulators of AKT activity***

AKT can be negatively regulated by a number of factors. FANCI has been shown to be a negative regulator of AKT. Depletion of FANCI induces spontaneous phosphorylation of AKT, and a substantial reduction in apoptosis following radiation, in MCF10A cells (X. Zhang, Lu, Akhter, Georgescu, & Legerski, 2016). Breast cancer susceptibility gene 1 (BRCA1) has also been shown to negatively regulate AKT via ubiquitin degradation (Xiang et al., 2008). PH domain leucine-rich repeat protein phosphatase (PHLPP) has been shown to dephosphorylate AKT at Ser473 and

promote apoptosis and suppress tumour growth (Gao, Furnari, & Newton, 2005). PTEN has also been shown to negatively regulate AKT via dephosphorylation on PIP_3 (Figure 3).

1.10.1.3. *Downstream targets of AKT*

The downstream targets of AKT are many and have varied functions on cellular processes including control of growth, proliferation and survival (**Figure 5**)

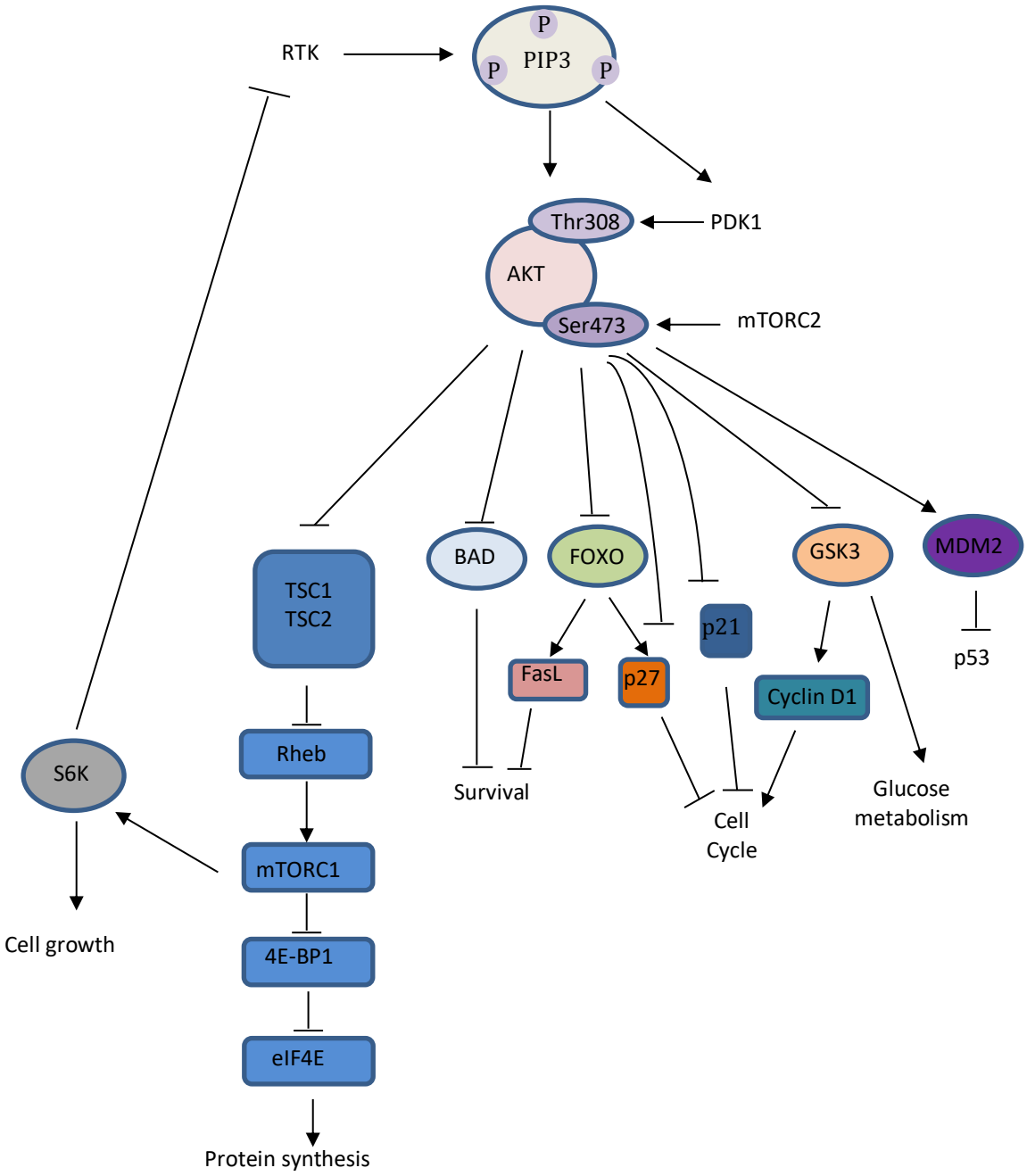

Figure 5 Downstream targets of AKT

AKT regulates many cellular processes including cell growth, protein synthesis, cell survival, cell cycle progression, glucose metabolism and cell death. Downstream targets include the TSC complex, BAD, FOXO's, GSK3 and MDM2. Cell cycle targets include GSK3β, and the CDK inhibitors ($p21^{Kip1}$ and $p27^{Cip1}$). Protein synthesis is regulated by the TS complex, which negatively regulates RTK's via S6K. Phosphorylation of MDM2 negatively regulates p53. AKT negatively regulates BAD, a pro-apoptotic member of the Bcl-2 family of proteins. GSK3β impacts on both cell cycle, via Cyclin D1, and glucose metabolism. FOXO's impact on both cell survival and cell cycle progression (1.10.1.4).

1.10.1.4. *The Forkhead Box transcription factors (FOXOs)*

The Forkhead Box (FOXO) transcriptional factors influence cell cycle functions including IGF1 signalling, regulation of insulin, metabolism, proliferation and growth (Manning & Toker, 2017). There are currently four recognised FOXO transcription factors comprised of FOXO 1, 3, 4 and 6 in mammals (Benayoun, Caburet, & Veitia, 2011). Essentially phosphorylation by AKT inactivates FOXO's by nuclear exclusion resulting in their accumulation within the cytoplasm. This in turn results in a reduced transactivation of target genes such as CDKN1B (negative cell-cycle regulators), CDKN1A, p130(RB2), cyclin D, Bim, TRAIL, Fas Ligand (FasL) and BAD/Bcl-X_L which are required for cellular functions including cell proliferation, apoptosis and differentiation (Hui et al., 2008). Associated P27/Kip1 mutations have been frequently identified in paediatric cancers including T-cell leukaemia and acute myeloid leukaemia (Markaki et al., 2006). Specifically to NBL, expression of p27/Kip1 has been shown to be prognostically significant independent of N-Myc (Bergmann et al., 2001).

GSKBβ regulates cyclin D1 expression and CDK4 & CDK6 are cyclin D1 binding partners with activated cyclin D1/CDK4 and cyclin D1/CDK6 required for progression from G_1 to S phase (Takahashi-Yanaga & Sasaguri, 2008). In glioblastoma, inactivation of PI3K/AKT signalling was accompanied by a G2/M phase arrest associated with down-regulation of CDKi and Cdc25C proteins (Yanchun Li et al., 2012). FOXO's also upregulate the pro-apoptotic BH3 only proteins including Bim and BNIP3, triggering cell death (Gilley, Coffer, & Ham, 2003).

1.10.1.5. *GSK3β*

Glycogen synthase kinase 3-beta (GSK3β) was one of the first substrates of AKT identified (Hermida, Dinesh Kumar, & Leslie, 2017). As suggested by its nomenclature GSK3β was initially shown to be involved in glucose metabolism, in particular that it negatively regulated glycogen synthesis (Embi, Rylatt, & Cohen, 1980; Maurer, Preiss, Brauns-Schubert, Schlicher, & Charvet, 2014). Insulin

signalling results in activation of AKT and subsequent inactivation of both isoforms GSK3α and GSK3β.

GSK3β has been shown to be a key regulator in the WNT/β-catenin pathway which has been implicated in paediatric tumours including neuroblastoma and medulloblastoma (Ellison et al., 2011; Northcott et al., 2012). GSK3 inhibitors have been shown to reduce NBL cell viability by regulating *MYCN* mRNA levels. RNA-seq analysis confirmed that activation of canonical WNT signalling contributed to NBL cell death in a p53 independent manner (Duffy, Krstic, Schwarzl, Higgins, & Kolch, 2014).

The first study suggesting GSK3β was involved in apoptosis found that the pro-apoptotic BCL-2 protein BAX required direct phosphorylation by GSK3β for its function (Linseman et al., 2004). In addition GSK3β phosphorylation of MCL-1, which antagonises pro-apoptotic BH3 only proteins including BAX, results in its degradation (R. Wang, Xia, Gabrilove, Waxman, & Jing, 2013). GSK3β has also been shown to regulate Cyclin D1 expression, which is required for progression from G_1 to S phase, by regulating mRNA protein transcription and degradation (Takahashi-Yanaga & Sasaguri, 2008).

1.10.1.6. ***p53/MDM2/ARF***

P53 mutations have been established as both germline and somatic drivers of human cancers. Around 50% of cancers contain a somatic p53 mutation, while 17% of human cancers harbor MDM2 gene amplifications (Nag, Qin, Srivenugopal, Wang, & Zhang, 2013). Most NBL tumours at diagnosis are p53 wildtype; however, at relapse a high frequency of NBL have mutations in the p53/MDM2/ $p14^{ARF}$ pathway. AKT negatively regulates p53, by enhancing murine double minute 2 (MDM2), which targets p53 for degradation (Abraham & O'Neill, 2014; Gottlieb, Leal, Seger, Taya, & Oren, 2002). In turn ARF promotes MDM2 degradation, thereby stabilizing p53 (Y.

Zhang, Xiong, & Yarbrough, 1998). Finally when AKT phosphorylates MDM2 it mediates p53s ubiquitination and subsequent degradation (Ogawara et al., 2002).

1.10.1.7. ***AKT and apoptosis***

Apoptosis occurs via two main pathways. There is the intrinsic pathway which is mediated by mitochondria and which results in serial activation of caspases 9 and 3. Alternatively, there is the extrinsic pathway that relies on the activation of Fas and TNRFs via activation of caspase 8 (Fulda & Debatin, 2006; Kiechle & Zhang, 2002). The role of the BCL-2 family of proteins in apoptosis has been well established (Czabotar, Lessene, Strasser, & Adams, 2013). The BH3-only group consists of pro-apoptotic proteins including BMF, BAD, BIK, Bim, EGI-1, NOXA, BID, BNIP3, PUMA and Beclin-1. AKT regulates apoptosis via inhibition of FOXOs which normally transactivate pro-apoptotic Bim and BNIP3 (Gilley et al., 2003). FOXO3a transcriptionally upregulates PUMA and FOXO4 suppresses the expression of the BCL-2 family member Bcl-XL (pro-survival). FOXOs also promote the extrinsic apoptotic pathway by upregulating the transcription of proapoptotic factors such as TRAIL and FasL (X. Zhang, Tang, Hadden, & Rishi, 2011). AKT can directly phosphorylate BAD, blocking BAD induced apoptosis in a site-specific manner (Datta et al., 1997). There is also emerging evidence to suggest that AKT directly phosphorylates caspase 9 at Ser196 to inhibit its activity (P. Li et al., 2017). Apoptosis signal-regulating kinase 1 (ASK-1) is a mediator of MAPK and involved in stress induced apoptosis. Phosphorylation of ASK-1 at Ser83 reduces ASK-1 activity and its regulation of apoptosis (A. H. Kim, Khursigara, Sun, Franke, & Chao, 2001) (Figure 6).

1.10.1.8. ***NFκB signalling***

NFκB is a family of five transcriptional factors that include p50, p52, p65 (Rel-A), RelB and c-Rel and are key positive cell regulators by their impact on both pro-survival and anti-apoptotic genes such as XIAP, Bcl-2 and Bcl-X1 (Hussain et al., 2012). Studies in B lymphomas have confirmed significant cross talk between NFκB signalling, STAT3 and the PI3K/AKT/mTOR pathway (Han et al., 2010).

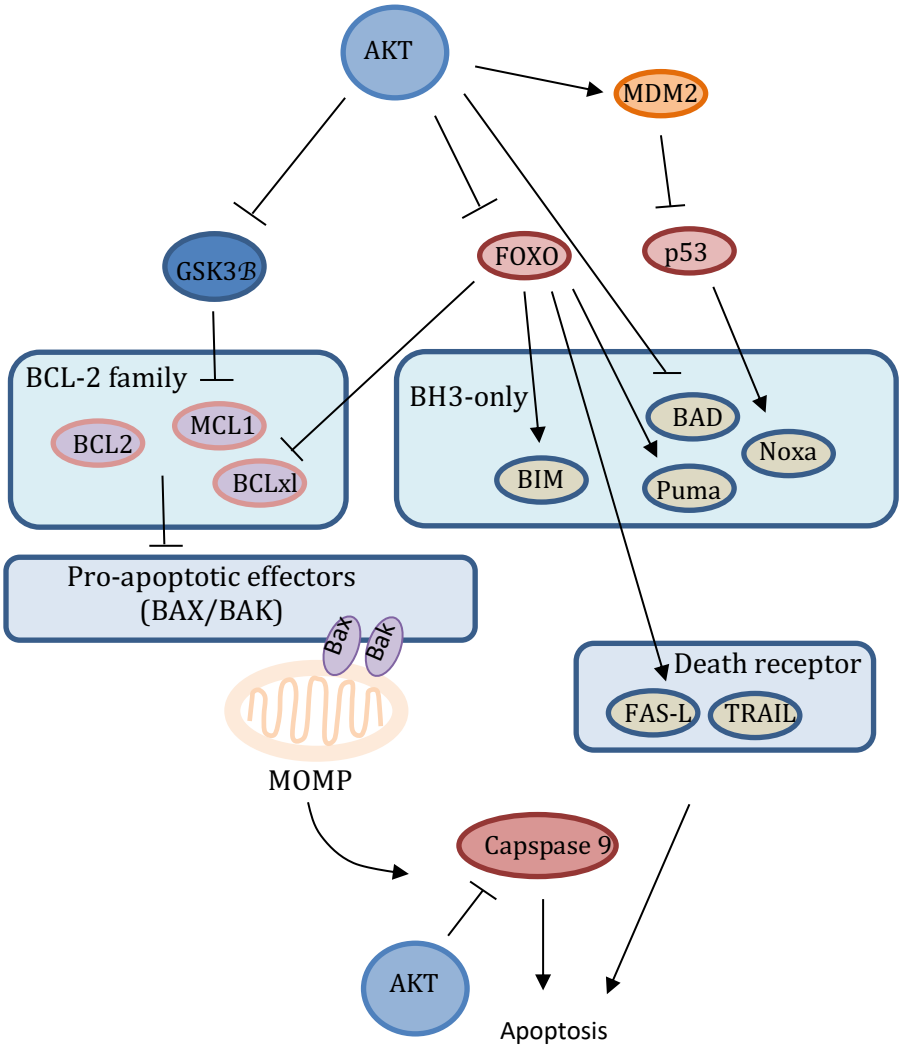

Figure 6 AKT and apoptosis

AKT regulates apoptosis through both the BCL-2 (pro-survival) and the BH3-only (pro-apoptotic) family of downstream apoptotic effectors. It directly inhibits the death receptors FAS-L and TRAIL and can negatively regulate caspase-9. Phosphorylation of GSK-3β stabilises anti-apoptotic MCL-1 levels. Phosphorylated FOXO's are likewise sequestered to reduce Bim and FAS-L levels. AKT stabilises p53 via phosphorylation of MDM2. Downstream of MOMP, phosphorylation by AKT reduces the susceptibility of caspase-9 to cleavage. MOMP; Mitochondrial outer membrane complex.

1.10.1.9. *AKT in neuroblastoma*

Activation of AKT has been shown to impart a poor prognosis in NBL patients. When the phosphorylation status of AKT was examined in 116 primary human NBL samples, not only was AKT shown to be upregulated frequently but that upregulated phosphorylation was associated with survival outcomes, imparting a poor prognosis (Opel et al., 2007). As summarised previously (Figure 5) AKT has numerous downstream impacts on cellular processes so it is reasonable to expect that over-expression of AKT in NBL will contribute to tumour formation and treatment resistance (Sartelet et al., 2008). Retinoic acid, used in the maintenance phase of NBL therapy to promote differentiation, is also reliant on AKT signalling, demonstrated by the fact that inhibition of PI3K by LY294002 impairs the retinoic acid induced differentiation (Lopez-Carballo, Moreno, Masia, Perez, & Barettino, 2002).

1.10.1.10. *Non-AKT regulators of the PI3K pathway*

PDK1, which is responsible for the phosphorylation of Thr308 (Figure 3) can be regulated by MAPK or PKCα (Faes & Dormond, 2015). It has also been shown that PDK1 contributes to the regulation of proliferation and survival in cancers where PI3K and MAPK are constitutionally activated (Z. Lu, Boyapati, Kirschmeier, & Windsor, 2008). SGK3 has been identified as an important downstream regulator of this process. SGK 1, 2 and 3 are PI3K dependent serine/threonine kinases that are structurally related, and with similar substrate specificity, to AKT. Consequently they mimic the functions of AKT (Bruhn, Pearson, Hannan, & Sheppard, 2013). mTORC2 has been shown to regulate PI3K in glioblastoma cell lines in an NFκB dependent but AKT independent manner (Tanaka et al., 2011) . The role of RAC proteins in tumourigenesis is complicated but appears to be through PI3K mediated MAPK activation (Ebi et al., 2013).

1.11. The mammalian target of rapamycin

Rapamycin (AY,22,989) was first isolated from Streptomyces hygroscopicus in 1975, from soil samples collected from the South Pacific island Rapa Nui, and initially classed as an anti-fungal (Vezina, Kudelski, & Sehgal, 1975). Coincidently rapamycin was noted to have a structure similar to tacrolimus (FK-506), a potent immunosuppressant (Sabatini, 2017). Subsequently, rapamycin went on to be used as an immunosuppressive therapy in organ transplantation, due to its ability to inhibit antigen induced T and B cell proliferation and antibody formation (Seto, 2012). The protein target of rapamycin was isolated in 1995 and named the mTOR (Sabers et al., 1995).

mTORC1 is defined by its three core components: mTOR, Raptor (regulatory protein associated with mTOR) and mLST8 (mammalian lethal with Sec13 protein 8). Like mTORC1, mTORC2 also contains mTOR and mLST8. However, instead of Raptor it contains Rictor (rapamycin insensitive companion of mTOR). As the name suggests Rictor renders mTORC2 insensitive to the effects of the rapamycin-FKBP12 complex which strongly inhibits mTORC1 (Saxton & Sabatini, 2017) (Figure 7).

In order to grow and divide a cell must be able to co-ordinate the doubling of cell contents and DNA material in concert with the cell cycle. At the same time, it must suppress competing catabolic pathways thereby balancing the impacts of cellular anabolism and catabolism in response to environmental stimuli. mTORC1 is primarily responsible for this regulation of cell growth (Saxton & Sabatini, 2017) (1.9.5). mTORC2, on the other hand, is responsible for phosphorylating the family of AGC protein kinases (1.10) the most important of which is the phosphorylation and activation of AKT (1.10.1).

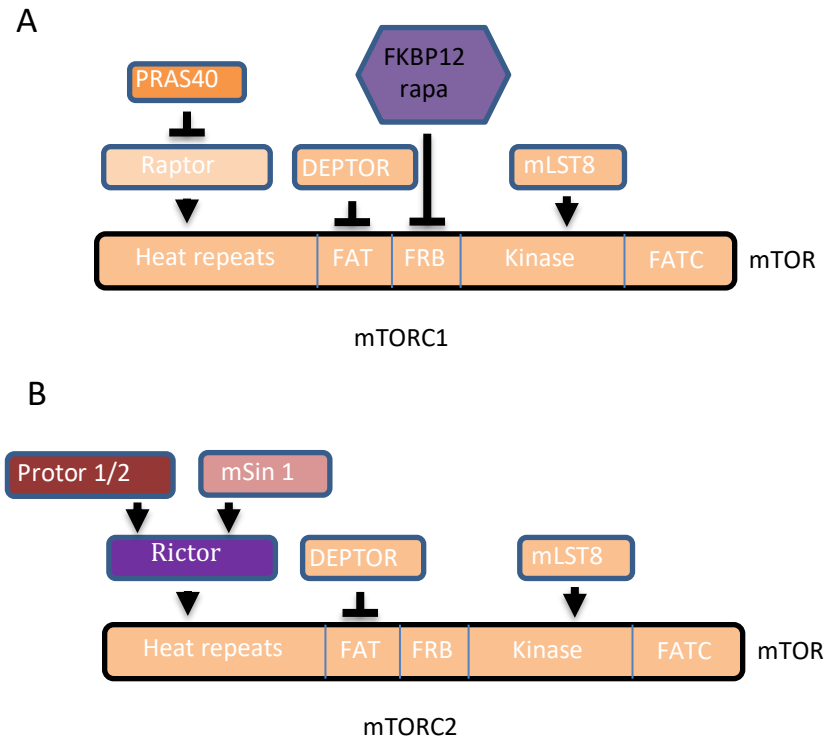

Figure 7 Established components of (A) mTORC1 and (B) mTORC2

Rictor renders mTORC2 insensitive to the effects of the rapamycin-FKBP12 complex which strongly inhibits mTORC1 (Sabatini, 2017).

1.11.1. Regulation of 5 'cap-dependent translation

In preparation for cell growth and in response to extracellular stimuli, mTORC1 regulates protein synthesis, ribosomal biogenesis and lipid synthesis via the eukaryotic initiation factor eIF4F complex. The eIF4F subunit eIF4E interacts directly with the mRNA 5' cap structure to recruit 40S ribosomal subunits. mTORC1, via its phosphorylation and inactivation of 4E-BP (or 4E-BP1), correspondingly activates eIF4E. In its de-phosphorylated state 4E-BP1 competes with eIF4G to bind eIF4E. The functionality of the eIF4F complex relies on the association between eIF4E and eIF4G. However, the binding of 4E-BP1 to eIF4E displaces eIF4E from eIF4G and thus inhibits 5' cap-dependent translation. mTORC1 controls whether or not 4E-BP1 binds

eIF4E by controlling 4E-BP1 phosphorylation (Buchkovich, Yu, Zampieri, & Alwine, 2008) (Figure 8).

4E-BP1 phosphorylation is a multi-step process and to date seven phosphorylation sites have been identified; Thr37, Thr46, Ser65, Thr70, Ser83, Ser101, and Ser112 (Qin, Jiang, & Zhang, 2016). The initial step involves phosphorylation of Thr37 and Thr46 which then primes 4E-BP1 for subsequent phosphorylations (Gingras et al., 1999) at Thr70 and finally Ser65 (Qin et al., 2016).

Traditionally mTORC1 has been considered responsible for phosphorylation of all four sites; however, recent evidence suggests that other kinases may be involved (Sikalidis, M Mazor, Kang, Liu, & Stipanuk, 2013). For example, GS3Kβ has been shown to phosphorylate 4E-BP1 at Thr37 and Thr46 (Ito et al., 2016). UVB damage can induce phosphorylation of 4E-BP1 at multiple sites mediated by p38MAPK and MSK1 (Hara et al., 1997). ERK has also been shown to phosphorylate 4E-BP1 at Ser65 (Rolli-Derkinderen et al., 2003).

4E-BP1 acts as a cross talk point between the PI3K/AKT and ERK signalling pathways as evidenced by the fact that mutations in both pathways occurs in several human tumours. Inhibition of either pathway alone does not result in a significant anti-tumour effect, whereas inhibition of both pathways induces a significant anti-tumour effect. In such tumours, knockdown of 4E-BP1 reduced their dependence on both pathways (She et al., 2010).

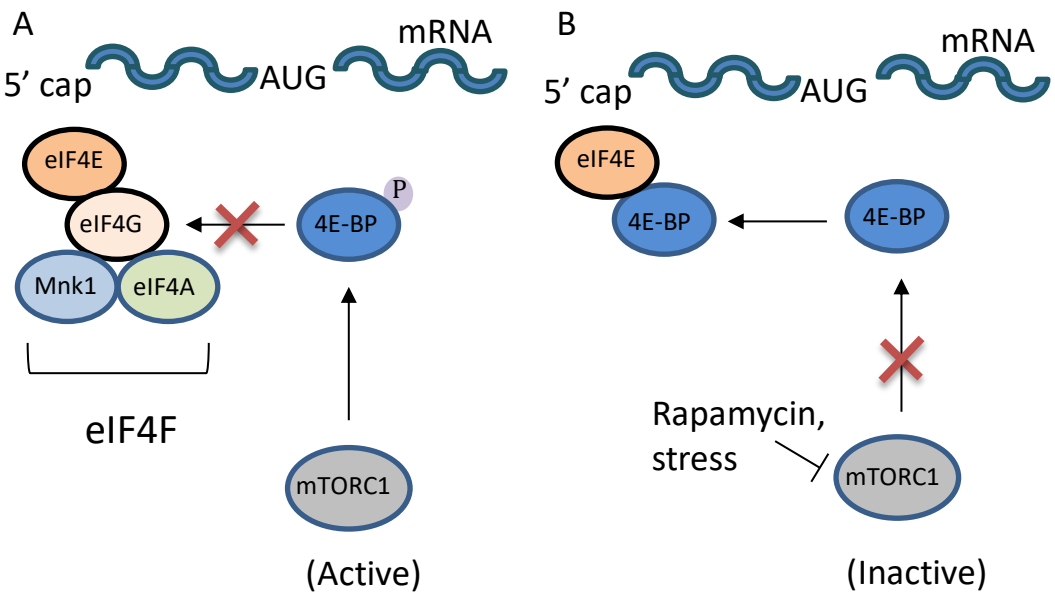

Figure 8 mTORC1 activity control 5' cap-dependent translation

Under positive growth conditions (A), mTORC1 phosphorylates 4E-BP, which is therefore unable to bind to eIF4E. eIF4E is then free to bind to eIF4G, which completes the eIF4F complex on the 5′ cap and permits translation to proceed. Under negative growth conditions (B), mTORC1 is inactive; 4E-BP therefore becomes hypo-phosphorylated and binds efficiently to eIF4E, thereby removing it from the eIF4F complex and inhibiting 5' cap-dependent translation.

1.11.2. Regulation of ribosomal biogenesis

One of the major downstream targets of mTORC1 is ribosomal biogenesis which is primarily mediated by SK6. SK6 is activated by serial phosphorylation; mTORC1 initially phosphorylates Thr389, which allows PDK1 to phosphorylate Thr229 (Gentilella, Kozma, & Thomas, 2015). Interestingly, tissues that lack SK6 has been shown to have a defect in ribosomal biogenesis (Chauvin et al., 2014). The first identified target of SK6 was ribosomal protein 6 (rpS6) which is a component of the 40S ribosomal subunit (Magnuson, Ekim, & Fingar, 2012). Ribosomes with the

highest proportion of phosphorylated rpS6 have an advantage in mobilisation into polysomes (Ruvinsky et al., 2005) and therefore transcription.

The coordinated actions of the RNA polymerases are essential to ribosomal biogenesis. These are designated RNA Pol I, II and III. Of the three, RNA Pol I mediated transcription is thought to be the rate limiting step of ribosomal biogenesis. RNA Pol I transcribes 47S pre-rRNA in the nucleolus which is then cleaved into 18S, 5.8S and 28S rRNAs. RNA Pol II transcribes ribosomal protein encoding genes in the nucleoplasm. RNA Pol III is responsible for the nucleoplasmic transcription of 5S rRNA and the tRNAs. The proteins of the ribosomal subunits are then transported into the nucleolus to be assembled with their respective ribosomal subunit (Chaillou, Kirby, & McCarthy, 2014). There is also cooperation between the RNA polymerases and the PI3k/AKT/mTOR pathway as evidenced by the fact that combination therapy targeting POL I and mTORC1 synergistically extends survival in MYC driven lymphoma (Devlin et al., 2016).

1.11.3. **mTORC2**

The structure of mTORC2 has been previously discussed (1.11.3) (Figure 7). Although thought to be insensitive to the effects of the rapamycin-FKBP12 complex (Saxton & Sabatini, 2017), prolonged exposure to rapamycin can indirectly inhibit its activity (Sarbassov et al., 2006). It appears that PDK1 phosphorylates AKT at Thr308, increasing AKT kinase activity. Subsequently AKT phosphorylates SIN1 at Thr86 which results in phosphorylation of AKT Ser473 by mTORC2 (G. Yang, Murashige, Humphrey, & James, 2015). Rictor has also been shown to be phosphorylated by SK6 at Thr1135 and by GSK3β at Se1235 (Oh & Jacinto, 2011). mTORC2 has also recently been implicated in signalling through insulin/IGF-1 receptors and has the ability to phosphorylate proteins on tyrosine residues (Xuemin Wang & Proud, 2015).

1.11.3.1. ***mTORC2 outputs***

mTORC2 functions in a number of cellular processes by mediating the phosphorylation of conserved motifs in AGC kinases to promote their maturation, stability and allosteric activation. mTORC2 phosphorylates AKT at Thr450 and Ser 473. Catalytic activation of these AGC kinases requires phosphorylation of the activation loop by PDK1. In the absence of Ser473 phosphorylation, AKT can still phosphorylate some of its substrates, such as TSC2 and GSK3. AGC kinases phosphorylate a multitude of substrates that mediate numerous cellular functions. These functions of mTORC2 promote cell growth. Whether mTORC2 can play a role in cellular and organismal aging via regulation of AGC kinases or other substrates remains to be elucidated (Oh & Jacinto, 2011).

1.11.3.2. ***mTOR in neuroblastoma***

Given the role that mTOR plays in cell growth and proliferation it is not surprising that it has been implicated in the progression of many cancers including NBL (Mei, Wang, Lin, & Tong, 2013). What is of particular interest in NBL is the role mTOR plays in stabilising N-Myc via GSK3β making it a potential therapeutic target. In fact, GSK3β inhibitors have been shown to be effective in pre-clinical models of NBL (Kunnimalaiyaan, Schwartz, Jackson, Clark Gamblin, & Kunnimalaiyaan, 2018). GSK3β phosphorylates Myc at Thr58 and enhances its ubiquitination (Gregory, Qi, & Hann, 2003). Several E3 ubiquitin ligases for MYC proteins have been described. The best known is SCF^{Fbw7}. Regulation of MYC by SCF^{Fbw7} is in a phosphorylation dependent manner. Phosphorylation of MYC at Ser62 stabilises the protein. Subsequent phosphorylation by GSK3β at Thr58 allows to the de-phosphorylation of the stabilising Ser62 and SCF^{Fbw7} mediated degradation via the 26S proteasome (Farrell & Sears, 2014). GSK3β is regulated by activated AKT which in turn requires mTORC2 for phosphorylation of Ser473 (Figure 5)

Indeed, inhibition of PI3K upstream of mTOR has been shown to reduce N-Myc protein levels without affecting mRNA (L. Chesler et al., 2006). NBL cell lines

expressing higher levels of N-Myc have also been shown to be more sensitive to mTOR inhibition with resultant reduction in N-Myc protein levels (Johnsen et al., 2008). It appears that complete block of mTOR kinase activity is more important than blocking PI3K activity in N-Myc protein degradation (Vaughan et al., 2016).

1.12. Targeting the PI3K/AKT/mTOR pathway

All aspects of the PI3K/AKT/mTOR pathway can potentially be therapeutically targeted. To date, despite the fact that over 40 compounds targeting this pathway have been used in human clinical trials, only the mTOR inhibitors temsirolimus and everolimus and the PI3K inhibitors idelalisib and copanlisib have been approved by the FDA for clinical use in adult cancers. This has been primarily due to both the limited anti-tumour activity and the associated drug toxicities (D. A. Fruman et al., 2017; Janku, Yap, & Meric-Bernstam, 2018).

1.12.1. Inhibitors upstream of the PI3K/AKT/mTOR pathway

1.12.1.1. *Monoclonal antibodies*

Monoclonal antibodies (Mab) that target upstream regulators of the PI3K/AKT/mTOR pathway, such as cell surface GRP78, a major endoplasmic reticulum chaperone protein, are an attractive target. Accordingly, Mab159, an anti GRP78 Mab, has been shown to have pre-clinical anti-tumour activity with associated inhibition of the PI3K/AKT/mTOR pathway and compensatory up-regulation of the MAPK pathway (R. Liu et al., 2013). In ovarian cancer, combined use of an EGFR inhibitors with PI3K inhibitors had synergistic activity compared to each therapy when used in isolation (Glaysher et al., 2013).

1.12.1.2. *Tyrosine kinase inhibitors*

The role of tyrosine kinase inhibitors (TKi) in paediatric cancer has been most extensively investigated in haematological malignancies such as AML and ALL. Although PI3K/AKT/mTOR inhibitors have been shown to act independently of TKi's

in leukaemia cell lines (Badura et al., 2013), TKi's and PI3K inhibitors have been shown to act synergistically in BCR/ABL mutated cell lines (Ciarcia et al., 2013). In some tumours, the PI3K/AKT/mTOR pathway has been linked to the resistance that develops to TKi's such as Imatinib (J. Li et al., 2015; Quentmeier, Eberth, Romani, Zaborski, & Drexler, 2011). Inhibition of IGF-1R, using small molecule inhibitors such as NVP-AEW541 has been shown to inhibit cell growth in NBL cell lines and xenograft models via inhibition of PI3K/AKT/mTOR signalling (King, Yeomanson, & Bryant, 2015). ALK is another RTK that affects PI3K/AKT/mTOR signalling and has been shown to be a significant mutation in a subset of neuroblastoma patients (Schulte et al., 2013) making it a potential upstream target of PI3K/AKT/mTOR. Combination therapy with the ALK inhibitor crizotinib and a combined PI3K/mTOR inhibitor was more effective than crizotinib alone, or crizotinib with an mTOR inhibitor, in ALK-mutated neuroblastoma (N. F. Moore et al., 2014).

1.12.1.3. ***Tumour microenvironment***

Inhibition of the PI3K/AKT/mTOR pathway has been shown to inhibit tumour angiogenesis (J. Kang et al., 2008). It therefore makes sense that other agents that control tumour microenvironment may also interact with the PI3K/AKT/mTOR pathway. MicroRNA's have been shown to promote angiogenesis in ovarian cancer via the PI3K/AKT/mTOR and MAPK/Erk pathways (W. Wang et al., 2014). In breast cancer miR-564 acts as a potent dual inhibitor of the PI3K/AKT/mTOR and MAPK pathways inhibiting breast cancer proliferation and invasion (Mutlu et al., 2016). Therefore miR-564 agonists would be an attractive therapeutic approach in such diseases. Thalidomide, currently being investigated as an anti-angiogenic therapy in CNS tumours, acts via inhibition of endothelial Slit2/Robo1 signalling to block the PI3K/AKT/mTOR pathway (Y. Li et al., 2014).

1.12.2. Agents directly targeting the PI3K/AKT/mTOR pathway

Given the central role of the PI3K/AKT/mTOR pathway plays in many cellular processes, and its frequent dysregulation in cancer (The Cancer Genome Atlas Research et al., 2008) it is not surprising that much research has been conducted in targeting this pathway. A recent meta-analysis of 46 randomised controlled trials (RCT) in humans showed that the addition of PI3K/AKT/mTOR inhibitors to the treatment of solid tumours significantly improved progression free survival (PFS) (X. Li et al., 2018). These include ATP-competitive, dual inhibitors of class I PI3K and mTOR, "pan" PI3K inhibitors that target all four isoforms of class I PI3K (α,β,δ and γ) or isoform specific PI3K inhibitors, and ATP-competitive inhibitors of mTOR only (Dienstmann, Rodon, Serra, & Tabernero, 2014). The current status of inhibitors is summarized (Table 2). Although over 40 compounds have been identified and tested this thesis focus on the combined PI3K/mTOR inhibitor PF-04691502 (PF-502) and the mTOR inhibitor temsirolimus (CCI-779).

Agent	Company	Selectivity	Clinical status
Dactolisib (BEZ235)	Novartis	PI3K/mTOR	Phase I/II
Apitolisib (GDC-0980)	Genentech	PI3K/mTOR	Phase II
Gedatolisib (PF-05212384)	Pfizer	PI3K/mTOR	Phase I/II
Buparlisib (BKM120)	Novartis	Pan-PI3K	Phase II /III
Pictilisib (GDC-0941)	Genentech	Pan-PI3K	Phase II
Bimiralasib PQR309	PIQUR	Pan-PI3K	Phase II

Copanlisib (BAY80-6946)	Bayer	PI3K-p110α, δ > β, γ	Phase III / IV
Taselisib (GDC-0032)	Genentech	PI3K-p110α, δ ,γ > β	Phase III
Alpelisib (BYL719)	Novartis	PI3K-p110α	FDA approved to treat hormone receptor-positive, HER2-negative, PIK3CA-mutated breast cancer
Serabelisib (TAK-117, MLN1117)	Takeda	PI3K-p110α,	Phase II
GDC-0077	Genentech	PI3K-p110α,	Phase I
Idelalisib (CAL-101)	Gilead	PI3K-p110δ	FDA approved for CLL, NHL and small lymphocytic leukaemia
Duvelisib (IPI-145)	Infinity	PI3K-p110δ, γ	Phase II/III
IPI549	Infinity	PI3K-p110γ	Phase I
Capivasertib (AZD5363)	Astra Zeneca	AKT1/2/3	Phase II
Ipatasertib (GDC-0068)	Genentech	AKT1/2/3	Phase II
Sirolimus (Rapamycin)	Pfizer	mTORC1	FDA approved for lymphangioleiomyomatosis
Temsirolimus (CCI-779)	Pfizer	mTORC1	FDA approved for renal cell carcinoma (RCC)
Everolimus (RAD001)	Novartis	mTORC1	FDA approved for HR+/HER2- breast cancer,

			RCC and pancreatic neuroendocrine tumours
Vistusertib (AZD2014)	Astra Zeneca	mTORC1/2	Phase I
TAK-228 (INK128, MLN0128)	Takeda	mTORC1/2	Phase I/II
CC-223	CelGene	mTORC1/2	Phase I/II

Table 2 Targeted inhibitors of the PI3K/AKT/mTOR pathway

List of approved and investigational agents targeting kinases in the PI3K/AKT/mTOR pathway (D. A. Fruman et al., 2017).

1.12.2.1. *ATP-competitive combined PI3K/mTOR or mTOR only inhibitors*

Because both PI3K and mTOR belong to the family of PI3K-related kinases (PIKK) they share many structural domains that can be dual targeted by certain compounds. In theory this combined inhibition should abolish the AKT activation, via the mTORC1/S6K negative feedback which has been observed when inhibiting mTOR in isolation (Rozengurt, Soares, & Sinnet-Smith, 2014) and can lead to drug resistance.

The two most studied pan-PI3K inhibitors, buparlisib (BKM-120, NVP-BKM120) and pictilisib (GDC-0941) are both in early phase II/III clinical trials. Because both pan-PI3K inhibitors and PI3K/mTOR inhibitors act upstream of AKT they should have a more pronounced pro-apoptotic effect than mTOR inhibitors alone (Dienstmann et al., 2014). Buparlisib has been trialled in a number of human tumours with mixed results. Pre-clinical studies using Buparlisib in glioblastoma multiforme (GBM) have shown promising results (Netland et al., 2016) and accordingly early phase studies in this indication have been approved (NCT01339052). However, buparlisib was shown to be ineffective with unacceptable toxicity in patients with recurrent endometrial

carcinoma (Heudel et al., 2017). Pictilisib is currently in early phase clinical trials for patients with advanced solid tumours with 22% of patients demonstrating an evaluable response to the drug (Sarker et al., 2015).

Dual PI3K/mTOR inhibitors in development include dactolisib (BEZ-235, NVP-BEZ235), voxtalisib (SAR245409, XL765) and gedatolisib (PF-502). Despite the promising pre-clinical activity of dactolisib (Shortt et al., 2013), early phase studies in adult patients with renal cell carcinoma (RCC) and transitional cell carcinoma (TCC) have shown unacceptably high rates of toxicity with little clinical activity (Carlo et al., 2016; Seront et al., 2016). Gedatolisib (PF-502) has also shown promising pre-clinical activity (J. Yuan et al., 2011) with little anti-tumour activity seen in early phase studies (Britten et al., 2014). Of the isoform selective inhibitors, the p110δ inhibitor idelalisib (GS-1101, CAL-101) is perhaps the most studied and is in Phase III trials for non-Hodgkin lymphoma (NHL) (NCT01306643) and chronic lymphocytic leukaemia (CLL) (NCT01659021).

ATP-competitive mTORC inhibitors have an advantage in that they inhibit both mTORC1 and mTORC2 (Schenone, Brullo, Musumeci, Radi, & Botta, 2011). Additionally, their ability to antagonise 4EBP-1 phosphorylation at rapamycin resistant sites, is an advantage over allosteric inhibitors. However, this inhibition may be incomplete and contribute to drug resistance (Ducker et al., 2013). Several of these inhibitors have shown pre-clinical promise and are now being evaluated in humans. AZD8055 is currently registered for early phase studies in recurrent gliomas (NCT01316809). OSI-027 has been trialled in patients with advanced solid tumours with very little in the way of tumour response and only 5% of patients registering stable disease (Mateo et al., 2016). Sapanisertib (INK128) has been shown to not only have anti-tumour effects in pre-clinical NBL models alone, but can also synergistically enhance the effectiveness of traditional agents such as anthracyclines (Huiyuan Zhang et al., 2015).

1.12.2.2. ***AKT inhibitors***

AKT inhibitors are classed as either ATP-competitive inhibitors or allosteric inhibitors. AKT competitive inhibitors are non-selective against AKT isoenzymes and have many "off-target" effects due to their similarity with other kinases. Efforts to identify AKT specific inhibitors have resulted in the allosteric inhibitors (Nitulescu et al., 2016) which in theory should be more specific and have a lower toxicity profile. Despite the large number of compounds identified, to date only miltefosine, an alkylphosphoslipid allosteric inhibitor, has FDA approval for cutaneous leishmaniasis, a non-cancer indication. Many other AKT inhibitors are currently in early phase clinical studies. Perhaps their ultimate contribution to cancer therapy will be in combination with other agents (Brown & Banerji, 2017). MK-2206, a 2,3-Diphenylquinoxaline analogue, has been shown in pre-clinical studies to enhance the chemotherapeutic effect of conventional agents such as 5-Fluorouricil and doxorubicin (P. Jin et al., 2016). MK-2206 is currently in early phase trials for adult solid tumours in combination with lapatinib (Wisinski et al., 2016), and bendamustine in leukaemias (Larsen et al., 2017).

1.12.2.3. ***Rapamycin analogues: the allosteric mTOR inhibitors***

Rapamycin, a potent and specific mTORC1 inhibitor, has been an invaluable tool in the dissection of the mTOR pathway. Because of this, the upstream and direct modulation of mTORC1 is better understood than mTORC2 (Zhou, Luo, & Huang, 2010). Rapamycin was initially discovered as an anti-fungal agent and then was subsequently found to have immunosuppressive properties (Yatscoff, LeGatt, & Kneteman, 1993). Despite extensive research the exact mechanism that rapamycin inhibits mTORC1 remains uncertain. It is thought that the rapamycin-FKBP12 complex binds to the C terminus of TOR proteins and interferes with the interaction of mTOR and raptor (Oshiro et al., 2004), exerting its inhibitory effects.

Rapamycin has been shown to be efficacious in TS, and inherited genetic conditions of the TS complex (Franz & Capal, 2017). The most promising role for rapamycin as

an anti-cancer therapy has been seen in advanced renal cell carcinoma (RCC) (Voss, Molina, & Motzer, 2011). Recent evidence suggests a role in the treatment of a variety of haematological conditions including lymphomas (Y. Liu et al., 2017). The mTORC1 inhibitor everolimus has been FDA approved for RCC (Buti, Leonetti, Dallatomasina, & Bersanelli, 2016), SEGA (and other TSC associated tumours) (Franz & Capal, 2017) and ER+ breast cancer in combination with exemestane (Hortobagyi, 2015).

Temsirolimus is a water soluble pro-drug of rapamycin which is rapidly metabolised to sirolimus through de-esterification (Voss et al., 2011). The Children's Oncology Group (COG) has recently demonstrated that temsirolimus was superior to bevacizumab in the treatment of high-risk rhabdomyosarcoma. Currently it is being investigated in combination with irinotecan and temozolomide with relapsed or refractory paediatric solid tumours, including NBL (Bagatell et al., 2014). However, the combination of irinotecan, temozolomide and dinutuximab was found the be superior to irinotecan, temozolomide and temsirolimus in refractory or relapsed NBL (Mody et al., 2017).

1.12.2.4. ***Indirect modulation of mTOR via energy sensing pathways***

The ability of organisms to adapt to fluctuations in available nutrients is essential to survival. In response to fluctuations in cellular nutrients, such as glucose and oxygen, AMP dependent protein kinase (AMPK) has been shown to interact with the TSC and modulate mTOR signalling (**Error! Reference source not found.**) (Howell & M anning, 2011). Metformin has been shown to down-regulate AMPK in a caspase dependent manner as well as mTOR signalling (Abdelmonsif, Sultan, El-Hadidy, & Abdallah, 2018; Howell et al., 2017). Interestingly metformin has been shown to reduce the risk of cancer in Type II diabetes patients who have been taking the therapy for glucose management (H. J. Kim et al., 2018).

1.12.3. **Downstream of mTOR**

Agents targeting processes downstream of mTORC1, such as protein translation, are gaining more interest as potential cancer therapeutic strategies. Primarily this involves modulation of protein translation which can be targeted by a variety of approaches (Showkat, Beigh, & Andrabi, 2014).

1.12.3.1. ***Inhibitors of protein translation***

Viruses such as hepatitis A and poliovirus hijack the 5'-cap binding complex to replicate (Avanzino, Fuchs, & Fraser, 2017). Many viruses can impact on 5'-cap dependent translation directly. Hepatitis B and C, human papillomavirus (HPV) and EBV contribute to 10-15% of human cancers (Shih, Fang, & Chen, 2014). Preventing these viruses, through the use of vaccination programs, can reduce these virally associated cancers as has been demonstrated with HPV and cervical cancer (Szarewski, 2012). One mechanism by which these viruses promote cancer is not only by activating the PI3K/AKT/mTOR pathway but also countering cell mechanisms that inactivate it via stress signalling (Buchkovich et al., 2008). DNA viruses such as SV-40 induce accumulation of hypo-phosphorylated 4E-BP1 which prevents eIF4F assembly and 5'-cap dependent translation (Avanzino et al., 2017; Walsh, Mathews, & Mohr, 2013). It therefore makes sense that anti-viral therapies may indirectly attenuate the cell growth impacts of the PI3K/AKT/mTOR pathway. Accordingly, acyclovir has been tested in MCF7 breast cancer cell lines and has induced significant cell inhibition (Shaimerdenova, Karapina, Mektepbayeva, Alibek, & Akilbekova, 2017).

Many antibiotics work by inhibiting the ribosomal bacterial subunits inhibiting bacterial protein synthesis. For example aminoglycosides inhibit either 30S or the 40S ribosomal subunit and are potent antibacterial agents (Mingeot-Leclercq, Glupczynski, & Tulkens, 1999) but potentially useful as anti-cancer therapies. A new synthetic aminoglycoside, NB124, strongly suppresses tumour cell growth by

promoting apoptosis via p53 and APC genes (Bidou, Bugaud, Belakhov, Baasov, & Namy, 2017).

A recent high throughput multiplexed translation screen identified 14 compounds with promising inhibition of protein synthesis. One of those compounds identified, NSC 119889, is a potent inhibitor of poliovirus cap dependent replication (Novac, Guenier, & Pelletier, 2004).

1.12.3.2. ***Targeting ribosomal biogenesis***

The PI3K/AKT/mTOR pathway has been linked to ribosomal biogenesis (1.6.3.2) and regulates RNA polymerases in response to IGF-1 and nutrients (James & Zomerdijk, 2004; Tee, 2018). Together Pol I and Pol III account for up to 80% of the nuclear transcription activity, which is regulated by mTOR in response to growth factors (Tsang, Liu, & Zheng, 2010). Pre-clinical research validates the potential role of Pol I inhibitors, such as CX-5461, as anti-cancer therapies (Bywater et al., 2012; Hein et al., 2017; H. Xu et al., 2017).

Interestingly the nucleolus has been shown to be integral in the function of p53 in response to cellular stress. Given that the nucleolar stress response is regulated by RNA polymerases it follows that Pol I inhibitors can modulate the p53 response in cancer cells and activate p53 dependent apoptosis (Bywater et al., 2012; Hannan, Drygin, & Pearson, 2013). CX-5461 has also been shown to induce p53-independent cell cycle checkpoints mediated by ATM/ATR signalling in the absence of DNA damage (Quin et al., 2016). Co-ordinated therapy targeting both RNA polymerases and TOR, with CX-5461 and mTORC1 inhibition acted synergistically in MYC-driven lymphoma (Devlin et al., 2016). Accordingly, CX-5461 in now in early phase trials for both haematological and solid tumours (NCT02719977).

1.13. PI3K-related kinases and the DNA-damage response

Cancer cells must develop methods to evade repair and resist apoptosis in order to survive. Inherited mutations of genes involved in DNA repair, such as the BRCA1 and BRCA2 genes, predispose carriers to much higher lifetime risks of both breast and ovarian cancers. The PI3K/AKT/mTOR pathway has been shown to co-operate with the DNA damage repair (DDR) pathway (De, Carlson, leyland-jones, & Dey, 2016) to regulate the DNA-damage response. PI3K inhibitors can induce DNA damage by inhibiting essential elements such as Rib phosphate and amino acids required for deoxynucleotide synthesis (Juvekar et al., 2016). Also, PI3K inhibitors can augment the DNA damage repair response as seen when they are used in combination with radiation therapy as radio-sensitisers (J. H. Park et al., 2017). In fact, full activation of AKT by phosphorylation of Ser473 is potentially ATM dependent in response to ionising radiation (Bensimon, Aebersold, & Shiloh, 2011). Central to the effectiveness of conventional chemotherapeutic agents, as well as radiation therapy, is their ability to cause DNA damage. In theory, rapidly dividing cells should be more sensitive to such therapies than non-replicating functional cells. Cancer cells can evade the effects of such therapies by activating DDR (Woods & Turchi, 2013). Accordingly small molecule inhibitors that target DDR proteins such as poly (ADP-ribose)-polymerase (PARP) have been shown to be highly effective in treated BRCA mutated cell lines (Davar, Beumer, Hamieh, & Tawbi, 2012).

1.13.1. ATM, ATR and DNA-PK

The inability to repair DNA double strand breaks (DSBs), which can be caused by many exogenous stimuli, is typically lethal to cells. Therefore cells have adapted and developed many cellular mechanisms, to repair these defects (Davis, So, & Chen, 2010). ATM and ATR are Ser/Thr kinases, with overlapping protein substrates, that are activated by DNA damage and DNA replication stress (Maréchal & Zou, 2013). The DDR is also important in the response of cancer cells to DNA damaging agents, and it is not surprising that many human tumours show functional loss or

deregulation of many key proteins involved in DDR and cell cycle regulation, in particular p53 and ATM (The Cancer Genome Atlas Research et al., 2008; Weber & Ryan, 2015).

Ataxia telangiectasia (AT), an inherited germline mutation of ATM, presents with ataxia, ocular telangiectasia, dysarthria and an increased cancer risk in the context of DNA damage (McKinnon, 2004) such as radiation therapy. ATM plays a crucial role in the activation of the G1/S phase cell cycle checkpoint which is meant to ensure cells with damaged DNA do not progress through the cell cycle. ATM directly phosphorylates the tumour suppressor protein p53 on Ser15, followed by phosphorylation of Ser20 by CHK2. This in turn prevents MDM2-mediated ubiquitination and degradation and stabilises p53 (Weber & Ryan, 2015). In response to damage of DNA replication forks, ATR phosphorylates CHK1 which in turn prevents CDK1/Cyclin8 activation (Rundle, Bradbury, Drew, & Curtin, 2017) and ultimately inhibits cell cycle progression at the G2/M phase. ATM, ATR and DNA-PK are all involved in AKT activation, although the exact mechanisms are not clear (Q. Liu, Turner, Alfred Yung, Chen, & Zhang, 2014). DNA-PK indirectly stabilises p53 by blocking its interaction with MDM2 (J. Li & Kurokawa, 2015). DNA-PK also directly promotes CHK1 to promote cell cycle arrest (Abdelmonsif et al., 2018). Both AKT and MYC have also been proposed as direct targets of DNA-PK (Cui et al., 2015; Stronach et al., 2011) (Figure 9).

Combined PI3K/mTOR inhibitors such as dactolisib (BEZ235) have shown substantial activity against ATM and ATR (Maira et al., 2008) and have been shown to be effective radiosensitisers in RAS activated tumours (Konstantinidou et al., 2009).

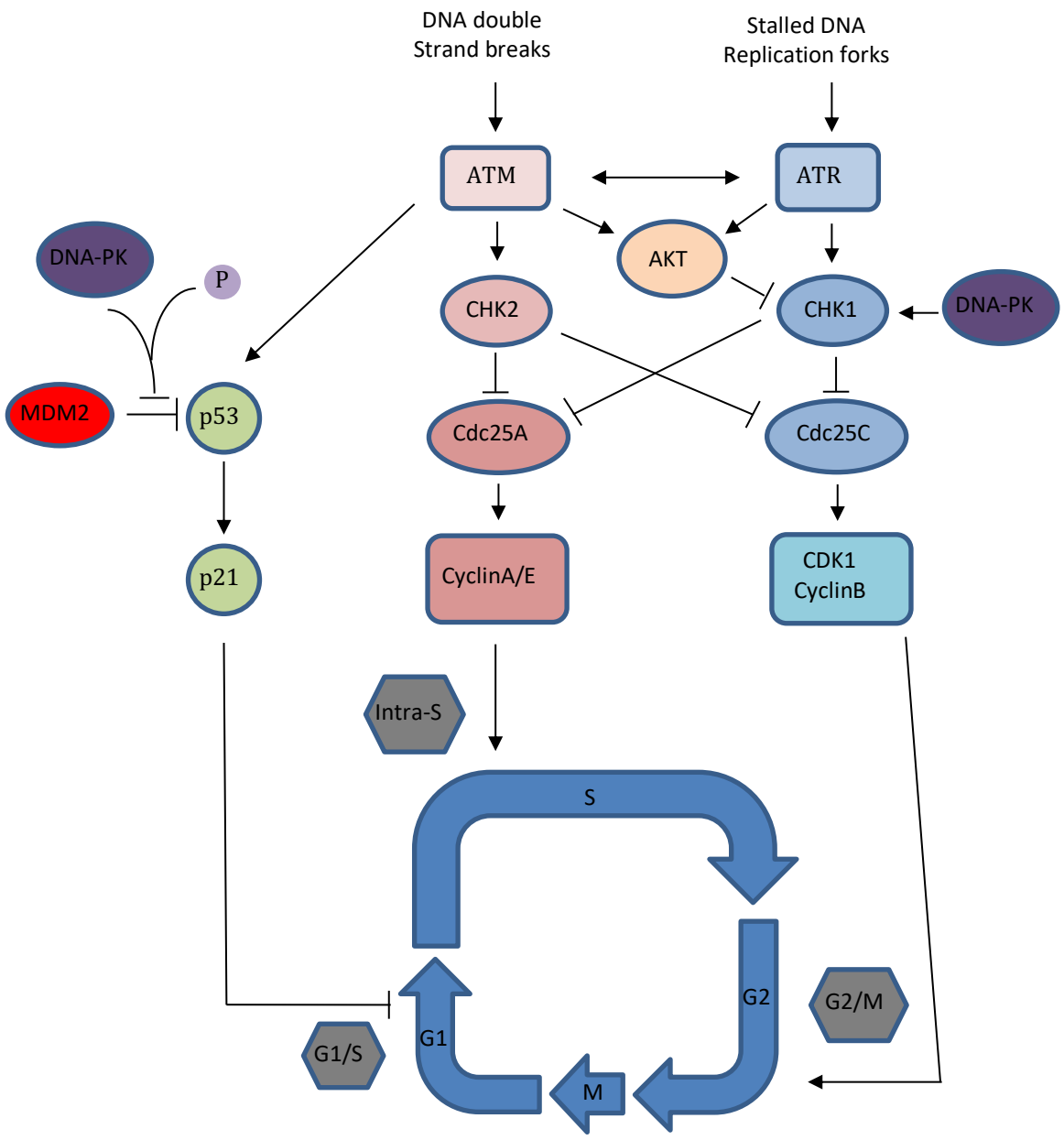

Figure 9 Activation of DDR kinases

DNA double strand breaks (DSB's) are recognised by the MRN complex that recruits and activates ATM. Phosphorylated ATM monomers activate a range of substrates including CHK-2 and p53 to arrest the cell cycle at G1 and G2 checkpoints. Concurrent activation of DNA repair effectors including DNA-PK induces activation of CHK1 and negative regulation of p53. Alternatively, single stranded DNA recruits and activates ATR kinase upstream of CHK-1 at the G2 – M checkpoint.

1.14. Histone Deacetylase inhibition in paediatric solid tumours

1.14.1. Histone Deacetylases

Allfrey was the first to postulate that HDACs were involved in the regulation of transcription (Allfrey, Faulkner, & Mirsky, 1964). Histone Deacetylases (HDACs) and histone acetyl transferases (HATs) were first identified in the 1990's (Rundlett et al., 1996). Subsequent research has shown that HDACs are essential to normal mammalian development. HDAC-1 null mice die before embryonic day 10.5 with severe associated growth and development defects (Haberland, Montgomery, & Olson, 2009). Conditional deletion of conditional HDAC1 or HDAC2 in mice, thereby bypassing early lethality, does not result in end organ phenotypic changes. If both HDAC1 and HDAC2 are conditionally deleted the results are severe phenotypic changes in organs such as the heart and liver (Montgomery et al., 2007). Further to this HDAC4 has been implicated in normal skeletogenesis (Vega et al., 2004), HDAC5 and HDAC9 have been implicated in normal cardiovascular growth (S. Chang et al., 2004) and HDAC7 controls endothelial function (S. Chang et al., 2006). Both class I and class II HDACs are essential in CNS development and function (Morris & Monteggia, 2013).

Simplistically histones can either be acetylated or deacetylated and the balance between these two states depends on the balance of activity between HDACs and HAT's. When HDACs predominate, the positive charge of the lysine residue located on the terminal chains of the histones is restored thereby condensing the structure of the nucleosomes (Davie, 1998). When HAT's predominate, acetylation neutralises the charge of the histones and generates a more open DNA conformation. This more open conformation allows for access to transcription factors, and the expression of relevant genes is promoted (Davie, 1998; Kouzarides, 1999) (Figure 10).

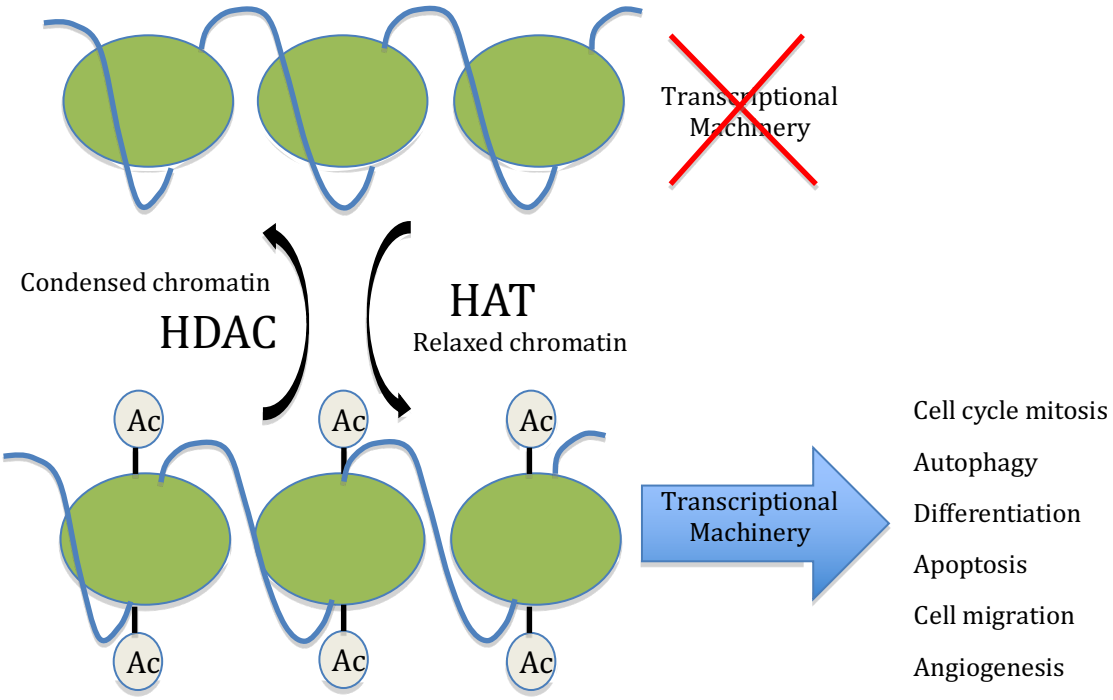

Figure 10 Schematic representation of the competing roles of HDACs and HAT's on transcription

Histones can either be acetylated or deacetylated and the balance between these two states depends on the balance of activity between HDAC's and HATs. When HDACs predominate, the positive charge of the lysine residue located on the terminal chains of the histones, is restored thereby condensing the structure of the nucleosomes. When HATs predominate, acetylation neutralises the charge of the histones and generates a more open DNA conformation.

1.14.2. **HDAC classes**

There are 18 HDACs in humans. Eleven of these are zinc dependent, classified on the basis of homology to yeast HDACs, and these are typically the targets of HDAC inhibitors (HDACi). These are often referred to as the classical classes: I, II and IV (Witt, Deubzer, Milde, & Oehme, 2009). Class III HDACs have a dependence on NAD^+ are therefore not targeted by traditional Histone HDACi (P. A. Marks & Xu, 2009).

1.14.2.1. ***Class I HDAC's***

Class I HDACs consist of HDAC1 (chromosome 1p34.1), HDAC2 (chromosome 6p21), HDAC3 (chromosome 5q31) and HDAC8 (chromosome Xq13) (P. A. Marks & Xu, 2009). All Class I HDACs are located within the nucleus, except HDAC8 which is located in both the nucleus and cytoplasm (New, Olzscha, & La Thangue, 2012). HDAC1, 2 and 3 are responsible for transcriptional repression (S. Hong, Derfoul, Pereira-Mouries, & Hall, 2009; Karagianni & Wong, 2007). The DNA damage response is also controlled by Class I HDACs via hypoacetylation of histone H3 K56, which represses transcription and allows DNA repair to take place (Miller et al., 2010). HDAC8 is X-linked in humans and its activity is independent of additional co-factors (Chakrabarti et al., 2015). HDAC8 also controls proteins such as cohesin, oestrogen receptor α and cortical actin-binding protein, and these proteins are involved in diverse functions such as sister chromatid separation, energy homeostasis, microtubule integrity and muscle contraction (Olson et al., 2014). Mutations in HDAC8 are found in Cornelia de Lange syndrome (Kaiser et al., 2014) which has a cancer predisposition to Wilms tumour (Maruiwa et al., 1988). When mRNA expression in a large range of human neuroblastoma samples was interrogated there was a clear association between HDAC8 expression and advanced disease with metastatic disease. Conversely it was down-regulated in Stage IVS disease which typically spontaneously regresses and causes minimal harm (Oehme et al., 2009). Finally, HDAC8 substrates include p53 (Chakrabarti et al., 2015) an essential gene in the control the human cell cycle.

1.14.2.2. ***Class II HDAC's***

Class II HDACs are present in either the cytoplasm or the nucleus. They tend to have tissue specific functions (New et al., 2012) and most of them are highly expressed in heart, brain, skeletal muscle and thymus which is consistent with their important role in cell differentiation (X.-J. Yang & Grégoire, 2005). They are further sub-divided into class IIa and class IIb.

1.14.2.3. ***Class IIa HDACs***

Class IIa HDACs consist of HDAC4 (chromosome 2q372), HDAC5 (chromosome 17q21), HDAC7 (chromosome 12q13) and HDAC9 (chromosome 7p21-p15) (P. A. Marks & Xu, 2009). All class IIa members have a conserved N-terminal domain which is homologous to yeast γ HDA1, first identified in 1996 (Rundlett et al., 1996). Like yeast γ HDA1, class IIa mammalian HDACs mainly function as transcriptional corepressors. HDAC4 partners with the Runx2 transcription factor to regulate skeletal development including chondrocyte hypertrophy and endochondral bone formation (X. Sun, Wei, Chen, & Terek, 2009; Vega et al., 2004). When HDAC9 is partnered with MEF2 it can impact on regulation of cell differentiation, death and survival (Verdin, Dequiedt, & Kasler, 2003), and aberrant MEF2 proteins have been identified in pre-B acute lymphoblastic leukaemia, the most common paediatric malignancy (Barneda-Zahonero et al., 2015; Yuki et al., 2004). When partnered with 53BP1 HDACs can impact on p53 binding protein that regulates cell cycling in response to DNA damage (Kao et al., 2003). The DNA damage response has been repeatedly shown to be critical in the development and treatment of cancer (O'Connor, 2015). From a therapeutic point of view, novel class IIa selective HDACi have been identified (Hsu et al., 2017).

1.14.2.4. ***Class IIb HDAC's***

Class IIb HDACs consist of HDAC6 (chromosome Xp11.22-33) and HDAC10 (chromosome 22q13.31-33) (P. A. Marks & Xu, 2009). In general class IIb members have been linked to the cellular stress response, protein degradation and autophagy

(Ridinger et al., 2018). HDAC6 has several functions some of which are independent of its HDAC activity (New et al., 2012) and it is unique in its ability to form substrates with non-histone proteins (Y. Li, Shin, & Kwon, 2013). HDAC6 interacts with numerous proteins that control functions such as cell migration, transcription, immune response, cell proliferation and cell death (Y. Li et al., 2013). The over-expression of HDAC6 has been shown in human breast and ovarian cancer (Bazzaro et al., 2008) and this may be related to the fact that the HDAC6 gene is an oestrogen regulated gene (Inoue et al., 2002). HDAC10 plays a key role in DNA repair (Radhakrishnan et al., 2015; Ridinger et al., 2018) and has been identified as a prognostic marker in high-risk neuroblastoma where it promotes chemo-resistance (Oehme et al., 2013). HDAC10 may also regulate vascular endothelial growth factor receptor (VEGFR) degradation via HSP90 acetylation (Bruns et al., 2012; J. H. Park et al., 2008). The central role of vascular endothelial growth factors in the development of cancer, especially during periods of rapid tumour growth and relative hypoxia, is well established (Goel & Mercurio, 2013). Class II b HDACs can co-operate with class IIa HDACs as evidenced by the interaction between HDAC6 and HDAC9 in neuronal cell survival and movement (Salian-Mehta, Xu, McKinsey, Tobet, & Wierman, 2015).

1.14.2.5. ***Class III HDACs (sirtuins)***

Class III HDACs consist of seven members nominated SIRT1 (chromosome 10q21.3), SIRT2, (chromosome 19q31.2), SIRT3 (chromosome 11p15.5), SIRT 4 (chromosome 12q24.23-q24.31), SIRT 5 (chromosome (6p23), SIRT6 (chromosome 19p13.3) and SIRT7 (chromosome 17q25.3) (Dai & Faller, 2008; T. Liu, Liu, & Marshall, 2009). SIRT1 has been shown to be consistently up-regulated in malignant cells from patients with leukaemia, glioblastoma, prostate, colorectal and skin cancer (T. Liu et al., 2009). By inducing histone deacetylation and methylation, transcriptional repression and deacetylation of tumour suppressor proteins SIRT1 may promote, or initiate, cancer cell growth by blocking senescence, differentiation and apoptosis while at the same time promoting cell growth and angiogenesis (T. Liu et al., 2009).

1.14.2.6. ***Class IV HDACs***

Class IV HDACs consists of HDAC 11 (chromosome 3p25.2) (P. A. Marks & Xu, 2009). Very little is known about HDAC11. HDAC11 shows tissue and cell type specific expression and regulates diverse immune functions via repression of IL-10 gene transcription (Yanginlar & Logie, 2018). HDAC11 has also been shown to regulate the expression of OX40L in Hodgkin's lymphoma, making HDACi a potential therapeutic target in this disease (Buglio et al., 2011).

1.14.2.7. ***Histone Deacetylase deregulation in cancer***

Imbalances between the activity of HDACs and HATs and their deregulation play a key role in the development of human cancers (Johnstone, 2002; Ropero & Esteller, 2007). In fact, the critical balance between their acetylation state and their deacetylation state plays an essential role in gene expression (Ropero & Esteller, 2007) (Figure 10). HATs induced acetylation is associated with gene transcription whilst HDAC induced deacetylation is associated with gene silencing (Davie, 1998; Kouzarides, 1999). Ultimately, the balance between these and the subsequent impact on chromatin remodelling, affects the expression of key genes that regulate vital cellular functions such as cell proliferation, cell-cycle regulation, differentiation and apoptosis (Johnstone, 2002; P. A. Marks, Richon, & Rifkind, 2000; New et al., 2012; Ropero & Esteller, 2007; Waldeck et al., 2016).

In addition, HDACs can promote cancer development via their non-histone substrates (B. N. Singh et al., 2010). Select examples of targets of non-histone substrates, among others, include GATA-1/2 which has been implicated in acute myeloid leukaemia (AML) via repression of RUNX1 target genes (Mandoli et al., 2014). FLT3, which is commonly present in multi-drug resistant AML, is driven by the MAP kinase transcription factor AP-1 and RUNX1 via a unique chromatin signature (Cauchy et al., 2015). Finally, the tumour suppressor function of p53 can be impacted due to reduced transcriptional activity (Luo et al., 2001).

HDAC8 and HDAC10 have been linked to advanced disease and poor survival in NBL (Oehme et al., 2009; Oehme et al., 2013; Rettig et al., 2015). HDAC 2, HDAC 5 and HDAC 9 have been similarly shown to be associated with advanced disease and poor prognosis in paediatric medulloblastoma (Ecker et al., 2015; Milde et al., 2010)

When these essential cell processes are deregulated it can drive or maintain human cancer. Germline mutations in the CRP gene, which encodes HAT's, are associated with the cancer predisposition syndrome Rubinstein-Taybi syndrome (Petrij et al., 1995). Aberrant HDAC expression has been implicated in a number of human cancers although the prognostic significance of these findings, in the context of other critical pathway changes, is still uncertain (P. A. Marks & Xu, 2009; New et al., 2012). As a result, strategies targeting HDAC are an attractive therapeutic option in human cancer (Johnstone, 2002). The rationale for their use is that inhibitors of HDACs may relieve transcriptional repression caused by the products of certain oncogenes such as MYC (Waldeck et al., 2016), leading to gene reactivation. The role of reactivating genes is to reactivate tumour suppression or death pathway genes, which have been abnormally silenced in the generation of the malignant phenotype. This reactivation may lead to cell cycle arrest, induction of apoptosis, or differentiation (Glozak & Seto, 2007; P. Marks et al., 2001; Waldeck et al., 2016; Weidle & Grossmann, 2000).

Although it is predicted that HDACi will have an anti-cancer effect there are in some cancers it has been found in which genetic inactivation of HDACs might have tumorigenic effects. Class II HDACs may also function as tumour suppressors in certain circumstances. For example, low expression of HDAC10 is associated with poor prognosis in lung and gastric cancer patients (Z. Jin et al., 2014; Osada et al., 2004).

1.14.2.8. ***Histone deacetylase inhibitors***

HDACi's are potent anti-cancer agents and have been shown to promote both apoptosis and differentiation in aggressive pre-clinical models (Cain et al., 2013; Muscat et al., 2016). Many compounds are either currently in early phase clinical trials or have been approved in defined diseases by the United States of America (USA) Food and Drug Administration (FDA). Currently panobinostat has been FDA approved for multiple myeloma (Laubach, Moreau, San-Miguel, & Richardson, 2015) and vorinostat, belinostat and romidepsin have been FDA approved for cutaneous T-cell lymphoma (Moskowitz & Horwitz, 2017). HDACis are classified by their chemical structure (Table 3).

Classification by chemical structure	Named examples	HDAC specificity	Clinical status
Hydroxamates	Vorinstat (SAHA)	Pan-inhibitor	FDA approved
	Belinostat (PXD101)	Pan-inhibitor	FDA approved
	Panobinostat (LBH589)	Classes I and II	FDA approved
	Givinostat (ITF2357)	Pan-inhibitor	Phase II
	Resminostat (4SC-201)	Pan-inhibitor	Phase II
	Abexinostat (PCI 24781)	Classes I and II	Phase II
	Trichostatin A (CAS 58880-19-6)	Pan-inhibitor	Pre-clinical
	Quisinostat (JNJ-26481585)	Pan-inhibitor	Phase I
	Rocilinostat (ACY-1215)	Class II	Phase I
	Pracinostat (SB939)	Class I, II and IV	Phase II
	CHR-3996	Class I	Phase I
Cyclic peptides	Romidepsin (FK228)	Class I	FDA approved
Benzamides	Entinostat (MS-275)	Class I	Phase II/III
	Mocetinostat (MGCD0103)	Class I	Phase II
	Tacedinaline (CI994)	Class I	Phase III
	4SC202	Class I	Phase I
Aliphatic fatty acids	Valproic Acid	Class I and IIa	FDA approved for epilepsy, Phase II for cancer
	Butyrate	Class I and IIa	Phase II
	Phenylbutyric acid	Class I and II	Phase I

Table 3 HDAC inhibitors classification by chemical structure, specificity and clinical status

HDACi classification by chemical structure, specificity and clinical status (Adapted and updated from (New et al., 2012).

1.14.2.9. *Mechanisms of Histone deacetylase inhibitors action in cancer*

HDACi play an important role in the treatment of human malignancies, with a variety of cellular targets (Clawson, 2016; Eckschlager, Plch, Stiborova, & Hrabeta, 2017).

1.14.2.10. *Cell cycle arrest*

HDAC1 and HDAC2 may co-operate to promote G_1-S phase progression (Yamaguchi et al., 2010). It is not surprising then that HDACi block cell cycle progression at G_1 in many pre-clinical cancer cell types including multidrug resistant sarcoma cell lines (Bernhart et al., 2017). Specifically, suppression of Cdk2 and CdK4 kinase activity due to p21 overexpression plays a critical role in HDACi induced cell cycle arrest (He et al., 2005; Y. B. Kim, Ki, Yoshida, & Horinouchi, 2000). In prostate cancer cell lines HDACi induced G_2/M arrest via an increase in p21 and a reciprocal decrease in cyclin A and cyclin B1 (Z. Dong et al., 2018). In both these instances p21 regulation was the key player in cell cycle arrest. As stated earlier HDACs modulate p53 (Chakrabarti et al., 2015) and research has shown that p53 controls both the G_1 and G_2/M checkpoints (Agarwal, Agarwal, Taylor, & Stark, 1995) and that p21 expression is in turn modulated by p53 in response to DNA damage (Karimian et al., 2016).

1.14.2.11. *Apoptosis*

It has been shown that HDACi induces apoptosis via different transcriptional pathways in a tumour cell specific manner (Bolden et al., 2013). For example, human neuroblastoma cell lines have been shown to undergo apoptosis in response to HDACi exposure via upregulation of BMF and BIM (Waldeck et al., 2016), whereas in prostate cancer cell lines, apoptosis was induced by an increase in the BH3-only proteins Noxa and Hrk (Z. Dong et al., 2018). Regardless of the transcription pathway, they are potent inducers of apoptosis preferentially via the BH3-only BCL-2 family proteins (Elkholi, Floros, & Chipuk, 2011).

1.14.2.12. ***Differentiation***

Analysis using knockout mice, incorporating primarily HDAC 1, 2 and 3 gene deletions, have reinforced their crucial role in embryonal differentiation, in particular cardiac and neuronal differentiation (Humphrey et al., 2008; Montgomery et al., 2007). In addition, mouse embryonic stem cells can be epigenetically programmed to differentiate into neural cells when exposed to HDACi (X. Yao et al., 2010). Research focussing on NOTCH mediated smooth muscle differentiation demonstrate that HDAC activity is required for NOTCH differentiation signalling through both the PI3K pathway and the MAPK pathways (Tang, Boucher, & Liaw, 2012). Research looking at wing development in *Drosophila* suggests this is primarily through NOTCH1 signalling (Z. Wang et al., 2018). Although the exact mechanism is not clear, there is evolving pre-clinical evidence in paediatric cancer models that, when particularly used in continuous low-dosing schedules, HDACi result in terminal differentiation and prolonged survival of several embryonal cancer models (Cain et al., 2013; Muscat et al., 2016).

1.14.2.13. ***Autophagy***

Autophagy is the process by which the body consumes its own tissue as a result of certain metabolic processes or diseases (Heras-Sandoval, Pérez-Rojas, Hernández-Damián, & Pedraza-Chaverri, 2014). There are several proposed mechanisms via which HDACi induce autophagy including inactivation of mTOR signalling, reactive oxygen species (ROS) activation, upregulation of p21, NF-κB hyperacetylation and p53 acetylation (Mrakovcic, Kleinheinz, & Fröhlich, 2017). It is the inactivation of the PI3K/AKT/mTOR pathway that has the most interest and has identified mTORC1 as the major player in this process via inhibition of ULK1 (Rabanal-Ruiz, Otten, & Korolchuk, 2017; Zachari & Ganley, 2017). HDACi appear to inhibit mTORC1 via an increase in LC3B-II which in turn inhibits the mTOR complex (Campbell, Bruckman, Chu, & Spector, 2015). Interestingly HDACi has also been shown to protect against cisplatin induced nephrotoxicity by activating autophagy in proximal tubular cells (J. Liu et al., 2018).

1.14.2.14. ***Cell signalling***

Of particular recent interest is the impact HDACi has on cell signalling pathways including those involved in differentiation (2.2.7.3). Long-term, continuous, low-dose panobinostat has been shown to induce terminal differentiation in three separate pre-clinical paediatric cancer models. This was first reported in pre-clinical osteosarcoma models (Cain et al., 2013). In MRT cell lines exposed to low dose panobinostat there was evidence of multi-lineage differentiation with the induction of neural, renal and osteoblast differentiation pathways (Muscat et al., 2016). Another important pathway is WNT signalling which has been implicated in many human cancers including medulloblastoma, colon cancer, breast cancer and melanoma (Eckschlager et al., 2017). HDAC2 appears central to this pathway as a functional target of APC/β-catenin (Schneikert & Behrens, 2007).

1.14.2.15. ***Angiogenesis***

HDACi can act as anti-angiogenic agents primarily via their regulation of HIF-1α (Ellis, Hammers, & Pili, 2009). Hypoxia induces HDAC expression, which deacetylates HIF-1α and subsequently increase its translational activity (M. S. Kim et al., 2001). In glioblastoma (GBM) panobinostat treatment resulted in increased HIF-1α instability and degradation, and decreased VEGF expression (Z. G. Yao et al., 2017).

1.14.2.16. ***DNA damage response***

HDAC influences the DNA damage response via several mechanisms. In leukaemia cells, HDACi triggers increases in reactive oxygen species and DNA damage (Robert & Rassool, 2012). In breast cancer, HDACi has been shown to regulate p53-dependent DNA damage signalling by diminished phosphorylation of ATM, BRCA1, CHK2 and p53 (Thurn, Thomas, Raha, Qureshi, & Munster, 2013). Radiation therapy causes DNA damage and several chemotherapeutic agents are considered radio-sensitisers due to their impact on increasing the efficacy of radiation. Exposure to vorinostat radio-sensitises many different cancer cell lines, including melanoma, osteosarcoma

and colon cancer, to the effect of radiation (Groselj, Sharma, Hamdy, Kerr, & Kiltie, 2013).

1.14.2.17. ***Interaction with MYC***

N-Myc regulation of chromatin in the human genome includes not only specific genes but also genomic domains that invoke functions independent of a classic transcription factor (Cotterman et al., 2008). This N-Myc genomic regulation is strongly linked to AcK9 H3K9ac and H3K4triMe, with induced loss of N-Myc significantly reducing cellular pools of these two key peptides. CHiP verification assays also established that N-Myc can regulate H3K9ac and H3K4triMe at genomic regions that it does not bind to, indicating it has both direct and indirect effects on chromatin (Cotterman et al., 2008). An extensive CHiP-Seq interrogation of mouse embryonic stem cells confirmed the regulatory role of MYC/MAX in chromatin modifiers such as Setd3, MII1, MII3 and Wdr5 (Krepelova, Neri, Maldotti, Rapelli, & Oliviero, 2014).

In addition, MAX has the ability to form dimers with MAD1, Mxi1, Mad3, Mad4 and Mnt. These heterodimers bind to E-boxes and repress transcription by recruiting HDAC complexes (Figure 11). In proliferating cells, the balance between MYC/MAX heterodimers and MAX/Mad heterodimers is in favour of the former. In resting cells the MAX/Mad complexes are in excess (Adhikary & Eilers, 2005). It has also been shown that HAT's can acetylate MYC, making it less susceptible to ubiquitination, thereby prolonging its effect (Vervoorts et al., 2006).

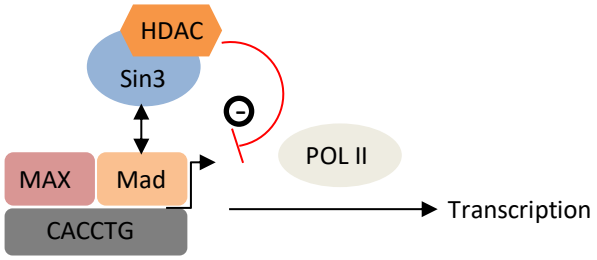

Figure 11 Interaction between histone deacetylase complexes and MYC transcription

MAX/Mad repress transcription at E-Box sites by recruitment of Sin3/HDAC complexes.

HDAC1 is also recruited to MYC-Sin3 complexes and its deacetylase activity is required for the action of Sin3 on MYC (Alland et al., 1997; Garcia-Sanz et al., 2014). In leukaemia cells and fibroblasts, Sin3b silencing led to Myc upregulation, whereas Sin3b overexpression induced Myc deacetylation and degradation. As Sin3 is also required for the transcriptional repression by Mxd-Max complexes, these results suggest that, at least in some cell types, Sin3 limits Myc activity through two complementary activities: Mxd dependent gene repression and reduction of Myc levels (Garcia-Sanz et al., 2014). p53 regulated transcriptional repression of c-Myc is accompanied by a decrease in the level of acetylated H4 at the c-Myc promoter, and by recruitment of Sin3 (Ho et al., 2005).

Finally, the histone chaperone FACT has been shown to co-operate with MYC in a forward feedback loop to maintain mutually high levels and promote *MYCN* transcription. FACT inhibitors, such as CBL0137, markedly reduced neuroblastoma tumour initiation and progression *in vivo* (D. R. Carter et al., 2015).

1.14.3. Histone deacetylase inhibitor resistance

Resistance to HDACi is mediated by a number of cellular mechanisms common to drug resistance seen with other chemotherapeutic agents. These include resistance mediated by efflux mechanisms, HDAC mutations, antioxidant generation to combat oxidative stress, downstream epigenetic and chromatin alterations and overexpression of anti-apoptotic proteins such as BCL-2 (Fantin & Richon, 2007).

1.14.4. Histone deacetylase inhibitors in paediatric cancer

Early pre-clinical studies identifying HDACi potential therapeutic benefit in neuroblastoma demonstrated that they cause apoptosis of human neuroblastoma cells *in-vitro* with an enhanced inhibitory effect when combined with retinoic acid (Coffey et al., 2001; Coffey et al., 2000). Furthermore, in xenograft models of neuroblastoma in SCID mice, HDACi inhibited tumour growth in a dose-dependent manner, and acted synergistically with all-trans retinoic acid, rendering lower doses of HDACi effective (Coffey et al., 2000). Retinoids exert their effect via a nuclear receptor complex that has been recently found to contain HDAC. It is hypothesised that HDAC inhibitors potentiate the de-repression of retinoid responsive genes in the presence of ligand (Glick et al., 1999).

HDACs and HATs interact with methyl-CpG binding proteins and the SWI/SNF chromatin re-modelling complex (mutated in rhabdoid tumours) to regulate chromatin structure. The HDAC inhibitor, MS-27-275, has been shown to inhibit the growth of rhabdoid tumour cell lines in which INI1 was deleted (Biegel et al., 2002). Preliminary evidence of tumour response has been observed in adult Phase I studies in advanced solid tumours and non-Hodgkins lymphoma with particular reference to cutaneous T-cell lymphoma (Prince et al., 2007). These results could be translated to the paediatric populations of non-Hodgkin's lymphoma patients. The COG currently has Phase I studies open using the related HDACi, vorinostat, in paediatric patients with refractory solid tumours and leukaemias. Vorinostat has been used in combination with temozolomide in refractory or relapsed CNS tumours in a dose

finding, Phase I trial. The drugs were well tolerated and 21% (4/19) of patients exhibited stable disease or better (Hummel et al., 2013). One of the earliest Phase I dose finding studies of panobinostat in paediatric patients with haematological malignancies again demonstrated that the drug was well tolerated (Goldberg et al., 2014). HDACi have a dual role of potentiating the actions of platinum based therapies (Gueugnon et al., 2014) and protecting against their nephrotoxic effects (J. Liu et al., 2018). Platinums are commonly used in paediatric cancer. Recent evidence in breast cancer which demonstrates how HDACi potentiates the effectiveness of immunotherapy, via up-regulation of PD-L1 and HLA-DR, in breast cancer can also be translated to paediatrics as this is an ever-expanding area of therapy (Terranova-Barberio et al., 2017). Finally, the compelling evidence, including that presented in this thesis, that HDACi promotes terminal differentiation in paediatric pre-clinical models, such as NBL, osteosarcoma and ATRT, has generated a Phase II study, in Australia and New Zealand (ANZCTR trial ID ACTRN12618000321246), which is investigating this as a potential therapeutic option (Cain et al., 2013; Muscat et al., 2016; Waldeck et al., 2016).

These results suggest that HDACi alone or in combination with other chemotherapeutic or differentiating agents may prove to be very useful in the treatment of neuroblastoma, rhabdoid tumours as well as other solid and haematological malignancies in children.

1.15. **Hypothesis and Aims**

In summary HR NBL remains a disease that has particularly poor outcomes when compared to other paediatric malignancies. N-Myc amplification has repeatedly been shown to be associated with HR disease and imparts a poor prognosis. The concept of oncogene addiction suggests that if we can target N-Myc we may be able to reverse its ability to maintain elements critical to tumour growth, including TME. To date, however, there have been no therapeutic strategies that target N-Myc directly. Given *MYCN* co-operates with other oncogenic pathways, including PI3K/AKT/mTOR, it

may be possible to indirectly alleviate the impact of N-Myc by targeting these pathways instead. In addition, it might be possible the alleviate the impacts of N-Myc at a post-transcriptional level by inhibiting HDACs. Therefore, both inhibition of the PI3K/AKT/mTOR pathway and histone deacetylases are promising therapeutic strategies in NBL.

This thesis will explore the use of inhibitors of the PI3K/AKT/mTOR pathway and HDAC in both human/murine NBL cell lines and an aggressive mouse model that accurately mirrors the human form of the disease. Specifically, it will explore the survival benefit, the tolerability and the mode of action of such inhibitors. It will also attempt to fill a gap in currently available NBL mouse models by using TH-*MYCN* derived cell lines orthotopically in WT-littermates thereby creating a model with an intact immune system that can also be manipulated. Finally, the tolerability of panobinostat will be explored in a Phase I study of paediatric patients with refractory solid tumours. As part of this Phase I study we will also attempt to validate potential drug biomarkers to demonstrate a pharmacodynamic value in early phase studies.

2 Materials & Methods

2.1.**Human Tissue Samples**

Human neuroblastoma tissue samples were obtained following Human Research Ethics Committee (HREC) approval from the both the Royal Children's Hospital (RCH) and Peter MacCallum Cancer Centre (PMCC).

2.1.1. **Immunohistochemistry (IHC), human and mice.**

Formalin-fixed, paraffin embedded specimens were cut at 4 micron (μm) and baked overnight (minimum 2 hours) at 60^{O}C. The slides were then de-waxed (Jung Autostainer XL, Leica Biosystems, Wetzlar, Germany) and re-hydrated prior to antigen retrieval in sodium citrate 10mM (pH 6.0) for two minutes at 125^{O}C and 15-18 PSI pressure (pressure cooker). Slides were then rinsed three times in distilled water for five minutes and then once in Tris-HCL 50mM (pH 7.6)/0.1% Tween for five minutes. This was followed by peroxidase blocking (3% H_2O_2) for 10 minutes, and then appropriately diluted primary antibody (Table 4) labelling was performed for one hour at room temperature for all antibodies except pAKT (Ser473) which was extended to two hours. Appropriate secondary antibody detection (Table 4) was performed for one hour. Finally, DAB (DAB peroxidase, DAKO, Glostrup, Denmark) was applied. There were five-minute washes using Tris-HCL 50mM (pH 7.6)/0.1% Tween buffer in between labelling steps. The steps from peroxidase blocking onwards were performed on the DAKO autostainer (DAKO Universal Staining System, Glostrup, Denmark). Slides were then rinsed in distilled H_2O and counterstained with haematoxylin (Jung Autostainer XL, Leica Biosystems, Wetzlar, Germany) prior to dehydration and cover slipping. Images were acquired on a BX-51 Olympus contrast microscope with the DP70 digital camera system, software DP2-BSW (Ver 2.2) (Olympus, Center Valley, PA, USA).

For human neuroblastoma tissue samples, staining intensity was scored by an anatomical pathologist.

2.1.2. **Antibodies for Western blotting and IHC**

Antibody	Supplier	Molecular Weight	Dilution	Source
Acetyl Histone H3	Merck Millipore #06-599	15kDa	WB 1:2000	Rabbit
β-actin	MP Biologicals #691002	42kDa	WB 1:20000	Mouse
Bcl-2	Cell Signalling #15071/2870	26kDa	WB 1:1000 IHC 1:400	Mouse
BIM	Cell Signalling #2933	12, 15, 23kDa	WB 1:1000	Rabbit
BMF	EnzoLifeSciences ALX-804-508	25kDa	WB 1:500	Mouse
Chromogranin	DakoCytomation #A0430	20kDa	IHC 1:400	Rabbit
Enolase 2	Thermo Scientific PA5-27452	47kDa	IHC 1:500	Rabbit
pAKT (Ser473)	Cell Signalling WB #9271 IHC #3787	60kDa	IHC 1:50 WB 1:1000	Rabbit
tAKT	Cell Signalling #9272	60kDa	WB 1:1000	Rabbit
pERK (Thr202/Tyr204)	Cell Signalling WB #9101 IHC #4370	42,44 kDa	IHC 1:200 WB 1:2000	IHC Rabbit WB Mouse
tERK	Cell Signalling #9102	42, 44kDa	WB 1:2000	Rabbit
pS6 WB(Ser240/244) IHC(Ser235/236)	Cell Signalling WB #2215 IHC #2211	32 kDa	IHC 1:200 WB 1:1000	Rabbit
tS6	Cell Signalling #2217	32kDa	WB 1:1000	Rabbit
P4EBP1 (Thr37/46)	Cell Signalling #2855	15-20kDa	IHC 1:400 WB 1:1000	Rabbit
Cleaved Caspase-3	Cell Signalling WB #9662 IHC # 9664	17, 19kDa	IHC 1:250 WB 1:1000	Rabbit
Mcl-1	Cell Signalling #5453	40kDa	WB 1:1000	Rabbit
N-myc	Calbiochem #OP13	62kDa	IHC 1:200 WB 1:1000	Mouse
S100	Dako #Z0311	50kDa	IHC 1:3000	Rabbit
SSTR2	Abcam #134152	75-80kDa	IHC 1:250	Rabbit

Rabbit anti-mouse	Dako #P0447	N/A	1:2000	N/A
Goat anti-rabbit	Dako #P0448	N/A	1:2000	N/A

Table 4 Antibodies used for Western blotting and IHC

This table summarises the antibodies used for Western blotting and IHC including dilutions and secondary antibodies.

2.2. Tissue culture methods

2.2.1. Culture of TH-*MYCN* Murine derived neuroblastoma cells

TH-*MYCN* derived NHO1A and NHO2A cell lines were obtained from the Children's Cancer Institute, Sydney, Australia (Cheng et al, 2007). Cells were cultured in either T25 or T75 flasks (CELLSTAR® , Greiner Bio-One, Kremsmünster, Austria) using RPMI-1640 with additional supplements (2.2.1.1) in a humidified 37^{o}C incubator containing 5% CO_2 in air. NHO1A cells were split at 1:5 once per week. NHO2A cells were split 1:20 to 1:40 twice a week. Freeze down cells in 90% FCS with 10% DMSO.

2.2.1.1. *NH02A and NHO1A media*

RPMI-1640 (Invitrogen™, Life Technologies™, CA, USA)
L-glutamine (2mM) (Sigma-Aldrich, MO, USA)
Sodium pyruvate (1mM) (Sigma-Aldrich, MO, USA)
MEM Non-essential amino acids (1x) (Gibco™, Life Technologies™, CA, USA)
50μM β-mercaptoethanol (Calbiochem, EMD chemicals, CA, USA)
20% heat-inactivated FCS (SAFC Biosciences, Lenexa, KS, USA)

2.2.2. Culture of Human neuroblastoma cell lines

The IMR-32 (*MYCN*-amplified) and SK-N-SH (non-*MYCN*-amplified) human neuroblastoma cells lines were purchased from DSMZ, Germany. Cells were cultured

in six-well plates (CELLSTAR®, Greiner Bio-One, Kremsmünster, Austria) using DMEM with additional supplements (2.2.2.1 & 2.2.2.2) in a humidified 37^{o}C incubator containing 5% CO_2 in air. Freeze down cells in 90% FCS with 10% DMSO.

2.2.2.1. ***Media IMR-32***

DMEM (Invitrogen™, Life Technologies™, CA, USA)
L-glutamine (2mM) (Sigma-Aldrich, MO, USA)
Sodium pyruvate (1mM) (Sigma-Aldrich, MO, USA)
MEM Non-essential amino acids (1x) (Gibco™, Life Technologies™, CA, USA)
50μM β-mercaptoethanol (Calbiochem, EMD chemicals, CA, USA)
10% heat-inactivated FCS (SAFC Biosciences, Lenexa, KS, USA)

2.2.2.2. ***Media SK-N-SH***

DMEM (Invitrogen™, Life Technologies™, CA, USA)
L-glutamine (2mM) (Sigma-Aldrich, MO, USA)
MEM Non-essential amino acids (1x) (Gibco™, Life Technologies™, CA, USA)
50μM β-mercaptoethanol (Calbiochem, EMD chemicals, CA, USA)
10% heat-inactivated FCS (SAFC Biosciences, Lenexa, KS, USA)

2.3.**Preparation of chemical compounds for *in-vitro* studies**

PF-502 (Pfizer®) was made in a stock solution of 10mM in DMSO.
Temsirolimus (Pfizer®) was made in a stock solution of 10mM in DMSO.
Stock solutions were aliquoted and stored at -20^{o}C.

2.4.**Sulforhodamine B (SRB) Assay**

For a typical experiment, cells were inoculated into 96 well microtiter plates (CELLSTAR®, Greiner Bio-One, Kremsmünster, Austria) in 100 μL of media (2.2.1.1, 2.2.2.1 & 2.2.2.2) at plating densities ranging from 500 to 5000 cells per well depending on the doubling time of individual cell lines. A cell count (Beckman Coulter

Multisizer 3, Life Sciences, Brea, CA, USA) was performed to determine number in cells in cell stock media prior to making a solution with a standard cell concentration per ml. A multi-channel pipette can be used at this stage to deliver an equal number of cells in each treatment well. After cell inoculation, the microtiter plates are incubated for 24 hours prior to addition of drug. After the time that drug is added, designated "time zero", the wells of one plate are fixed using 50% trichloroacetic acid (TCA) (Sigma-Aldrich, MO, USA). This represents the cell density when drug was added. Experimental drugs are solubilised, and serial dilutions are made to provide a total of 11 drug concentrations, and a vehicle control. All empty wells around the edge of the plate were filled with media to ensure a consistent temperature in experimental wells. The desired drug concentration was achieved when 100 μL of the drug dilution was added to the 100 μL of media already in the well. Following addition of drug, plates were incubated for an additional 72 hours.

At the end of the experiment wells were fixed with 50% TCA, washed and then stained with 0.4% SRB (Sigma-Aldrich, MO, USA) that had been filtered (filter paper). SRB stains proteins in a way that can be used to quantify the protein content per well as an indirect measure of cellular content. The SRB was allowed to sit for 30 minutes. The plates were washed again with cold tap water and then rinsed twice with 1% acetic acid (safety glasses must be worn for this step). The plates were then air dried and inverted on a paper towel. At this stage the plates can be stored once dry. The absorbance of individual wells was measured at 550 nm using a Versa max Microplate Reader and analysed with SoftMax Pro software v 5.4 (Molecular Devices, Sunnyvale, CA, USA). Data was then transferred to either Microsoft Excel ™ or GraphPad Prism software for Mac OS X (Version 5.0d, GraphPad Software INC, La Jolla, CA, USA) to analyse and plot dose-response curves. From this an IC_{50} for drug concentration could be obtained.

2.5. Determination of cell cycle arrest by fluorescence-activated cell sorting (FACS)

A minimum of 1.0 x 10^5 cells were fixed in 400µL of a 50:50 ethanol:PBS solution for twelve hours (overnight) at 4^{0}C. Following this they were washed in PBS and re-suspended in 50µL propidium iodide (PI) buffer (PI 69mM in Sodium citrate 38mM) containing 1% RNase A (Sigma-Aldrich, MO, USA). Cell nuclei were then analysed on the LSRII or FACSCantoll cytometer (BD Biosciences, San Jose, CA, USA) and analysed using FlowJo software (Version 9.3, Tree Star Incorporated, Ashland, OR, USA). Apoptosis was defined by the percentage population of sub-G1 cells.

2.6. Protein techniques

2.6.1. Preparation of protein samples for in vitro assays

2.6.1.1. *RIPA Buffer*

EDTA (stock 500mM, ph 8)	1ml
NP-40	5 ml
Sodium deoxycholate	2.5 g
SDS	0.5 g
Sodium Flouride (mwt=42)	1.05
Pyrophosphate (tetra sodium, mwt=446.06)	0.23 g
Make to 500mL with PBS	

Add just before using, per 10 ml buffer:
1 x Complete EDTA-free protease inhibitor cocktail (Roche Diagnostics Australia Pty Ltd, Castle Hill, NSW, Australia)
100 µl 100 mM Sodium Vanadate (x100)
100 µl 100 mM PMSF (x100)

2.6.1.2. ***Preparing in vitro cells for lysis***

Media was removed from cells and transferred into a 15ml centrifuge tube (ThermoFisher Scientific, Ma, USA). The plate was then washed with warm PBS. If required, 2 ml of trypsin (Sigma-Aldrich, MO, USA) was added, and the plate incubated for 10 minutes. The plate was then inspected to ensure all cells had detached. If cells were still adherent a pipette was used to dislodge the cells. The media was then tipped back into the plate and the entire solution collected back into the centrifuge tube and spun at 1000 rpm for 5 minutes. The media was then removed, and cells were resuspended in 1 ml of PBS and transferred to an eppendorf tube (SSIBio, Lodi, CA, USA). The eppendorf tube was then spun at 8000 rpm for 10 seconds to form a cell pellet. The PBS was then removed, and cell pellets stored at -80^{O}C until ready to perform protein extraction.

2.6.1.3. ***Preparation of lysates from cells***

RIPA buffer (2.6.1.1) was prepared as required and protease inhibitors and PMSF (2.6.1.1) were added immediately prior to use. Frozen cell pellets were lysed for 30 minutes on ice using RIPA buffer. Lysates were then micro-centrifuged at 13,000 rpm for 10 minutes, at 4^{O}C to remove insoluble material. Protein content determination was then performed (2.6.1.4). Lysates were then stored at -80^{O}C prior to use.

2.6.1.4. ***Protein content determination***

Protein content was determined using the Bio-Rad DC (Bio-Rad, Hercules, CA, USA) protein concentration estimation, standardised against a bovine serum albumin (BSA) (Promega, Madison, WI, USA) concentration gradient. Two ul of unknown lysates were pipetted into the wells of a flat bottom 96 well plate (CELLSTAR®, Greiner Bio-One, Kremsmünster, Austria). Then 25 ul of Reagent A (supplied) and 200 ul of Reagent B (supplied) were added to the wells. The plate was then agitated for 5 seconds. After 15 minutes the absorbance of individual wells was measured at 750nm using a Versa max Microplate Reader and analysed with SoftMax Pro software v 5.4 (Molecular Devices, Sunnyvale, CA, USA).

2.6.2. **Preparation of protein samples for in vivo assays**

2.6.2.1. ***Crushing tumours***

One large, and one small dewar were filled with liquid nitrogen and all instruments required were also cooled in liquid nitrogen. The tumour tissue was placed in the homoginiser on a wooden platform. The frozen tumours were then crushed in the homoginiser using a hammer then the tumour pieces were scraped into the middle of the homoginiser and crushed again. This process was repeated until a fine powder was obtained. Using a spatula, the required amount of tumour was transferred into a labelled eppendorf tube for protein extraction. The remaining tumour was transferred to a second labelled eppendorf tube for storage at -80^{O}C.

2.6.2.2. ***Preparation of lysates from tumours***

RIPA buffer (2.6.1.1) was prepared as required and protease inhibitors and PMSF (2.6.1.1) were added immediately prior to use. RIPA buffer was added to each tumour sample in an eppendorf tube on ice. The mixture was then agitated using a syringe with a 21-gauge needle. The eppendorf tube was then placed on a tube rotator and rotated for 30 minutes, at 4^{O}C. Lysates were micro-centrifuged at 13,000 rpm for 10 minutes, at 4^{O}C. Protein content determination was then performed (2.6.1.4). Lysates were then stored at -80^{O}C prior to use.

2.7.**Western blotting**

Whole cell lysates (25 – 50ug) were heated to 95^{O}C for five minutes in 5x SDS sample loading buffer (2.7.1) and proteins were separated by polyacrylamide gel electrophoresis using 8 – 15% polyacrylamide gels in SDS running buffer (Tris-HCl 25mM, glycine 192mM, 10% SDS in water). Pre-stained molecular weight standards (10uL, PageRuler™ Prestained Protein Ladder, Fermentas Life Sciences, Burlington, Ontario, Canada) were run on each gel to ascertain the molecular weight of proteins of interest. Gels were transferred to Immobilon-P PVDF membrane (Millipore,

Bedford, MA, USA) by electroblotting in Western transfer buffer (Tris-HCl 25mM [pH 8.3], glycine 192mM, 15% methanol), that had been pre-soaked in methanol, in wet transfer apparatus (Biorad, Hercules, CA, USA) at 100V for 90 minutes at 4^{O}C. Membranes were then blocked for one hour at room temperature in PBS/5% w/v skim milk powder. Blocked membranes were incubated with the appropriate primary antibody solution (Table 4) in PBS/5% BSA at 4^{O}C overnight. Following primary antibody staining, membranes were thrice washed in PBS for five minutes and then incubated for one hour at RT with the appropriate HRP- conjugated secondary antibody (Table 4) in PBS/5% skim milk. Excess secondary antibody was then removed with three further five-minute washes in PBS prior to visualisation with enhanced chemoluminescence reagents (Amersham™ ECL™ or Amersham™ ECL™ Plus, GE Healthcare, Uppsala, Sweden) detected by FUJIFILM Super RX (FujiFilm, Brookvale, NSW, Australia) according to the manufacturer's instructions. Film was developed using an Agfa CP1000 developer (Agfa, Mortsel, Belgium). All membranes were subsequently stained with anti-β-actin antibodies to confirm equal loading.

2.7.1. **SDS Sample Loading Buffer (5x)**

Tris-HCL 250nM, pH 6.8
10% SDS
50% glycerol
β-mercaptoethanol

2.8.**Experimental animals**

2.8.1. **Animal housing and sources**

Experimental mice were housed in pathogen free facilities at the PMCC, East Melbourne. All mouse experiments were performed in accordance with guidelines administered by the PMCC Experimental Animal Ethics Committee and conducted in compliance with the Australian code of practice for the care and use of animals for

scientific purposes. TH-*MYCN* mice were originally generated at the University of California, San Francisco, CA, USA (Weiss et al., 1997). The TH-*MYCN* mice (on an SV-129 background) were kindly provided by the CCIA, Sydney.

2.8.2. **Genotyping of TH-*MYCN* model**

2.8.2.1. ***TKM Buffer***

Tris-hydrochloride (HCL), pH 7.6
$MgCL_2$ 4mM
KCL 10mM
EDTA 2mM

2.8.2.2. ***Tris-EDTA (TE) Buffer, pH8***

5ml Tris-HCL
EDTA 1mM
Sterile water to 500mls

2.8.2.3. ***3M NaOAc, pH 5.2***

408.1g Sodium Acetate-$3H_2O$ in 800mls water
Glacial acetic acid for pH 5.2
Sterile water to 1000ml
Autoclave

2.8.2.4. ***DNA/RNA extraction***

Mouse tail clips were stored in the fridge until required in Eppendorf tubes. Tail clips were labelled with each mouse identification number and the date of clipping. A solution of TKM + 20% Chelex (Bio-Rad) (w/v) + 0.75% Sodium Dodecyl Sulphate (SDS) was then made. 300ul of this mixture to was added to each tail clip. The Eppendorf tube was heated to 56^{O}C for 30 min on a Thermomixer (setting 14). Then the heat was turned up to 95^{O}C and heated for another 15 minutes. The Eppendorf

tube was transferred to a rotary wheel and spun for 15 min at 4^{O}C. Transfer The Eppendorf tube was transferred to a centrifuge and spun at 13,000 rpm at 4^{O}C for 5 min. The resultant supernatant was transferred, using a pipette, into a fresh Eppendorf tube (usually between 120-150ul). At all stages the samples were be stored on ice except when specified. Alternatively, RNA from tumours was prepared and processed using the High Pure Tissue Isolation kit (Roche, Basel, Switzerland) and SYBR Green detection method in a StepOne PCR machine as previously described (Bolden et al., 2013).

2.8.2.5. ***Phenol chloroform extraction (performed at 4^{O}C)***

Bring the volume obtained from DNA extraction (2.8.2.4) to 200ul minimum volume with sterile water. Add an equal volume (200ul) of phenol/chloroform/isoamyl alcohol mix (Sigma-Aldrich). Invert the Eppendorf tube 10 times manually. Transfer to a centrifuge, 4^{O}C, and spin at 13,000 rpm for 5 min. Take the aqueous (top layer) and transfer into fresh Eppendorf tube (120-140ul). Add an equal volume of chloroform (120-140ul). Invert this manually 10 times. Transfer to centrifuge, 4^{O}C, and spin at 13,000 rpm for a further 5 min. Take the aqueous (top layer) and transfer into fresh Eppendorf tube (80-100ul).

2.8.2.6. ***Ethanol precipitation***

Bring the volume obtained from phenol chloroform extraction (3.5.2.4) to a volume of 200ul with sterile water. Add 1:10 volume (20ul) 3M Sodium Acetate (NaOAc). Then add 2 volumes (440ul) of 100% ethanol and incubate at -20^{O}C for at least 1-2 hours. This can be left overnight. Transfer to centrifuge, 4^{O}C, and spin at 13,000 rpm for 20 min. There is usually a visible pellet at the bottom of the Eppendorf tube. Discard as much supernatant as possible, leaving the pellet, and add 500ul 70% ethanol. Transfer to centrifuge, 4^{O}C, and spin at 13,000 rpm for 20 min. Using a pipette, remove the majority of supernatant and then either dry on the bench, at room temperature, for 1 hour with cap open, or at 37^{O}C for no longer than 1 hour, to ensure evaporation. Then re-suspend the remaining pellet in 20ul TE buffer. This can be

stored at -20^{0}C until RT-PCR is performed. Use 1.5ul of the final DNA extraction, from each tail preparation, for RT-PCR.

2.8.2.7. ***Genotyping using Real Time Polymerase Chain Reaction (RT-PCR). Materials and equipment.***

ABI PRISM 770 RT-PCR Machine (Applied Biosystems)
Taqman Master Mix (Applied Biosystems)
VIC and FAM Fluorogenic Probe (Applied Biosystems)
Primers/Probes (GeneWorks)
PCR Grade Water
96-well plate (Applied Biosystems)
SYBR Green (Applied Biosystems)
StepOne PCR machine (Applied Biosystems)

2.8.2.8. ***Primers and Probes***

Gene	Primer sequence
Human NMyc Transgene	**717s**: 5' CGA CCA CAA GGC CCT CAG TA-3' **837a**: 5' CAG CCT TGG TGT TGG AGG AG-3'
Beta-Actin	NHM**ActF**: 5' TGC GTC TGG ACY TGG CTG-3' NHM**ActR**: 5' TAG CCM CGC TCG GTC AGG-3'

Gene	Probe sequence
Human NMyc Transgene	**FAM**-5' CGC TTC TCC ACA GTG ACC ACG TCG-3'
β-Actin	**VIC**-5' CGG GAC CTG ACT GAC TAC CTC ATG-3'

2.8.2.9. ***RT-PCR Master Mix***

The following formula of master mix is required for each RT-PCR reaction:

Taqman Universal Master Mix	10μL
717s primer (100ng/μL)	0.32μL
837a primer (100ng/μL)	0.4μL
ActF (100ng/μL)	0.4μL
ActR (100ng/μL)	0.24μL
FAM NMyc probe (100ng/μL)	0.04μL
VIC actin probe (100ng/μL)	0.04μL
Sterile water (100ng/μL)	7.0μL

Each well of the 96-well RT-PCR plate is loaded with 1.5ul of DNA tail preparation (2.8.2.4) and 18.4ul of RT-PCR master mix. Each tail preparation sample is run in triplicate. Each RT-PCR run contains four control wells (all run in triplicate): water only, known wild-type (WT) NMyc mouse, known hemizygotic (Hemi) NMyc mouse and known homozygotic (Homo) NMyc mouse. Once all required wells have been plated, place the 96-well plate in a centrifuge and spin at 1300rpm for 30 seconds.

2.8.2.10. ***RT-PCR run***

Place 96-well plate in RT-PCR machine.

For experimental properties assign:

- Experimental name (date_NMYC_initials)
- 96 wells
- Standard curve
- Taqman Reagents

- Standard (2 hours)

For plate setup assign:

- Define targets: FAM for NMyc, VIC for Actin
- Define samples: controls & all unknowns
- Assign targets. Each well needs to be assigned NMyc and Actin
- Assign samples (in triplicate). Each triplicate of wells needs to be nominated for the assigned targets NMyc and Actin.

Begin run.

2.8.2.11. ***RT-PCR. Analysing results***

Raw data was transferred to an NMyc genotyping Microsoft Excel® template. The Ct column represents the PCR cycle at which the amplification crossed the assigned threshold. The average VIC (Actin probe) value was subtracted against the average FAM (NMyc probe) and normalised against the NMyc Hemi control results. This will give us a value known as the dct. We now average the dct values for the Hemi control and deduct this number from all of the previously obtained dct values for the unknown samples to give a new value designated the ddct. To obtain the transgene dose apply the following formula to the ddct values: (=power(2,-w3)). One can then find the average transgene dose and assign it to the unknown samples. This data can now be presented as a column graph (Figure 12).

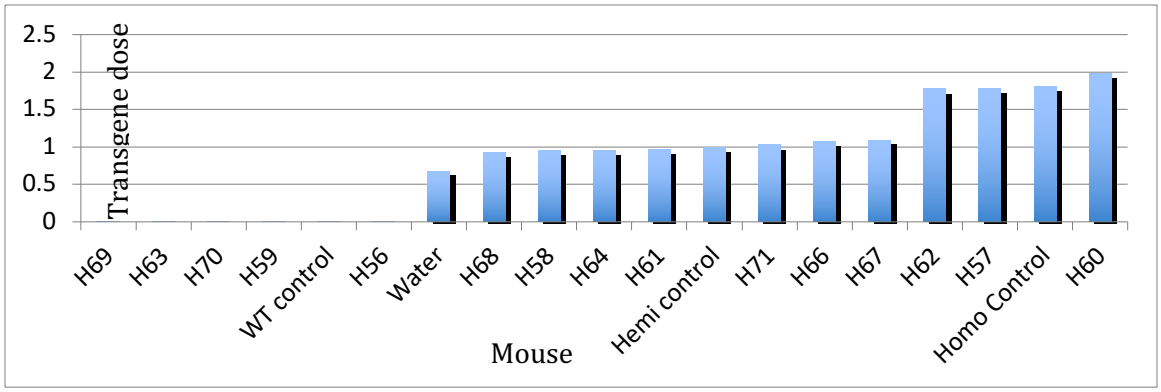

Figure 12 RT-PCR analysis

Representative example of final analysis of RT-PCR transgene read out showing relative NMyc copy number in unknown versus control samples. A transgene read out of zero is consistent with a WT littermate. A transgene read out of one is consistent with a hemizygote (Hemi). A transgene read out of two is consistent with a homozygote (Homo).

2.9. Administration of therapeutics

2.9.1. Preparation of drugs for *in-vivo* use

PF-502 and temsirolimus were prepared as per Pfizer recommendations. PF-502 was suspended in 0.5% methylcellulose solution (MP Biomedicals, Solon, OH, USA) and then sonicated (Unisonics Pty. Ltd., Sydney, NSW, Australia) for 30 minutes. Temsirolimus was dissolved in a solution of 4% ethanol, 2% Tween 80 (Sigma-Aldrich, MO, USA), 5% PEG 400 (Sigma-Aldrich, MO, USA) in 5% dextrose. The vehicle was made by sequencially adding ingredients to the ethanol and sonicating prior to the next ingredient. The temsirolimus was finally added and the solution sonicated for 30 minutes. Panobinostat was prepared as per Novartis recommendations.

Panobinostat was suspended in lactic acid in 5% glucose solution and then sonicated (Unisonics Pty. Ltd., Sydney, NSW, Australia) for 30 minutes.

2.9.2. **Drug administration**

PF-502 was given by oral gavage using a 20-gauge feeding tube (Intech Laboratories, Plymouth, PA, USA) at a dose of 10mg/kg daily (0.025ml/10g mouse). Temsirolimus was given by tail vein injection once weekly, using a 26-gauge needle (Terumo Medical Corporation, Somerset, NJ, USA) at a dose of 30mg/kg (0.1ml/10g mouse). Panobinostat was given by intraperitoneal injection once daily, using a 26-gauge needle (Terumo Medical Corporation, Somerset, NJ, USA) at a dose of 5mg/kg (0.1ml/10g mouse).

2.9.3. **Clinical assessment of tumour burden and drug toxicity**

Mice were assessed and weighed daily. Signs of distress included a scruffy appearance, cool extremities, increased respiratory rate, reduced mobility, distended abdomen or weight loss > 20% from baseline. Mice were ultrasounded twice weekly to assess tumour size. A tumour size of 600mm^3 was roughly equivalent to a tumour weight of 1 gram. Mice that were deemed to be in distress were immediately euthanised by cervical dislocation.

2.9.4. ***In vivo*** **neuroblastoma assays**

2.9.4.1. ***Biomarker studies and acute dosing schedules***

Homozygote mice were identified by genotyping (2.8.2) as these mice had a 100% tumour penetrance. From 5 weeks of age they underwent twice weekly abdominal ultrasounds until a tumour was visualised with a volume > 50 mm^3. Mice could then be randomised to receive drug or vehicle, minimum of n=3 per group. Mice would then be harvested (2.9.5.1) at a specific timepoint, usually two to three hours after the final dose of drug or vehicle.

2.9.5. In vivo survival studies in TH-MYCN neuroblastoma

Homozygote mice were identified by genotyping (2.8.2) as these mice had a 100% tumour penetrance. From 5 weeks of age they underwent twice weekly abdominal ultrasounds until a tumour was visualised with a volume > 50 mm^3. Mice could then be randomised to receive drug or vehicle. Mice would then be inspected daily (2.9.3) for signs of toxicity and twice weekly ultrasounds. Survival curves were plotted, and statistical significance calculated, using GraphPad Prism software for Mac OS X (Version 5.0d, GraphPad Software INC, La Jolla, CA, USA) (3.9).

2.9.5.1. *Harvesting of mice*

Mice demonstrating a significant disease burden were selected for harvest. This was either determined by their physical appearance or the presence, on ultrasound, of a tumour > 600mm^3. Tumour bearing mice were culled by cervical dislocation and disease involvement documented at autopsy. Tumours were photographed, removed and weighed. Tumours were divided and stored in 10% NBF (Australia Biostain Pty. Ltd., Traralgon, VIC, Australia), OCT and snap frozen in liquid nitrogen.

2.10. Imaging techniques

2.10.1. Ultrasound

Small animal ultrasound (US) was performed in the PMCC small animal imaging facility. Mice were fasted for three hours prior to the procedure. Mice are then anaesthetised using isoflurane (2.5% in 1:10 oxygen and air delivered at 200ml/min) and placed on the heated ultrasound mat in contact with electrode strips to electronically monitor heart rate and breathing during the experimental period (usually approximately 10 minutes). The instrument is also equipped with a murine rectal probe to monitor body temperature during scanning if required. The probe is not used routinely but will be employed for the longer duration scans involving contrast agents described below. A depilatory cream (Nair®) is used to remove hair

from the area of skin covering the tumour to reduce sound wave scattering and the area is then covered with non-toxic gel to aid in transmission of sound waves to and from the tissue. An ultrasound probe is placed in contact with the gel and signals collected through the probe producing a real time image of the tumour. This procedure takes approximately 5 minutes before the anaesthetic is discontinued and the mouse allowed to recover. Mice may be subjected to ultrasound imaging several times during the lifetime of the mouse, which should cause minimal discomfort or trauma. In some experiments, a contrast agent will be injected via tail vein (50ul, 27-gauge needle) and ultrasound data collected for approximately 10-15 minutes thereafter. These non-toxic agents are similar to those used in human MRI experiments and help to delineate blood flow in tumours. Particularly for smaller tumours or systemic models, non-invasive imaging technology should aid in early identification and localisation of tumours, potentially helping to minimise the duration of the study.

2.10.2. **18F-fluoro-deoxyglucose positron emission tomography (PET)**

PET scanning was performed in the PMCC small animal imaging facility. Mice were fasted and aneasthetised as for US (2.10.1). Mice were injected in the tail vein with 400-500uCi 18F-FDG. Mice were re-anaesthetised ninety minutes after tracer injection, and imaged for five minutes on a Phillips MOSAIC small animal PET scanner (Cleveland, OH, USA) as previously described (Cullinane et al., 2005). For quantitative analysis, tracer uptake in the tumour was measured and compared to background tissue uptake. The background region was chosen to represent regional uptake in non-tumour tissue. Areas of increased physiological uptake such as the bladder were not chosen. Typically, the liver was the organ of choice. Tumour to background FDG uptake ratios could then be calculated by taking the standard uptake value (SUV) of the tumour and dividing it by the SUV of the liver (or equivalent background region).

2.11. Histological techniques

2.11.1. IHC stains

IHC was performed on mice as described previously (2.1.1).

2.11.2. Terminal deoxynucleotide transferase dUTP nick end labelling (TUNEL) assay

Tumours were resected and fixed in 10% NBF prior to embedding in paraffin. The Apoptag® Peroxidase *in-situ* apoptosis detection kit was used on tumour sections cut to 4μm thickness. Mounted slides had paraffin removed and were then rehydrated with Proteinase K (20 μg/ml in PBS) for 15 minutes at room temperature. The slides were then washed twice with sterile water. A 3% peroxide solution was then applied for five minutes. Slides were then rinsed again with sterile water twice. The slides were then incubated in the supplied equilibrium buffer with terminal deoxynucleotidyl transferase (TdT) enzyme in a humidified chamber at 37^{O}C for one hour. Prior to removal from chamber, slides were agitated and then transferred to the supplied stop/wash buffer for 10 minutes. Slides were then removed and incubated with the supplied Anti-Digoxigen-Peroxidase for 30 minutes at room temperature. Slides were then washed in PBS and then DAB (peroxidase substrate) was added for three to five minutes until optimal staining was achieved. Slides were then counterstained with haematoxylin prior to dehydration and cover slipping. The positive control used was a BEZ235 treated lymphoma with a constitutively active (myristoylated) AKT construct (Shortt et al., 2013). Images were acquired on the BX51 Olympus contrast microscope with the DP70 digital camera system.

2.11.3. CD31 expression by IHC

Tumours, previously processed in optimal cutting temperature compound (OCT) (ProSciTech, Thuringowa, QLD, Australia) were cut to 7 um frozen sections and stored at 4^{O}C. Sections were brought to room temperature for 5 minutes and then

fixed in ice-cold acetone (4^{0}C) for 10 minutes. Slides were then washed with PBS. The primary antibody (Rat anti-mouse CD31 (DAKO #K8006) (1:200 in antibody diluent) was applied for 90 minutes at room temperature. The slides were then washed in PBS. The slides were then exposed to the secondary antibody (Goat anti-rat (Abcam #568) (1:700) in antibody diluent for 75 minutes at room temperature. DAPI (Sigma-Aldrich, MO, USA) was applied and slides were mounted. Images were acquired on a BX-51 Olympus contrast microscope (Olympus, Center Valley, PA, USA). The percentage of CD31 positive staining was calculated using MetaMorph software (Molecular Devices, San Jose, CA, USA). Results were expressed as mean percentage +/- standard error of the mean (SEM).

2.11.4. **SA-β-GAL staining.**

Tumours, previously processed in optimal cutting temperature compound (OCT) (ProSciTech, Thuringowa, QLD, Australia) were cut to 4 um frozen sections and stored at 4^{0}C. The sections were mounted on positively charged slides. Immediately after cutting the sections, they were fixed with 300 ul of 0.5% glutaraldehyde (40% v/v) and incubated for 15 minutes at room temperature. The excess PBS was removed, and a peroxidase anti-peroxidase (Pap) pen was used to outline the tissue. The 300ul of SA-β-GAL stain was added (2.11.4.1). Slides were placed in a humidified chamber and left for 18 hours at 37^{0}C. The slides were then rinsed with PBS. Sections were then counter stained using nuclear fast red (Sigma-Aldrich, MO, USA) for 5 minutes. Sections were then coverslipped and images were acquired on a BX-51 Olympus contrast microscope (Olympus, Center Valley, PA, USA). Positive controls used were everolimus treated Eu-Myc lymphomas (Wall et al., 2013).

2.11.4.1. ***SA-β-GAL staining solution***

50ul 20mg/ml Xgal (5-bromo-4-chloro-3-indolyl-β-galactopyranoside) in DMF

4 ml of citric acid/sodium phosphate solution, pH 6.0 (2.11.2)

1 ml of 100mM potassium ferrocyanide

1 ml of 100 mM potassium ferricyanide

0.6 ml of 5 M NaCl

40 ul of 1 M $MgCl_2$

Make up to 20 ml with distilled water.

2.11.4.2. ***Citric Acid/Sodium Phosphate solution, pH 6.0***

36.85 ml of 0.1 M citric acid

63.15 ml of 0.2 M dibasic sodium phosphate

2.12. **RNA sequencing and data analysis**

RNA was extracted from four baseline (0-hour timepoint) and four panobinostat treated mice (24-hour timepoint) following two treatments with either vehicle or 5mg/kg panobinostat 24 hours apart. RNA was extracted using using the Qiagen miRNAeasy kit (QIAGEN, Hilden, Germany) and quality assessed using the Agilent 2100 Bioanalyzer (Agilent Technologies, Santa Clare, CA, USA). RNA sequencing libraries were prepared using the IlluminaTruSeq V^2 RNA-Seq (Illumina, San Diego, CA, USA) and paired-end 50 base pair RNA-seq reads were generated using HiSeq 2500 (Illumina, San Diego, CA, USA). Reads were quality checked by FastQC (Wellcome Sanger Institute, Hinxton, UK) and trimmed if necessary, for low base quality using Cutadapt v1.6 (Gensoft, Lyndhurst, USA). Alignment was then performed against the mouse reference genome GRCm38 using TopHat (Top Hat, Ontario, Canada) v 2.0.12 with Max multihits set to 1 and using the option to map first to the reference transcriptome. HTseq v 0.5.4p5 ((Anders, Pyl, & Huber, 2015) with mode intersection-nonempty used to count the number of reads per gene using gene definition from Ensemble Release 73 (European Bioformatics Institute, Cambridgeshire, UK). Prior to differential expression analysis genes with very low counts were removed; genes with greater than 1 count per million in at least two samples were used for analysis. The limma-voom method v3.22.1 (Law, Chen, Shi, & Smyth, 2014) was used to identify differentially expressed genes. Gene Set Enrichment Analysis (GSEA) (Subramanian et al., 2005), was performed over the

MSigDB C2 gene sets with the additional HDAC inhibitor differentiation signature published by Frumm et al (Frumm et al., 2013). Pathway mapping of significant genes (p values < 0.05, expression change threshold 0.25) was undertaken using GeneGo Metacore software (Clarivate Analytics, London, UK). RNA-seq data is made publicly available (GEO accession number GSE69869).

2.13. **Orthotopic transplant in mice**

Heat pads were turned on and set up one hour prior to procedure. Next, cell suspensions were made up at a concentration of $1x10^5$ cells/20ul in 0.9% sterile normal saline. Suspended cells were kept on ice until required. Mice were fasted for three hours prior to the procedure. The mouse was weighed and injected with 100ul/10g of Xylazine (500ul)/Ketamine (800ul)/PBS (9000ul) anaesthetic mixture via intra-peritoneal route. Lacri-lube® or Polyvisc® was applied to the eyes of the mouse to prevent drying. When anesthetised, the right hand flank of mouse was shaved. The mouse was then positioned on the heat pad, right side up. 70% alcohol was applied to the shaved area to sterilize the skin. This also helped to identify kidney through the skin. A sterile technique was used throughout the procedure. An incision was made in right flank of mouse between 1-2cm in length and a similar 1-2cm incision through the peritoneum was made with forceps. Using curved, blunt end tweezers, the white fat body, which is attached to kidney was located. Pulling on this ensured the kidney came out of the abdominal cavity. Throughout this part of the procedure the mouse was kept hunched as this removed tension on blood vessels of kidney. During the procedure, sterile 0.9% normal saline was dropped onto the kidney to keep it moist. Once the kidney was exteriorised, 20ul of cell suspension was injected into subcapsular space of kidney. When finished, the kidney was placed back in renal bed. The peritoneum was then sutured using 6.0 dissolving sutures using one to two stitches at most. Then the skin was clipped together using 1-2 skin staples. If mouse was bleeding excessively, then one ml of sterile saline was injected IP when finished. The mouse was then placed in the box on a heat pad covered with towel. This prevented the mouse becoming too hot. The box was then covered with a towel

and then heat lamp applied. The mice were monitored carefully until they woke up, which took approximately one hour.

2.13.1. Monitoring after the procedure

Mice were checked on the afternoon of the experiment prior to removing from heat pads. It may be necessary to leave them on heat pads overnight. Mice will also be checked the day after the procedure. If they have been left on the heat pads overnight, they can be removed the next day. Mice will then be weighed & palpated for tumours (right flank) twice weekly. Clips will be removed 7-10 days after the procedure

Once tumours are reliably palpated in one mouse of the group those mice can then be moved to Ultrasound/PET facilities where they will undergo serial US and potentially be randomised into experiments. If no tumours have formed by 12 weeks post procedure, the mice will be culled. If during a mouse falls sick, has pale extremities, is non-responsive, is hunched, has ruffled fur, has excessive tumour burden noticeable when scruffed, we will assess it and aim to harvest the mouse as soon as possible depending on the condition of the mouse.

2.14. Retroviral transduction

2.14.1. Polyethylenimine (PEI) of 293T cells for virus production

PEI (Polysciences, Warrington, PA, USA) stock solution (1mg/ml) was defrosted and the stored at $4^{O}C$. HEK 293T cells were seeded at a concentration of 3×10^{6} into T75 flasks (CELLSTAR®, Greiner Bio-One, Kremsmünster, Austria) with a desired confluence of 50-60% at the point of transfection. NHO1A cells were plated in separate T25 flasks (CELLSTAR®, Greiner Bio-One, Kremsmünster, Austria) at a concentration of 450,000 cells per 10 mls. On the second day the media on the HEK 293T cells was changed (DMEM, 10% FCS, GlutaMax 2mM (Invitrogen™ Life Technologies Corporation, Carlsbad, CA, USA). The DNA (3 ug per T75 flask)/DMEM (500 ul) mix was then made: 3 ug of DNA (BCL2 or empty vector construct with 6 ug

of amphotericin B (Gibco™, Life Technologies™, CA, USA). Both the BCL2 and empty vectors were kind gifts of the Johnson laboratory, PMCC. The solution was then vortexed (Ratek Instruments Pty Ltd, Boronia, VIC, Australia). Then 4.5 ul of PEI (1mg/ml) per ug of DNA was added. This solution was vortexed again and incubated at room temperature for 10 minutes. This solution was then "flicked" to mix and added dropwise to the HEK 293T cells in the retroviral room. The transfection process took approximately six hours after which the media was replaced.

2.14.1.1. ***Retroviral transduction of murine NHO1A neuroblastoma cells***

The viral harvest took place the next morning. The 10 mls of the viral media was removed from the HEK 293T cells and put through a 0.45 um filter. If the 293T cells looked healthy the media could be replaced for a second harvest. For each one ml of viral media, one ul of protamine sulphate (10mg/ml) stock solution was added. Five mls of this final viral media was added to each T25 flask containing NHO1A cells. The viral media was replaced three times over the next 48 hours.

2.14.1.2. ***FACS sorting of MSCV/BCL2 transduced cells***

Virally infected NHO1A cells were washed and suspended in virus free media for FACS sorting based on green flourescent protein (GFP) expression. After sorting, GFP positive cells were washed and re-suspended in media (2.2.1.1).

2.15. Statistical analysis

Statistical analysis included 2-tailed student's t-test, 1-way ANOVA, 2-way ANOVA and Pearson's correlation coefficients. Calculations and graphical representations were performed on GraphPad Prism software for Mac OS X (Version 5.0d & 6.01, GraphPad Software INC, La Jolla, CA, USA). A p value < 0.05 was considered significant.

2.16. A Phase I study of LBH589 in paediatric patients with refractory solid tumours including CNS tumours

2.16.1. Study purpose and Objectives

The primary endpoints of this study were:

1) To determine the maximum tolerated dose (MTD) of panobinostat.
2) To recommend a Phase II dose of panobinostat for paediatric patients with solid tumours.
3) To define and describe the associated toxicities of panobinostat for patients dosed at MTD.
4) To characterise the pharmacokinetics (PK) of panobinostat for paediatric patients.

The secondary endpoints, where possible, were to define any anti-tumour activity observed in the paediatric population. Also, where possible, to assess the biologic activity of panobinostat by measuring histone acetylation status primarily in peripheral blood mononuclear cells (PBMNC), but also in bone marrow and fresh tumour tissue specimens in all patients (when available).

2.16.2. Patient Selection

This was a Phase I (3+3 design), open label trial conducted at eight centres in both Australia and New Zealand. Patients eligible to be enrolled included: paediatric patients defined as < 18 years of age and patients with refractory solid and central nervous system (CNS) tumours. Patients must have a histological diagnosis of a solid tumour (including CNS tumours) at the time of entering the study. This tumour must be refractory to conventional therapy. All patients required measurable lesions according to RECIST criteria. Additional inclusion criteria: either a Karnofsky performance level of ≥60% (patients > 10yr of age), or Lansky performance levels ≥60% (patients ≤10yrs of age), an estimated life expectancy of ≥ 8 weeks, patients

must also have recovered from the toxic side-effects of all prior therapies, prior to entering the study and patients with CNS tumours who required dexamethasone were on a stable/decreasing dose for at least 1 week. The following parameters must be tested within one week of registration. Adequate bone marrow function: peripheral blood absolute neutrophil count (ANC) > 1000/μL (or 1 x 10^9/L), platelet > 100 000/μL (or 100 x 10^9/L), haemoglobin > 8g/dL (or >80 g/L). Adequate renal function: age-adjusted normal serum creatinine or GFR >70ml/min/1.73m^2. Adequate liver function: total bilirubin ≤1.5 x institutional upper limit of normal (IULN) for age, SGPT (ALT) ≤5 x IULN for age, and albumin ≥ 2g/dL (20g/L). Adequate serum calcium, magnesium and potassium concentrations: all were ≥ institutional lower limit of normal (ILLN) for age with or without supplementation. The following parameters must be tested within two weeks of registration. Adequate cardiac function: shortening fraction of > 27% by echocardiogram OR ejection fraction of ≥ 50% by gated radionuclide study. Adequate pulmonary function: no evidence of dyspnoea at rest, no exercise intolerance and pulse oximetry (SaO2) >94%. Adequate CNS function was defined as: seizure free for 2 months prior to study entry. If the patient was female and post-menarchal, a negative pregnancy test was mandatory. If of reproductive potential the patient must have agreed to use effective contraceptive method. If the patient was female and lactating, they must have agreed not to breastfeed.

Exclusion criteria were defined as follows: having received any chemotherapy and/or biologic therapy within three weeks (four weeks if prior nitrosourea) of enrolment, having received radiotherapy (small port) within two weeks of study entry, having received craniospinal (CS) radiotherapy within three months of study entry, having received >50% radiation of the pelvis within three months of study entry, having received other substantial bone marrow radiation within six weeks of study entry, having received allogeneic stem cell transplant within six months of study entry, having received growth factor(s) within one week of study entry. Patients were also excluded if: they were receiving enzyme inducing anticonvulsant therapy, they were

receiving medications associated with prolongation of QTc interval, they were receiving hydrochlorothiazide while on study, they were receiving metronidazole and/or disulfiram, they had uncontrolled sepsis, they had previously received panobinostat, they had symptoms of congestive heart failure, uncontrolled cardiac rhythm disturbance, or a QTc ≥ 450msec.

2.16.3. Panobinostat Treatment Plan

Panobinostat was administered as a weekly (Days 1, 8) 30-minute infusion starting at a dose of 15mg/m^2. A starting dose of 15 mg/m^2 represented 80% of the maximum tolerated dose (MTD) established in the adult patient study population (Prince et al., 2007). One course was defined as 21 days. Inter-patient dose escalation or reductions, at increments of 5mg/m^2, were planned in successive cohorts, until an MTD was reached. There was no intra-patient dose escalation. Pharmacokinetic (PK) data was collected on each patient during course one. Ultimately the planned dose escalations, were not possible due to discontinuation of the study drug.

2.16.4. Assessments

2.16.4.1. *Dose limiting toxicities*

Dose limiting toxicities (DLT's) were defined as those toxicities attributable to drug during the first course only. For the purposes of this trial, haematologic and non-haematologic DLT's were defined differently. Non-haematologic DLT's were defined as any Grade III or Grade IV non-haematologic toxicity directly attributable, or potentially attributable, to the investigational drug with the following exclusions: Grade III nausea and vomiting controlled with adequate antiemetic medications, Grade III transaminase (AST/ALT) elevations that recover to Grade ≤ I prior to the next treatment course, or Grade III transaminase (AST, ALT) elevations that occur before the completion of the first course and recover to < grade II, before the next treatment dose, Grade III fever or infection, Grade III or greater fatigue that recovers to ≤ grade II by the next dose treatment course. Dose limiting prolongation of the

QTcF was defined as a QTcF >480 msec in a patient with confirmed normal serum electrolytes. If the patient had abnormal serum electrolytes these needed to be corrected, and the QTcF repeated. A QTcF >480 msec was not considered dose-limiting if it normalised following correction of the electrolyte disturbances. The following haematologic toxicities were considered to be DLTs: Grade IV neutropaenia of > seven days' duration, Grade IV thrombocytopaenia that required two or more platelet transfusions in the first 21 days, any haematologic toxicity that resulted in a treatment delay of > seven days beyond the planned interval between treatment courses and/or individual doses within treatment courses. Bone marrow aspirate and/or biopsy should be considered before removing a patient for hematologic toxicity if there is a possibility of bone marrow tumour involvement. Additionally, toxicities that resulted dose delays or dose reductions during the first course of therapy were also considered DLT's.

2.16.4.2. *Common Terminology Criteria for Adverse Events (CTCAE)*

This study utilised the CTCAE v3.0 of the national Cancer Institute (NCI) for toxicity and performance reporting.

2.16.5. Requirements for Subsequent Courses of Chemotherapy

Patients must have demonstrated haematological recovery before, and within 24 hours, of each course of panobinostat as defined: Haemoglobin ≥ 8 g/dL (80.0 g/L) (with or without transfusion support), Absolute Neutrophil Count ≥ 1000/μL (1 x 10^9/L), Platelets ≥ 75,000/μL (75 x 10^9/L) (independent of transfusion). Patients' serum total calcium (or ionized calcium if hypoalbuminaemia), magnesium and potassium must be greater than or equal to the institutional lower limit of normal for age (with or without supplementation), before each dose of panobinostat.

2.16.6. **Response assessment**

Tumours responses were assessed using the RECIST criteria.

2.16.7. **Pharmacokinetic Studies**

Plasma samples were collected at the following time-points:
Course 1, Day 1: Pre-dose, end of infusion, then 0.25-hour, 1 hour, 3 hours, 6 hours, 24 hours post infusion.
Course 1, Day 2; 26-70 hours post infusion.
Non-compartmental analysis was implemented in Phoenix® WinNonlin® (Pharsight, Mountain View, CA, USA), and was used to estimate pharmacokinetic parameters of panobinostat and its metabolite(s) from individual plasma concentration versus time profiles.

2.16.8. **Panobinostat studies**

Blood samples were collected at baseline, time 0, and 6, 24 and 48-hours post-treatment. Ten mls of blood was collected into Li-Heparin tubes and 2mLs into EDTA tubes. Qualitative histone acetylation assessment by ICC and quantitative histone acetylation analysis using flow cytometry (Li-Heparin), and quantitative Western blotting of acetylated histones (EDTA) were performed. The 697-leukemia cell line (ATCC) was used as a control throughout.

2.16.8.1. ***Immunocytochemistry***

Qualitative data was obtained by immunocytochemistry (ICC) on fixed sample slides as previously described (Ronzoni, Faretta, Ballarini, Pelicci, & Minucci, 2005). Antibodies used were rabbit anti-acetyl histone H3 K9/K14 (Millipore #06-755), rabbit anti-acetyl histone H4 (Millipore #07-108), followed by incubation with an AlexaFluor488 conjugated donkey anti-rabbit IgG secondary antibody (Invitrogen #A-21206) for one hour at room temperature. Slides were analysed using a Leica DM IRE2 confocal microscope (Leica Microsystems, Wetzlar, Germany).

2.16.8.2. ***Flow cytometry***

Histone acetylation in peripheral blood was examined using flow cytometry as previously described (Algar, Brickell, Deeble, Amor, & Smith, 2000; Rigby, Muscat, Ashley, & Algar, 2012).

Histone acetylation was detected by incubation with polyclonal rabbit anti-acetylated histone H3 (Millipore #06-755) or rabbit anti-acetylated H4 antibodies (Millipore #06-866), and AlexaFluor488-conjugated donkey anti-rabbit IgG secondary antibody (Invitrogen #A-21206). Flow cytometric analysis was performed on a LSRII flow cytometer (Becton Dickinson, Franklin Lakes, NJ, USA) acquiring at 15,000 events per sample. Data were collected using the BD FACS Diva software and a right shift in fluorescence, relative to pre-treatment blood cells, defined increased histone acetylation.

2.16.8.3. ***Western blotting***

Whole cell lysates were prepared from cell pellets and 20µg of total protein was subjected to SDS-PAGE and immunoblotted as previously described (Ronzoni et al., 2005). Cell pellets were prepared as follows: three volumes of red cell lysis buffer (RCL) (155mM NH_4Cl, 10mM $KHCO_3$, 1mM Na_2EDTA, pH 7.4) was added to two mls of whole blood and incubated for ten minutes at 4°C. Cells were then spun at 400g for 10 minutes at 4°C. The resultant cell pellet was then re-suspended in 200µL of RCL buffer and spun again for five minutes. Cells were then washed in PBS, pelleted and stored at -80°C.

Membranes were probed with the following antibodies: rabbit anti-acetyl histone H3 K9/K14 (Millipore #06-599), rabbit anti-acetyl histone H3 K9/K14 (Cell signalling #9677) or rabbit anti-acetyl histone H4 (Millipore #06-866). HRP conjugated donkey anti-rabbit IgG (Cell Signalling #7074) secondary antibody was detected by chemiluminescence using Super-Signal West Dura Extended Duration Substrate (Thermo Fisher Scientific, Waltham, MA, USA). Protein levels were quantitated using

the volume analysis tool with local background subtraction within the Image Lab 4.1 software (Biorad, Hercules, CA, USA).

2.16.9. **Statistical Methods**

As previously stated, this was a phase I (3+3 design) evaluation of panobinostat with the starting dose of 15mg/m^2 (80% of the adult MTD). A minimum of three evaluable patients were to be entered at each dose level until an MTD was established.

Data analysis was performed using GraphPad Prism® version 6.01 (GraphPad software). A paired one-tailed t-test and a probability score less than or equal to 0.05 was considered to indicate statistically significant acetylation of H3 and H4.

3 Targeting the mTOR/AKT/PI3K pathway in neuroblastoma

3.1. Introduction

3.1.1. mTOR inhibition

Temsirolimus is an allosteric mTORC1 inhibitor that has received FDA approval for treatment in advanced RCC following evidence that it significantly prolongs survival in patients when compared with interferon-α (Hudes et al., 2007; B. I. Rini et al., 2014). Low-dose single agent temsirolimus has also been shown to be effective in mantle cell lymphoma (MLC) patients with an overall response rate of 41% (Ansell et al., 2008) including refractory MCL (Hess et al., 2009).

Temsirolimus has been used in the Phase II setting at a low dose of 75mg/m^2 weekly, in heavily pretreated children with high-grade glioma, rhabdomyosarcoma and NBL. Disease stabilisation was observed in 32% of patients with NBL, 41% of patients with glioma and 6% of patients with rhabdomyosarcoma (Geoerger et al., 2012). Specifically to *MYCN* amplified NBL, and inhibitors of the PI3K/mTOR pathway, the ability of inhibitors to degrade *MYCN* requires complete blockade of mTOR but not PI3K (Vaughan et al., 2016). As demonstrated in most pre-clinical studies, rapalogs used alone are cytostatic in most tumour types and primarily stabilise disease (Meric-Bernstam & Gonzalez-Angulo, 2009).

Like most rapalogs temsirolimus preferentially targets mTORC1; however, prolonged exposure to rapamycin has been shown to reduce mTORC2 levels below what is required to maintain AKT/PKB signalling (Sarbassov et al., 2006). The treatment benefits of inhibiting both mTORC complexes remains unclear. When Ku0063794, a dual mTORC1 mTORC2 inhibitor was compared to Temsirolimus it displayed more effective anti-tumour effects in RCC cell lines; however, this benefit did not translate to xenograft models where impacts on tumour microenvironment, such as angiogenesis, become more important (H. Zhang et al., 2013). Combined inhibition, however, may overcome the observed drug resistance seen in RCC which is

associated with compensatory mTORC2 signalling and upstream activation of AKT (B. I. Rini & Atkins, 2009). The mechanisms by which targeted therapies inhibit the PI3K/AKT/mTOR pathway are summarised (Figure 13).

The activation status of PI3K/mTOR pathway in neuroblastoma has been previously described (Johnsen et al., 2008). In this study 30 primary neuroblastoma samples were investigated for the expression of activated AKT and mTOR using antibodies directed against phosphorylated AKT (ser473) and phosphorylated mTOR (ser2448). All 30 samples analysed showed specific expression of phosphorylated AKT (ser473) and phosphorylated mTOR (ser2448) (Johnsen et al., 2008). In a similar study 101 patients (median age 2.5 years, range: 0–13) with resected neuroblastoma (16 stage I; 7 stage II; 22 stage III; 48 stage IV and 8 stage IVS) were included (Sartelet et al., 2008). Tissue microarrays were constructed containing 101 primary tumours, 39 paired metastases and 56 paired normal tissues. IHC staining was performed on sections using antibodies against PI3K, total Akt and pAkt (ser473). The expression of downstream proteins (phospho-p70S6 kinase, 4eBP1) was studied. Interestingly 60% of the tumours expressed PI3K, 80% total AKT and 73% pAKT (ser473). In addition, phospho-p70S6 kinase and p4EBP1 were expressed in 95% and 85%, respectively. All these proteins had a significantly higher expression in tumours as compared with paired normal tissues (Sartelet et al., 2008). Akt and pAkt showed a tendency for higher expression in metastases as compared to paired primary tumors ($p<0.05$). A significant positive correlation was found between pAkt and the following: VEGFR1, VEGFR2 and IGF1Rβ ($p<0.001$), phospho-p70S6 kinase and mTOR ($p<0.01$) (Sartelet et al., 2008). In a similar study which specifically looked at the mRNA expression, through microarrays, quantitative RT-PCR and protein levels via WB analysis, demonstrated that the over expression of these PI3K genes can predict aggressive disease, and indicates stage-dependent involvement of PI3K-pathway members in neuroblastoma (Fransson, Abel, Kogner, Martinsson, & Ejeskar, 2013).

The PI3K/Akt pathway is activated in neuroblastoma and could be an attractive target for novel therapies. In addition, the data suggests that VEGFR and IGF1R are preferentially committed to this pathway activation.

This chapter explores the role of mTOR signalling in NBL with an emphasis on the cellular phenotype that results from mTORC1 inhibition. These results suggest that temsirolimus not only promotes cellular senescence, but also has anti-angiogenic effects. When the TH-*MYCN* model of NBL was treated with temsirolimus, there was no clear evidence of apoptosis.

3.1.2. **Combined PI3K/mTOR inhibition in neuroblastoma**

The importance of the PI3K/AKT/mTOR pathway will be demonstrated in a small cohort of high risk NBL patients (3.2), and is consistent with previously published data that confirms this as a valid therapeutic target in NBL (Fulda, 2009; Spitzenberg et al., 2010). The first generation of PI3K inhibitors included compounds like Wortmannin and LY294002 which were considered "pan-PI3K inhibitors". They have been extensively used in pre-clinical research but never translated into human trials. Newer agents with more favourable pharmacokinetic and toxicity profiles have subsequently been developed (Porta, Paglino, & Mosca, 2014).

Dual PI3K/mTOR inhibitors have now been trialled in a number of human cancers, with a meta-analysis of 46 of these RCT's demonstrating that addition of PI3M/mTOR inhibitors to the therapy of patients with advanced solid tumours significantly improves PFS (X. Li et al., 2018). With such clear benefits demonstrated in adult cancer populations it makes sense that paediatric tumours, such as NBL, may also benefit. Accordingly, PI3K/mTOR inhibitors such as LY3023414 are currently being investigated in early phase studies in paediatric patients with relapsed or refractory advanced solid tumours (A Pediatric MATCH treatment trial; NCT03213678).

NBL is the most common extra-cranial solid tumour in paediatrics (J. M. Maris et al., 2007), and the most commonly identified somatic mutation involves the ALK tyrosine kinase receptor gene (Pugh et al., 2013). Pre-clinical studies in *MYCN* amplified, ALK-mutated NBL have shown that crizotinib, an ALK inhibitor currently being trialed in human NBL, is more effective when used in combination with a dual PI3K/mTOR inhibitor than when used with an ATP-competitive mTOR inhibitor alone (N. F. Moore et al., 2014) confirming that the addition of PI3K/mTOR inhibitors may be beneficial in the most commonly mutated forms of NBL.

The immune checkpoint inhibitors ipilimumab, nivolumab and pembrolizumab are three immunotherapy drugs that have been approved for the treatment of advanced melanoma (Karlsson & Saleh, 2017) showing significant clinical benefits in this patient population. The addition of anti-GD2 based immunotherapy has been shown to significantly increase the OS of high risk NBL patients (1.6.5) (A. L. Yu et al., 2010) and is now considered standard of care. It has been established that the efficacy of cancer immunotherapies depends on priming and generation of tumour neo-antigen specific T cells that can mediate effector functions against tumour cells (Wherry & Kurachi, 2015). Combining immunotherapy with PI3K/mTOR inhibitors may improve the efficacy of immunotherapies by virtue of their immunomodulatory capacity (Smyth, Ngiow, Ribas, & Teng, 2016) which further supports their potential role in the treatment of NBL.

PF-502 is an ATP-competitive dual PI3K/mTOR inhibitor with excellent oral bioavailability. PF-502 inhibits full length human PI3Kα kinase activity with a Ki value of 1.2nM, and human mTOR kinase activity with a Ki value of 9.1nM. PF-502 inhibits the mouse PI3Kα kinase activity with a value of 1.7nM, which is similar to that seen in humans (H. Cheng et al., 2013).

This chapter investigates the role of combined PI3K/mTOR inhibition in paediatric NBL using the dual inhibitor PF-502. PF-502 has a dual role in the TH-*MYCN* mouse

model in that it promotes both apoptosis and has a significant anti-angiogenic effect. When the impact of its pro-apoptotic mechanisms is abrogated by BCL2 overexpression, there is still a survival benefit observed due to its anti-angiogenic effect.

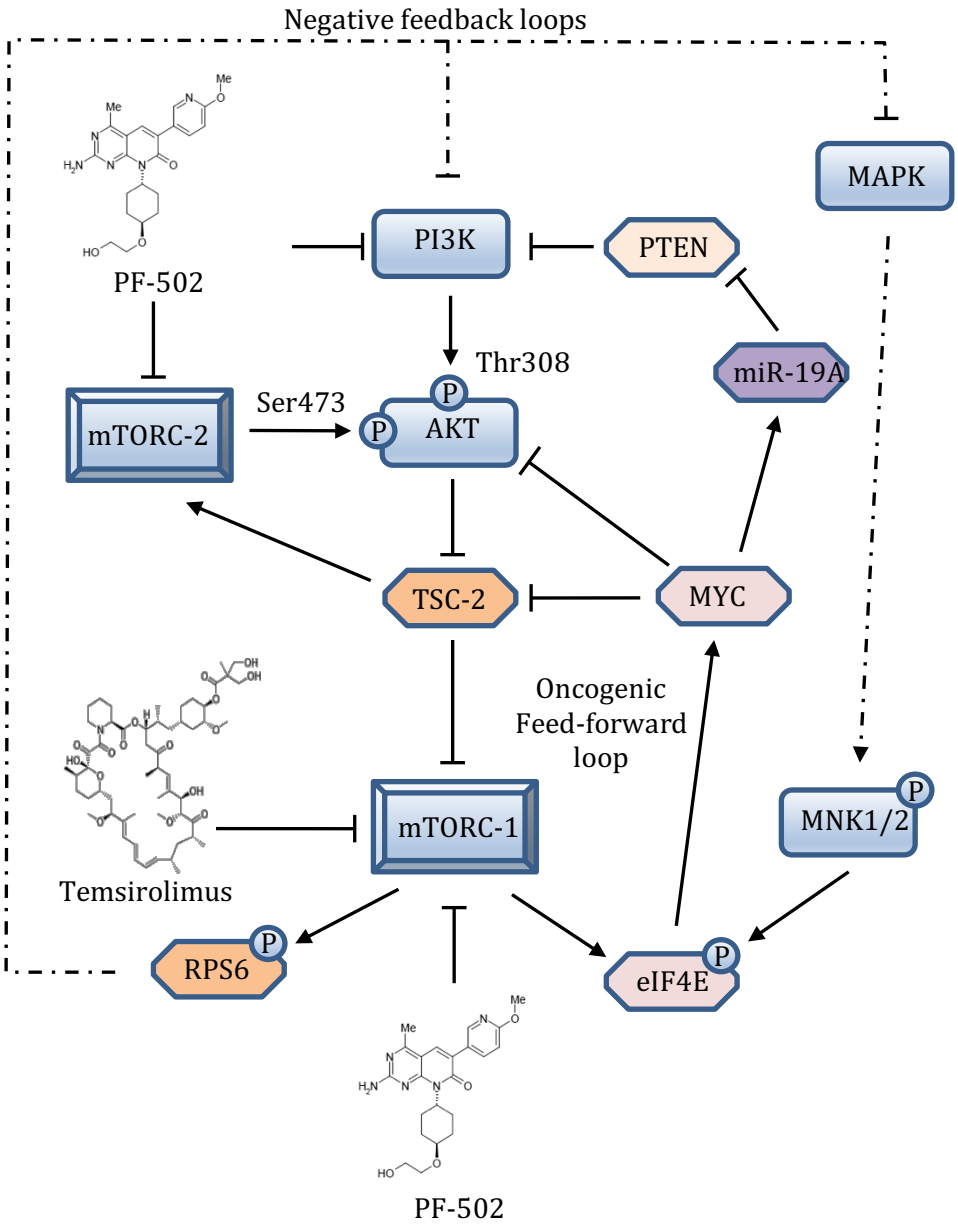

Figure 13 Schematic representation of the potential effects of PF-502, temsirolimus and MYC on the PI3K/AKT/mTOR pathway.

Myc dysregulation promotes mTORC1 signalling via multiple mechanisms including repression of TSC2 and AKT. The net result is activation of mTORC1 signalling and promotion of 5'cap-dependent translation. mTORC1 inhibition (temsirolimus) relieves the negative feedback, via RPS6, to promote PI3K/AKT activity and cross talk with the MAPK pathway. Dual mPI3K/mTOR inhibition (PF-502) in theory should suppress this feedback that occurs in response to mTORC1 inhibition.

3.2. Results for human tissue analysis

3.2.1. Patient characteristics of human neuroblastoma tissue samples

Thirty-seven patient samples were identified from the RCH Haematology and Oncology database that had tissue samples that included fresh frozen tissue (FFT) & paraffin embedded tissue. These were from 22 females and 15 males with the average age at diagnosis of 2.6 years (0.3-7.3 years). The overall mortality in this group was 47% (Table 5).

Patient Stage	Number	NMyc amplified	Mortality
I	3	0	0%
II	4	0	25%
III	7	0	29%
IV	24	12/24 (50%)	67%
IVS	3	0	0%

Table 5 Patient characteristics

Patient characteristics of 37 NBL patients with varying disease stages. As expected the majority of patients had Stage IV disease which was consistent with previously published data, with 50% of these patients having *MYCN* amplification (J. M. Maris et al., 2007). The mortality rate of 67% in the Stage IV patients was consistent with published data in the pre-immunotherapy era (Katherine K. Matthay et al., 2016).

Of these, eight patients were referred to PMCC between October 2008 and January 2012 for consideration of Gallium-68 DOTA-Octreotate (GaTATE) therapy. The average age at diagnosis of these patients was 2.7 years (0.5-5.3 years). The average age when they were referred to Peter MacCallum Cancer Centre was 5.4 years (2.0-8.2 years). These HR patients are often treated with multiple cycles of salvage therapy after they relapse, which may include radiation therapy, prior to being referred to PMCC.

Seven patients had stage IV (HR) disease and one patient had stage III, (IR) disease. Of these seven patients, five patients had paraffin embedded tissue available for IHC. All Stage IV patients would have been heavily pre-treated prior to referral to PMCC (1.6).

These patients were identified and their tumour samples were requested, as part of a project looking at the experience of GaTATE therapy in relapsed neuroblastoma patients from Melbourne, Australia (Kong et al., 2016). These human neuroblastoma tissue samples were interrogated for IHC evidence of activation of the PI3K/mTOR pathway.

The diagnosis of NBL is typically made with either a biopsy of the primary tumour or the presence of bone marrow disease with positive urinary catecholamine metabolites. Therefore, in some instances, the only available tumour sample was from a bone marrow trephine.

3.2.2. **Patient example. Primary abdominal and relapsed tumour.**

This patient was diagnosed at 20 months of age with a large inoperable, retroperitoneal abdominal NBL, with metastasis to liver, bone marrow, cortical bone and lymph nodes. The tumour was N-Myc negative. She commenced on standard chemotherapy which included six cycles of induction therapy. Evaluation imaging after four cycles was consistent with a partial response. At that stage an additional

six cycles of salvage therapy, including topotecan, was administered. Topotecan has been shown to be effective in relapsed NBL (Ashraf, Shaikh, Gibson, Baruchel, & Irwin, 2013) and is now incorporated in upfront induction therapy. Imaging and bone marrow aspirates confirmed that the skeletal and bone marrow disease had resolved; however, the liver and retroperitoneal disease was still active.

At this point in time the patient was referred to PMCC for consideration of MIBG therapy. Two doses of MIBG therapy, 2000MBq and 1890 MBq were delivered with a confirmed partial response. At this point in time, given the intensity of the treatment to date, a decision was made to observe the patient.

Two years later, imaging confirmed progressive disease with multiple osseous and nodal recurrences. Thirteen cycles of salvage chemotherapy, which included irinotecan and temozolomide were given with a partial response. This combination of chemotherapy was shown to be well tolerated in relapsed patients with a reasonable response rate (Bagatell et al., 2011). It has subsequently been combined with anti-GD2 therapy as the standard of care in relapsed NBL (Mody et al., 2017). Following this, and five years after initial diagnosis, a further biopsy, which confirmed active disease, and then the residual retroperitoneal tumour was partially removed (4.2.5).

A subsequent cycle of stem cell supported chemotherapy was administered, followed by one additional cycle of irinotecan and temozolomide before being referred for LuTate therapy.

Despite being a candidate for GaTate therapy, the patient progressed quickly and instead received palliative radiation therapy and oral melphalan. The patient passed away in 2010, six years after diagnosis.

A (i) (ii)

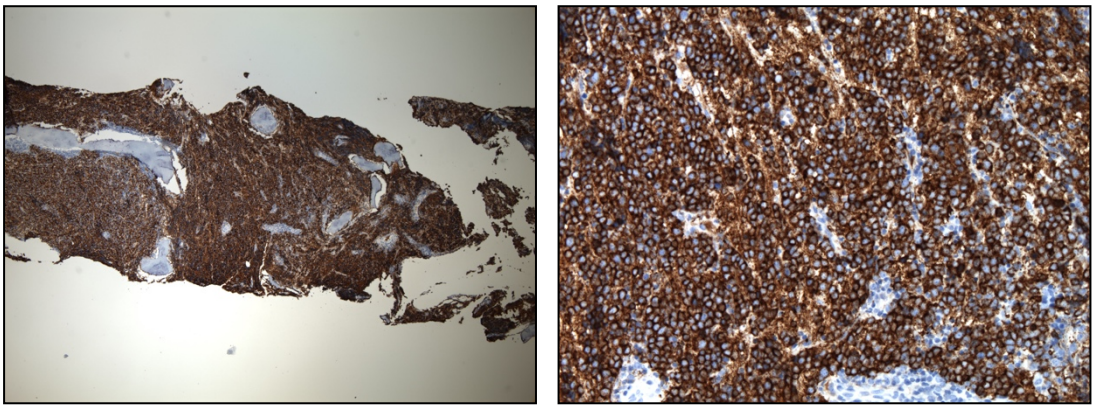

B (i) (ii)

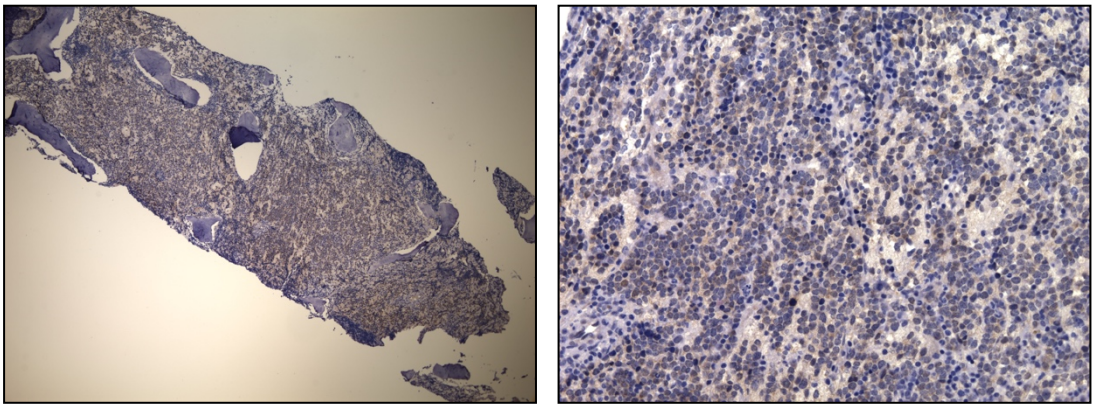

C (i) (ii)

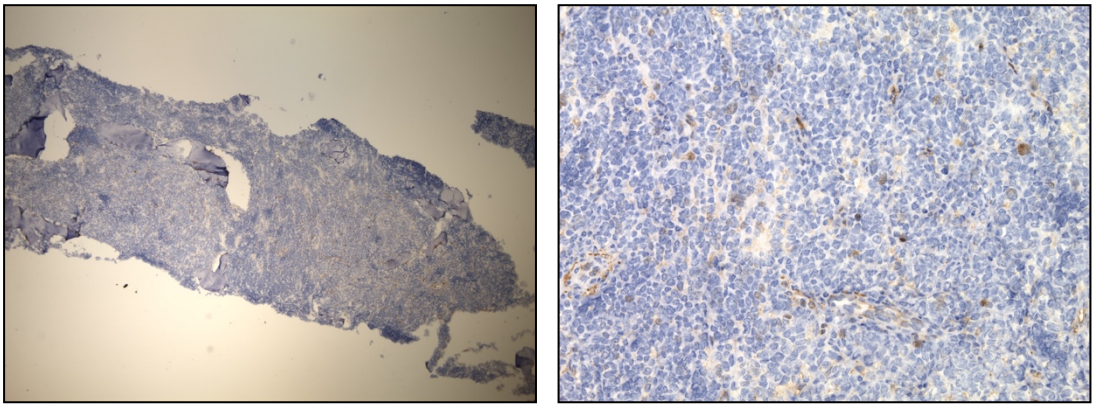

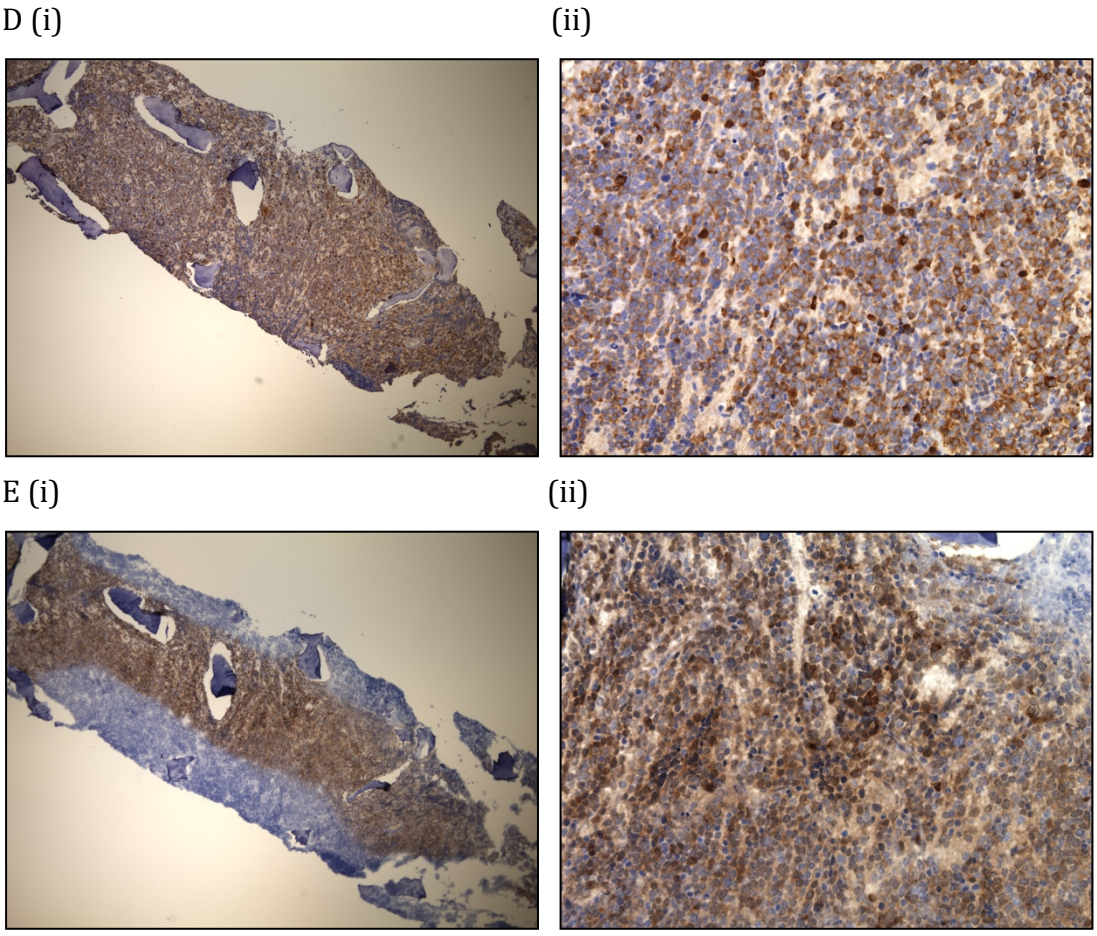

Figure 14 Immunohistochemistry of a primary abdominal tumour

Once embedded in paraffin the tissue was the sliced to 4-micron thickness and placed on glass slides. Tissue was probed via immunohistochemistry as previously described for chromogranin and for biomarkers of the PI3K/AKT/mTOR pathway including included A (i) Chromogranin x 4 (ii) Chromogranin x 20, B (i) pAKT (ser473) x 4 (ii) p AKT (ser473) x 20, C (i) p ERK (Thr202/Tyr204) x 4 (ii) p ERK (Thr202/Tyr204) x 20, D (i) pS6 (ser235/236) x 4 (ii) pS6 (ser235/236) x 20, E (i) p4EBP1 (Thr37/46) x 4 (ii) p4EBP1 (Thr37/46) x 20.

3.2.3. **Relapsed tumour.**

IHC performed on the relapsed tumour as described in (3.2.2).

A (i) (ii)

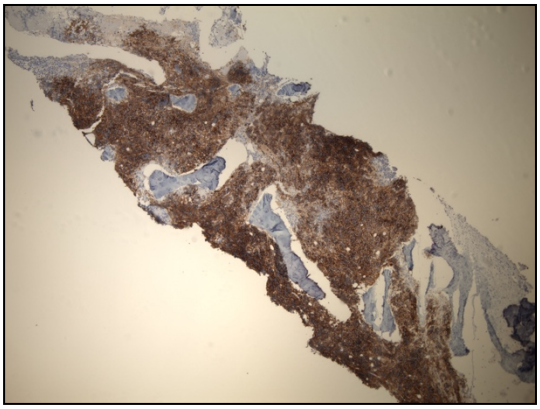
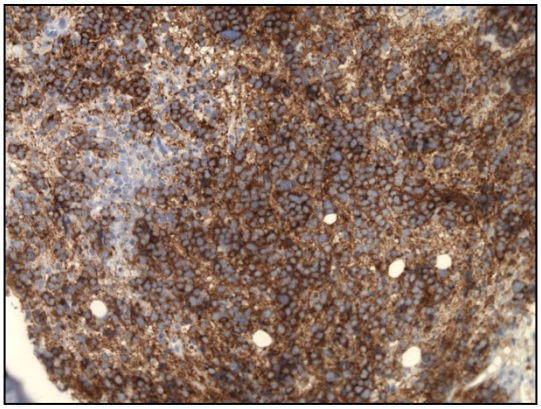

B (i) (ii**)**

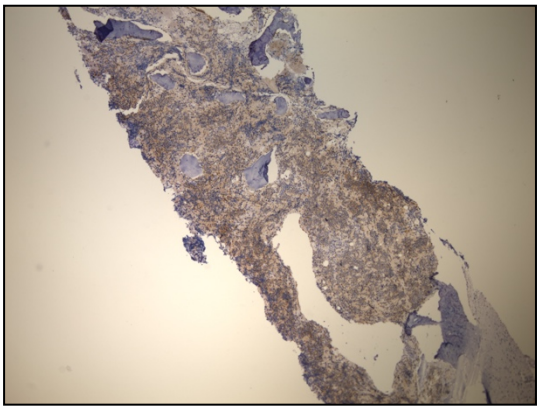
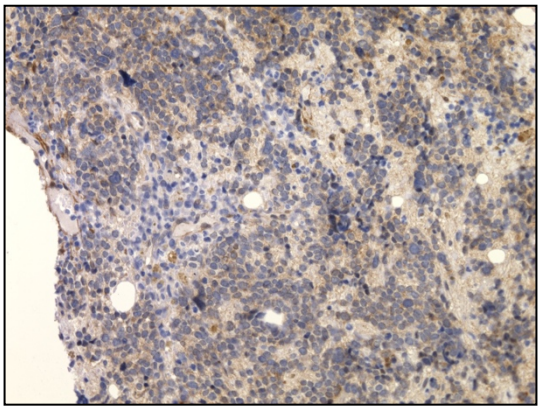

C (i) (ii)

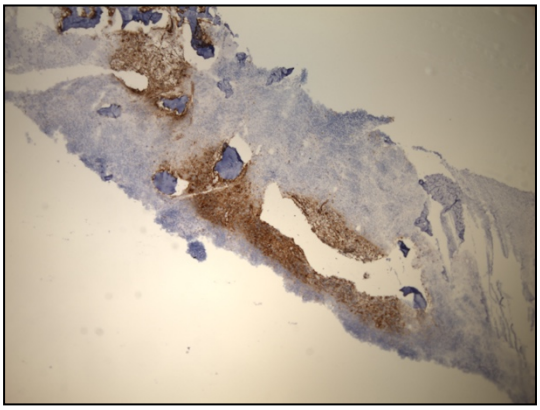
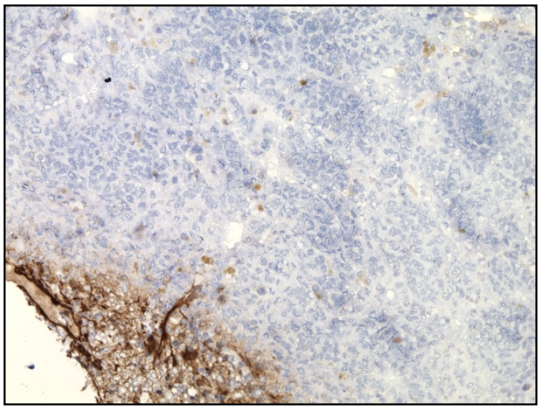

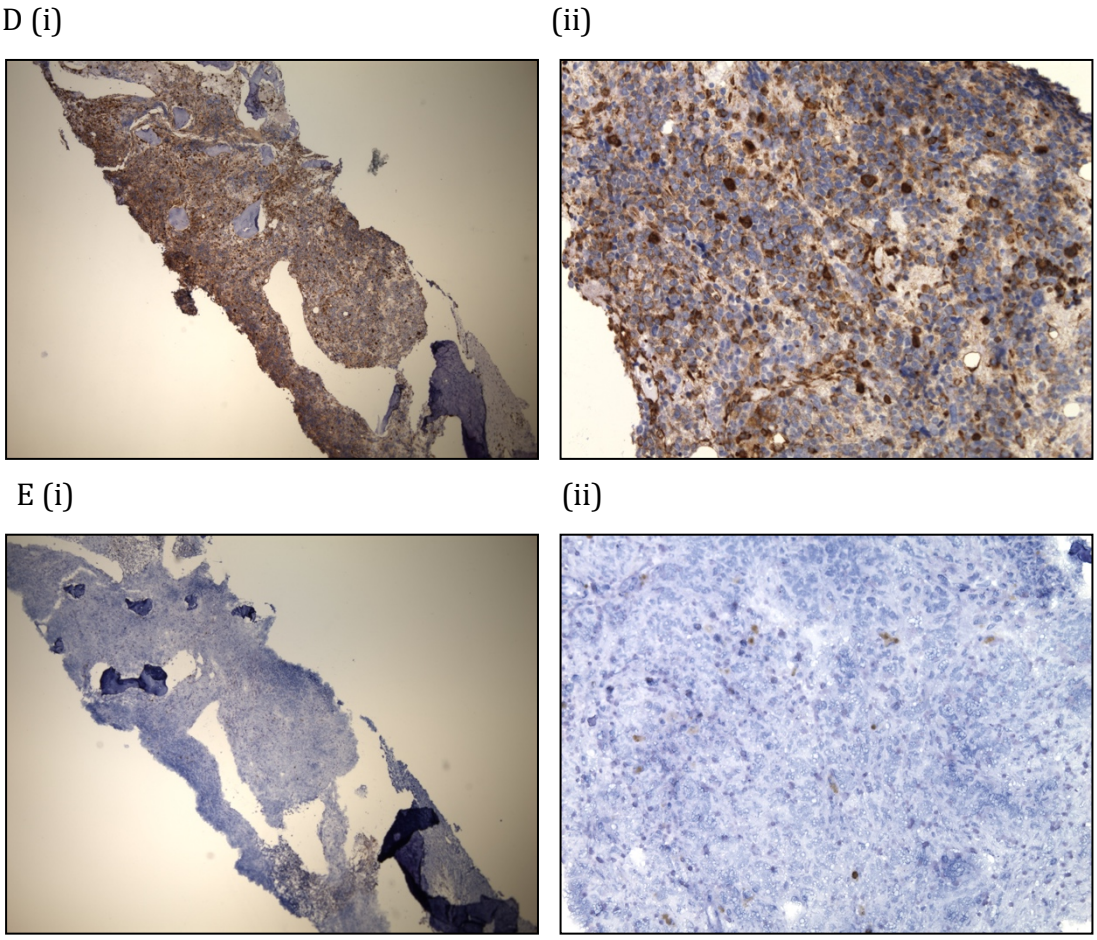

Figure 15 Immunohistochemistry of the relapsed tumour

Once embedded in paraffin the tissue was the sliced to 4-micron thickness and placed on glass slides. Tissue was probed via immunohistochemistry as previously described for chromogranin and for biomarkers of the PI3K/AKT/mTOR pathway including included A (i) Chromogranin x 4 (ii) Chromogranin x 20, B (i) pAKT (ser473) x 4 (ii) p AKT (ser473) x 20, C (i) p ERK (Thr202/Tyr204) x 4 (ii) p ERK (Thr202/Tyr204) x 20, D (i) pS6 (ser235/236) x 4 (ii) pS6 (ser235/236) x 20, E (i) p4EBP1 (Thr37/46) x 4 (ii) p4EBP1 (Thr37/46) x 20.

3.2.4. **Summary of immunohistochemistry staining.**

Slides were independently scored by a PMCC pathologist using a quantitative scoring system according to intensity and distribution of staining (Table 6) (Yan et al., 2012). Chromogranin has been validated as a marker of neuroendocrine tumours, including neuroblastoma, and is particularly useful in identifying patchy disease such as is observed in bone marrow samples (Georgantzi et al., 2018).

Patient	Chromogranin	pAKT	pERK	pS6	P4EBP1
1	3 +	2 +	2 +	3 +	3+
2	1 +	2 +	3 +	3 +	0 +
3 Primary	3 +	2 +	1 +	2 +	3 +
3 Relapse	3 +	2 +	2 +	3 +	1 +
4	3 +	2 +	3 +	3 +	3 +
5	2 +	2 +	3 +	3 +	2 +

0 + No staining

1 + Minimal staining

2 + Moderate staining

3 + Diffuse, intense staining

Table 6 Summary of IHC staining for patient samples

Five patients, representing six samples (one patient with primary and relapsed samples), were scored for IHC staining of members of the PI3K/AKT/mTOR pathway. All tumour samples demonstrated intense staining (3+) of at least one member of the PI3K/AKT/mTOR pathway.

3.3.**mTOR inhibition in the TH-MYCN neuroblastoma mouse model**

3.3.1. **The mTOR inhibitor temsirolimus treatment induces an incomplete cytostatic response with an associated G1/G0 phase cell cycle arrest**

When temsirolimus was added to human neuroblastoma cell lines in increasing concentrations there was incomplete cell death up to concentrations of 10,000 nM. This predominantly cytostatic response was observed in both *MYCN* amplified IMR32 cells as well as *MYCN* single copy SK-N-SH cells (Figure 16). This is consistent with published data using everolimus in human NBL cell lines which demonstrated that all cell lines tested, both *MYCN* amplified and *MYCN* single copy, were insensitive to everolimus based purely on IC_{50} data (Lang & Sandoval, 2014).

(A)

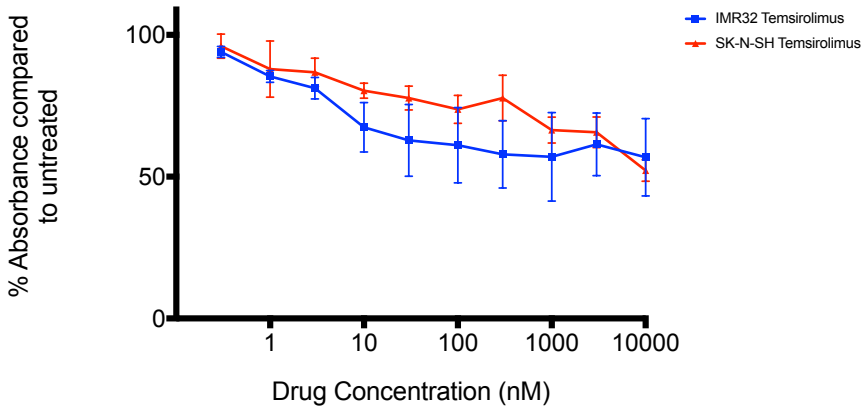
IMR32 Temsirolimus
SK-N-SH Temsirolimus
% Absorbance compared to untreated
100
50
0
1
10
100
1000
10000
Drug Concentration (nM)

(B)

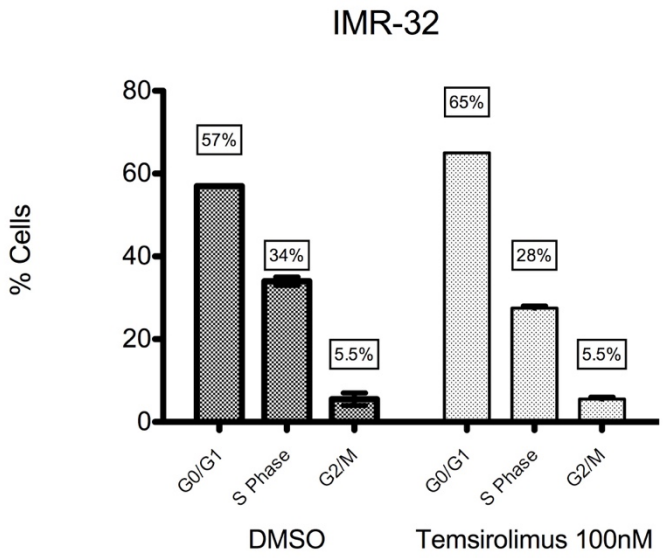
IMR-32
% Cells
80
60
40
20
0
57%
34%
5.5%
65%
28%
5.5%
G0/G1
S Phase
G2/M
G0/G1
S Phase
G2/M
DMSO
Temsirolimus 100nM

Figure 16 Efficacy of Temsirolimus established in human neuroblastoma cell lines

(A) Human IMR32 (*MYCN* amplified) and SK-N-SH (*MYCN* single copy) cells were cultured in 96 well plates and appropriate media (2.2.2.1 & 2.2.2.2) for 24 hours prior to addition of drug. Temsirolimus was added in escalating doses and cells were left exposed for 72 hours. Plates were incubated at $37^{O}C$, 5% CO_2. Plates were processed after 72 hours according to our standard SRB protocol (2.4). Absorbance of SRB was determined as a measure of cell number. Data was processed, and drug curves processed by Prism software. (B) FACS analysis of IMR32 cells exposed to 100nM of Temsirolimus for 72 hours. Cells were fixed and harvested according to the standard FACS protocol (2.5). Temsirolimus induced a significant G_0/G_1 cell cycle arrest when compared to DMSO. Experiments were performed in triplicate and data expressed as mean (+/- SEM), $p<0.05$, Students *t*-test.

3.3.2. **Temsirolimus inhibits the mTOR pathway in an equivalent manner to other mTOR inhibitors**

3.3.2.1. ***In vitro inhibition in human NBL cell lines***

In order to determine if temsirolimus was indeed acting as an mTOR inhibitor in its own right, and in an equivalent manner to other mTOR inhibitors as evidenced by its biomarker activity, it was compared to the several known inhibitors of mTOR at equivalent dosing. Temsirolimus did inhibit the downstream biomarkers of mTOR, phospo-S6 and phospo-4EBP1 in a manner equivalent to the mTORC1 inhibitors everolimus and sirolimus and the combined PI3K/mTOR inhibitor PF-502 (Figure 17).

3.3.2.2. ***In-vivo inhibition in the TH-MYCN mouse model***

This inhibition of mTORC1 was then confirmed *in-vivo*. Prior to this, tolerability studies were performed that confirmed a dose of 30mg/kg weekly was tolerated (Figure 18). TH-*MYCN* mice exposed to a single dose of temsirolimus 30mg/kg, and then harvested three hours later, had a reduction in the expression of both phospo-S6 and phospho-4EBP1 when compared to vehicle treated mice (Figure 19).

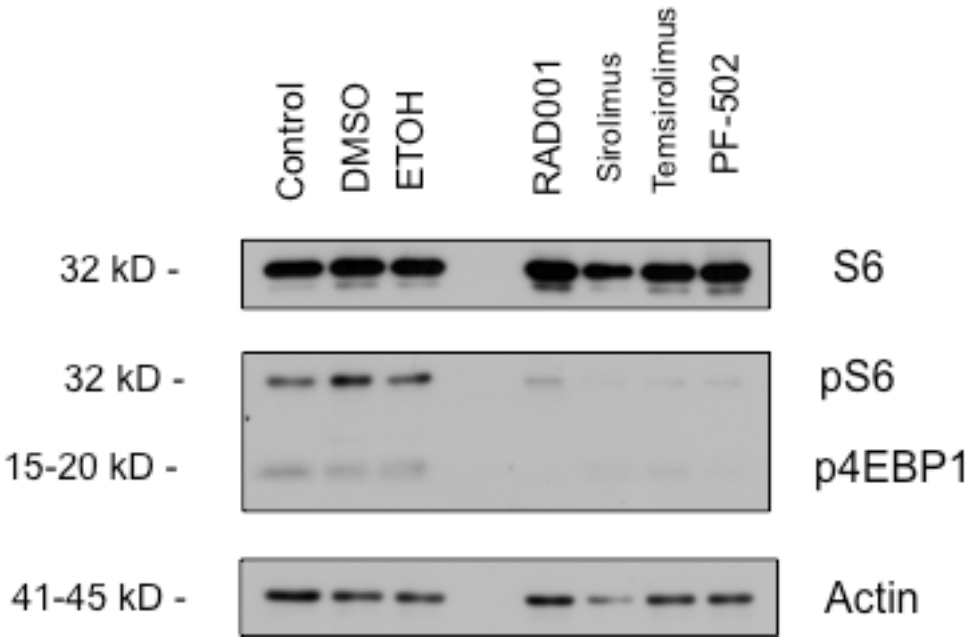

Figure 17 Western Blot (WB) analysis of protein lysates from IMR32 cells exposed to varying mTORC1 inhibitors, and the combined PI3K/mTOR inhibitor PF-502 at IC_{70} concentrations.

IMR32 cells were exposed to IC_{70} concentrations of Everolimus (RAD001), Sirolimus, Temsirolimus and PF-502 and their corresponding vehicles for 3 hours. WB membranes were probed for biomarkers of mTORC1 activity included total S6, phospo-S6 (ser240/244), & phosphor-4EBP1 (Thr37/46). Actin was used as a loading control. IC_{70} concentrations of all inhibitors used was associated with a decrease in biomarkers including pS6 (ser240/244) and p4EBP1 (Thr37/46) indicating that these pathways had been inhibited. Experiments were performed in triplicate.

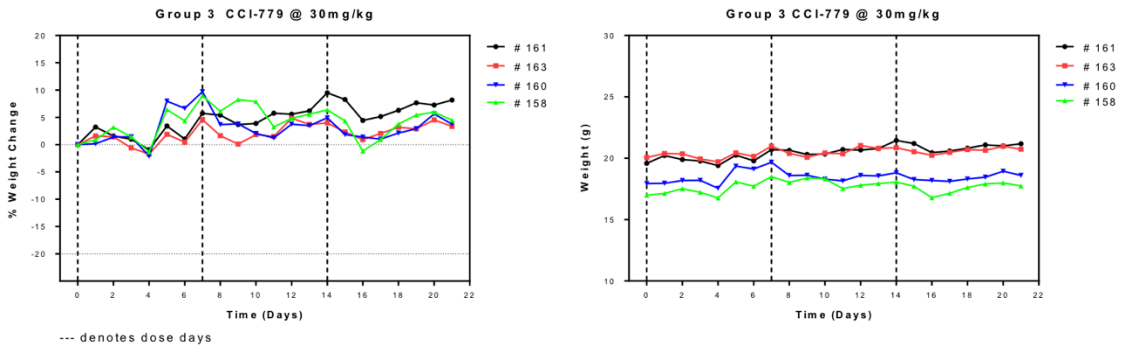

Figure 18 Maximum tolerated dose (MTD) of temsirolimus in TH-*MYCN* mice

Confirm tolerability of the temsirolimus (CCI-779) in TH-*MYCN* WT non-tumour bearing mice. Dose escalations are continued until a tolerable dose has been defined. Mice were weighed and inspected for signs of distress daily. Weight loss of more than 20% from baseline defined toxicity. Mice found to be in distress were carefully monitored and sacrificed, if required, to avoid distress. A dose of 30mg/kg given intravenously once weekly was deemed tolerable. Each line represents a mouse.

(A) (i)

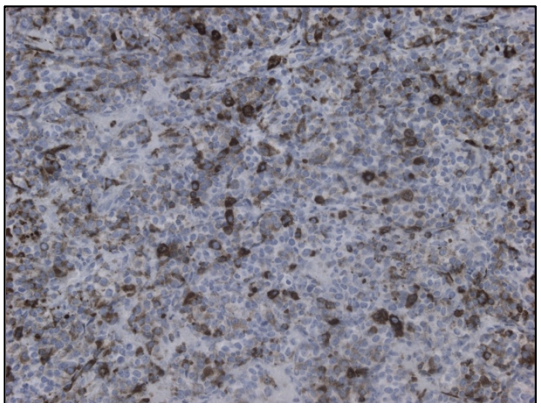

(ii)

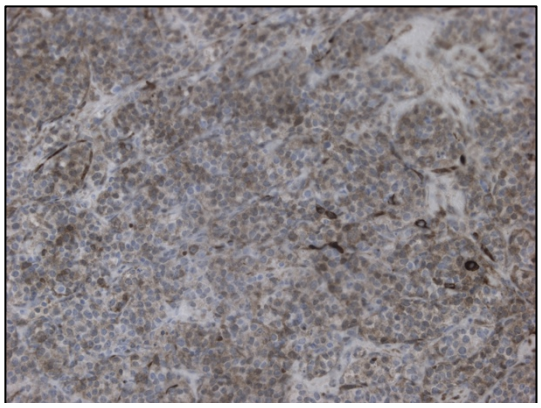

(B) (i)

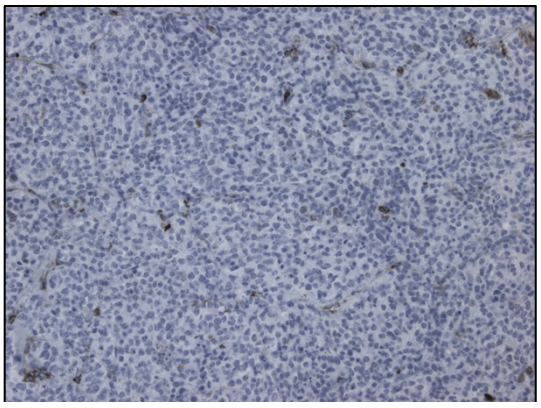

(ii)

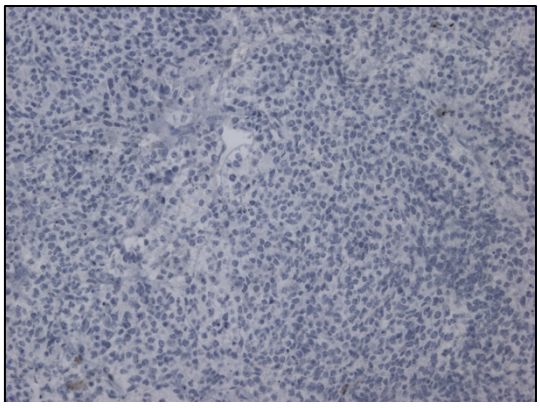

Figure 19 Immunohistochemistry of tumours exposed to a fixed dose of temsirolimus and harvested at 3 hours

Mice homozygous for the TH-*MYCN* transgene were identified and underwent ultrasound to confirm the presence of abdominal tumour. Mice then received, by tail vein injection, (A) 4% ethanol; 2% Tween 80; 5% PEG 400 in dextrose 5% (D5W) (vehicle) (n=5) of (B) Temsirolimus 30mg/kg (n=6). Tumours were harvested at 3 hours and fixed in 10% neutral buffered formalin (NBF). Once embedded in paraffin the tissue was the sliced to 6-micron thickness and placed on IHC glass slides. Tissue was probed via immunohistochemistry for biomarkers of the PI3K/AKT/mTOR pathway including included (i) pS6 (Ser235/236) x 20 & (ii) p4EBP1 (Thr37/46) x 20. A visual reduction in the distribution and intensity of staining was noted for both pS6 (Ser235/236) and p4EBP1 (Thr37/46) indicating that the PI3K/AKT/mTOR pathway had been inhibited.

3.3.3. **Efficacy of Temsirolimus in TH-MYCN transgenic murine model**

Having established that the PI3K/AKT/mTOR pathway is active in a small sample of human neuroblastomas both at initial diagnosis and at relapse (3.2) and knowing that temsirolimus was able to abrogate biomarkers of this pathway effectively (Figure 20), a survival analysis was performed in the TH-*MYCN* mouse model. As stated earlier (1.7), this model recapitulates the human NBL phenotype accurately both in its behaviour and chromosomal changes.

When mice were exposed to weekly doses of temsirolimus it conferred a significant survival advantage (Figure 20A). Concurrent ultrasound scans performed also demonstrated an initial reduction on tumour volume, which remained relatively static, until the temsirolimus was ceased at day 35 (Figure 20B). This was consistent with a partial response according to the International NBL response criteria (INRC) (J. R. Park et al., 2017). However, when dosing was ceased at day 35, 100% of mice relapsed quickly and then died in a timeframe similar to the vehicle control mice.

(A)

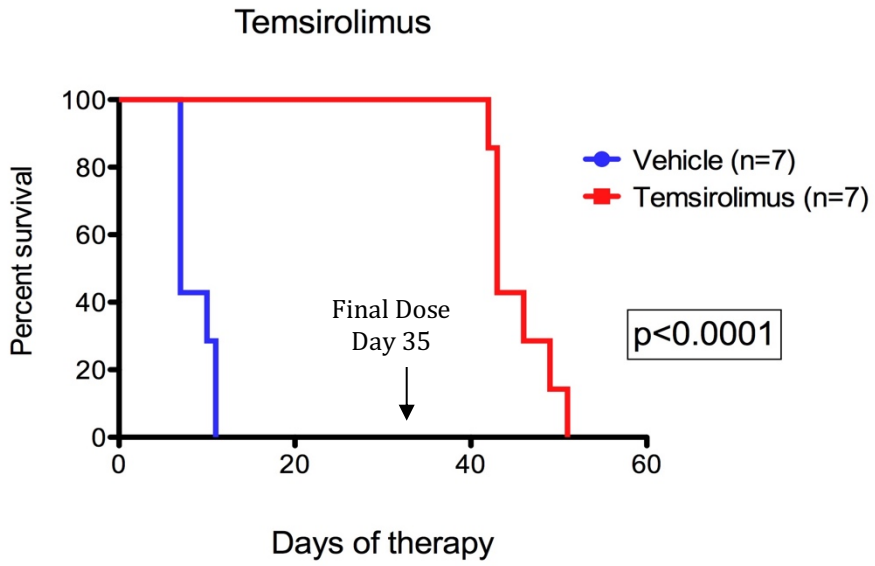

(B)

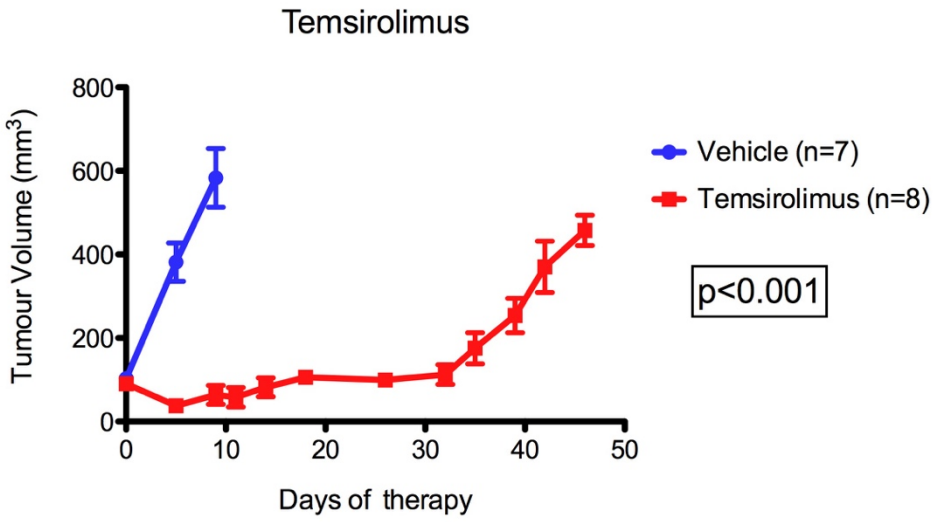

Figure 20 Efficacy of Temsirolimus in TH-*MYCN* transgenic murine model

(A) A significant difference in survival in mice treated with temsirolimus 30mg/kg when compared with 4% ethanol; 2% Tween 80; 5% PEG 400 in D5W (vehicle), ($p<0.0001$, one-way ANOVA) (B) A significant inhibition of tumour growth as evidenced by 3D tumour volumes (abdominal US), in mice treated with temsirolimus 30mg/kg when compared with 4% ethanol; 2% Tween 80; 5% PEG 400 in D5W (vehicle) ($p<0.001$, two-way ANOVA).

3.3.4. **Functional imaging as a marker of response**

Functional imaging has been validated as a useful tool in drug development (Waaijer et al., 2018), and has an established role in the assessment of tumour response in pre-clinical mouse models (Cullinane et al., 2005). Essentially, radio-labelled glucose is used as a measure of tumour metabolism and is therefore a measure of treatment effect. In NBL, as is the case with many solid tumours, a residual lesion will be present after a course of induction therapy. This typically requires surgical removal for complete local control. At the point of surgical resection the percentage of viable cells remaining in the tumour can often be a prognostic factor (Xin Li, Ashana, Moretti, & Lackman, 2011) and directly influence future therapies such as the need for radiation. In other cancers such as Hodgkin's lymphoma, FDG-PET has been validated and has become the standard of care in tumour response assessment (Subocz, Hałka, & Dziuk, 2017).

FDG-PET can be equally valuable in giving that researchers an indirect way of determining tumour viability in pre-clinical models. Within 48 hours of treatment with temsirolimus, TH-*MYCN* mice had significantly lower glucose uptake, and metabolic activity, when compared to vehicle treated mice (Figure 21). Given the tumour/background ratio compares glucose uptake in the tumour, to the glucose uptake in a background organ such as the liver, this indicates that although the tumour has had a significant reduction in metabolism, it is still more active than organs such as the liver.

The combination of small animal ultrasound and FDG-PET gives pre-clinical researches a way of assigning tumour response in a similar manner to that used in human clinical trials. In this case the combination of a significant but incomplete reduction in tumour volume with the partial metabolic response seen on FDG-PET would be consistent with a partial response as per the new International Neuroblastoma Response Criteria (INRC) (J. R. Park et al., 2017) (Figure 21).

(A)

Tumour/Background ratio 4.343

Temsirolimus

(B)

Tumour/Background ratio 1.475

(C)

Tumour/Background ratio 2.393

Vehicle

(D)

Tumour/Background ratio 3.757

(E)

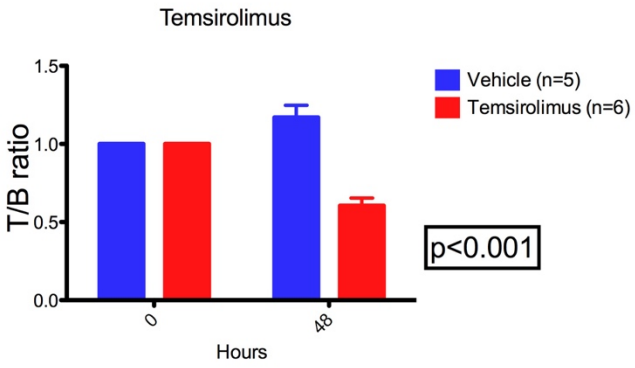

Figure 21 Efficacy of Temsirolimus in TH-*MYCN* transgenic murine model using FDG-PET

(A) FDG-PET image, showing central abdominal tumour, of TH-*MYCN* mouse treated with 30mg/kg temsirolimus at time 0 hours. (B) FDG-PET image, showing central abdominal tumour, of TH-*MYCN* mouse treated with 30mg/kg temsirolimus at time 48 hours. (C) FDG-PET image, showing central abdominal tumour, of TH-*MYCN* mouse treated with 4% ethanol; 2% Tween 80; 5% PEG 400 in D5W (vehicle) at time 0 hours. (D) FDG-PET image, showing central abdominal tumour, of TH-*MYCN* mouse treated with 4% ethanol; 2% Tween 80; 5% PEG 400 in D5W (vehicle) at time 48 hours. (E) A significant difference in FDG-PET avidity, as a measure of metabolism, over a 48-hour period in mice treated with temsirolimus when compared with vehicle ($p<0.001$, two-way ANOVA).

3.3.5. **N-Myc expression**

The NBL tumours that develop in the TH-*MYCN* mouse model of neuroblastoma are under the targeted expression of *MYCN* and are transgene dose dependent (Weiss et al., 1997). In addition, the importance of N-Myc as a negative prognostic factor in NBL has also been established (J. M. Maris et al., 2007). It therefore makes sense that any therapy that aims to effectively treat HR NBL must alleviate the transcriptional activities of *MYCN*.

TH-*MYCN* mice were treated with temsirolimus and had evidence or reduced *MYCN* expression three hours after the dose (Figure 22). Although the expression was clearly reduced, it was not complete. By reducing the *MYCN* expression, temsirolimus can also reduce the myriad of tumour promoting downstream targets of *MYCN* (1.4.1).

(A) (B)

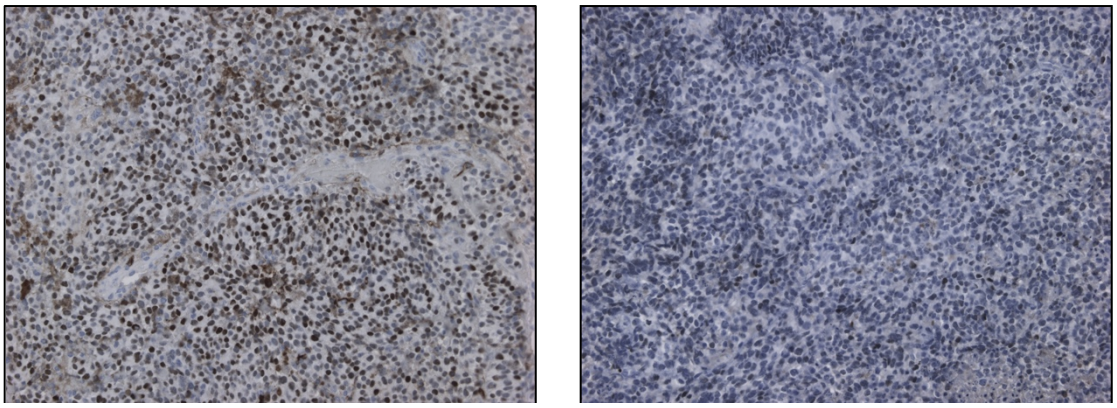

Figure 22 N-Myc in TH-*MYCN* transgenic murine model following treatment with temsirolimus

Mice homozygous for the TH-*MYCN* transgene were identified and underwent ultrasound to confirm the presence of abdominal tumour. Mice then received, by tail vein injection, (A) 4% ethanol; 2% Tween 80; 5% PEG 400 in D5W (vehicle) (n=5) or (B) 30mg/kg of temsirolimus (n=6). Tumours were harvested at 3 hours and fixed in 10% neutral buffered formalin (NBF). Once embedded in paraffin the tissue was the sliced to 6-micron thickness and placed on glass slides. Tissue was probed via immunohistochemistry for N-Myc (x 20). Temsirolimus treated mice had a visual reduction in *MYCN* expression at 3 hours.

3.3.6. **Temsirolimus and apoptosis**

In May 2007, temsirolimus received FDA approval for the treatment of advanced renal cell carcinoma (RCC). In a phase III clinical trial involving 626 patients with advanced RCC and poor prognosis temsirolimus significantly prolonged OS by 49% compared to interferon-α (Hudes et al., 2007). This improvement in overall survival has also been seen in other retrospective analysis (Afshar, Pascoe, Whitmarsh, James, & Porfiri, 2015).

In most pre-clinical solid tumour models mTOR inhibitors such as temsirolimus were primarily cytostatic, did not induce significant apoptosis, but had significant anti-angiogenic effects (Del Bufalo et al., 2006; Moriya et al., 2014; Yazbeck et al., 2006; H. Zhang et al., 2013). Apoptosis has been reported on occasion, primarily in pre-clinical liquid tumour models such as acute lymphoblastic leukemia (ALL) (Teachey et al., 2006).

TH-*MYCN* mice treated with temsirolimus were investigated for markers of apoptosis. On H&E staining, features of apoptosis include cell shrinkage and pyknosis or chromatin condensation. These are clearly visible on light microscopy (Elmore, 2007). There are currently 13 known caspases associated with apoptosis. The measurement of cleaved caspase-3 is perhaps the most validated marker and can be measured by WB analysis of protein samples (Porter & Janicke, 1999). The TUNEL method of measuring apoptosis identifies cells with DNA strand breaks *in situ* by using terminal deoxynucleotidyl transferase (TdT) to transfer biotin-dUTP to the cleaved ends of the DNA. These can be detected and visualised with appropriate staining (Elmore, 2007) and can differentiate between cell apoptosis and cell necrosis (Muppidi, Porter, & Siegel, 2004).

The half-life of temsirolimus is approximately 17 hours. It is then metabolised to sirolimus which has a half-life of 55 hours. This potentially provides a long window in which to probe for markers of apoptosis post dose. I have previously demonstrated

that the PI3K/mTOR pathway was impacted, as measured by phospo-S6 and phosphor-4EBP1 reduced expression, at 3 hours. However when apoptosis has been observed in pre-clinical models it was typically seen 12-24 hours after exposure to the drug (Teachey et al., 2006). Therefore, mice were harvested 24 hours after exposure to either temsirolimus or vehicle (4% ethanol; 2% Tween 80; 5% PEG 400 in D5W), and tumours probed for markers of apoptosis. Positive TUNEL staining, cleaved caspase-3 and the characteristic features of apoptosis on H&E were all absent in treated mice when compared to vehicle. This is consistent with previous literature suggesting apoptosis is not a hallmark of anti-tumour effect of temsirolimus (Figure 23).

(A) (i) (ii)

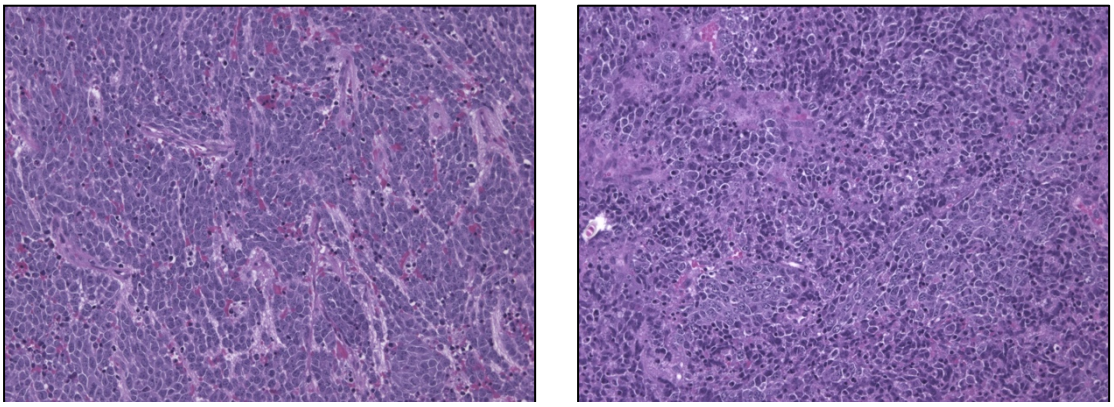

(B) (i) (ii)

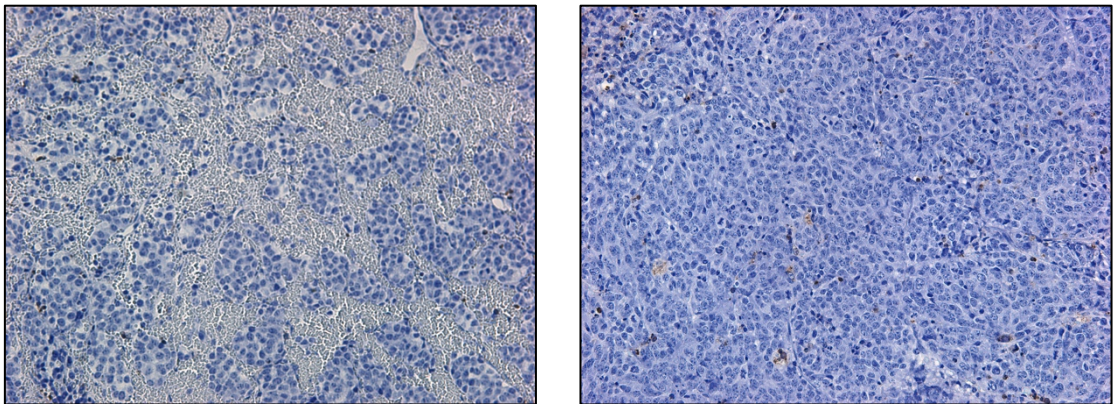

(C)

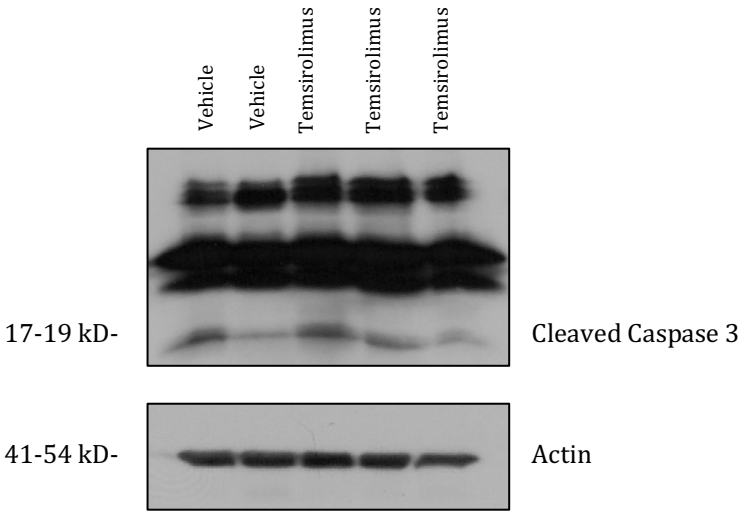
Vehicle
Vehicle
Temsirolimus
Temsirolimus
Temsirolimus
17-19 kD-
Cleaved Caspase 3
41-54 kD-
Actin

Figure 23 Apoptosis in TH-*MYCN* transgenic murine model

(A) H&E staining of spontaneous neuroblastoma that have been treated with a single dose of, (i) Temsirolimus 30mg/kg weekly via injection, (ii) 4% ethanol; 2% Tween 80; 5% PEG 400 in D5W (vehicle) and harvested 24 hours later (B) TUNEL staining of spontaneous neuroblastoma having been treated with a single dose of (i) Temsirolimus 30mg/kg via intravenous injection (ii) 4% ethanol; 2% Tween 80; 5% PEG 400 in D5W (vehicle) and harvested 24 hours later (x20) (C) Western blot analysis of tumour lysates demonstrate no significant increase in caspase 3 in TH-*MYCN* mice treated with a single dose of (i) Temsirolimus 30mg/kg via intravenous injection (ii) 4% ethanol; 2% Tween 80; 5% PEG 400 in D5W (vehicle) and harvested 24 hours later. Results do not demonstrate significant apoptosis in mice treated with temsirolimus when compared with vehicle treated mice.

3.3.7. **Temsirolimus and angiogenesis**

CD31, also known as platelet endothelial cell adhesion molecule-1 (PECAM1), acts as an endothelial cell marker (Tahergorabi & Khazaei, 2012). Specifically, CD31 is enriched at endothelial cell intercellular junctions where it regulates leukocyte trafficking, mechano-transduction, and vascular permeability (Lertkiatmongkol, Liao, Mei, Hu, & Newman, 2016). Accordingly measurement of CD31 can be used as an indicator of vascularity (Tahergorabi & Khazaei, 2012).

In pre-clinical models the primary mode of anti-tumour activity of temsirolimus has been repeatedly linked to anti-angiogenesis via impaired levels of VEGF and HIF-1α (Wan, Shen, Mendoza, Khanna, & Helman, 2006). A predominantly anti-angiogenic phenotype, in combination with the lack of apoptosis seen (4.3.6) would potentially explain the partial cytostatic effect of temsirolimus seen *in vitro* (4.3.1).

CD31 staining in temsirolimus mice confirmed a significant reduction in tumour vasculature when compared to vehicle treated mice ($p<0.001$), consistent with inhibition of angiogenesis (Figure 24).

(A) (B)

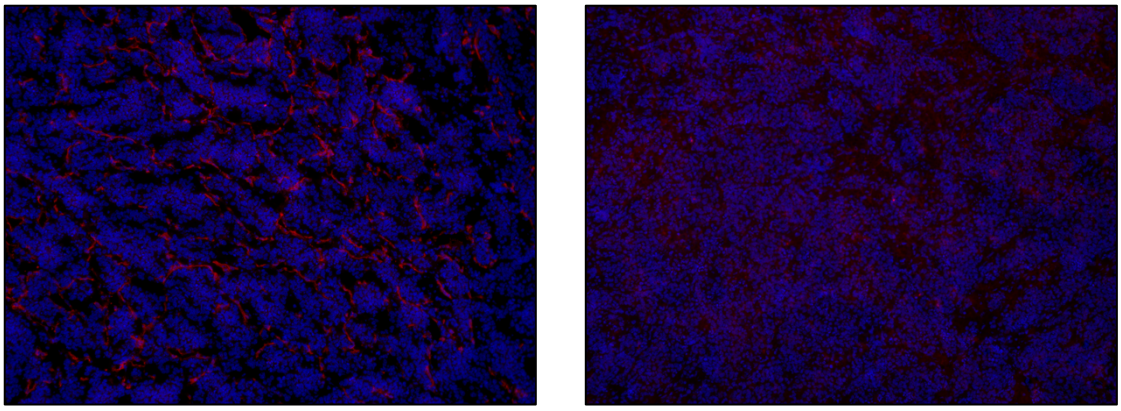

(C)

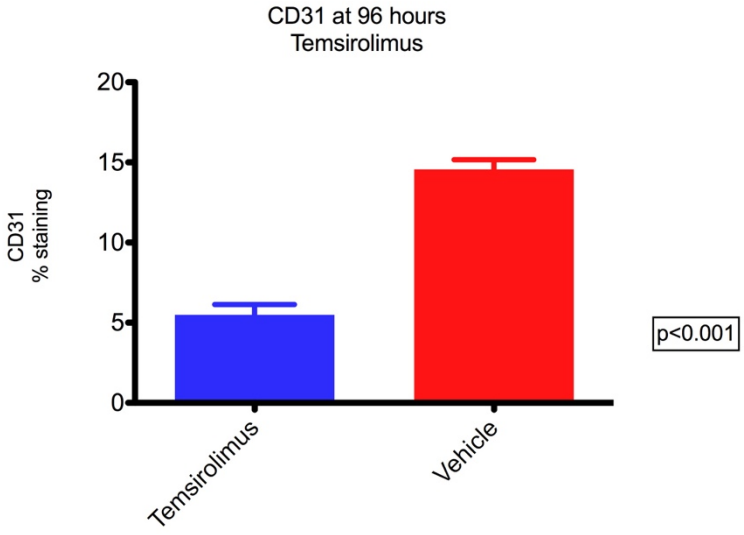

Figure 24 Angiogenesis in TH-*MYCN* transgenic murine model

(A) CD31 staining (red is endothelial) of spontaneous neuroblastoma having been treated for 96 hours with 4% ethanol, 2% Tween 80, 5% PEG 400 in 5% dextrose (vehicle) (n=3) 10ul/100g weekly via intra-venous injection or (B) Temsirolimus 30mg/kg weekly (n=3) via intra-venous injection (x20). (C) Quantitative metamorph analysis of CD31 staining of spontaneous neuroblastoma demonstrates a highly significant difference at 96 hours, in mice treated with Temsirolimus or vehicle, ($p<0.001$, Student *t*-test). This is consistent with Temsirolimus exerting a significant anti-angiogenic effect.

3.3.8. **Temsirolimus and senescence**

The mTOR pathway has been repeatedly implicated in cellular aging processes such as cellular senescence (B. Carroll et al., 2017; Soto-Gamez & Demaria, 2017; Weichhart, 2018). Indeed inhibition of mTORC1 extends life span by driving cellular senescence, although the exact mechanisms by which this occurs remains unclear (B. Carroll et al., 2017). It has also been shown to improve immune functions and reduce infections in the elderly (Mannick et al., 2018).

In pre-clinical cancer models such as lymphoma, the mTORC1 inhibitor everolimus (RAD-001) has been able to promote a cellular senescence phenotype (Wall et al., 2013). In this model, everolimus restored p53 activity and restored a normal pattern of B cell differentiation. In pre-clinical acute myeloid leukaemia models (AML) everolimus synergises with all trans retinoic acid (ATRA) to promote differentiation (Nishioka et al., 2009).

Cellular senescence is initiated in response to both intra-cellular and extra-cellular stresses. By "locking" cells in a state of senescence, this process prevents eventual malignant transformation of cells (Coppé, Desprez, Krtolica, & Campisi, 2010). In contrast, the process of differentiation transforms cells from a malignant phenotype to a more benign phenotype that more closely resembles the cell of origin (Waldeck et al., 2016). Differentiation has also been shown to be mTOR dependent in multiple pre-clinical models (Tyler et al., 2009; Zeng & Chi, 2017). Regardless, the distinction between cellular senescence and differentiation is not often clear (Rodier & Campisi, 2011; Tosh & Slack, 2002). Pre-clinical research in human NBL cells treated with ATRA often show two distinct phenotypic cell types; the well-differentiated NBL cells and a more "flattened" sub-clone of cells whose phenotype is more consistent with senescence. The difference between phenotypes may be the result of the interaction between $p21^{Cip1}$ and $p16^{INK4A}$ in response to ATRA. Over-expression of $p21^{Cip1}$ is associated with the differentiation phenotype and is due to sustained CDK activity in

NBL cell lines that do not show rapid cell cycle arrest (Wainwright, Lasorella, & Iavarone, 2001).

Autophagy and senescence are also closely related cellular processes and in fact may be activated in a sequential fashion, with autophagy preceding senescence, and initiating the secretion of senescence associated proteins (Kwon, Kim, Jeoung, Kim, & Kang, 2017). The interplay between these two cellular processes is complex. During oncogene induced senescence, autophagy generates recycled amino acids and other cellular metabolites which mTORC1 uses to generate the Senescence-Associated Secretory Phenotype (SASP) factors (C. Kang & Elledge, 2016). In the TH-*MYCN* model of neuroblastoma, mice exposed to temsorilimus for 96 hours showed significant expression of SA-β-Gal staining, consistent with induction of senescence (Figure 25).

(A) (B)

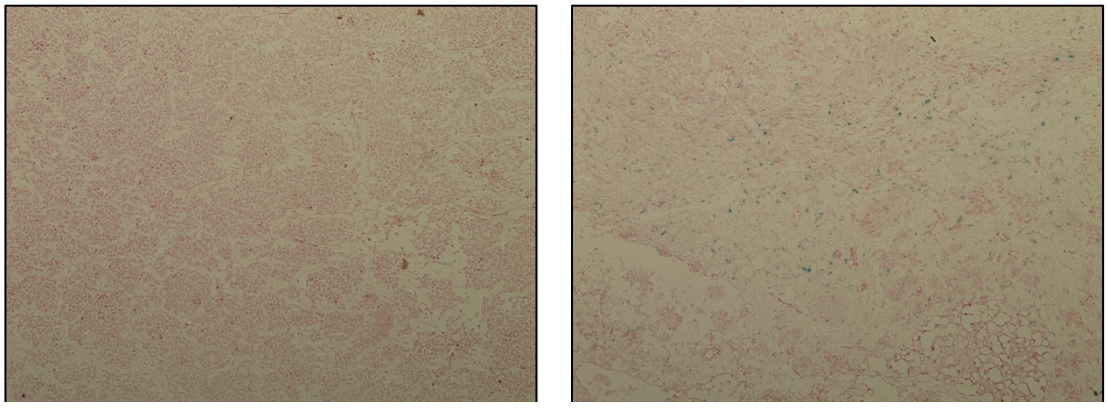

Figure 25 Senescence in TH-*MYCN* transgenic murine model

(A) SA-B-gal staining of spontaneous neuroblastoma having been treated for 96 hours with, (i) 4% ethanol, 2% Tween 80, 5% PEG 400 in 5% dextrose (vehicle) (n=3) 10ul/100g weekly via intra-venous injection or (ii) Temsirolimus 30mg/kg weekly (n=3) via intra-venous injection (x20). Increased Sa-β-gal staining is consistent with the induction of senescence.

3.4. Dual PI3K/mTOR inhibition in the TH-MYCN neuroblastoma mouse model

3.4.1. The dual PI3K/mTOR inhibitor PF-502 induces cell death with G1/G0 cell cycle arrest.

PF-502 treatment resulted in cell death with an IC_{50} of 300nM in IMR32 cells and 100nM in SK-N-SH cells (Figure 26) which is similar to published IC_{50} data B-cell lymphoma cell lines (D. Chen et al., 2016). This cell death was associated with a G_1/G_0 arrest (Figure 26) which is consistent with data published in other pre-clinical models (Herzog et al., 2013). Other combined PI3K/mTOR inhibitors such as BEZ-235, have been shown to induce a G_1/G_0 arrest in chronic myelogenous leukaemia (CML) (Xin et al., 2017) and glioma (Z. Yu et al., 2015) cell lines.

The observation that *MYCN* amplified IMR32 cells were less sensitive to combined PI3K/mTOR inhibition than *MYCN* single copy SK-N-SH cells was consistent with previously published data in NBL using BEZ-235 where the IC_{50} of IMR32 cells was tenfold that of SK-N-SH cells (Lang & Sandoval, 2014). This is contrary to data obtained when the small molecule PI3K inhibitor PI103 was used in NBL cell lines (Segerstrom et al., 2011).

(A)

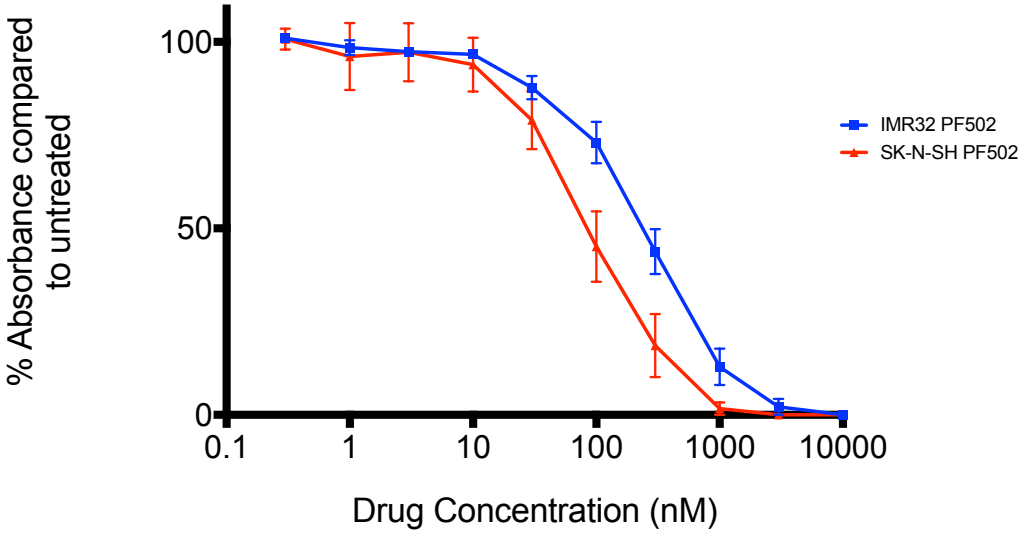
% Absorbance compared to untreated
100
50
0
0.1
1
10
100
1000
10000
Drug Concentration (nM)
IMR32 PF502
SK-N-SH PF502

(B)

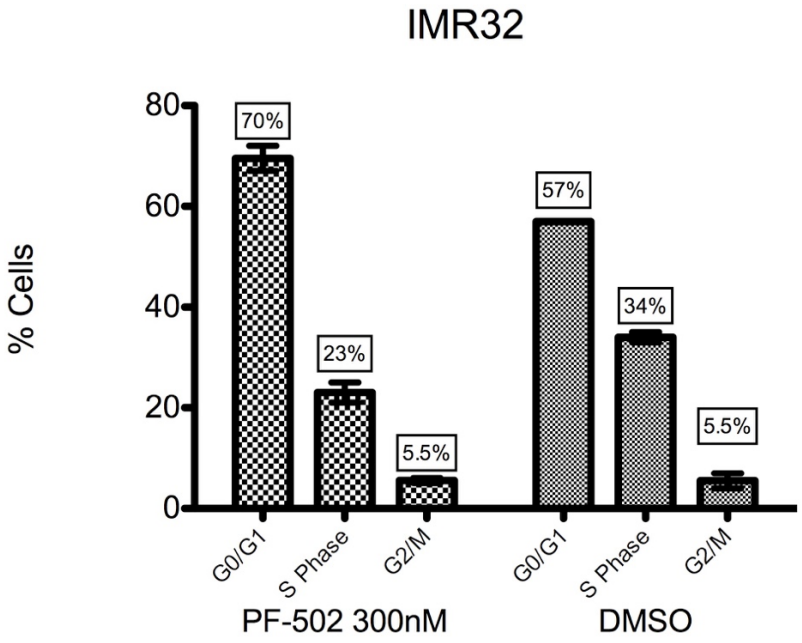
IMR32
% Cells
80
60
40
20
0
70%
23%
5.5%
57%
34%
5.5%
G0/G1
S Phase
G2/M
G0/G1
S Phase
G2/M
PF-502 300nM
DMSO

Figure 26 Efficacy of PF-502 established in human neuroblastoma cell lines

(A) IMR32 (*MYCN* amplified) and SK-N-SH (*MYCN* single copy) cells were cultured in 96 well plates and cell specific media for 48 hours prior to addition of drug. Drug was added in escalating doses and cells were left exposed for 72 hours. Plates were incubated at 37^0C, 5% CO2. Plates were processed after 72 hours according to our standard SRB protocol. Absorbance of SRB was determined as a measure of cell number. Data was processed, and drug curves processed by Prism software. (B) FACS analysis of IMR32 cells exposed to 300nM of PF-502 (IC50) for 72 hours. Cells were fixed and harvested according to the standard FACS protocol. PF502 induced a significant G_0/G_1 cell cycle arrest compared to DMSO ($p< 0.05$). Experiments were performed in triplicate and data expressed as mean (+/- SEM), $p<0.05$, Students *t*-test.

3.4.2. **PF-502 inhibits the PI3K/AKT/mTOR pathway in vitro**

When increasing concentrations of PF-502 were added to IMR32 human NBL cells, a dose dependent inhibition of the downstream targets phospo-S6 and phosphor-4EBP1 was observed. However, there was no apparent effect on the levels of phospo-AKT. Ideally AKT, which is downstream of PI3K, should also be inhibited with an associated down-regulation of phospho-AKT. This result was consistent with incomplete inhibition of the PI3K/AKT/mTOR pathway. However, using IHC in the TH-*MYCN* NBL model, a significant reduction in the expression of phospho-AKT was observed (Figure 29) consistent with previous studies that have demonstrated a reduction in the expression of phospho-AKT in response to PF-502 (D. D. Fang et al., 2013). Together these results are consistent with inhibition of the PI3K/AKT/mTOR pathway.

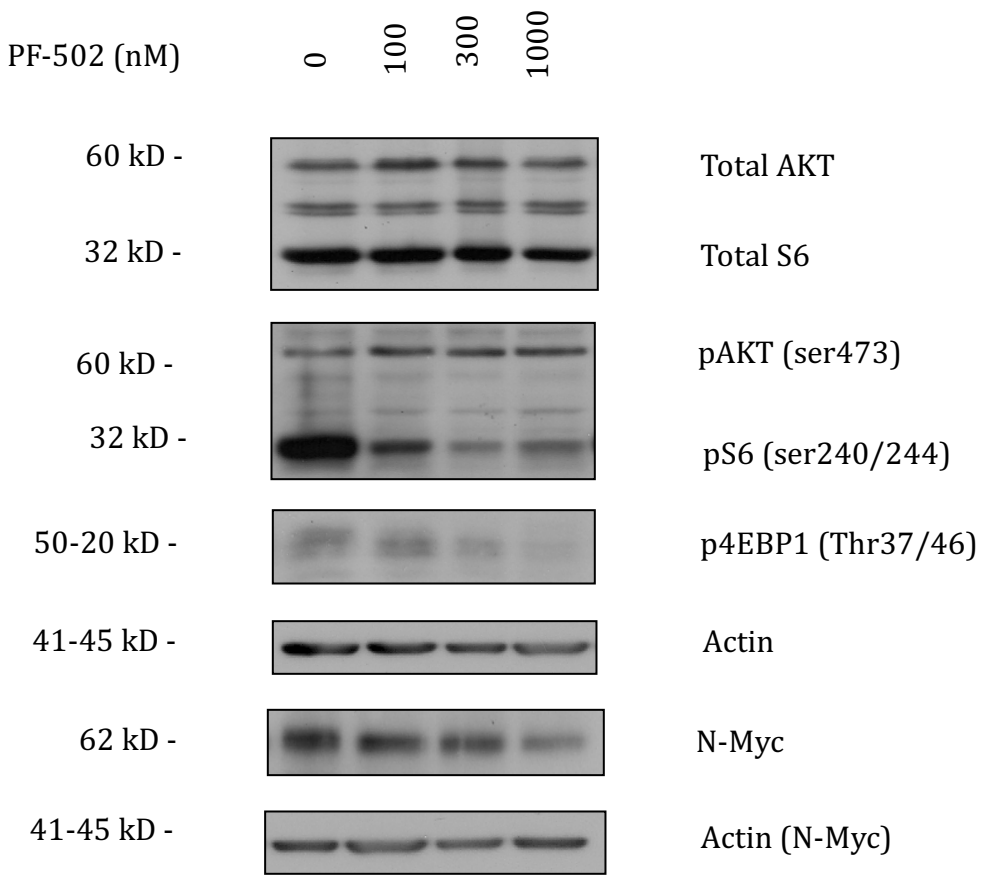

Figure 27 Western Blot (WB) analysis of protein lysates from IMR32 cells exposed to varying concentrations of PF-502

IMR32 cells were exposed to varying concentrations of PF-502 for 3 hours. WB membranes were probed for biomarkers of PF-502 activity including total AKT, pAKT(ser473), total S6, pS6 (ser240/244), p4EBP1 (Thr37/46) & NMYC. Actin was used as a loading control. Escalating concentrations of PF-502 was associated with a dose dependent decrease in biomarkers including pAKT (ser473), pS6 (ser240/244) and p4EBP1 (Thr37/46) indicating that these pathways had been inhibited. NMYC protein levels were also reduced in a dose dependent fashion.

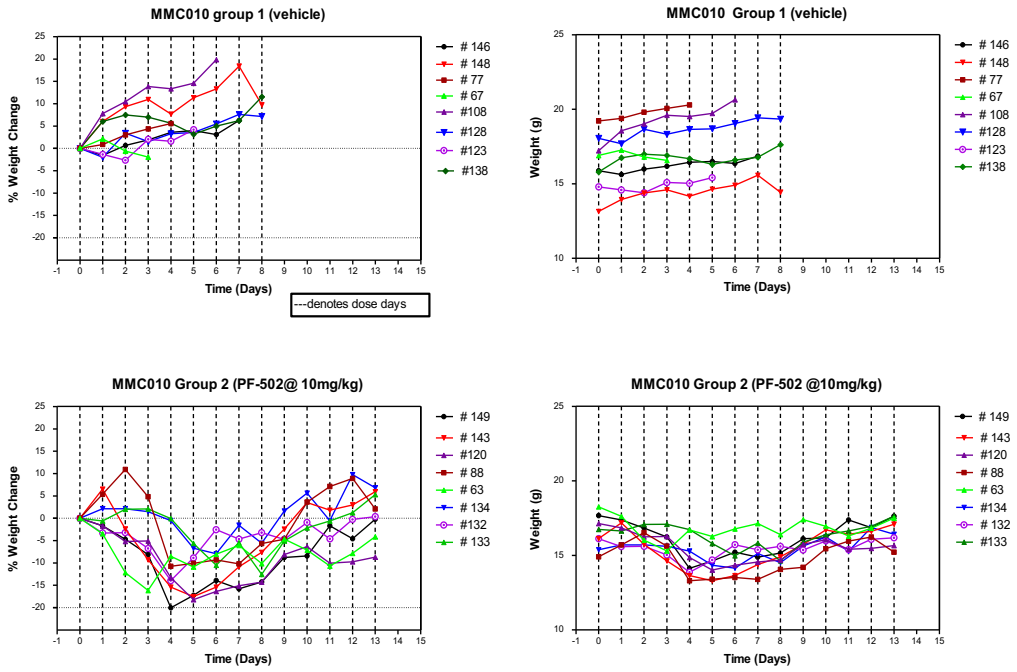

Figure 28 Maximum tolerated dose (MTD) of PF-502 in TH-*MYCN* mice

Confirmed tolerability of the PF-502 in TH-*MYCN* WT non-tumour bearing mice. Dose escalations are continued until a tolerable dose has been defined. Mice were weighed and inspected for signs of distress daily. Weight loss of more than 20% from baseline defined toxicity. Mice found to be in distress were carefully monitored and sacrificed, if required, to avoid distress.

3.4.3. PF-502 inhibits the PI3K/AKT/mTOR pathway in vivo

The inhibition of the PI3K/AKT/mTOR pathway was then confirmed *in-vivo*. Prior to this, tolerability studies were performed that confirmed an MTD of 10mg/kg daily (Figure 28). TH-*MYCN* mice exposed to a single dose of PF-502 10mg/kg, and then harvested 3 hours later, had a reduction in the expression of phospho-AKT, phospho-S6 and phospho-4EBP1 when compared to vehicle treated mice (Figure 29). This was important to demonstrate that the PF-502 had biological activity in this model.

(A) (i)

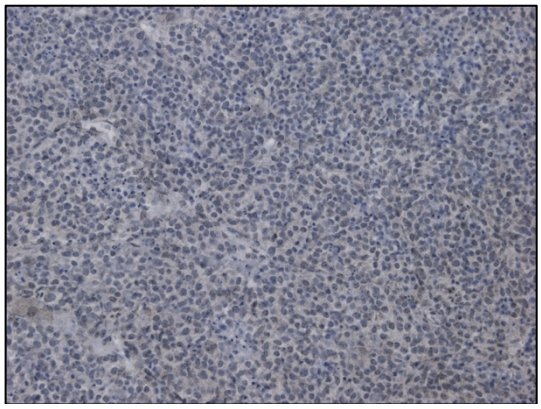

(ii)

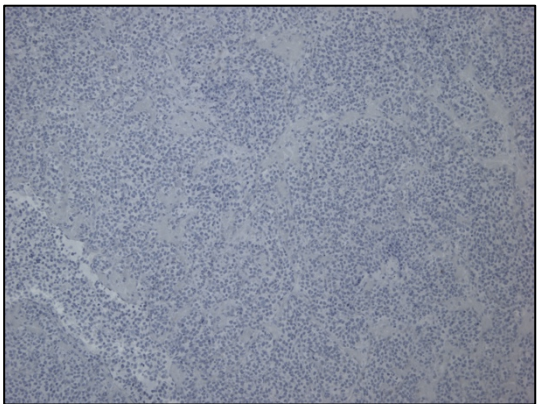

(B) (i)

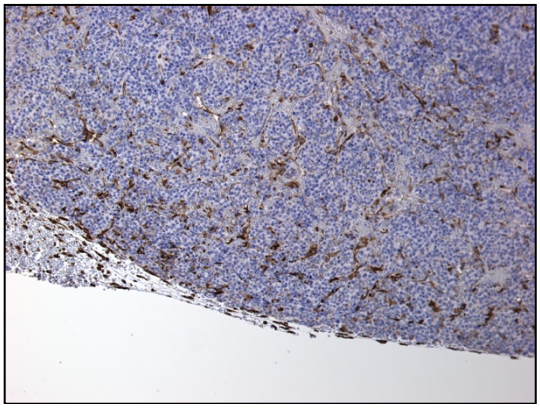

(ii)

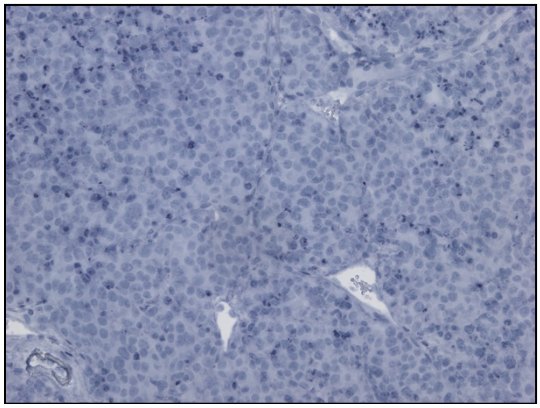

(C) (i)

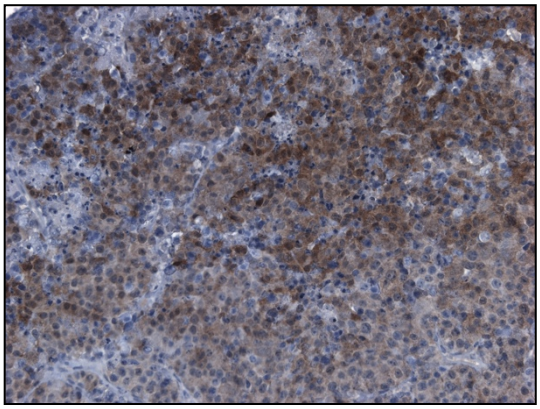

(ii)

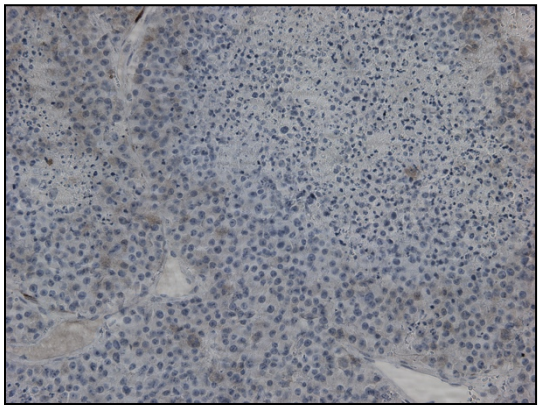

Figure 29 Immunohistochemistry of tumours, from TH-*MYCN* mice exposed to a fixed dose of PF-502 and harvested at 3 hours

Mice homozygous for the TH-*MYCN* transgene were identified and underwent ultrasound to confirm the presence of abdominal tumour. Mice then received, by oral gavage either (i) vehicle (n=5) or (ii) PF-502 10mg/kg (n=5). Tumours were harvested at 3 hours and fixed in 10% neutral buffered formalin (NBF). Once embedded in paraffin the tissue was the sliced to 6-micron thickness and placed on glass slides. Tissue was probed via immunohistochemistry as described for biomarkers of the PI3K/AKT/mTOR pathway including included (A) pAKT (ser473) x 20 (B) pS6 (Ser235/236) x 20 & (C) p4EBP1 (Thr37/46) x 20.

3.4.4. **Efficacy of PF-502 in TH-MYCN transgenic murine model**

Having established that the PI3K/AKT/mTOR pathway is active in NBL (3.2) (Johnsen et al., 2008), and knowing that PF-502 was able to abrogate this pathway effectively, a survival analysis was performed in the TH-*MYCN* mouse model. As stated earlier (1.7), this model recapitulates the human NBL phenotype accurately both in its behaviour and chromosomal changes.

When mice were exposed to daily dosing of PF-502 it conferred a significant survival advantage (Figure 30A). Concurrent ultrasound scans performed also demonstrated an inhibition of tumour growth without significant a reduction in tumour volume (Figure 30B). Collectively the murine tumours did not regress below baseline values but instead progressed at a much slower rate than the vehicle treated mice. This was consistent with a partial response. This was in contrast to the results seen when temsirolimus was administered to the TH-*MYCN* mice (Figure 20B) which inhibited tumour progression until the drug was removed at day 35.

In contrast to temsirolimus treated mice (Figure 20), mice treated with PF-502 relapsed as early as day 24, more than a week sooner than the planned cessation of drug at day 35. In fact, the majority of mice (78%) had relapsed while still on PF-502 by day 35. The toxicity of PF-502 is discussed in (3.4.10).

(A)

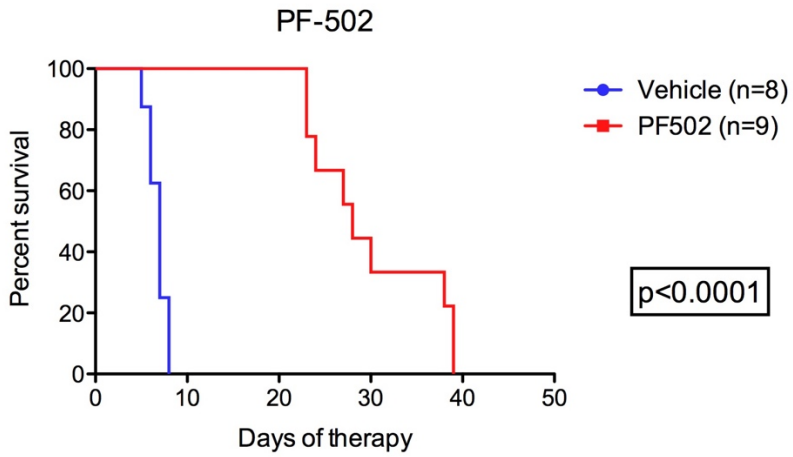

(B)

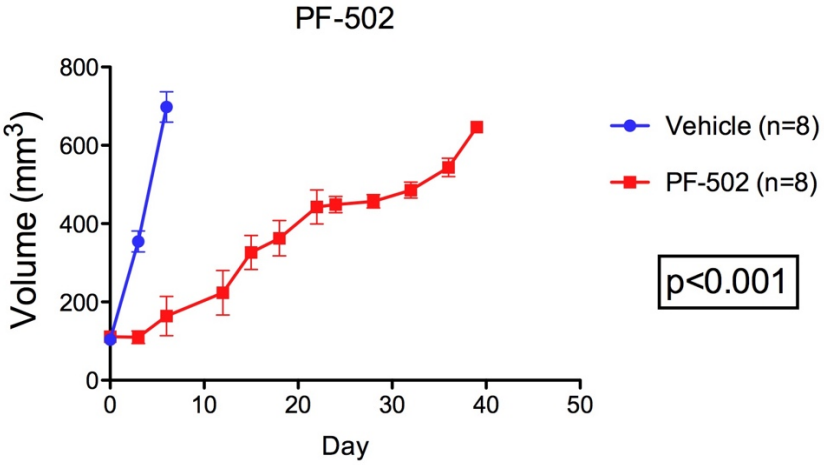

Figure 30 Efficacy of PF-502 in TH-*MYCN* transgenic murine model

(A) A significant difference in survival was observed in mice treated with PF-502 when compared with vehicle ($p < 0.001$, one way ANOVA). (B) A significant inhibition of tumour growth as evidenced by 3D tumour volumes, measured by abdominal US, in mice treated with PF-502 when compared with vehicle ($p < 0.001$, two way ANOVA)..

3.4.5. **Functional imaging as a marker of response**

The role of functional imaging combined with small animal US, in pre-clinical models, has been discussed (3.3.4). The PF-502 treated TH-*MYCN* mice showed a significant reduction in FDG-PET activity and a consistent and significant reduction in tumour metabolism, when compared to vehicle treated mice (Figure 31). This response was more pronounced than the response seen in temsirolimus treated mice (3.3.4). In this case the combination of a significant but incomplete reduction in tumour volume on small animal US, with the partial metabolic response seen on FDG-PET would be consistent with a partial response as per the new INRG (J. R. Park et al., 2017).

(A)

(B)

PF-502

Tumour/Background ratio 3.167

Tumour/Background ratio 2.069

(C)

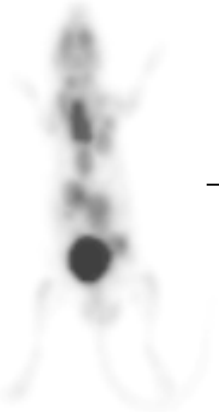

(D)

Vehicle

Tumour/Background ratio 4.328

Tumour/Background ratio 5.164

(E)

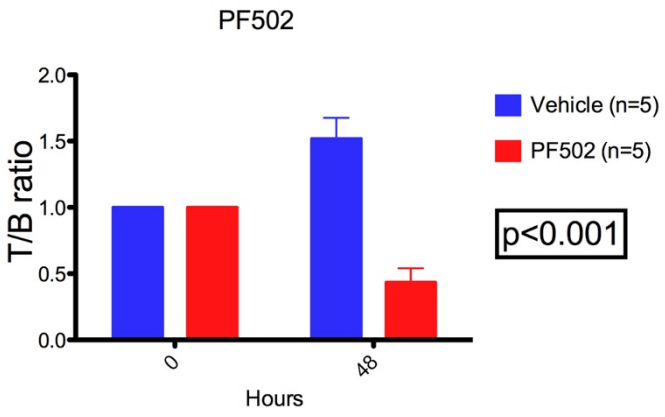

Figure 31 Efficacy of PF-502 in TH-*MYCN* transgenic murine model

(A) FDG-PET image showing central abdominal tumour of TH-*MYCN* mouse treated with 10mg/kg PF-502 at time 0 hours. (B) FDG-PET image showing central abdominal tumour of TH-*MYCN* mouse treated with 10mg/kg PF-502 at time 48 hours. (C) FDG-PET image showing central abdominal tumour of TH-*MYCN* mouse treated with vehicle at time 0 hours. (D) FDG-PET image showing central abdominal tumour of TH-*MYCN* mouse treated with vehicle at time 48 hours. (E) A significant difference in FDG-PET avidity, as a measure of metabolism, over a 48-hour period in mice treated with PF-502 when compared with vehicle ($p < 0.001$, two way ANOVA).

3.4.6. **N-Myc expression**

As stated previously the NBL tumours in the TH-*MYCN* mouse model of NBL are under the targeted expression of *MYCN* and are transgene dose dependent (Weiss et al., 1997). In addition, the prognostic significance of N-Myc amplification NBL has been established (John M. Maris, 2010) which has identified MYC as an important therapeutic target in NBL (Beltran, 2014). It was important to demonstrate that targeting the PI3K/AKT/mTOR pathway was result in reduced N-Myc expression consistent with the aims of this thesis. TH-*MYCN* mice treated with PF-502 had IHC evidence of reduced expression of *MYCN*. This treatment effect was maximal at 3-6 hours post the treatment dose and reduced *MYCN* expression persisted until 12, and to a lesser extent, 24 hours post treatment (Figure 32).

(A) (i)

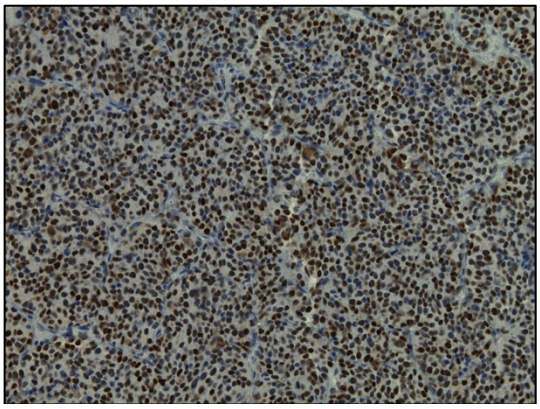

(B) (i)

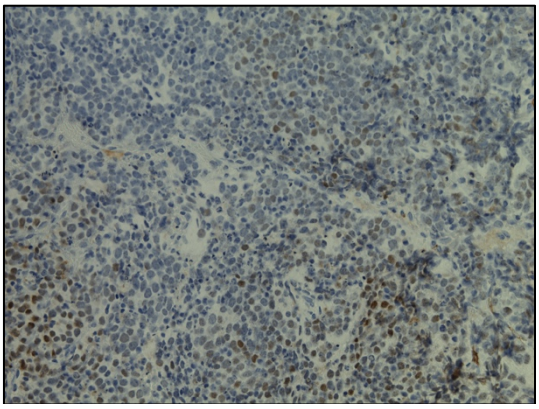

(A) (ii)

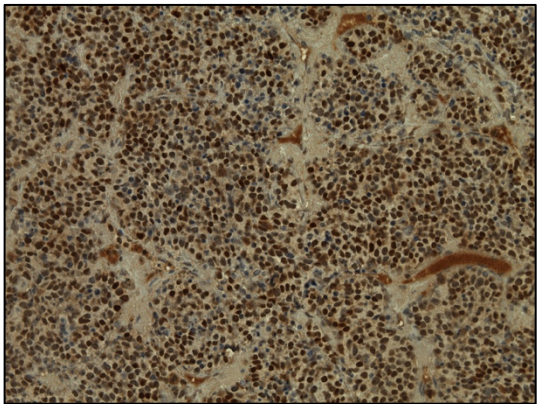

(B) (ii)

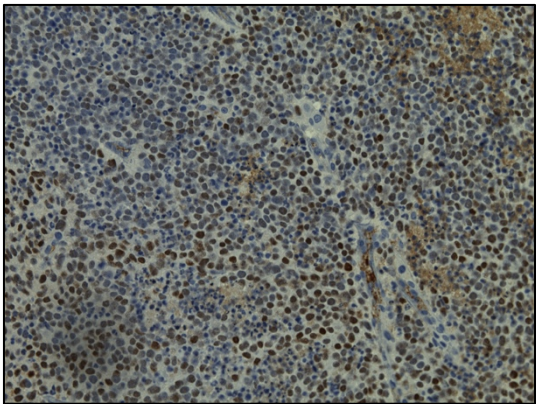

(A) (iii)

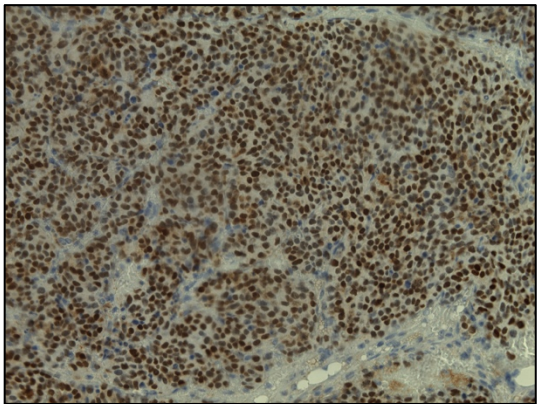

(B) (iii)

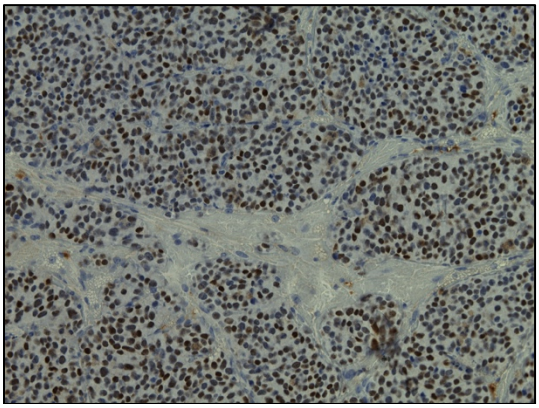

(A) (iv)

(B) (iv)

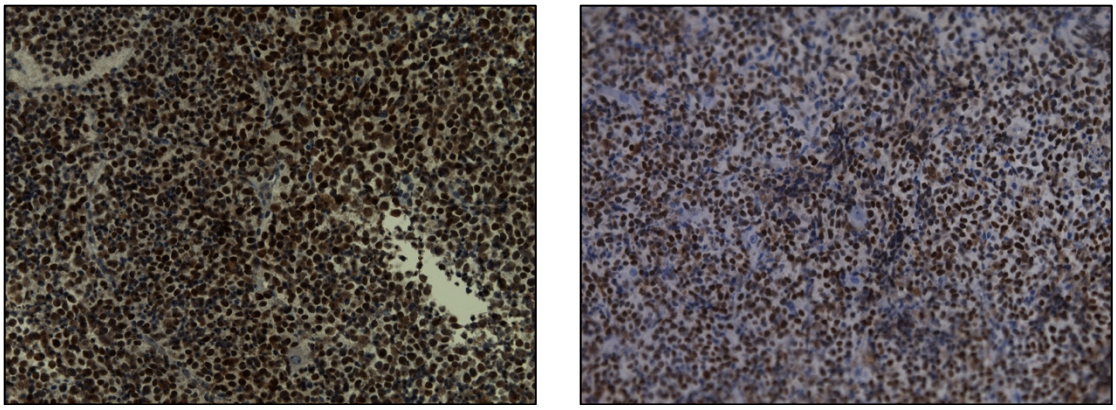

(C)

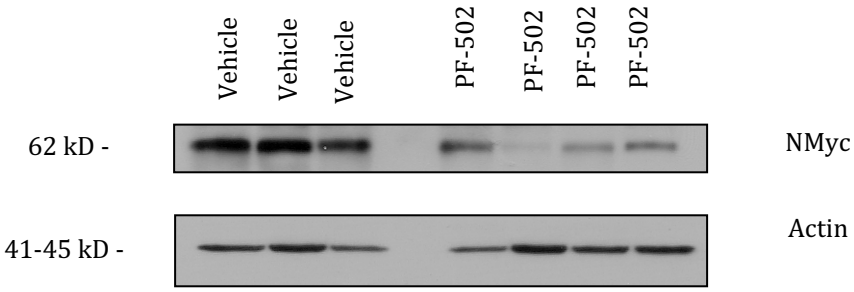

Figure 32 NMYC in TH-*MYCN* transgenic murine model following treatment with PF-502

Mice homozygous for the TH-*MYCN* transgene were identified and underwent ultrasound to confirm the presence of abdominal tumour. Mice then received, by oral gavage, (A) vehicle or (B) 10mg/kg of PF-502. Tumours were harvested at dedicated time-points (i) 3 hours (n=5/group) (ii) 6 hours (n=3/group) (iii) 12 hours (n=3/group) & (iv) 24 hours (n=3/group) and fixed in 10% neutral buffered formalin (NBF). Once embedded in paraffin the tissue was the sliced to 6-micron thickness and placed on glass slides. Tissue was probed via immunohistochemistry as described for NMYC. (C) Mice homozygous for the TH-*MYCN* transgene were identified and underwent ultrasound to confirm the presence of abdominal tumour. Mice then received, by oral gavage, vehicle or 10mg/kg of PF-502. Tumours were harvested 3 hours post treatment dose. WB analysis was then performed for N-Myc.

3.4.7. **PF-502 and apoptosis**

Combined PI3K/mTOR inhibitors have been previously demonstrated to induce apoptosis and PF-502 has been shown to induce apoptosis in many pre-clinical models including chronic lymphocytic leukaemia (Blunt et al., 2015), NHL (D. Chen et al., 2016), lung cancer (Fei et al., 2016) and hepatocellular carcinoma cell lines (F.-Z. Wang et al., 2013). In NBL, the dual class I PI3K/mTOR inhibitor PI103 has been shown to induce apoptosis in both NBL cell lines and mouse models. Neuroblastoma cells expressing higher levels of N-Myc were more sensitive to PI103 induced apoptosis (Segerstrom et al., 2011).

TH-*MYCN* mice exposed to daily dosing of PF-502 and harvested at 48 hours showed significant evidence of apoptosis as measured by characteristic changes in H&E stained tumour tissue including cell shrinkage and pyknosis (Figure 33 A). In addition, mice treated with PF-502 had a significant increase in TUNEL staining (Figure 33 B) and increased cleaved caspase 3 on WB analysis of protein lysates from tumours (Figure 33 C).

(A) (i)

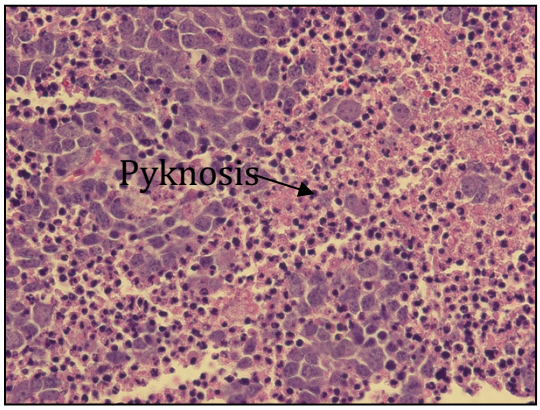

(ii)

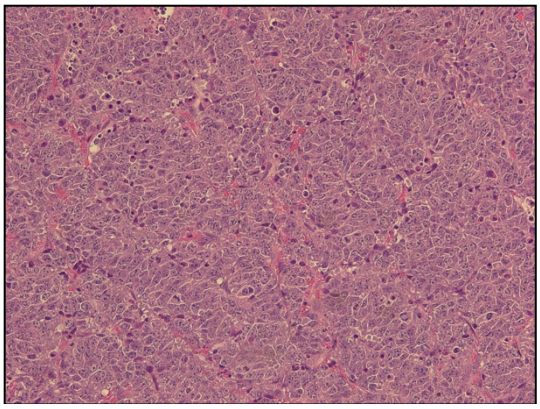

(B) (i)

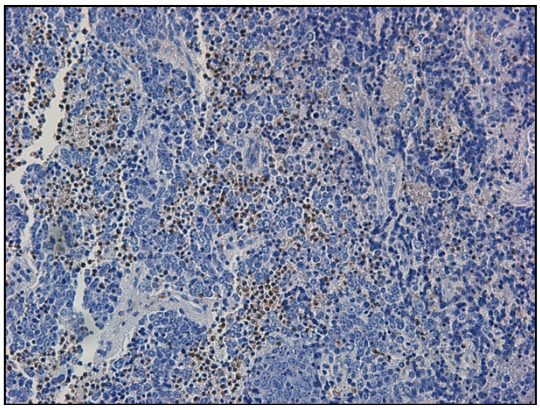

(ii)

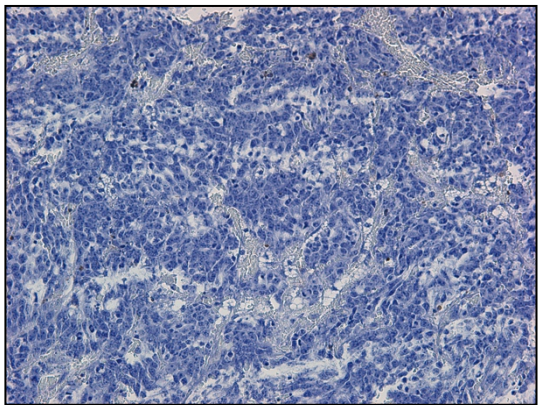

(C)

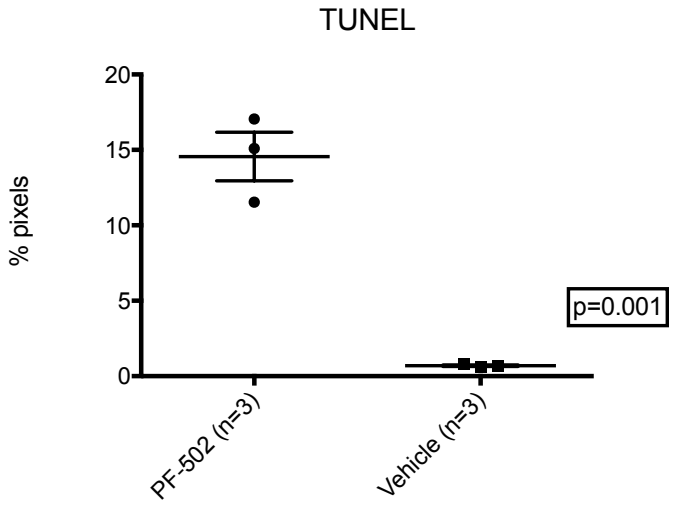

(D)

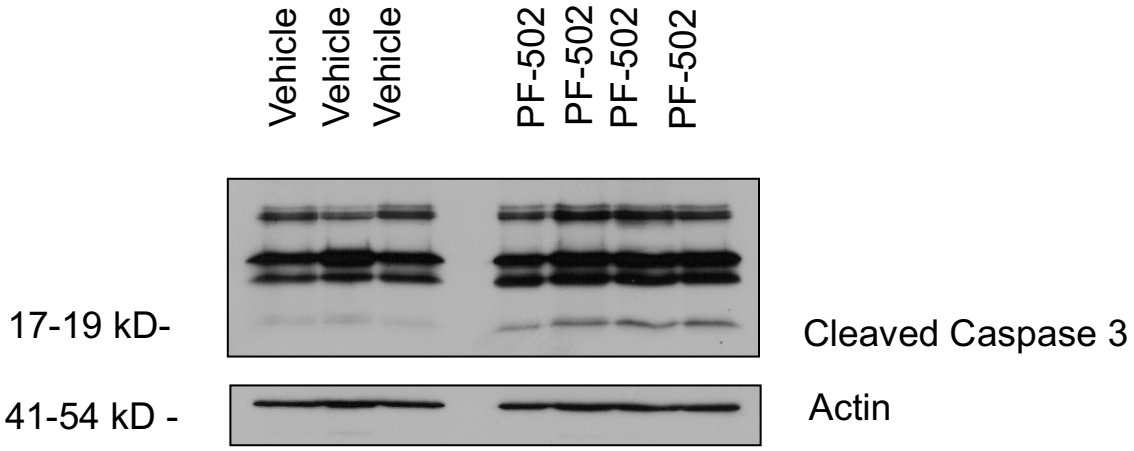

Figure 33 Apoptosis in TH-*MYCN* transgenic murine model

(A) H&E staining of spontaneous neuroblastoma having been treated for 8 days with (i) PF-502 10mg/kg daily via oral gavage, (x20) (ii) methylcellulose 0.5% 10ul/100g (vehicle) daily via oral gavage (B) TUNEL staining of spontaneous neuroblastoma having been treated for 48 hours with (i) PF-502 10mg/kg daily via oral gavage, (ii) methylcellulose 0.5% 10ul/100g (vehicle) daily via oral gavage, (x20) (C) A significant difference in TUNEL positive cells observed after exposure to PF-502 ($p=0.001$, student *t*-test) (D) Western blot analysis of tumour lysates demonstrates increased cleaved caspase 3 in TH-*MYCN* mice treated for 48 hours with (i) PF-502 10mg/kg daily via oral gavage, or methylcellulose 0.5% 10ul/100g (vehicle) daily via oral gavage. Results are consistent with PF-502 inducing apoptosis.

3.4.8. **PF-502 and angiogenesis**

The PI3K/mTOR pathway is intimately linked to angiogenesis. Activation of the pathway in tumour cells upregulated both HIF-1α and VEGF (Karar & Maity, 2011). mTORC1 inhibition significantly prolongs survival and induces tumour growth arrest in the TH-*MYCN* mouse model (3.3.3). This anti-tumour effect was accompanied by a significant anti-angiogenic effect (3.3.7). It therefore makes sense that a combined PI3K/mTOR inhibitor should also inhibit angiogenesis.

PF-502 has been shown to have anti-angiogenic effects in pre-clinical hepatocellular carcinoma models primarily by reduced expression of VEGF and HI-1α (F.-Z. Wang et al., 2013). Tumour anti-angiogenesis has also been observed when PI3K and mTOR are inhibited independently of each other (Zhong et al., 2000).

TH-MYCN mice were treated with a daily dose of PF-502 for two weeks. Mice were harvested at various timepoints and their tumours probed for CD31 expression, an endothelial cell marker. PF-502 treated mice showed a significant reduction in CD31 expression, when compared to vehicle treated mice consistent with reduced tumour angiogenesis (Figure 34).

(A) (i) (ii)

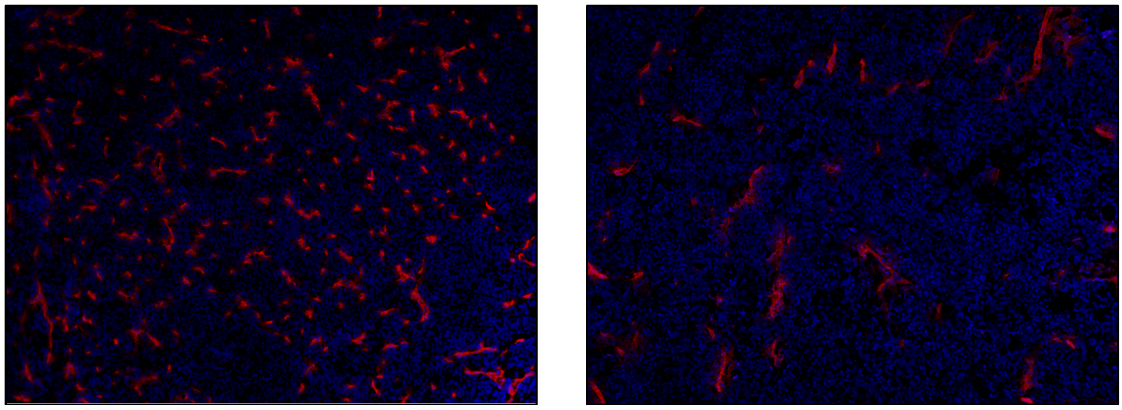

(B)

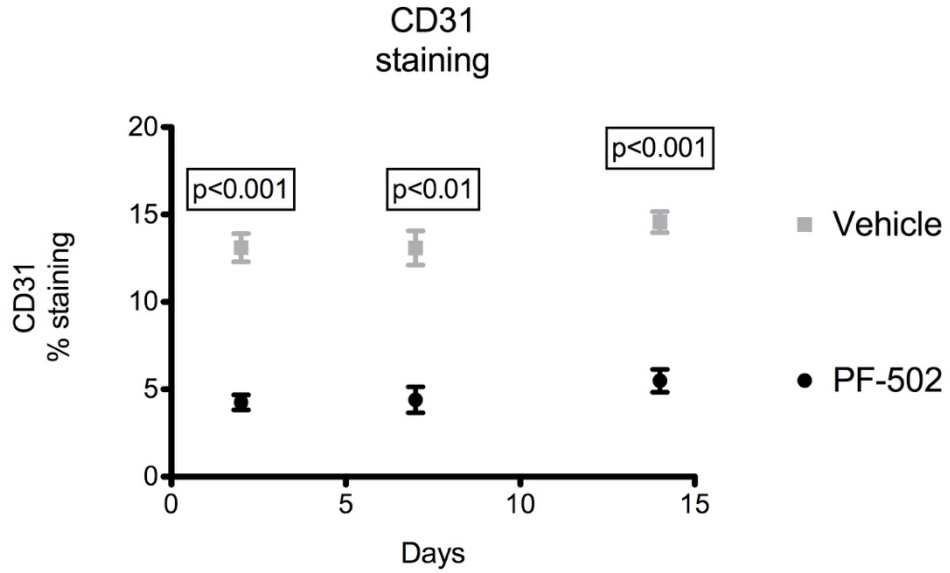
CD31
staining
CD31
% staining
20
15
10
5
0
0
5
10
15
Days
p<0.001
p<0.01
p<0.001
Vehicle
PF-502

Figure 34 Angiogenesis in TH-*MYCN* transgenic murine model

(A) CD31 staining of spontaneous neuroblastoma having been treated for 48 hours with, (i) methylcellulose 0.5% 10ul/100g (vehicle) daily via oral gavage. (x20) (ii) PF-502 10mg/kg daily via oral gavage, (x20) (B) Metamorph analysis of CD31 staining of spontaneous neuroblastoma demonstrates significant difference at 48 hours, 7 days and 14 days in mice treated with (i) PF-502 10mg/kg daily via oral gavage, or methylcellulose 0.5% 10ul/100g (vehicle) daily via oral gavage ($p < 0.01$, student *t*-test). Note: day 14 PF-502 treated samples were compared with vehicle treated samples from mice harvested beyond day 7 as no vehicle treated mice remained alive by day 14.

3.4.9. **PF-502 and senescence**

The PI3K/AKT/mTOR pathway has been linked to cellular ageing and senescence (Bent, Gilbert, & Hemann, 2016). Activated PI3K/AKT signalling may also impair other pathways associated with senescence, such as Ras-induced senescence (Kennedy, Adams, & Morton, 2011). PI3K/mTOR inhibitors such as LY294002 have been shown to induce cellular senescence by upregulation of $p27^{Kip1}$ (Collado et al., 2000). PF-502 has induced a senescence phenotype in A549 cells alongside significant apoptosis (Fei et al., 2016). There is, however, a paucity of published data linking combined PI3K/mTOR inhibitors to cellular senescence, especially in the setting of cellular apoptosis. Cellular senescence differs from apoptosis in that senescent cells are still able to influence surrounding cells via the secretion of SASP, although from an evolutionary stand-point the two processes may not be mutually exclusive in terms of involved cellular pathways involved (Childs, Baker, Kirkland, Campisi, & van Deursen, 2014).

mTORC1 inhibition induces a significant increase in SA-β-Gal positive cells consistent with cellular senescence (3.3.8). When TH-*MYCN* tumour bearing mice were treated for seven days with continuous daily dosing of PF-502, a slight, but not significant, increased expression of SA-β-GAL staining was observed (Figure 35). Therefore, senescence was not a significant phenotype associated with treatment with PF-502.

This result is interesting given PF-502 is a combined PI3K/mTOR inhibitor. The balance between apoptosis and senescence, in this case, appears to be tipped towards a predominantly apoptosis phenotype.

(A)(i) (ii)

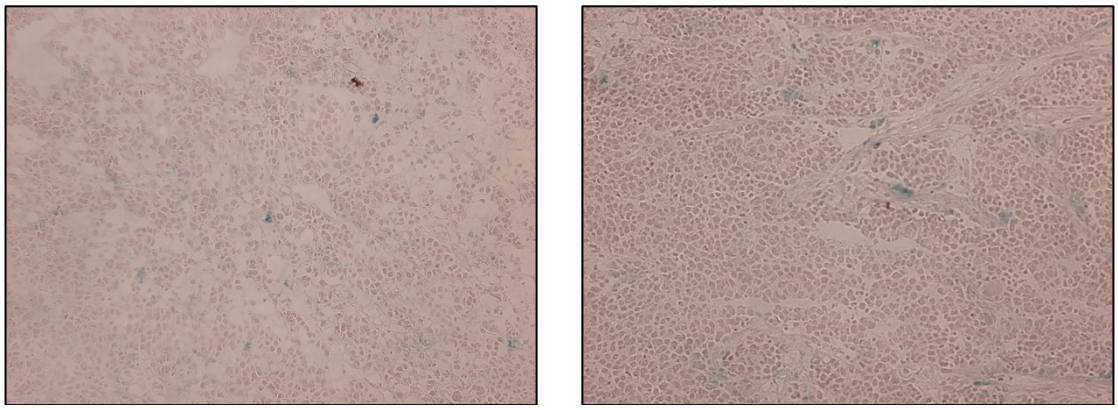

(B)

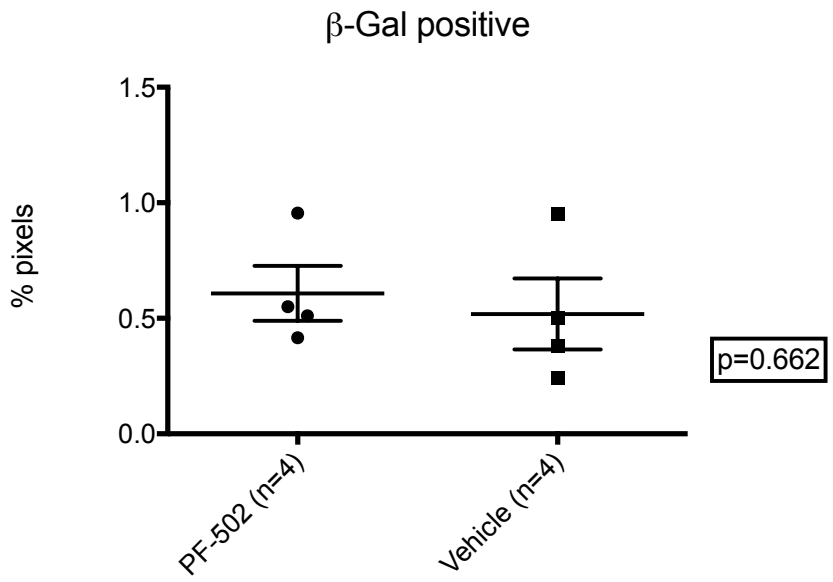

Figure 35 Senescence in TH-*MYCN* transgenic murine model

SA-B-gal staining of spontaneous neuroblastoma having been treated for 7 days with, (i) methylcellulose 0.5% 10ul/100g (vehicle) (n=4) daily via oral gavage x40 & (ii) PF-502 10mg/kg daily via oral gavage (n=4) (x40) (B) quantification of SA-B-gal staining (p=0.662, student *t*-test)..

3.4.10. **PF-502 and toxicity**

In early phase human studies of combined PI3K/mTOR inhibitors hepatotoxicity has been recognized as a significant toxicity seen in 5% of patients (Seront et al., 2016). Continuous dosing of PF-502 in the TH-*MYCN* NBL model demonstrated significant (Grade III) hepatic toxicity consistent with steatohepatitis (Takahashi & Fukusato, 2014) (Figure 36).

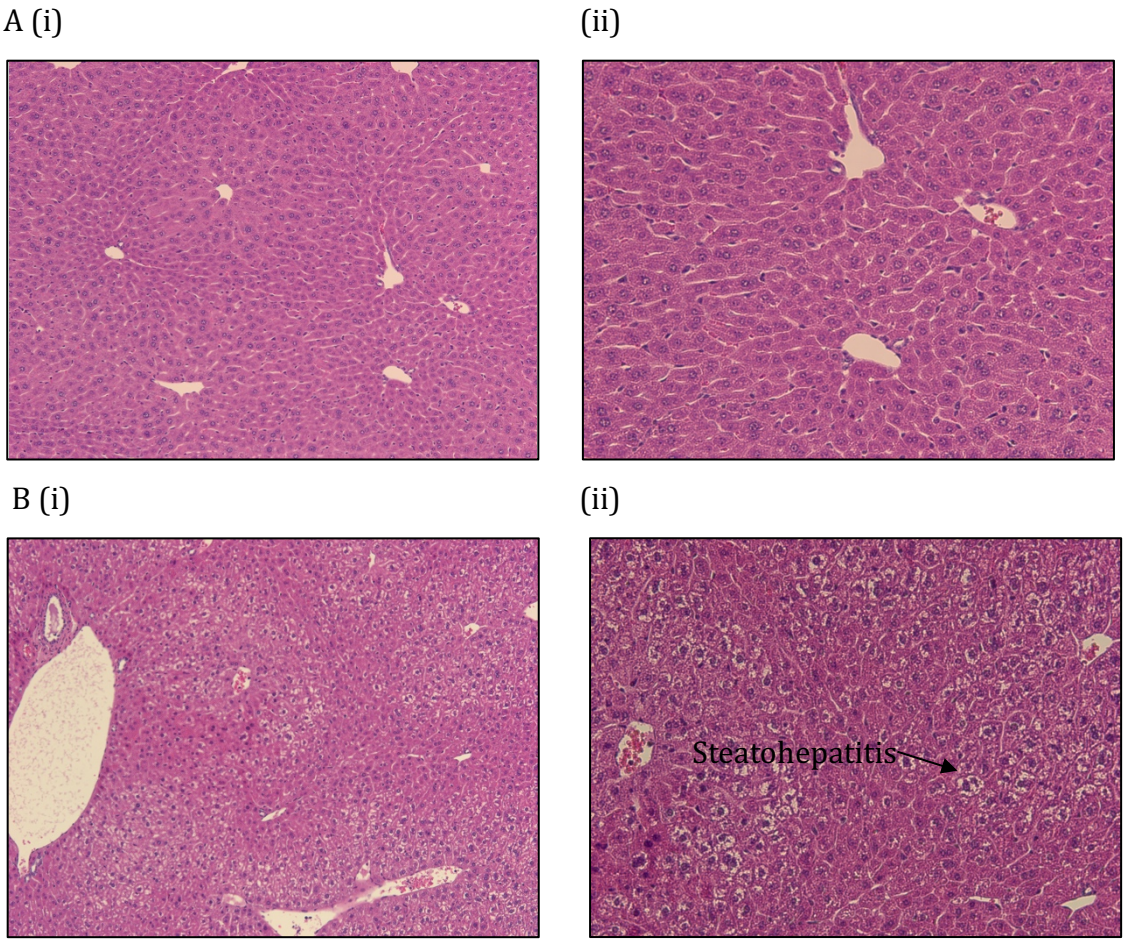

Figure 36 Hepatic toxicity of PF-502

H&E Liver. PF-502 induced hepatic steatohepatitis in TH-*MYCN* neuroblastoma. TH-*MYCN* mice were exposed to PF-502 daily. Mice were harvested at the time of culling. (B) PF-502 treated mice had significant hepatic steatohepatitis on H&E (i) x 20 magnification, (ii) x 40 magnification, compared with (A) vehicle treated mice (i) x 20 magnification, (ii) x 40 magnification.

3.4.11. PF-502 in TH-MYCN derived NHO1A cells

In an attempt to further evaluate the role of apoptosis in the mode of action of PI3K/mTOR inhibitors in NBL, an orthotopic transplant model of NBL, that could be manipulated, was developed. There were limited orthotopic models, in NBL, that were available at the time. Several cell lines that have been derived from the TH-*MYCN* model were available as tools (A. J. Cheng et al., 2007). The ability to use cell lines derived from the TH-*MYCN* model that could be potentially manipulated and then transplanted back into immuno-competent wild-type (WT) littermates was appealing. The value of an immuno-competent mouse model with the associated benefits such as an authentic tumour microenvironment is essential when evaluating drugs that may impact on tumour microenvironments (Arauchi et al., 2015). It was also important to confirm that NHO1A, cells derived from the TH-*MYCN* NBL model, responded in an equivalent manner to human IMR-32 NBL cell lines (4.2.1 & Figure 26).

NHO1A TH-*MYCN* derived tumour cells exposed to increasing concentrations of PF-502 were inhibited in a similar way to human IMR32 tumour cells (4.2.1 & Figure 37)with an equivalent inhibition of in the low nM range. Biomarkers of pathway inhibition, including phospho-AKT, phospho-S6 and phospho-4EBP1 were similarly inhibited in the low nM range (Figure 37).

(A)

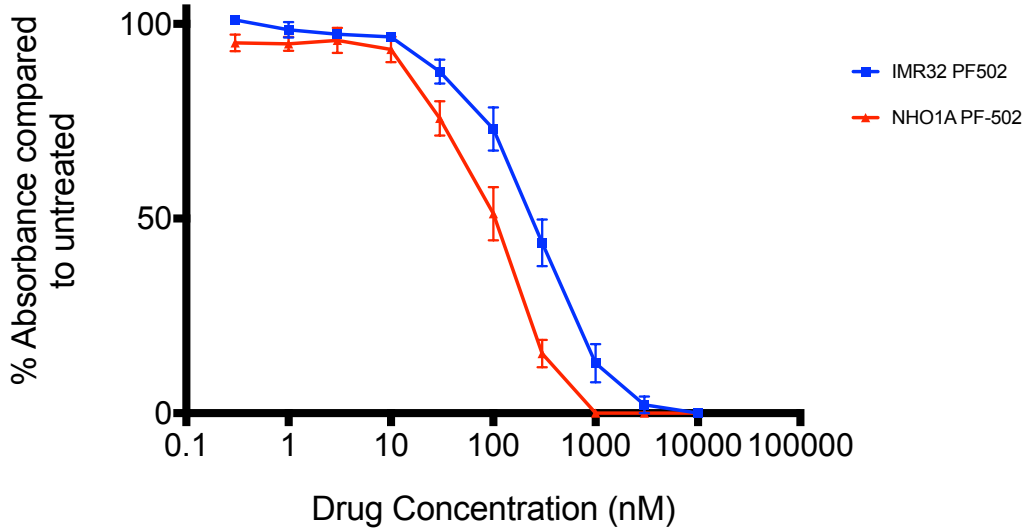
100
50
0
% Absorbance compared to untreated
0.1
1
10
100
1000
10000
100000
Drug Concentration (nM)
IMR32 PF502
NHO1A PF-502

(B)

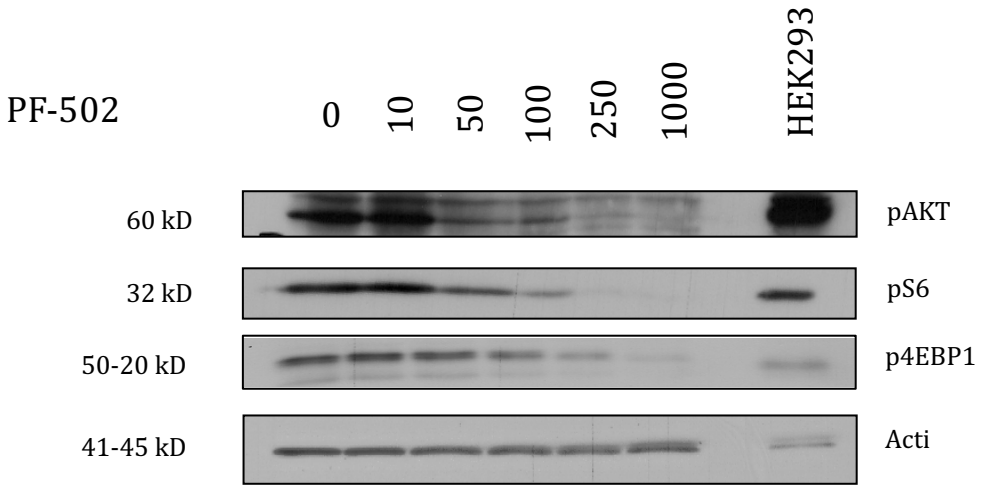
PF-502
0
10
50
100
250
1000
HEK293
60 kD
pAKT
32 kD
pS6
50-20 kD
p4EBP1
41-45 kD
Acti

Figure 37 Efficacy of PF-502 established in NHO1A cell lines

(A) NHO1A (murine derived *MYCN* amplified) and IMR-32 (human derived *MYCN* amplified) cells were cultured in 96 well plates and cell specific media for 48 hours prior to addition of drug. Drug was added in escalating doses and cells were left exposed for 72 hours. Plates were incubated at 37^0C, 5% CO2. Plates were processed after 72 hours according to our standard SRB protocol. Absorbance of SRB was determined as a measure of cell number. Data was processed, and drug curves processed by Prism software. IC_{50} of 100nM (NHO1A) and 380nM (IMR-32)(B) NHO1A cells were exposed to varying concentrations of PF-502 for 3 hours. WB membranes were probed for biomarkers of PF-502 activity including total pAKT (ser473), pS6 (ser240/244) & p4EBP1 (Thr37/46). Actin was used as a loading control. Escalating concentrations of PF502 was associated with a dose dependent decrease in biomarkers including pAKT (ser473), pS6 (ser240/244) and p4EBP1 (Thr37/46) indicating that these pathways had been inhibited.

3.4.12. **The orthotopic mouse model**

Ideally any orthotopic animal model system should faithfully re-capitulate the biology of the cancer that it is modelling (Antonello & Nucera, 2014). Human NBL are predominantly abdominal tumours that arise from the adrenal gland located just above either kidney. I therefore chose this location as the preferred site to transplant tumour cells. Once the right kidney was exteriorised, tumour cells were injected as close to the adrenal gland as possible. The procedure itself has been described in detail (2.13).

The procedure was tolerated well with a successful tumour engraftment in over 90% of mice. Mice were then monitored in a similar way to the TH-*MYCN* mouse model, primarily with small animal ultrasound, concentrating on the right flank of the mice. Once tumours had reached a specified volume, mice could then be randomised into experiments. The value of using wild-type littermates as the recipients was that they were immune-competent. The tumours harvested from these mice progressed in a similar way to the abdominal NBL in the TH-*MYCN* model, and importantly expressed high levels of N-Myc (Figure 38).

(A) (i) (ii)

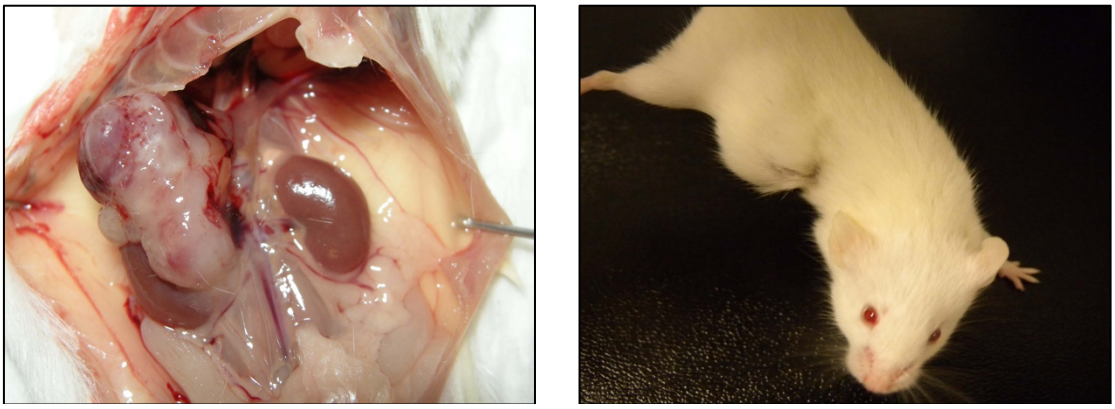

(B) (i) (ii)

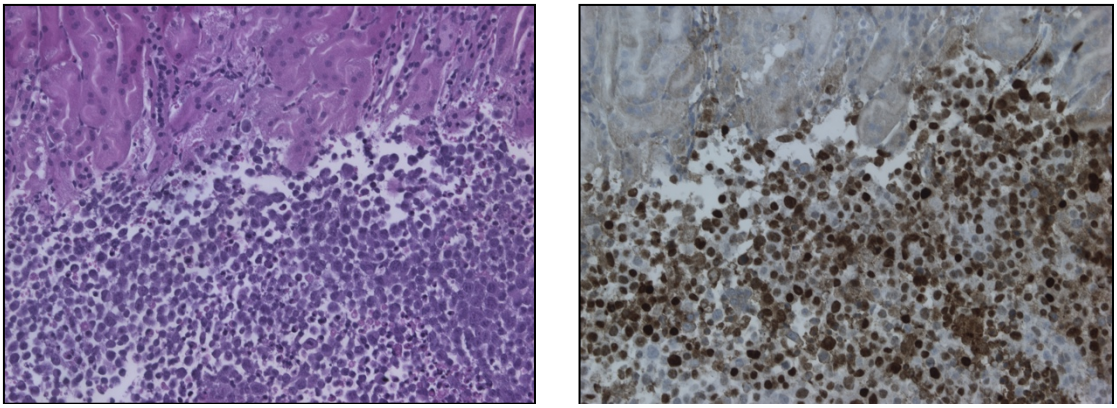

Figure 38 Orthotopic transplant of NHO1A neuroblastoma cells into TH-*MYCN* Wild-Type littermates

(A) (i) Orthotopic tumour as it appears following dissection and (ii) tumour as it appears in the flank of the mouse. (B) (i) H&E showing NHO1A tumour cells invading normal renal (kidney) tissue following orthotopic transplant. (x20) (ii) IHC for N-Myc confirming N-Myc over-expression. (x20).

3.4.13. **Efficacy of PF-502 in the NHO1A orthotopic model**

When mice were exposed to daily dosing of PF-502 it conferred a significant survival advantage (Figure 39 A). Tolerability studies previously confirming a PF-502 dose of 10mg/kg per day had been performed in wild type littermates, so the same dose was used in the NHO1A orthotopic model, as the host mice were wild type littermates. Concurrent ultrasound scans performed also demonstrated an inhibition of tumour growth, without a significant reduction in tumour volume (Figure 39 B). As observed in the TH-*MYCN* model, the NHO1A orthotopic tumours did not regress below baseline values but instead progressed at a much slower rate than the vehicle treated mice. This was consistent with a partial response. The NHO1A orthotopic mice did succumb to their tumours slightly earlier than their TH-*MYCN* counterparts.

FDG-PET studies performed after 48 hours of PF-502 dosing confirmed a significant reduction in avidity in PF-502 treated mice when compared with vehicle treated mice, consistent with a partial metabolic response (Figure 39 C).

(A)

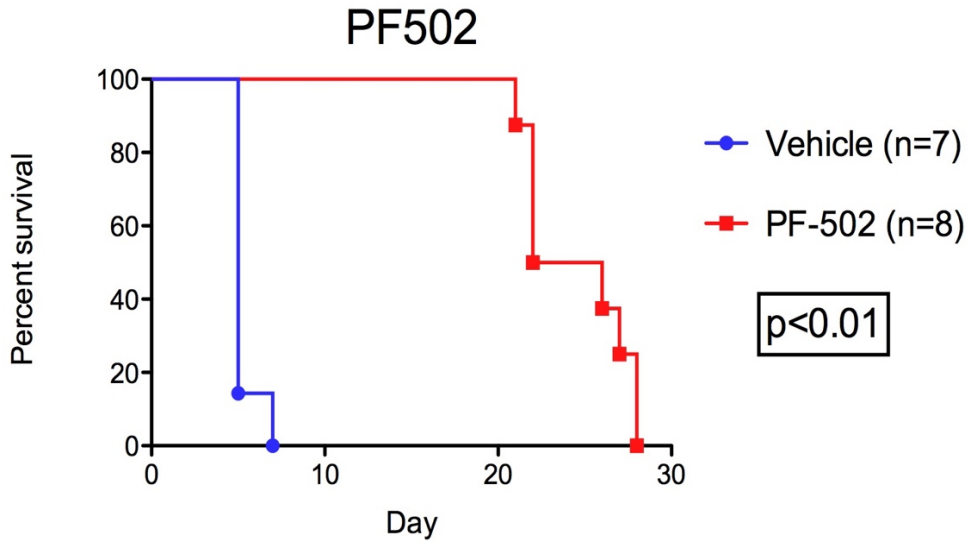
PF502
Percent survival
100
80
60
40
20
0
0
10
20
30
Day
Vehicle (n=7)
PF-502 (n=8)
p<0.01

(B)

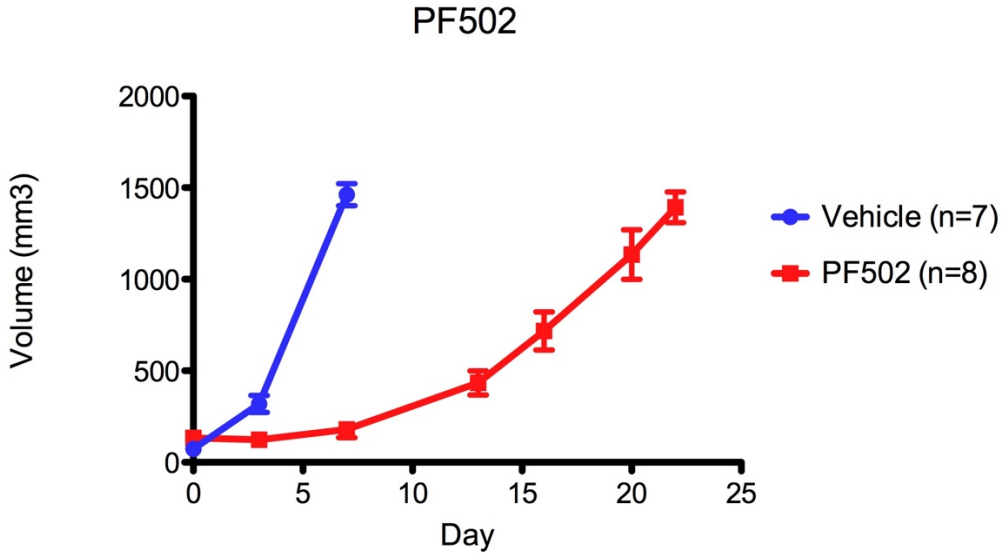
PF502
Volume (mm3)
2000
1500
1000
500
0
0
5
10
15
20
25
Day
Vehicle (n=7)
PF502 (n=8)

(C)

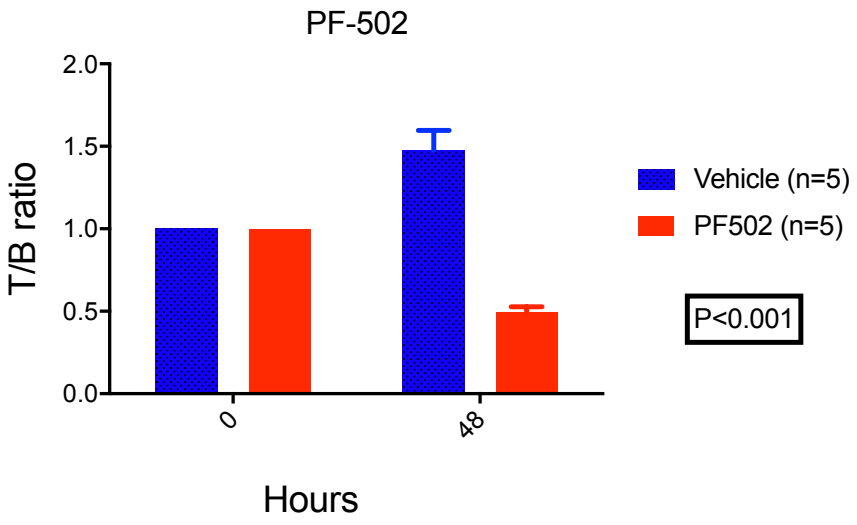

Figure 39 Efficacy of PF-502 in NHO1A orthotopic mouse model

(A) A significant difference in survival was observed in mice treated with PF-502 when compared with vehicle ($p < 0.01$, one way ANOVA). (B) A significant inhibition of tumour growth as evidenced by 3D tumour volumes, measured by abdominal ultrasound, in mice treated with PF-502 when compared with vehicle ($p < 0.01$, two way ANOVA) (C) A significant difference in FDG-PET avidity, as a measure of metabolism, over a 48-hour period in mice treated with PF-502 when compared with vehicle ($p<0.001$, two way ANOVA).

3.4.14. PF-502 inhibits the PI3K/AKT/mTOR pathway in vivo

The inhibition of the PI3K/AKT/mTOR pathway was then confirmed *in-vivo*. NHO1A orthotopic mice were exposed to a single dose of PF-502 10mg/kg, and then harvested three hours later. Mice had a reduction in the expression of phospho-AKT, phospo-S6 and phospho-4EBP1 when compared to vehicle treated mice (Figure 40) consistent with inhibition of the PI3K/AKT/mTOR pathway.

(A) (i) (ii)

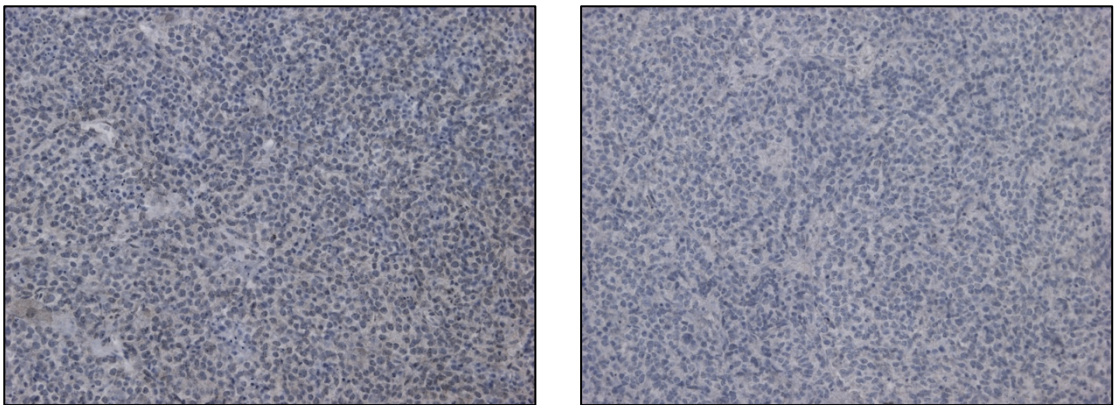

B (i) (ii)

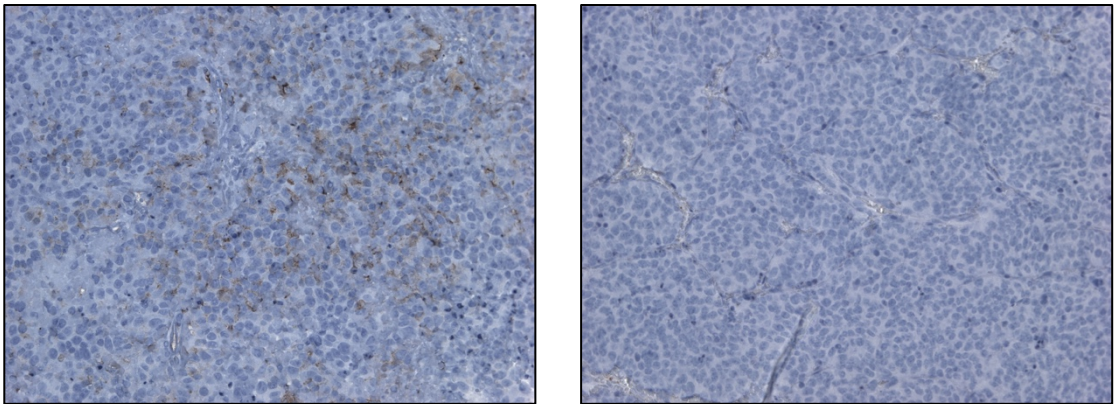

C (i) (ii)

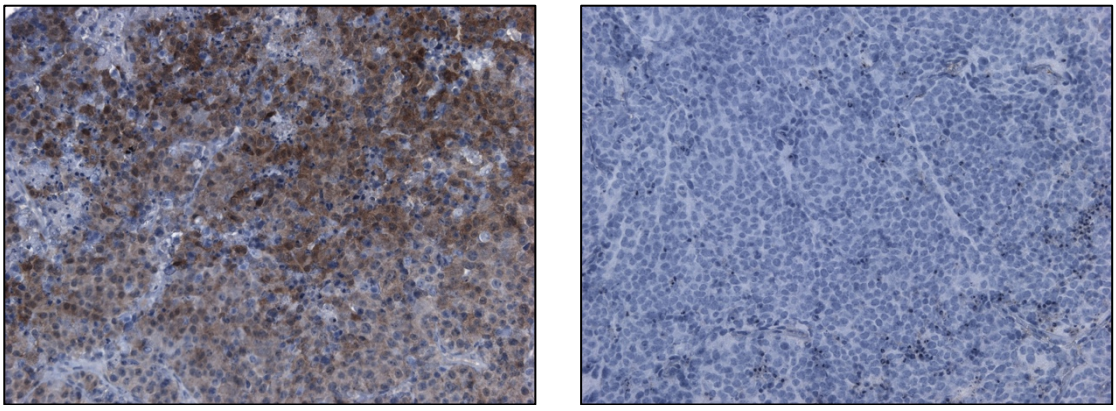

Figure 40 Immunohistochemistry of NHO1A orthotopic tumours exposed to a fixed dose of PF-502 and harvested at 3 hours

NHO1A orthotopic mice underwent ultrasound to confirm the presence of abdominal tumour. Mice then received, by oral gavage either (i) vehicle (n=7) or (ii) PF-502 10mg/kg (n=7). Tumours were harvested at three hours and fixed in 10% neutral buffered formalin (NBF). Once embedded in paraffin the tissue was the sliced to 6-micron thickness and placed on glass slides. Tissue was probed via immunohistochemistry as described for biomarkers of the PI3K/AKT/mTOR pathway including included (A) pAKT (ser473) (x20) (B) pS6 (Ser235/236) (x20) & (C) p4EBP1 (Thr37/46) (x20).

3.4.15. PF-502 reduces N-Myc expression in vivo

NHO1A orthotopic mice treated with PF-502 had IHC evidence of reduced expression of *MYCN* at 6 hours confirming the observations seen in the TH-*MYCN* model.

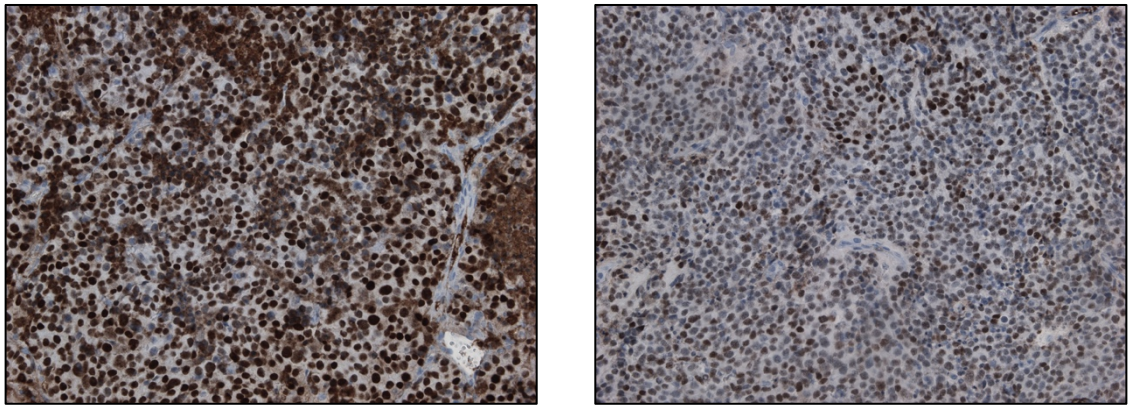

Figure 41 Immunohistochemistry of NHO1A orthotopic tumours exposed to a fixed dose of PF-502 and harvested at 6 hours

NHO1A orthotopic mice underwent ultrasound to confirm the presence of abdominal tumour. Mice then received by oral gavage either, (i) vehicle (n=3) or (ii) PF-502 10mg/kg (n=3). Tumours were harvested at 6 hours and fixed in 10% neutral buffered formalin (NBF). Once embedded in paraffin the tissue was the sliced to 6-micron thickness and placed on glass slides. Tissue was probed via immunohistochemistry for N-Myc (x20).

3.4.16. PF-502 and apoptosis in the NHO1A orthotopic mouse model

PF-502 induces apoptosis in the NHO1A orthotopic mouse model, consistent with that previously demonstrated in the TH-*MYCN* mouse model (Figure 42) (Figure 33) TUNEL was not performed.

(A) (i) (ii)

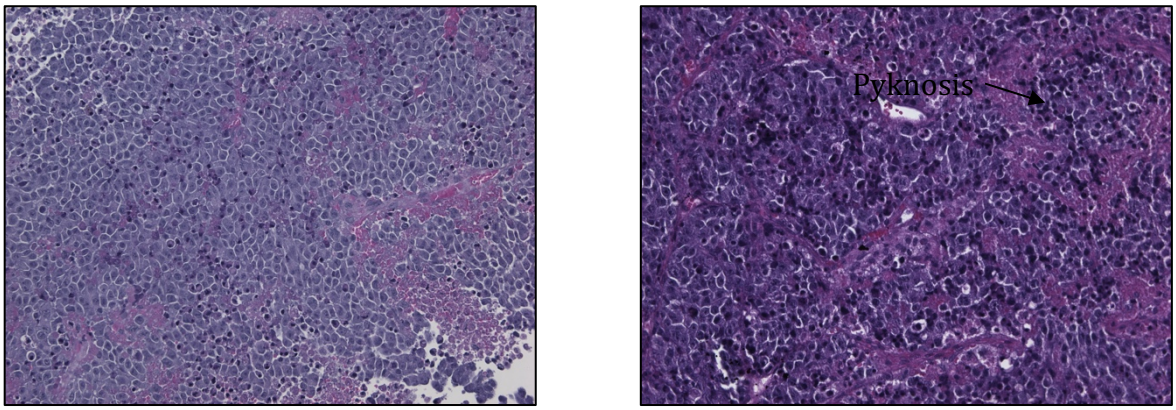

(B)

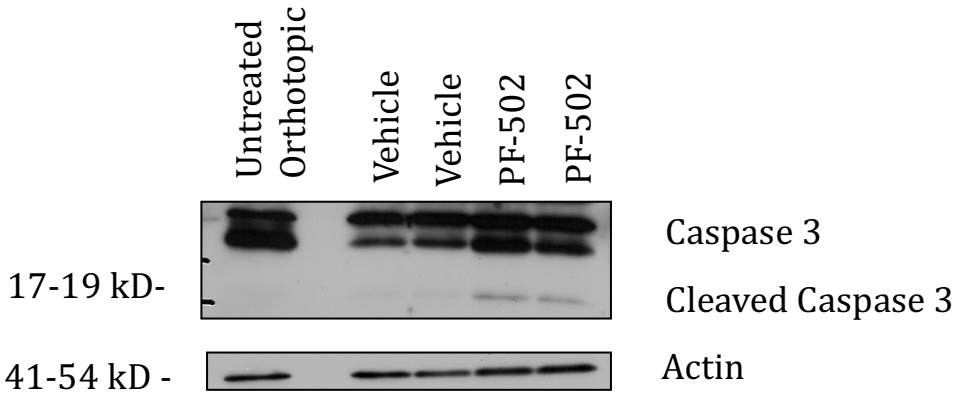

Figure 42 PF-502 and apoptosis in the NHO1A orthotopic mouse model.

(A) H&E staining of spontaneous neuroblastoma having been treated for 48 hours with, (i) methylcellulose 0.5% 10ul/100g (vehicle) daily via oral gavage (x20), (ii) PF-502 10mg/kg daily via oral gavage (x20) (B) Western blot analysis of tumour lysates demonstrate increased cleaved caspase 3 in NHO1A orthotopic mice treated for 48 hours with PF-502 10mg/kg daily via oral gavage, or methylcellulose 0.5% 10ul/100g (vehicle) daily via oral gavage. Results are consistent with PF-502 inducing apoptosis.

3.4.17. PF-502 and angiogenesis in the NHO1A orthotopic mouse model

PF-502 significantly inhibited angiogenesis after 48 hours of exposure in the NHO1A orthotopic mouse model in a similar manner as that seen in the TH-*MYCN* transgenic mouse model (Figure 43).

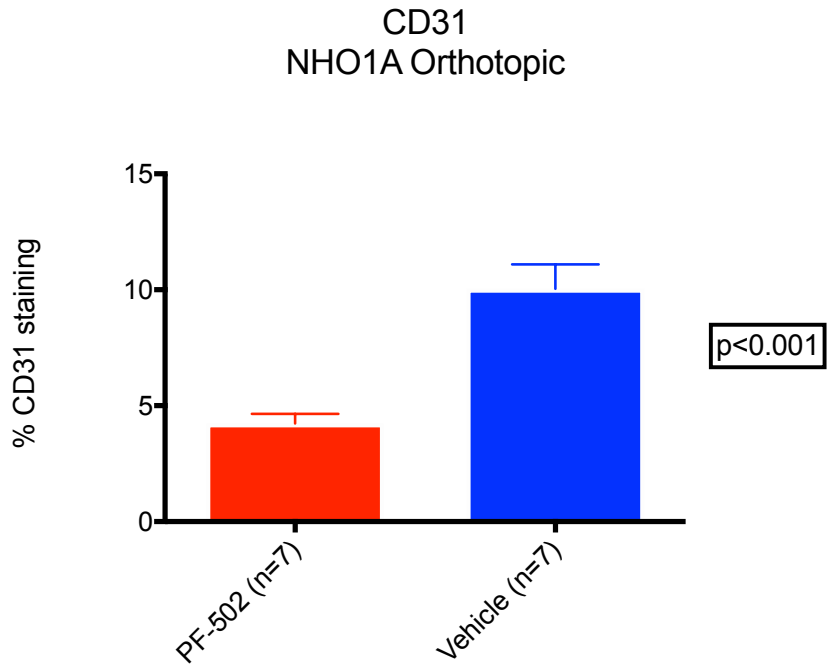

Figure 43 PF-502 and angiogenesis in NHO1A orthotopic mouse model.

Quantitative CD31 staining of NHO1A orthotopic mice having been treated for 48 hours with methylcellulose 0.5% 10ul/100g (vehicle) daily via oral gavage or PF-502 10mg/kg daily via oral gavage ($p < 0.001$, student *t*-test)..

3.4.18. Overexpression of Bcl-2 in NHO1A cells

In order to further determine the balance between the contribution of apoptosis and angiogenesis to the efficacy of PF-502, a biological system was required to negate the impact of one or the other. Over-expression of Bcl-2 has been previously shown to induce resistance to apoptosis in other experimental models (Douarre et al., 2005; Langenau et al., 2005) including lymphoma and other transgenic mouse models (Hotchkiss et al., 1999; Wall et al., 2013).

The intrinsic apoptotic pathway is controlled by the Bcl-2 family members of proteins. Bcl-2 inhibits apoptosis as do its close homologs Bcl-X_L, Bcl-w, Mcl-1, A1 and in humans Bcl-B (Jerry M. Adams & Cory, 2007). The intrinsic pathway of apoptosis is initiated by mitochondrial outer membrane permeabilisation, leading to the release of apoptogenic factors such as cytochrome c or Smac from the mitochondrial intermembrane space into the cytosol (Figure 6). Mitochondrial outer membrane permeabilisation is tightly controlled by both the pro- and anti-apoptotic proteins of the Bcl-2 family and these are in turn modulated by the PI3K/AKT/mTOR pathway (Fulda & Debatin, 2006; Leibowitz & Yu, 2010). Small-molecule PI3K inhibitors prime cancer cells to mitochondrial apoptosis by tipping the balance towards pro-apoptotic Bcl-2 proteins, resulting in increased mitochondrial outer membrane permeabilization. Thus, Bcl-2 mediated mitochondrial apoptotic events play an important role in PI3K inhibitor-mediated sensitization for apoptosis (Bender et al., 2011; Fulda, 2013). It is therefore reasonable to expect that over-expression of Bcl-2 in the NHO1A orthotopic mouse model should antagonise PF-502 induced apoptosis.

Over-expression of Bcl-2 in NHO1A cells was achieved by the PEI transfection protocol (2.14.1). These cells were then orthotopically transplanted in wild-type TH-*MYCN* littermates as previously described (2.13). Tumours were then harvested and stained for Bcl-2 which confirmed significant over-expression when compared to

mice injected with MSCV (empty vector) NHO1A cells. The degree of Bcl-2 staining was equivalent to a follicular lymphoma positive control (Figure 44).

(A) (i) (ii)

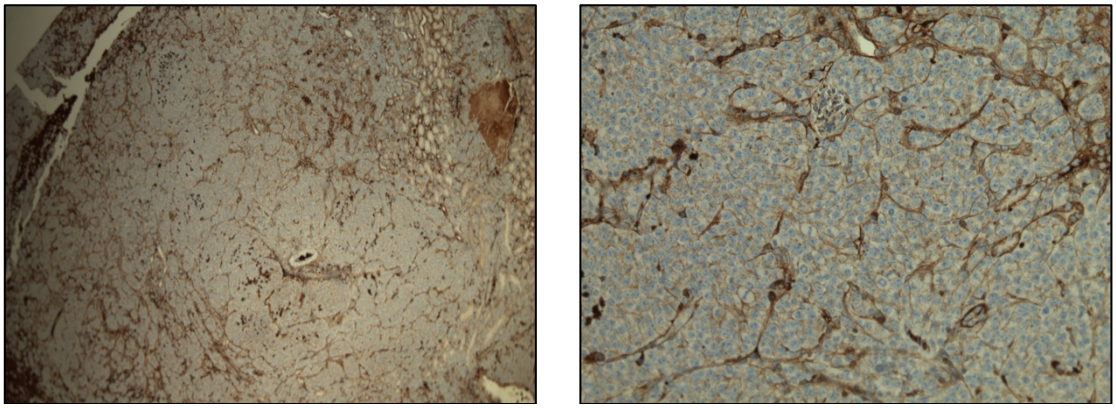

(B) (i) (ii)

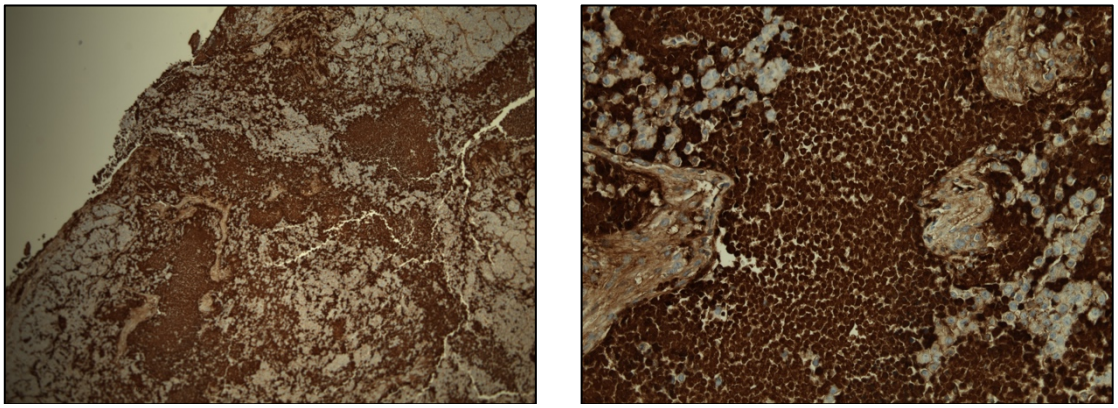

(C) (i) (ii)

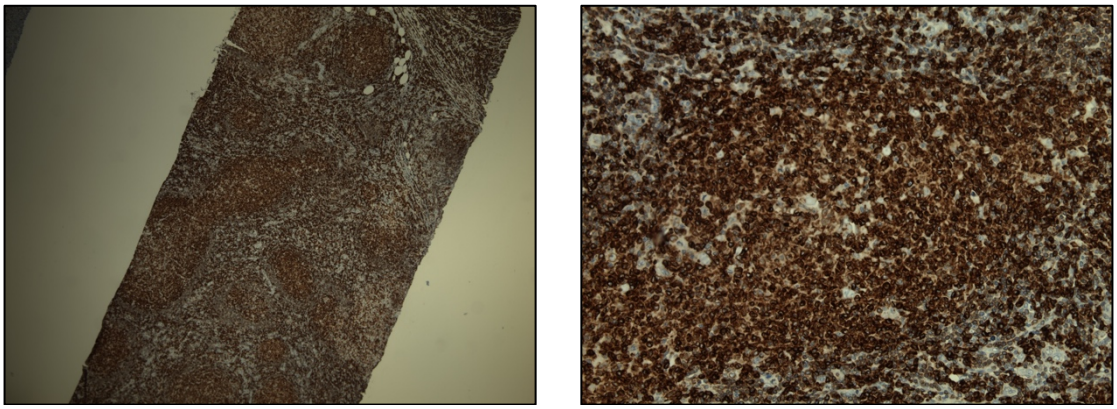

Figure 44 Over-expression of Bcl-2 in orthotopic model

1 x 10 ^{6} NHO1A neuroblastoma cells were suspended in 20ul of normal saline. Cells were engineered to either over-express (A) MSCV (empty vector) or (B) Bcl-2. (i) Immunohistochemistry for Bcl-2 x 4 (ii) IHC for Bcl-2 (x20). (C) (i) Follicular lymphoma, positive control, IHC for Bcl-2 (x4) (ii) Follicular lymphoma, positive control, IHC for Bcl-2 (x20).

3.4.19. PF-502 inhibits Bcl-2 over-expressing NHO1A cells in vitro at higher IC50

PF-502 was added in escalating doses to NHO1A, NHO1A over-expressing Bcl-2 and MSCV (empty vector) cells. The IC_{50} of NHO1A (90nM) and MSCV (160nM) cells was similar. However, when the contribution of apoptosis was inhibited by Bcl-2 over-expression, the IC_{50} was of PF-502 increased to 960nM with an incomplete cell death at 10000nM.

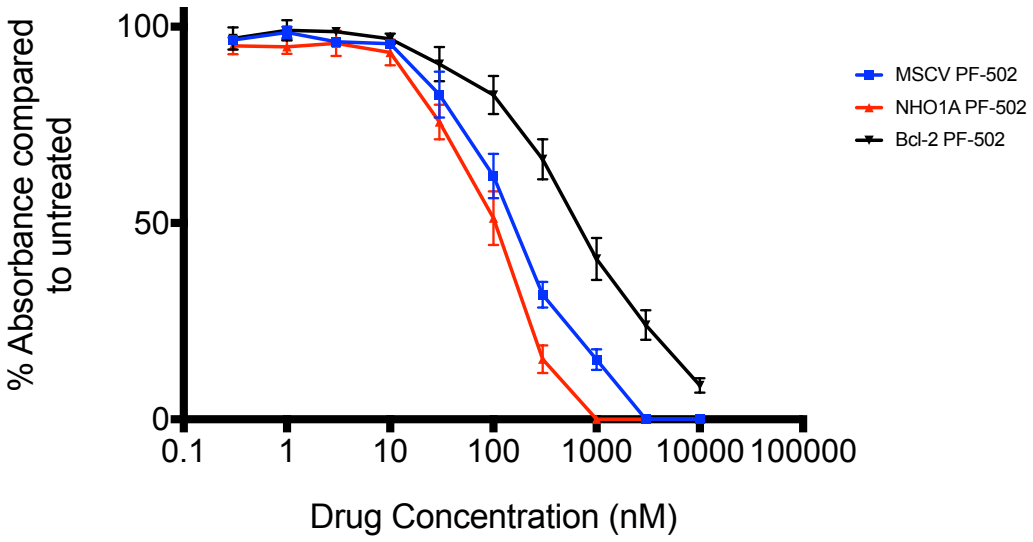

Figure 45 Efficacy of PF-502 established in Bcl-2 over-expressing NHO1A cell lines.

NHO1A (*MYCN* amplified), NHO1A Bcl-2 over-expressing and NHO1A MSCV (empty vector) cells were cultured in 96 well plates and cell specific media for 48 hours prior to addition of PF-502. Drug was added in escalating doses and cells were left exposed for 72 hours. Plates were incubated at 37^0C, 5% CO_2. Plates were processed after 72 hours according to our standard SRB protocol. Absorbance of SRB was determined as a measure of cell number. Data was processed, and drug curves processed by Prism software.

3.4.20. **PF-502 inhibits the PI3K/AKT/mTOR pathway in Bcl-2 over-expressing NHO1A cells in vitro**

There appeared to be altered expression of the pathways being interrogated in the transduced cells. When a fixed concentration of PF-502 (at IC70 doses) was added to Bcl-2 and MSCV (empty vector) NHO1A cells, inhibition of phospho-AKT, phospho-S6 and phospho-4EBP1 was observed. Together these results are consistent with inhibition of the PI3K/AKT/mTOR pathway (Figure 46). Given that these cells were orthotopically transplanted into the wild type littermates, it is reasonable to assume that the resultant tumours would respond to PF-502 in a similar fashion.

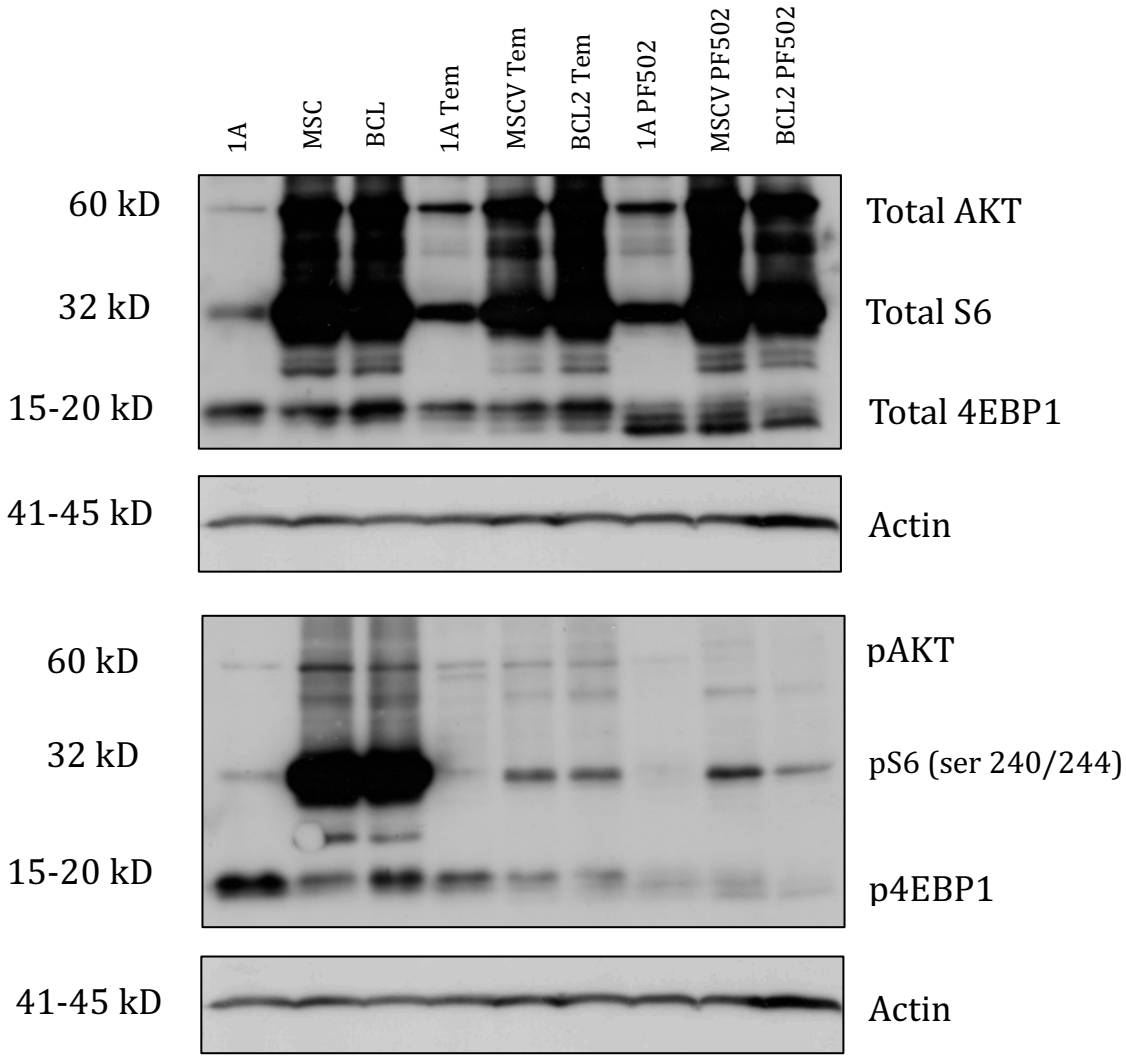

Figure 46 Western Blot (WB) analysis of protein lysates from NHO1A cells over-expressing Bcl-2 or MSCV (empty vector) exposed to fixed concentrations of PF-502 or temsirolimus.

NHO1A cells over-expressing Bcl-2 or MSCV (empty vector) were exposed to 300nM of PF-502 or 100nM of temsirolimus for three hours. WB membranes were probed for biomarkers of PF-502 and temsirolimus activity including total AKT, pAKT (ser473), total S6, pS6 (ser240/244), p4EBP1 (Thr37/46) & NMYC. Actin was used as a loading control. Addition of 500nM PF-502 was associated with a decrease in biomarkers including pAKT (ser473), pS6 (ser240/244) and p4EBP1 (Thr37/46) indicating that these pathways had been inhibited. Tem = temsirolimus.

3.4.21. PF-502 reduces expression N-Myc in Bcl-2 and MSCV (empty vector) over-expressing NHO1A cells in vitro

When a fixed concentration of PF-502 was added to Bcl-2 and MSCV (empty vector) NHO1A cells, a reduction in N-Myc was observed (Figure 47). Given that these cells were orthotopically transplanted into the wild type littermates, it is reasonable to assume that a similar response to PF-502 would be observed in the resultant tumours.

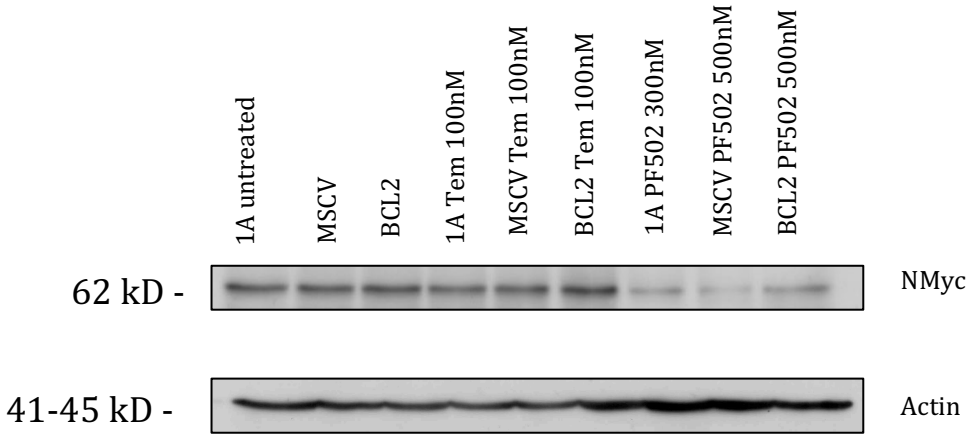

Figure 47 Western Blot (WB) analysis of protein lysates from NHO1A cells over-expressing Bcl-2 or MSCV (empty vector) exposed to fixed concentrations of PF-502 or temsirolimus.

NHO1A cells over-expressing Bcl-2 or MSCV (empty vector) were exposed to 300-500nM of PF-502 or 100nM of temsirolimus for three hours. WB membranes were probed N-Myc. Actin was used as a loading control. Addition of 500nM PF-502 and 100nM temsirolimus was associated with a dose dependent decrease in N-Myc expression.

3.4.22. **Efficacy of PF-502 in the NHO1A orthotopic mouse model over-expressing Bcl-2**

PF-502 significantly improves survival in the TH-*MYCN* neuroblastoma mouse model (3.4.4) and the NHO1A orthotopic model (3.4.13). It achieves this by both promoting apoptosis (3.4.7) and by inhibiting tumour angiogenesis (3.4.8). In order to understand the balance between these anti-tumour processes and their importance in the ultimate efficacy of PF-502, NHO1A orthotopic mice over-expressing Bcl-2 or MSCV (empty vector) were exposed to PF-502 or vehicle. Over-expression of Bcl-2 induces resistance to apoptosis and should therefore negate the impact of apoptosis on the final phenotype (Hotchkiss et al., 1999).

Mice bearing orthotopic tumours injected with MSCV (empty vector) NHO1A cells and treated with PF-502 had a significant survival difference compared to vehicle treated mice (Figure 48 A). This improvement in overall survival was comparable to that seen previously in the orthotopic model. A similar inhibition of tumour growth, measured by serial abdominal ultrasound scans, was also observed (Figure 48 B). Mice bearing orthotopic tumours injected with NHO1A cells over-expressing Bcl-2 and treated with PF-502 also had a significantly improved survival when compared to vehicle treated mice but their survival was significantly less than the MSCV (empty vector) treated mice when treated with PF-502 (Figure 48 A).

This significant difference in survival observed between the PF-502 treated Bcl-2 and MSCV mice suggests that the ability of PF-502 to both induce apoptosis and inhibit angiogenesis contribute to its anti-tumour effect in an additive fashion. When the impact of apoptosis is removed in the Bcl-2 over-expressing mice, a significant difference of survival was still observed, when compared to vehicle treated mice, possibly due to the anti-angiogenic effect of PF-502 (Figure 48).

(A)

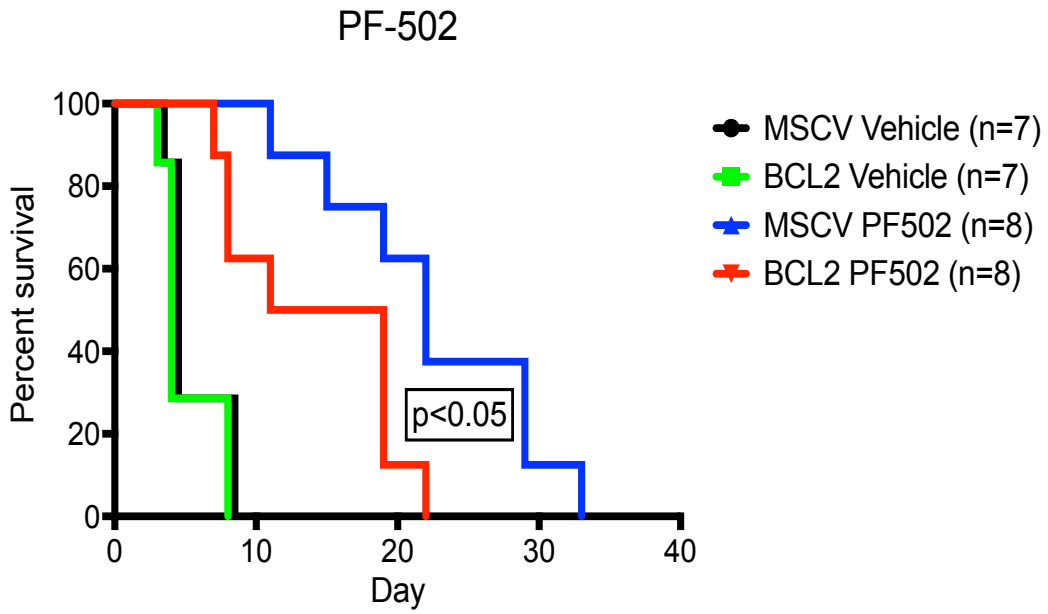
PF-502
Percent survival
100
80
60
40
20
0
0
10
20
30
40
Day
p<0.05
MSCV Vehicle (n=7)
BCL2 Vehicle (n=7)
MSCV PF502 (n=8)
BCL2 PF502 (n=8)

(B)

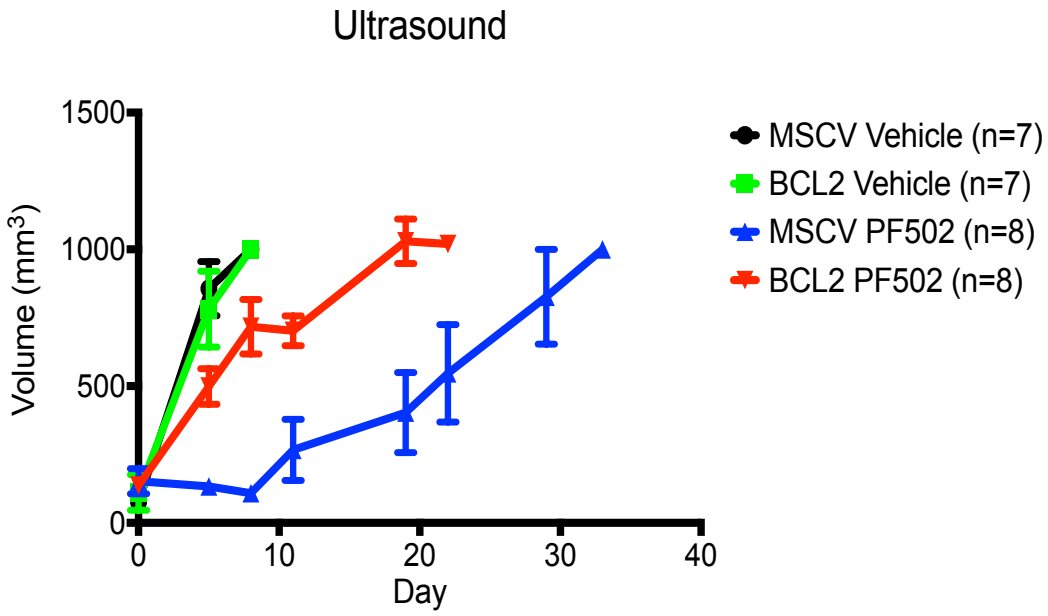
Ultrasound
Volume (mm3)
1500
1000
500
0
0
10
20
30
40
Day
MSCV Vehicle (n=7)
BCL2 Vehicle (n=7)
MSCV PF502 (n=8)
BCL2 PF502 (n=8)

Figure 48 Efficacy of PF-502 in NHO1A orthotopic mouse model over-expressing Bcl-2 or MSCV (empty vector).

(A) A significant difference in survival in mice treated with PF-502 was observed, when compared with vehicle treated mice. MSVC (empty vector) mice had a significantly prolonged survival when compared to both vehicle treated mice and Bcl-2 over-expressing mice ($p < 0.05$, one way ANOVA) (B) A significant inhibition of tumour growth as evidenced by 3D tumour volumes, in mice treated with PF-502 when compared with vehicle treated mice ($p< 0.05$, two way ANOVA). A difference was also observed between MSCV (empty vector) and Bcl-2 over-expressing mice ($p< 0.05$, two way ANOVA).

3.4.23. PF-502 and angiogenesis in the NHO1A orthotopic mouse model over-expressing Bcl-2

Due to a possible additive contribution of both apoptosis and anti-angiogenesis to the efficacy of PF-502 it was important to confirm that a significant anti-angiogenic effect was still being observed in both the Bcl-2 over-expressing and MSCV (empty vector) mice. Without a confirmed anti-angiogenic effect, its contribution to the anti-tumour activity of PF-502, when apoptosis is inhibited by Bcl-2 over-expression, could not be confirmed.

Both MSCV (empty vector) and Bcl-2 over-expressing mice demonstrated a significant reduction in CD31 staining when exposed to PF-502 when compared to vehicle treated mice (Figure 49). This confirms that the impact of PF-502 on angiogenesis remains intact in the absence of its ability to induce apoptosis. It is this ongoing anti-angiogenic effect that potentially contributes, or is in fact responsible for, the differences in survival seen between mice over-expressing Bcl-2 and MSCV (empty vector). The importance of the anti-angiogenic effect of the combined PI3K/mTOR inhibitor BEZ235 in NBL mouse models has been previously confirmed and is thought to be enhanced by paracrine signalling through *MYCN* (Chanthery et al., 2012).

(A) (i) (ii)

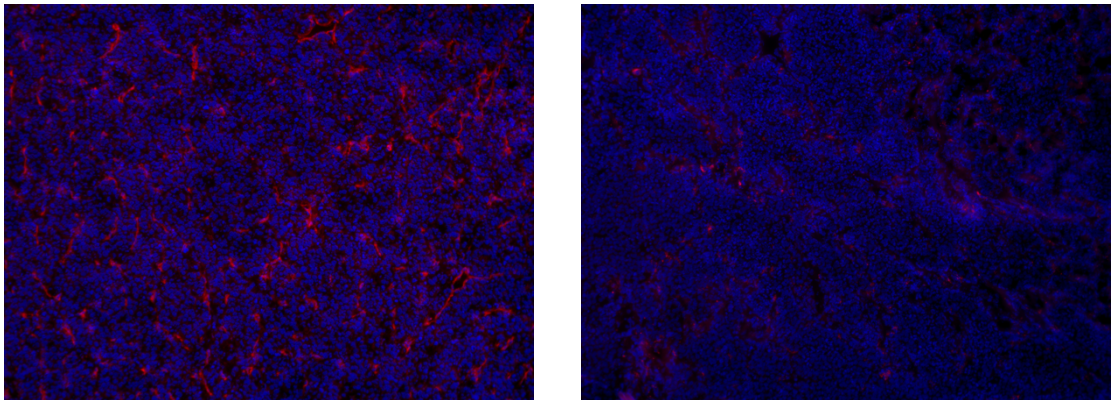

(B) (i) (ii)

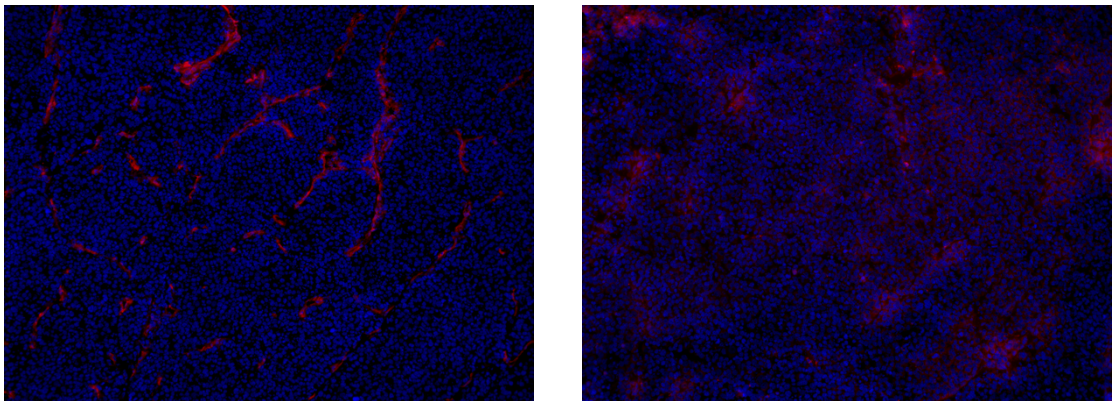

(C)

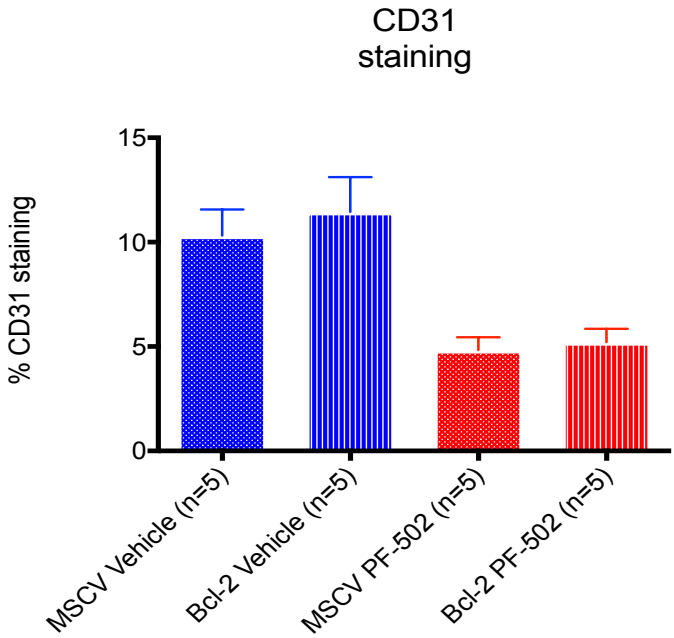
CD31 staining
% CD31 staining
15
10
5
0
MSCV Vehicle (n=5)
Bcl-2 Vehicle (n=5)
MSCV PF-502 (n=5)
Bcl-2 PF-502 (n=5)

Figure 49 Angiogenesis in the NHO1A orthotopic mouse model over-expressing Bcl-2 or MSCV (empty vector).

CD31 staining of (A) MSCV (empty vector) or (B) Bcl-2 over-expressing NHO1A orthotopic mice having been treated for 48 hours with (i) methylcellulose 0.5% 10ul/100g (vehicle) daily via oral gavage (x20) (ii) PF-502 10mg/kg daily via oral gavage (x20) (C) Quantitative metamorph analysis of CD31 staining of MSCV (empty vector) or Bcl-2 over-expressing NHO1A orthotopic mice having been treated for 48 hours with methylcellulose 0.5% 10ul/100g (vehicle) ($p< 0.05$, student *t*-test) daily via oral gavage or PF-502 10mg/kg ($p< 0.05$, student *t*-test)

3.4.24. **PF-502 and apoptosis in the NHO1A orthotopic mouse model over-expressing Bcl-2**

The anti-apoptotic protein Bcl-2 inhibits activation of caspases 2 and 3 (Swanton, Savory, Cosulich, Clarke, & Woodman, 1999). Therefore, the use of caspase 3 as a measure of apoptosis in a Bcl-2 over-expressed system may be influenced by Bcl-2 in a manner independent of drug induced apoptosis.

Ideally NHO1A Mice bearing orthotopic tumours, over-expressing Bcl-2 would have been enrolled in a short-term experiment where PF-502 was administered and tumour tissue harvested for markers of apoptosis including H&E and TUNEL staining. I had previously performed a short-term experiment, but all tumour tissue was processed in OCT for CD31 staining. However, due to a contamination in my Bcl-2 and MSCV cell lines I was not able to complete the planned short-term experiments.

3.5.**Discussion and Conclusions**

The value of archival human tissue samples, especially in the evolving era of personalised medicine, is well established (C. C. Cheung, Martin, & Asa, 2013). It is crucial to maintain these repositories and access this tissue responsibly. In particular, these archival tissue samples become even more important, as new methods of tumour interrogation are developed.

At the start of this PhD I had identified a subset of archival human NBL available from the RCH pathology biobank (Table 5). It was the intention to interrogate a larger sample size of tumours for expression of the PI3K/AKT/mTOR pathway. However, very similar data was published at this time (Johnsen et al., 2008) which reduced the potential scientific impact of reproducing this data.

When the opportunity arose to access these samples for another project that was unique at the time (Kong et al., 2016) it was reasonable to perform PI3K/AKT/mTOR pathway analysis in this limited, but representative, subset of patients. As stated earlier, the cure rates of LR and IR neuroblastoma are excellent and these are not the patient groups where research needs to be focused on improving patient outcomes (Katherine K. Matthay et al., 2016). It is the high-risk patients that frequently relapse or fail to respond to therapy that require this research focus. These high-risk patients are represented in this patient cohort. Clearly, in this small but representative cohort of high-risk human NBL tissue samples, the PI3K/AKT/mTOR pathway was strongly activated in all samples tested, confirming that it is a valid target in the treatment of NBL.

As part of this chapter the role of small animal imaging in pre-clinical translational research was explored. Tools such as small animal US and FDG-PET give researchers additional response assessments that go beyond simple survival analysis. Small animal US can measure three-dimensional tumour volumes and allow for a quantitative assessment of response. This response can then be compared to

standard measures often used in human subjects, such as the INRC (J. R. Park et al., 2017).

Functional imaging such as FDG-PET allows researchers to quantitatively assess the metabolic response within a tumour. This has become particularly important in diseases such as Hodgkin's Lymphoma where it is now considered standard of care in documenting tumour response (Subocz et al., 2017). Together, these small animal imaging techniques were well tolerated by the mice and contributed significant information to the response assessment in the mouse models studied.

Temsirolimus was effective in treating TH-*MYCN* tumour bearing mice and conferred a significant survival advantage, with a corresponding partial tumour response on small animal imaging. This partial response was documented by both small animal US and FDG-PET. Mice quickly relapsed when drug was removed at day 35.

There was no significant evidence of temsirolimus inducing apoptosis, and this is consistent with previously published data (4.3.6) (Del Bufalo et al., 2006; Moriya et al., 2014; Yazbeck et al., 2006; H. Zhang et al., 2013). Instead the anti-tumour effect was primarily mediated by an anti-angiogenic effect (4.3.7) (L. Wang et al., 2010). Correspondingly there was also evidence of cellular senescence which has also been reported with mTORC1 inhibitors (4.3.8) (Wall et al., 2013). Drugs that primarily induce cellular senescence or that work by inhibiting angiogenesis tend to be cytostatic in nature (S. K. Carter, 2000; Ewald, Desotelle, Wilding, & Jarrard, 2010).

Previously published data suggests that rapalogs are primarily cytostatic, not cytotoxic, and they achieve their anti-tumour benefit via disease stabilisation rather than regression (Fagone et al., 2013; Meric-Bernstam & Gonzalez-Angulo, 2009). This is consistent with the observation that they tend to be more effective when combined with other chemotherapeutic agents that are cytotoxic (B. Hong et al., 2017) or DNA damaging radiation therapy (D. Wang, Gao, Liu, Yuan, & Wang, 2017).

Other possible explanations for this include the fact that temsirolimus is converted to sirolimus *in vivo*, following removal of the dihydroxymethyl propionic acid ester group at C40, and therefore may require this conversion to be fully activated in the same way that many pro-drugs act (MacKeigan & Krueger, 2015; Mizuno et al., 2017). However, there is evidence that temsirolimus acts independently in its own right as an MTORC1 inhibitor with the additional benefit of sirolimus following its metabolism (Brian I. Rini, 2008). Studies that have been performed *in vitro* and *in vivo* directly comparing the anti-tumour activity of temsirolimus and sirolimus and have displayed almost equivalent anti-tumour activity (Fagone et al., 2013). Interestingly when temsirolimus and sirolimus were compared in prostate cancer cell lines a similar incomplete growth inhibition and G1 cytostatic arrest was observed (Fagone et al., 2013).

Another possibility is that temsirolimus may act by a mechanism that cannot be reproduced in certain *in vitro* culture systems. An example of this would be a drug that primarily acts via an anti-angiogenic mechanism as has been demonstrated for temsirolimus in many human cancers (Le Tourneau, Faivre, Serova, & Raymond, 2008; L. Wang et al., 2010). Temsirolimus primarily inhibits angiogenesis via decreased VEGF expression, both on RNA and protein levels (Liegl et al., 2014). A dose of 100nM temsirolimus was chosen for *in vitro* experiments which is consistent with the maximal observed effective dose in other cell lines (H. Zhang et al., 2013).

When considering the best way to evaluate cytostatic drugs in the pre-clinical setting, thought needs to be given to the different assay tools available. The SRB assay, which measures cellular protein content, is considered a cytotoxic assay and so was potentially not the most appropriate assay to measure the effects of drugs such as temsirolimus (Blois, Smith, & Josephson, 2011). Perhaps a better assay would have been an ATP assay which can distinguish between cytotoxic and cytostatic drugs based on the cellular ATP levels (Garewal, Ahmann, Schifman, & Celniker, 1986).

When evaluating the *in vivo* effect of cytostatic drugs in early phase human trials,

many clinicians are adopting the "cytostatic paradigm" and choosing to measure outcomes such as time to progression (TTP) rather than traditional measures such as EFS and OS (S. K. Carter, 2000). If using TTP as a more appropriate outcome measure it is interesting to note that the temsirolimus treated mice did not progress whilst on treatment. The role of small animal US is particularly relevant in this setting as the tumour volumes remained relatively static during this treatment period as well.

Pre-clinical animal model systems are essential for translational research. They allow researchers to confirm the efficacy and toxicity of treatments prior to human trials. In particular, animal models that can be manipulated to either under or over express biological functions or cellular pathways can be important in dissecting the contribution of these processes to the disease being studied. At the time of this research, the number of pre-clinical models for paediatric NBL was extremely limited. In fact, the TH-*MYCN* murine mouse model was established and published in the year prior to this research commencing (Weiss et al., 1997). Perhaps the best-known system for pre-clinical NBL research prior to that mouse model was the zebrafish (Casey & Stewart, 2018; Corallo, Candiani, Ori, Aveic, & Tonini, 2016).

In this chapter the mice bearing orthotopic tumours model has been validated as a model that can be genetically manipulated, as a new pre-clinical tool in the study of neuroblastoma. With an intact immune system, it provides a model in which mouse derived NBL cells can be manipulated and placed back into the model for further interrogation. Although the TH-*MYCN* murine mouse model has an intact immune system, it does not have the scope for further genetic modification. This is a contrast to xeno-transplanted mice which do not have an intact immune system. When exposed to PF-502 the NHO1A mice bearing orthotopic tumours model faithfully recapitulated many of the efficacy studies performed in the TH-*MYCN* mouse model. In addition, over-expression of Bcl-2 in the NHO1A cells prior to transplant was successful and produced a murine NBL phenotype that was potentially more resistant to apoptosis. Perhaps the biggest asset of this mouse model is the fact that it retains an intact immune system. This is particularly important when biological factors such

as tissue microenvironment can impact on treatment outcomes. In the evolving era of immune therapy this becomes particularly important. There is also evidence that epigenetic modifiers such as HDACi require an intact immune system to function (West et al., 2013).

PF-502 was effective in treating TH-*MYCN* tumour bearing mice and conferred a significant survival advantage with a corresponding partial tumour response on small animal imaging. This anti-tumour effect was mediated by both apoptosis and an anti-angiogenic effect. Although the anti-angiogenetic effect of PF-502 was significant at all time points, the impact on tumour growth was not as pronounced as that seen with temsirolimus (Figure 20). Temsirolimus treated mice were all alive at day 35 when drug was removed; however, the majority of PF-502 treated mice had succumbed to disease prior to this timepoint. Therefore, the addition of PI3K inhibition, with its associated anti-apoptotic benefits (Figure 33), did not provide an apparent advantage over mTORC1 inhibition alone.

Correspondingly there was no significant evidence of cellular senescence. Assuming the impact of apoptosis was removed by over-expression of Bcl-2, as this was not formally confirmed, the retained anti-angiogenic effect still had a significant anti-tumour effect and prolonged survival in an orthotopic mouse model. Both the combined anti-angiogenic effect and pro-apoptotic effect appear at least additive, if not synergistic, and necessary for the therapeutic benefit of PF-502. These results are consistent with previously published data for combined PI3K/mTOR inhibitors.

4 Histone deactylase inhibition in the TH-*MYCN* neuroblastoma mouse model.

4.1.**Introduction**

The amplification of the proto-oncogene *MYCN* in neuroblastoma remains one of the predictors of poor prognosis in children with NBL (Brodeur, 2003; J. M. Maris et al., 2007). As discussed earlier in this thesis, *MYCN* driven transcription can have a significant, often deleterious effect, on a wide variety of cellular processes including apoptosis and differentiation (Adhikary & Eilers, 2005; Arvanitis & Felsher, 2006; Cowling & Cole, 2006). Therefore modulating the epigenetic processes that contribute to this transcriptional process may undo those processes that are directly responsible for driving and maintaining neuroblastoma.

NBL is a cancer that is unique in many regards. In particular it has the ability to spontaneously differentiate into benign tissue that resembles its neuronal origins (Brodeur, 2003; J. M. Maris et al., 2007). This ability to spontaneously differentiate into benign tissue is characteristic of stage Ms disease, which is associated with infants < 18 months old. Interestingly one hallmark of stage Ms disease is the fact that *MYCN* amplification is extremely rare and, if present, changes the risk from low to high (Table 1) (Schleiermacher et al., 2003). There is evidence to support several possible mechanisms of spontaneous regression in neuroblastomas: neurotrophin deprivation, loss of telomerase activity, humoral or cellular immunity and most interestingly alterations in epigenetic regulation (Brodeur, 2018). Research focusing on stage 4s disease identified reduced promotor methylation in 97% of genes in which differential methylation was detected, and that these samples were enriched for genes involved in cellular differentiation (Brodeur & Bagatell, 2014). Whole genome sequencing of a comprehensive panel of neuroblastomas demonstrated that malignant tumors had recurrent defects in genes controlling neuritogenesis and differentiation (Molenaar et al., 2012). The possibility therefore exists that epigenetic modulators, such as HDACi, can drive this differentiation process and potentially transform malignant NBL into benign ganglioneuroma.

The role of HDACi in cellular processes including differentiation has been discussed previously (2.2.7.4). Importantly numerous proteins have been identified that act as substrates for HDACi, and these proteins are essential in many cellular processes including cell proliferation, cell death, cell migration and differentiation (Dokmanovic, Clarke, & Marks, 2007). The particular interest of using HDACi in NBL stems from the observation that *MYCN* and HDACi co-operate to regulate these cellular processes. In particular HDAC5 has been shown to block neuroblastoma cellular differentiation, and does so by co-operating with *MYCN* (Y. Sun et al., 2014), whilst selective inhibitors of HDAC8 have been shown to promote NBL differentiation (Rettig et al., 2015). The ability of HDACi to promote terminal differentiation has been demonstrated in pre-clinical models of other paediatric cancers including osteosarcoma and acute myeloid leukaemia (Bots et al., 2014; Cain et al., 2013).

In this chapter we explore the anti-tumour activity of the pan-HDACi panobinostat in the TH-*MYCN* mouse model of neuroblastoma. In particular we wish to investigate the potential of sustained, low-dose panobinostat, on the epigenetically driven differentiation process. Panobinostat was chosen as it is available in an oral formulation which is ideal for metronomic dosing, and there is some early phase safety data in paediatrics (Wood et al., 2018).

4.2.**Results**

4.2.1. **Panobinostat is tolerated in TH-*MYCN*wild type littermates.**

Panobinostat was administered daily by intraperitoneal injection at a dose of 5mg/kg/daily (35mg/week). Mice were examined daily for signs of toxicity as previously described (2.9.3). Doses of up to 25mg/kg three times a week (75mg/week) were currently being used in our institution in other mouse strains.

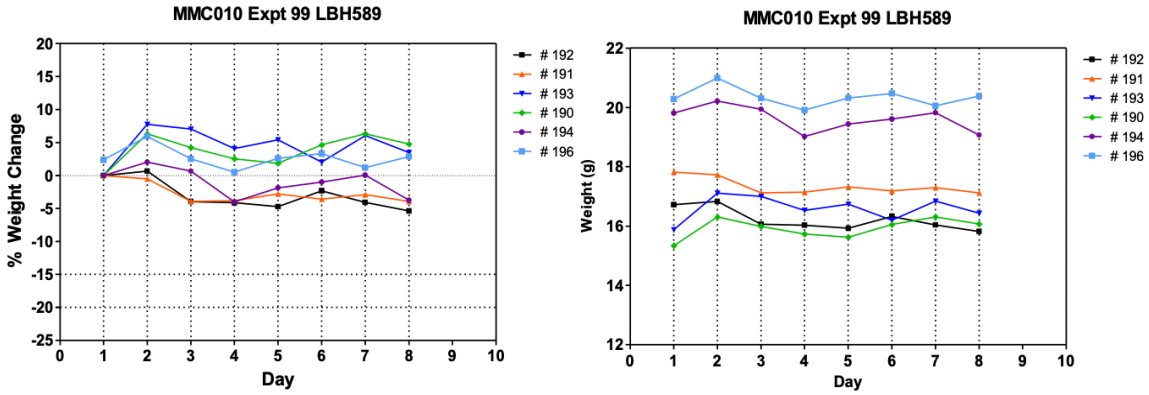

Figure 50 Maximum tolerated dose (MTD) of panobinostat in TH-*MYCN* mice

Tolerability of the panabinostat (LBH-589) in TH-*MYCN* WT non-tumour bearing mice was confirmed. Dose escalations were continued until a tolerable dose was defined. A dose of 5mg/kg given intraperitoneally once daily was deemed tolerable.

4.2.2. **Panobinostat prolongs survival and reduces tumour burden in TH-*MYCN* neuroblastoma mice**

TH-*MYCN* homozygous mice (2.8.2) with demonstrable disease on ultrasound (2.10.1) were randomised to receive vehicle or panobinostat 5mg/kg of panobinostat daily for a total of three or nine weeks. Typically, tumours develop by 4-6 weeks of age and grow rapidly in this mouse model (Rasmuson et al., 2012). Tumours in the vehicle treated group grew rapidly with a median time to sacrifice of 7 days. Mice treated for three weeks with panobinostat had a significant survival advantage over the vehicle treated group with a median survival of 68 days. All of the mice in this group eventually relapsed with neuroblastoma after panobinostat was ceased.

To investigate whether a longer period of treatment with panobinostat would result in a more prolonged survival benefit, panobinostat was administered daily for a total of nine weeks. The panobinostat was tolerated by the mice for this extended treatment period (2.9.3). With the exception of one mouse, which relapsed after six days from the completion of treatment, all mice remained well and tumour free 100 days post cessation of treatment. This was a significant survival benefit when compared to both the vehicle treated mice and the mice treated with panobinostat for three weeks, and potentially represented a curative response in this aggressive murine model of neuroblastoma. Mice treated with panobinostat has a rapid tumour response with no evidence of residual tumour, on ultrasound imaging (2.10.1) by day five of imaging.

(A)

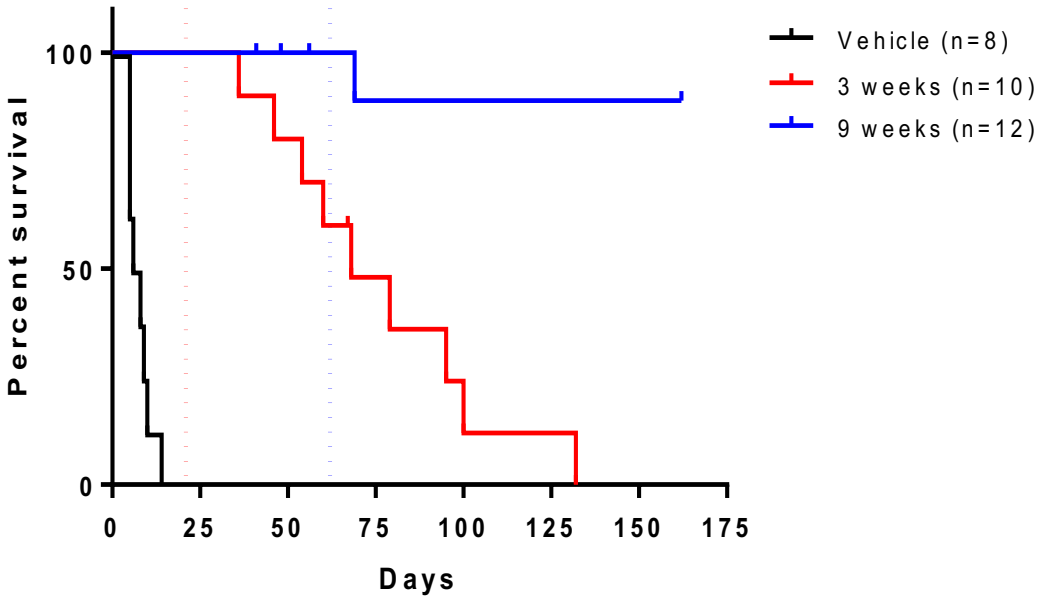
Percent survival
100
50
0
0
25
50
75
100
125
150
175
Days
Vehicle (n=8)
3 weeks (n=10)
9 weeks (n=12)

(B)

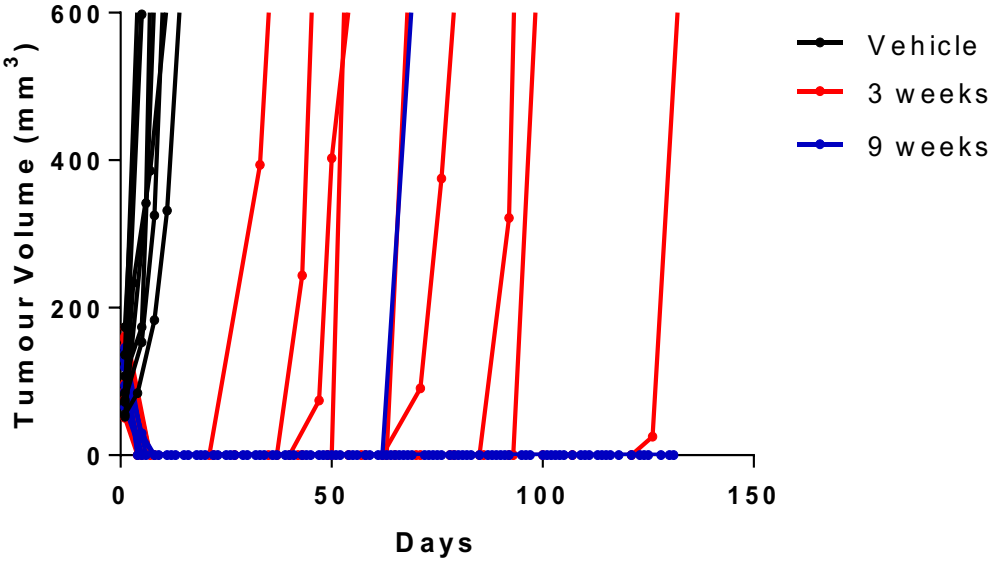
Tumour Volume (mm3)
600
400
200
0
0
50
100
150
Days
Vehicle
3 weeks
9 weeks

Figure 51 Panobinostat prolongs survival and reduces tumour burden in TH-*MYCN* neuroblastoma mice

(A) A significant difference in survival was observed in mice treated with panobinostat when compared with vehicle (n= 8-12) ($p<0.0001$ versus vehicle) in mice treated for either three weeks or nine weeks. A significant survival difference between mice treated with panobinostat for nine weeks as opposed to three weeks was also observed ($p<0.0001$). Dotted lines represent the last day of treatment for that group. (B) A significant and rapid tumour response, as measured by 3D tumour volumes, was observed in mice treated with panobinostat when compared with vehicle.

4.2.3. **Panobinostat induces apoptosis**

Given the rapid tumour response to panobinostat that was observed on serial abdominal ultrasounds, tumours were examined for markers of apoptosis. TH-*MYCN* homozygous mice were treated for 48 hours (2 doses) with either vehicle or 5mg/kg panobinostat (2.9.4). Tumours were then harvested (2.9.5.1) and prepared for immunostaining. Immunostaining of tumours revealed a dramatic increase in staining of cleaved caspase 3, as well as histological changes consistent with apoptosis. In addition, panobinostat induced acetyl-histone H3 expression, while BIM, Mcl-1 and BMF protein levels, members of the BCL-2 proapoptotic family, were increased consistent with previously published data (J. Zhang & Zhong, 2014). BCL-2 remained unaltered.

(A)(i)

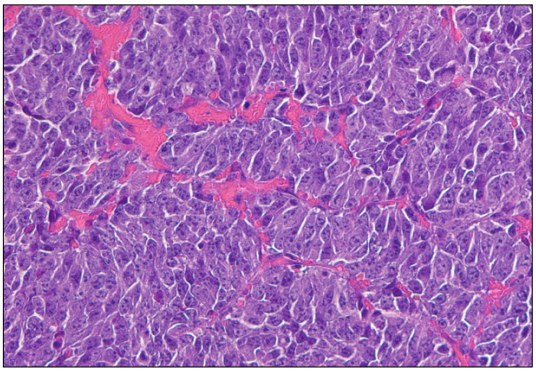

(ii)

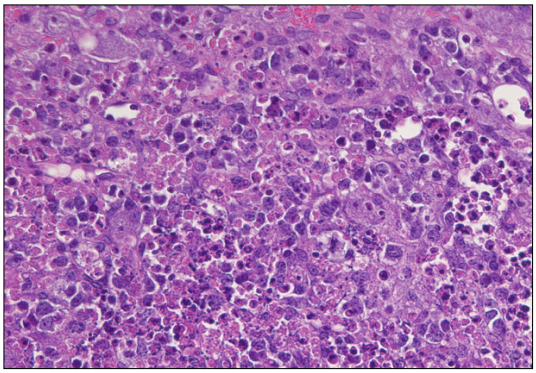

(B)(i)

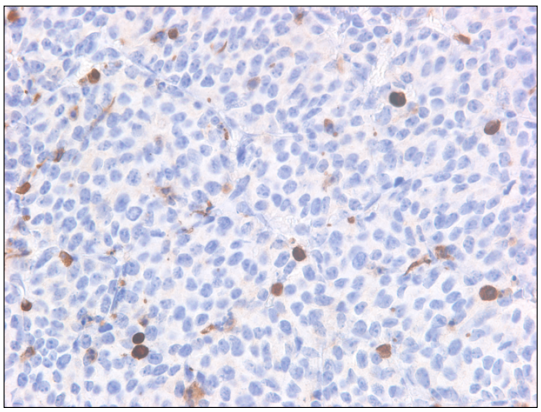

(ii)

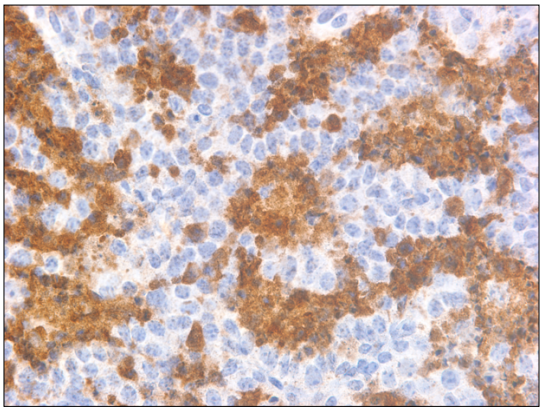

(C)

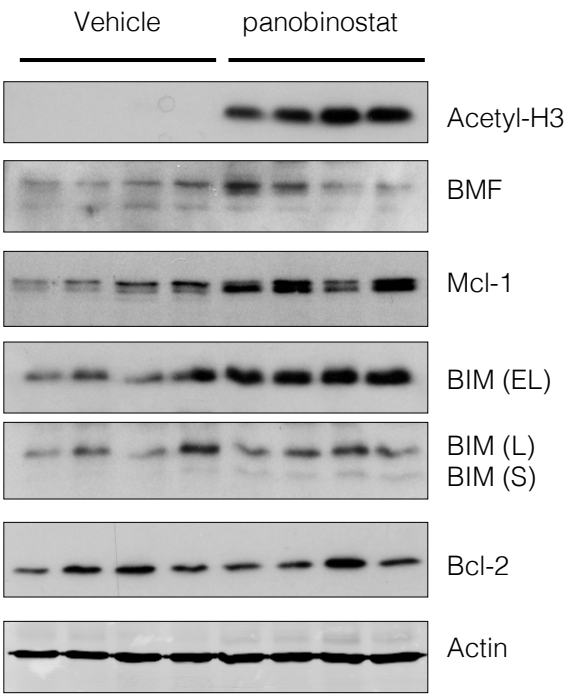
Vehicle
panobinostat
Acetyl-H3
BMF
Mcl-1
BIM (EL)
BIM (L)
BIM (S)
Bcl-2
Actin

Figure 52 Panobinostat treatment induces apoptosis in TH-*MYCN* tumour bearing mice

Tumour bearing mice (n=4) were exposed to either (i) vehicle or (ii) panobinostat for 48 hours (2 doses) and then harvested. Tumours were stained for markers of apoptosis including (A) H&E and (B) cleaved caspase 3. (C) Tumour lysates were immunoblotted for Acetyl Histone H3, BMF, BIM, Mcl-1, Bcl-2 and actin.

4.2.4. **Long term treatment of the TH-*MYCN* mouse model with panobinostat results in differentiation**

While the initial rapid tumour response to panobinostat was consistent with apoptosis (1.14.2.11), the difference that was observed between mice treated for 3 weeks and 9 weeks would suggest that a second process was required to explain the prolonged survival seen in those mice treated for 9 weeks. To this end, to assess whether terminal differentiation was observed in mice treated with panobinostat, tumours treated for 9 weeks were harvested and then assessed for markers of differentiation. H&E staining confirmed that mice treated for 9 weeks had tumours consistent with well differentiated ganglioneuroma. Interestingly, at Day 7 of treatment, samples harvested showed a mixed phenotype of both poorly and well differentiated cell types. Further to this, the number of Ki67, N-Myc positive cells was significantly reduced by Day 7 and then completely absent by Day 21 of treatment. In contrast, the expression of differentiation markers including S100, and somatostatin receptor 2 (SSTR2) increased throughout this time course. These data strongly suggest the induction of differentiation during panobinostat treatment.

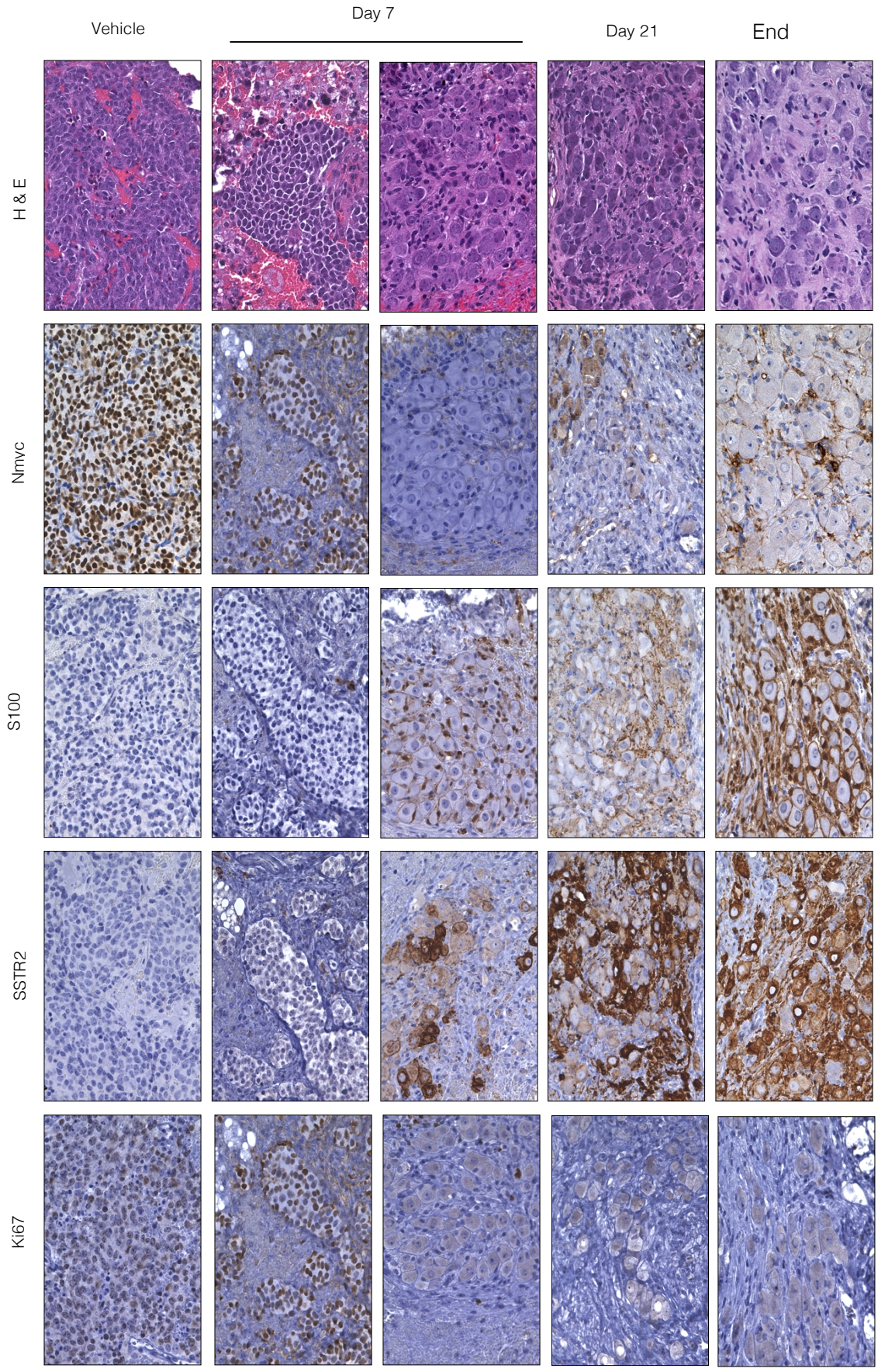
Vehicle
Day 7
Day 21
End
H & E
Nmvc
S100
SSTR2
Ki67

Figure 53 Panobinostat promotes differentiation

TH-*MYCN* mice were treated with either panobinostat or vehicle. Tumours were analysed at baseline or Days 7, 21 or at endpoint (100 days after cessation of treatment). Images from each timepoint are shown following staining with H&E, N-Myc, S100, SSTR2, and Ki67 expression.

4.2.5. **Gene expression profiling of panobinostat treated mice**

Differential gene expression analysis was performed on mice treated with either panobinostat or vehicle for 48 hours and harvested 4 hours after the second dose. Pathway enrichment analysis revealed that genes involved in many cellular processes including neurogenesis, chromatin modification, cytoskeletal remodelling and NOTCH signalling pathway were significantly altered following panobinostat treatment. In addition, targeted GSEA analysis comparing this data to that previously published (Frumm et al., 2013) shows that upregulated genes within that signature are significantly enriched for within this data set. It is important to note that the Frumm gene signature included 59 genes. This analysis excluded 8 control genes and 10 genes that did not have a mouse homologue or due to gene expression below the limit of detection. In total 68 % of genes upregulated in the Frumm data set were also upregulated in the TH-*MYCN* mice when treated with panobinostat. In addition, 60% of genes downregulated in the Frumm data set were present in both. This data suggests that induction of differentiation starts as early as 24 hours after starting panobinostat dosing.

(A)

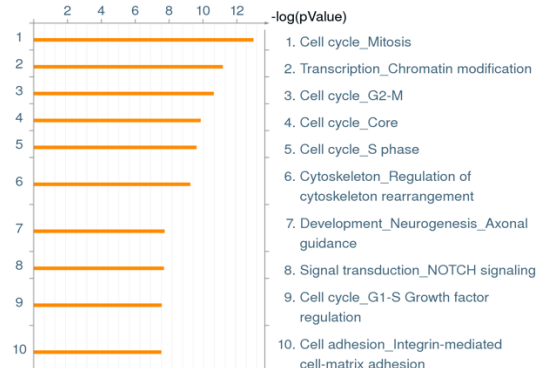
2
4
6
8
10
12
-log(pValue)
1
2
3
4
5
6
7
8
9
10
1. Cell cycle_Mitosis
2. Transcription_Chromatin modification
3. Cell cycle_G2-M
4. Cell cycle_Core
5. Cell cycle_S phase
6. Cytoskeleton_Regulation of cytoskeleton rearrangement
7. Development_Neurogenesis_Axonal guidance
8. Signal transduction_NOTCH signaling
9. Cell cycle_G1-S Growth factor regulation
10. Cell adhesion_Integrin-mediated cell-matrix adhesion

(B)

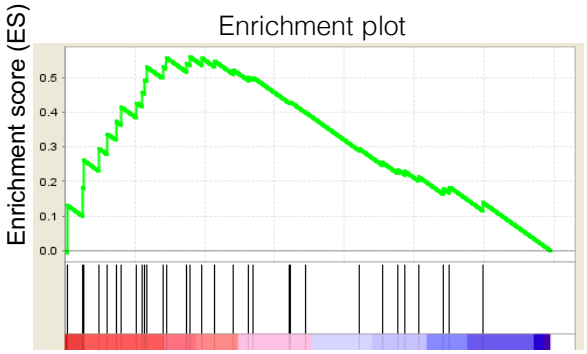
Enrichment plot
Enrichment score (ES)
0.5
0.4
0.3
0.2
0.1
0.0

(C)

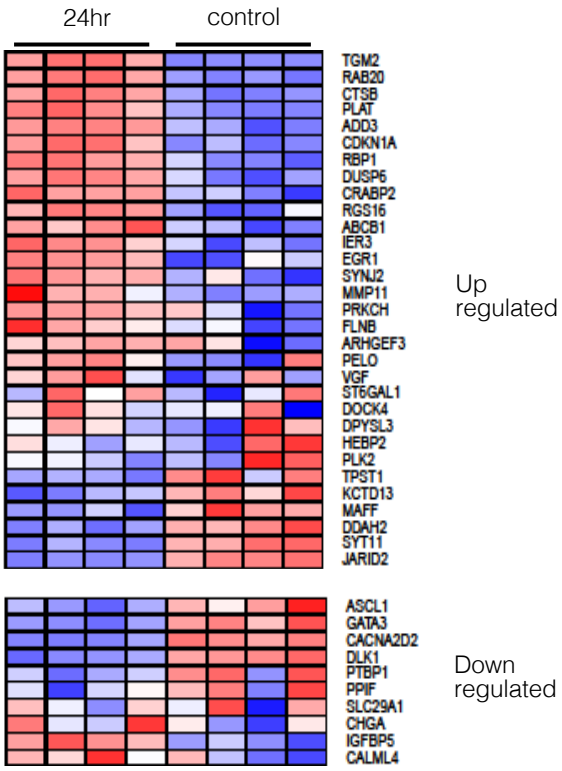
24hr
control
TGM2
RAB20
CTSB
PLAT
ADD3
CDKN1A
RBP1
DUSP6
CRABP2
RGS16
ABCB1
IER3
EGR1
SYNJ2
MMP11
PRKCH
FLNB
ARHGEF3
PELO
VGF
ST6GAL1
DOCK4
DPYSL3
HEBP2
PLK2
TPST1
KCTD13
MAFF
DDAH2
SYT11
JARID2
Up regulated
ASCL1
GATA3
CACNA2D2
DLK1
PTBP1
PPIF
SLC29A1
CHGA
IGFBP5
CALML4
Down regulated

Figure 54 Panobinostat promotes gene expression associated with differentiation

TH-*MYCN* treated mice were treated with daily panobinostat for 48 hours and then harvested 4 hours after the second dose. Tumours were then processed for RNA-seq and differential gene expression analysis. (A) GeneGo MetaCore pathway analysis showing the top ten pathways that have been significantly altered in response to panobinostat treatment (Expression fold change threshold 0.25). (B) GSEA enrichment plot of the upregulated genes (31 genes in total) from the Frumm differentiation gene signature, NES 1.56, FDR q-value 0.042. (C) Heat map of the expression of the 41 genes from the Frumm differentiation gene signature (red upregulated, blue downregulated). Top panel, genes upregulated within the Frumm gene signature (Frumm et al., 2013); bottom panel, downregulated genes. Genes are ranked by signal to noise ratio.

4.2.6. **Panobinostat on *MYCN* expression**

NMYC amplification remains one of the markers of poor prognosis in neuroblastoma (1.6.1). Therefore, therapeutic strategies aimed at reducing the impact of NMYC remain important in the treatment of HR neuroblastoma. The possibility exists to reduce the impact of NMYC expression via epigenetic manipulation. Treatment with panobinostat resulted in significant reductions in Nmyc mRNA expression, as well as other validated downstream markers including Polrb and ODC (Boon et al., 2001; Hogarty et al., 2008; G. Poortinga et al., 2011) (Figure 56).

(A)

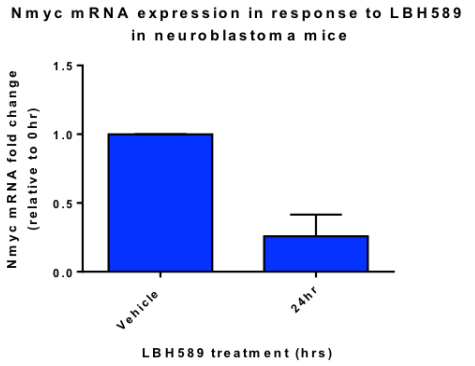

(B)

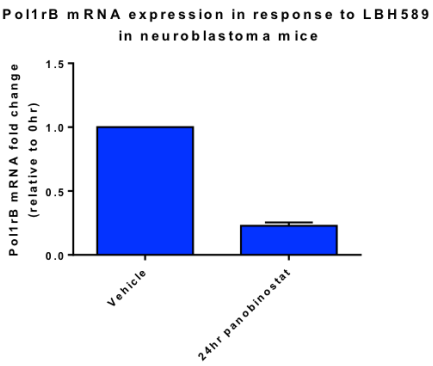

(C)

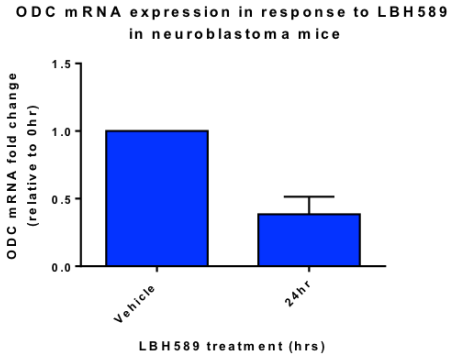

Figure 55 Panobinostat reduces *MYCN* expression

TH-*MYCN* treated mice were treated for 24 hours and harvested 4 hours after the second dose. Tumours were then processed via RT-PCR for (A) NMyc RNA expression as well as the downstream markers markers of *MYCN* expression (B) Polrb and (C) ODC.

4.3.**Discussion**

The successful treatment of HR NBL still remains a clinical challenge. In particular those patients that have no or a poor response to standard induction chemotherapy have an overall survival of < 10% (Brodeur et al., 1993). This is partly due to the infiltering nature of this tumour which often makes it impossible to completely remove it. Therefore, there is a need to explore new therapies for children in which residual disease imparts a poor prognosis.

NBL, ganglioneuroblastoma and ganglioneuroma are an inclusive spectrum of disease that primarily differ in their degree of differentiation and therefore their aggressive behavior. Ganglioneuroma, the most differentiated entity of this spectrum behaves like a benign tumour (Lonergan, Schwab, Suarez, & Carlson, 2002). As stated earlier, infant NBL has the ability to spontaneously regress. If this process can be replicated in older children with residual disease it may be possible to drive the malignant NBL into a more benign ganglioneuroma therefore reducing its ability to cause harm.

Differentiation therapy using retinoids for HR NBL is currently incorporated into many protocols and is certainly not a new concept (Reynolds et al., 2003). However, this class of drugs often have side-effects such as skin dryness that make them difficult to tolerate, especially for young children (David et al., 1988). Newer agents such as HDACi are emerging as potential alternatives and may in fact be the key to driving the differentiation process as early studies looking at the characteristic methylomes of stage 4s patients suggest (Brodeur & Bagatell, 2014). The bulk of early phase drug trials have concentrated on using HDACi in intermittent dosing schedules (Fouladi et al., 2010). Recent pre-clinical evidence in other pediatric tumour models suggest that these agents may in fact be more effective when used in continuous, low dosing schedules aimed at promoting differentiation (Cain et al., 2013; Muscat et al., 2016). The possibility exists that such a dosing schedule may be less toxic.

These results demonstrate that continuous, low dose panobinostat induces terminal

differentiation in the TH-*MYCN* murine model for neuroblastoma. This effect appears to be dependent on the overall exposure to the drug. Mice treated for three weeks had an excellent response, but all eventually relapsed. However, mice treated for nine weeks also had an excellent initial response with 90% remaining in long-term remission. This is a unique result for single agent therapy in this aggressive mouse model of NBL.

This exposure dependent response to panobinostat is in itself interesting given that RNA-seq analysis shows that pathways associated with differentiation were significantly upregulated as early as 24 hours after initial exposure. There are certainly two complimentary processes that can explain this remarkable response to panobinostat. The initial dramatic tumour response, as observed by serial tumour imaging, can be potentially explained by apoptosis whereas the prolonged survival seen in this model can be explained by terminal differentiation. The apopotosis effect in isolation does not appear sufficient to maintain a sustained anti-tumour effect as 100% of mice relapse when the drug is removed at three weeks. By this stage tumours were not visible on abdominal ultrasound. It is only when the mice were exposed to nine weeks of treatment, well beyond this initial rapid tumour response, that a sustained treatment effect was observed. The importance of this observation is that current HDACi dosing schedules based on intermittent dosing may not be providing adequate tumour exposure to drive the more sustained phenotype of terminal differentiation.

MYCN amplification has repeatedly been shown to impart a poor prognosis in patients with NBL (Rubie et al., 1997). Accordingly, much international effort has been expended on finding ways to ameliorate the impact of *MYCN*. In addition to the profound impact on differentiation, these results also demonstrate that HDACi have the ability to reduce the translational impact of *MYCN*. This impact can be significantly enhanced when combined with BET bromodomain inhibitors such as JQ1 (Shahbazi et al., 2016). Additionally, as a consequence of differentiation the expression of SSTR2 is upregulated, perhaps providing an additional therapeutic

target with the use of peptide receptor radionucleotide therapy (Kong et al, 2016).

Panobinostat has been shown to be safe in children (Goldberg et al., 2014). In addition, an oral formulation is now available which is perhaps more suited to sustained, low dose administration. Such oral formulations tend to be less invasive and less traumatic to administer to children. Given the main side-effect seen with HDACi is myelosuppression we must carefully think of the most suitable phase of treatment to administer the drug. If the is aim to achieve uninterrupted dosing then the most obvious choice is in the post consolidation phase which is not traditionally associated with chemotherapy induced myelosuppression. From a translational standpoint, these results suggest that panobinostat can perhaps be incorporated into the maintenance phase of NBL therapy as a substitute for Cis-RA therapy.

5 A Phase I Study of Panobinostat in Paediatric Patients with Refractory Solid Tumours, including CNS Tumours

5.1.**Introduction**

5.1.1. **Overall Study Design**

This was an open label Phase I study of panobinostat (LBH589) in paediatric patients with refractory solid tumours, including CNS tumours, aimed at determining the MTD of panobinostat as well as defining and describing the toxicities associated with its use. Pharmacokinetic data specific to the paediatric population was also collected and analysed.

Paediatric patients with refractory solid and CNS tumours were eligible to be enrolled with a planned maximum total sample size of 28 patients estimated for Part A and Part B of the study combined.

In Part A, panobinostat was administered I.V weekly (Days 1, 8) as a 30-minute infusion starting at a dose of 15mg/m^2. A starting dose of 15 mg/m^2 was chosen as this represented 80% of the MTD established in the adult patient study population. Each 21-day period was defined as one course. Inter-patient dose escalation or reductions occurred, in successive cohorts, at increments of 5mg/m^2 with corresponding dose levels of 20 mg/m^2, 25mg/m^2, 30 mg/m^2 in cohorts of 3-6 patients until an MTD is reached. There was no intra-patient dose escalation. During this dose escalation phase of treatment, PK data was collected on each patient, during course one of each successive cohort.

Part B commenced once the MTD was defined in Part A. A minimum of 4 patients per age group was required to accurately define PK studies at the MTD dosing level. It was anticipated that the adolescent age group would have already been represented in Part A of the study. Anticipated differences in PK between younger children (> 6 months - < 2 years) and older children (≥ 2 years - < 12 years) needed to be assessed. Therefore, additional children in these age ranges were enrolled to acquire PK data in children in the following group structure only if these patient age groups were not

already represented (n=4 per age group) in the PK evaluation of Part A of the study. Therefore, once the MTD was defined in Part A, additional patients were enrolled to acquire PK data in children in the following age groups if they were not adequately represented (n = 4 per age group) in the PK evaluation of Part A of the study:
Group 1: > 6 months- < 2 years
Group 2: ≥ 2 years- <12 years

The maximum number of additional patients that were enrolled was four per age group.

5.1.2. **Primary Aims**

- To determine the maximum tolerated dose (MTD) and recommend a Phase II dose of panobinostat for patients with progressive/recurrent solid tumours including CNS tumours of childhood.
- To define and describe the toxicities of panobinostat for patients on this schedule.
- To characterise the PK of panobinostat for patients in each age group with these refractory cancers.

5.1.3. **Secondary Aims**

- Where possible, to preliminarily define the anti-tumour activity of panobinostat within the confines of this Phase 1 study.
- Where possible to assess the biologic activity of panobinostat by measuring histone acetylation status in peripheral mononuclear cells (PMNC), bone marrow and fresh tumour tissue specimens in all patients (when available).
- Where possible to assess the biologic activity of panobinostat by measuring the effects of the drug on imprinting status and acetylation status in both fresh tumour tissue and PMNC in several target genes

including CDKN1C (p57) in all patients.

5.1.4. **Ethics**

All procedures performed in studies involving human participants were in accordance with the ethical standards of the institutional and/or national research committee and with the 1964 Helsinki declaration and its later amendments or comparable ethical standards.

Patient and/or their legal guardians have signed a written informed consent form.

5.2.**Results**

5.2.1. **Patient Demographics**

From February 2009 until May 2012 nine patients in total were enrolled with an average age of 9.6 years. Patient characteristics including diagnosis and prior therapies are summarised in (Table 7).

As is often the case with patients enrolled in early phase clinical trials, all patients had been exposed to all prior therapies that are currently considered standard of care in paediatric oncology: surgery, chemotherapy and radiation therapy (Saletta et al., 2014). This is consistent with the aggressive and often resistant nature of these tumours. By the time these children are enrolled in early phase studies their tumours have been selected for the population of the most treatment resistant cancer cells, potentially due to the expansion of a multi-resistant clone. This is thought to contribute to the poor success of early phase oncology drug trials (Worsley, Mayne, & Veale, 2016). In addition, the net outcome of these prior therapies is multi-organ toxicity, which can further impede the prospect of early phase therapeutics being effective (Adamson, Houghton, Perilongo, & Pritchard-Jones, 2014).

Age (years)	Sex	Diagnosis	Prior Chemotherapy	Prior Surgery	Prior Radiation
7	Female	Neuroblastoma	Yes	Yes	Yes
12	Male	Rhabdomyosarcoma	Yes	Yes	Yes
8	Female	Wilm's Tumour	Yes	Yes	Yes
13	Male	Rhabdomyosarcoma	Yes	Yes	Yes
8	Male	Ependymoma	Yes	Yes	Yes
13	Male	Medulloblastoma	Yes	Yes	Yes
13	Male	Medulloblastoma	Yes	Yes	Yes
9	Female	Primitive Neuroectodermal Tumour (PNET)	Yes	Yes	Yes
3	Female	Wilm's Tumour	Yes	Yes	Yes

Table 7 Patient Demographics

Demographics of patients enrolled on study including past treatments.

5.2.2. **Dose limiting toxicities**

Six patients were evaluable for dose limiting toxicities (DLT) (Table 8).

Dose Level	Number of Patients Entered	Number of Patients Evaluable	Number of Patients In-evaluable
15mg/m^2	9	6	3

Table 8 Evaluable patients

Six patients were evaluable for toxicities. Three patients were removed from the study prior to completion of course one due to disease progression.

DLT observed in patients are described in Table 9. The most commonly reported DLT's in previously published early phase studies were haematological toxicities that are reversible on cessation of the drug (Bauer et al., 2014; Bug et al., 2017; S. F. Jones et al., 2011). Interestingly cardiac DLT are reported infrequently (Andreu-Vieyra & Berenson, 2014; M. Anne, Sammartino, Barginear, & Budman, 2013; A. J. Yee & Raje, 2018) but tend to be associated with the intravenous formulation of the drug. Given this was one of the first early-phase clinical trials of panobinostat in paediatric patients, extra care and surveillance was performed to ensure early detection of cardiac toxicities.

Two DLTs were reported in patient CHW08 (Table 9):

Course 1, Day 4: T-wave flattening and then inversion (inferior & lateral leads) resulted in dose reduction from 15mg/m^2 to 10mg/m^2. T-wave inversion reverted back to normal in subsequent ECGs.
QT_cF remained normal throughout.

Course 1, Day 15: T-wave inversion (inferior leads). Action – surveillance only.

In this study two of six (33%) of patients experienced a Grade II QTcF change with one cardiac DLT, T-wave changes in inferior leads, reported at the 15mg/m^2 dosing level. This resolved when the patient de-escalated to a dose of 10mg/m^2. One patient experienced toxicity requiring a dose escalation to 10mg/m^2.

Dose Level	DLT Type	Number of Patients with DLT	Associated Patient ID's
15mg/m^2	T-wave inversion, inferior leads	1	CHW08
10mg/m^2	T-wave inversion, inferior leads	1	CHW08

Table 9 Dose Limiting Toxicity Information

Dose limiting toxicities attributable to panobinostat.

5.2.3. **Adverse events**

Treatment related adverse events (AE) for the six evaluable patients that completed course one are summarised in (Table 10).

Grade III-IV thrombocytopaenia was observed in 33% of patients. Grade III anaemia was observed in 17% of patients. Grade III neutropaenia was observed in 33% patients. Grade III-IV pain was observed in 50% patients studied. Myelosuppression has been previously documented as the most consistently observed toxicity (Prince et al., 2007).

Additional AE across all grades observed in this study were vomiting (67%), nausea (50%), diarrhoea (17%) and hypokalaemia (33%). We observed a Grade II QTcF change in 33% of patients with one cardiac DLT, T-wave changes, reported at the 15mg/m^2 dosing level.

Adverse Event	Grade 1		Grade 2		Grade3		Grade 4		All Grades (n=6)	
	Number (No)	%	No.	%	No.	%	No.	%	No.	%
Abdominal pain	2	33	0	0	0	0	0	0	2	33
Alanine aminotransferase increased	0	0	1	17	0	0	0	0	1	17
Alkalosis	0	0	0	0	1	17	0	0	1	17
Alopecia	0	0	1	17	0	0	0	0	1	17
Apnea	0	0	0	0	0	0	1	17	1	17
Arrhythmia	0	0	1	17	0	0	0	0	1	17
Arrhythmia supraventricular	1	17	0	0	0	0	0	0	1	17
Aspartate aminotransferase increased	1	17	0	0	0	0	0	0	1	17
Ataxia	0	0	1	17	0	0	0	0	1	17
Bilirubin increased	1	17	0	0	0	0	0	0	1	17
Blood bicarbonate decreased	1	17	0	0	0	0	0	0	1	17
Constipation	1	17	0	0	0	0	0	0	1	17
Cough	2	33	0	0	0	0	0	0	2	33
Creatine phosphokinase increased	0	0	1	17	0	0	0	0	1	17
Creatinine increased	2	33	0	0	0	0	0	0	2	33
Diarrhea	0	0	1	17	0	0	0	0	1	17

Dyspnea	0	0	1	17	1	17	0	0	2	33
Electrocardiogram QTc interval prolonged	0	0	2	33	0	0	0	0	2	33
Facial nerve disorder	0	0	1	17	0	0	0	0	1	17
Fatigue	1	17	0	0	1	17	0	0	2	33
Fever	1	17	0	0	1	17	0	0	2	33
Fracture	0	0	0	0	1	17	0	0	1	17
Gait abnormal	0	0	0	0	1	17	0	0	1	17
Headache	1	17	1	17	0	0	0	0	2	33
Hemoglobin decreased	0	0	1	17	1	17	0	0	2	33
Hydrocephalus	0	0	0	0	1	17	0	0	1	17
Infection	0	0	1	17	0	0	0	0	1	17
Insomnia	0	0	1	17	0	0	0	0	1	17
Laboratory test abnormal	2	33	0	0	0	0	0	0	2	33
Leukocyte count decreased	0	0	0	0	1	17	0	0	1	17
Lymphocyte count decreased	1	17	0	0	1	17	0	0	2	33
Muscle weakness lower limb	1	17	0	0	1	17	0	0	2	33
Musculoskeletal disorder	1	17	0	0	0	0	0	0	1	17
Nausea	3	50	0	0	0	0	0	0	3	50
Neck pain	2	33	0	0	0	0	0	0	2	33
Neutrophil count decreased	1	17	1	17	2	33	0	0	4	67
Nystagmus	0	0	1	17	0	0	0	0	1	17

Pain	1	17	0	0	1	17	2	33	4	67
Pain in extremity	0	0	2	33	0	0	0	0	2	33
Platelet count decreased	4	67	0	0	2	33	0	0	6	100
Pyramidal tract syndrome	1	17	0	0	0	0	0	0	1	17
Seizure	0	0	1	17	0	0	0	0	1	17
Serum magnesium decreased	1	17	0	0	0	0	0	0	1	17
Serum potassium decreased	2	33	0	0	0	0	0	0	2	33
Serum sodium decrease	1	17	0	0	0	0	0	0	1	17
Sinus arrhythmia	1	17	0	0	0	0	0	0	1	17
Skin disorder	0	0	1	17	0	0	0	0	1	17
Stomach pain	0	0	1	17	0	0	0	0	1	17
Supraventricular tachycardia	1	17	0	0	0	0	0	0	1	17
Urinary retention	1	17	0	0	0	0	0	0	1	17
Vision blurred	0	0	0	0	1	17	0	0	1	17
Vomiting	3	50	1	17	0	0	0	0	4	66
Weight loss	0	0	1	17	0	0	0	0	1	17
Wound dehiscence	1	17	0	0	0	0	0	0	1	17

Table 10 Adverse events and Grading

Adverse events attributable to panobinostat.

5.2.4. **Serious adverse events**

There were five serious adverse events (SAE's) reported in this trial with only one, central line infection, suspected as being related to the panobinostat therapy (Table 11). One patient experienced a pathological fracture due to a metastatic tumour deposit. One patient experienced hydrocephalus as a result of CNS tumour progression. One patient experienced ataxia which was due to posterior fossa tumour progression. One patient experienced musculoskeletal pain which was brief and resolved despite continuation of the trial drug.

All patients who experienced an SAE were hospitalised and treated according to standard institutional care.

Patient ID	SAE	Outcome	Action Required	Causality
CHB01	Musculoskeletal Pain	Improved	Nil	Not suspected
JHC02	Fracture	Improved	Nil	Not suspected
RCH04	Hydrocephalus	Improved	Nil	Not suspected
RCH05	Ataxia	Deteriorated due to disease progression	Nil	Not suspected
SCH06	Central line infection	Improved	Nil	Suspected

Table 11 Serious Adverse Events

Serious adverse events attributable to panobinostat

5.2.5. **Patient responses**

No objective responses were reported in the six evaluable patients. Two patients completed course 2 and one patient completed course 3 having demonstrated stable disease (SD) as defined by the treatment protocol. All patients eventually withdrew from the study due to disease progression. This is consistent with published data showing a pooled response rate, in early phase paediatric oncology trials, of 3.17% for solid tumours (Waligora et al., 2018).

5.2.6. **Pharmacokinetic results**

Non-compartmental analysis was implemented in Phoenix® WinNonlin® (Pharsight, Mountain View, CA), and was used to estimate pharmacokinetic parameters of panobinostat and its metabolites(s) from individual plasma concentration versus time profiles. Results are presented in Table 12. These results were comparable to previously published PK data on panobinostat (Savelieva et al., 2015; Srinivas, 2017; Van Veggel, Westerman, & Hamberg, 2018).

Parameter	Definition	Mean +/- Standard Deviation
C_{max}	The maximum (peak) observed plasma concentration after single dose (ng/ml)	235.20 (ng/ml) +/- 116.74
T_{max}	The time to reach maximum (peak) plasma, blood, serum or other body fluid drug concentration after single dose administration (hr)	0.83 (hours) +/- 1.0
AUC_{0-t}	The AUC from time zero to the last measurable concentration sampling time (t hours) (ng*hr/ml)	346.88 (hr.ng/ml) +/- 199.92
AUC $_{0-inf}$	The AUC from time zero to infinity (ng*hr/ml) where feasible	359.14 (hr.ng/ml) +/- 199.84
$T_{1/2}$	The elimination half-life when feasible	7.33 (hours) +/- 1.06
Cl	The total body clearance of drug from the plasma (L/hr) when feasible	48.09 ($L/hr.m^2$) +/- 13.55
Vz	The apparent volume of distribution during terminal phase (L) for panobinostat only	512.62 (L/m^2) +/- 169.46

Table 12 Pharmacokinetic Results

Pharmacokinetic results of intra-venous panobinostat.

5.2.7. **Biological activity of panobinostat**

The acetylation status of acetyl-Histone H3 and acetyl-Histone H4 increased over the time period measured, with maximal acetylation between six and 24 hours. Previously, acetylated H3 has been shown to correlate with detectable plasma levels of panobinostat, although not quantitatively (Bauer et al., 2014).

The role of biomarkers in the evaluation of therapeutic agents is rapidly expanding (A. F. Cohen, Burggraaf, van Gerven, Moerland, & Groeneveld, 2015; L. M. Yee, Lively, & McShane, 2018). Theoretically, if one can demonstrate significant inhibition of the biological target then further dose escalations in a Phase I drug trial may not improve efficacy but instead contribute to toxicity. However, the biomarker used must be validated and reproducible if significant decisions such recommendations of drug dosing are made (L. M. Yee et al., 2018). Acetylated H3 and H4 have been validated as reliable and reproducible markers of HDACi efficacy (Rigby et al., 2012).

At a dose of 15mg/m^2 there was significant acetylation of both H3 and H4 six hours post panobinostat dosing. This significant biological effect persisted until 24 hours post dose (Figure 56, Figure 57, Figure 58). It is possible that doses above 15mg/m^2 may not achieve additional activity but instead further contribute to drug toxicity, which has already been reported as significant at this dosing level (Table 10).

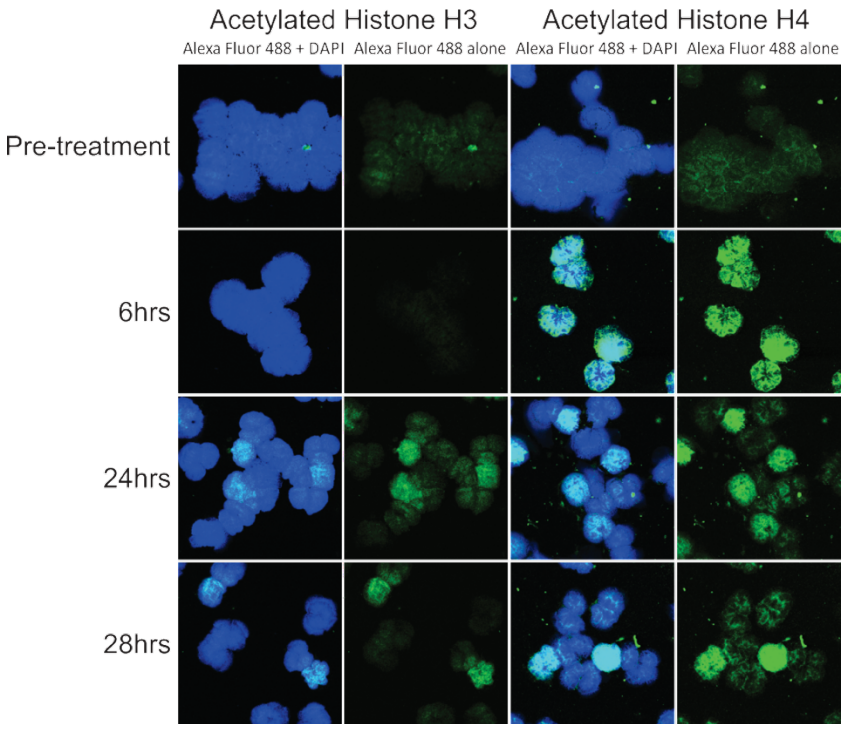

Figure 56 Immunocytochemistry of acetylated histone H3 and H4 in panobinostat treated patients at fixed time points

Immunocytochemistry (ICC) of PBMNC's, staining for Acetylated Histone H3 and Acetylated Histone H4 at designated time points following panobinostat dosing at pre-treatment, six hours, 24 hours and 28 hours post-treatment time points. Blue; Alexa Flour 88 + DAPI, Green; Alexa Flour 88 alone.

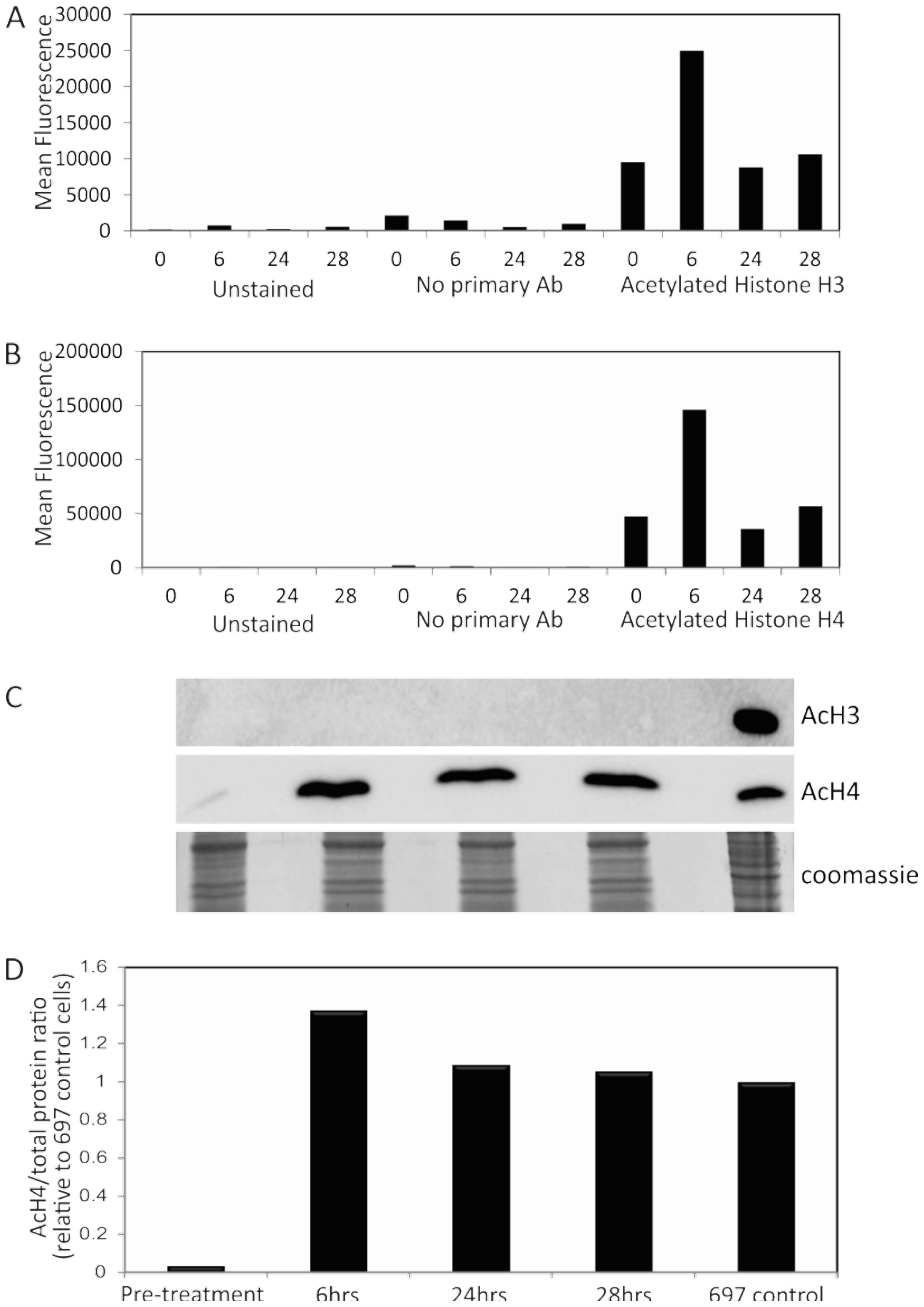
A
Mean Fluorescence
30000
25000
20000
15000
10000
5000
0
0 6 24 28 0 6 24 28 0 6 24 28
Unstained
No primary Ab
Acetylated Histone H3
B
Mean Fluorescence
200000
150000
100000
50000
0
0 6 24 28 0 6 24 28 0 6 24 28
Unstained
No primary Ab
Acetylated Histone H4
C
AcH3
AcH4
coomassie
D
AcH4/total protein ratio
(relative to 697 control cells)
1.6
1.4
1.2
1
0.8
0.6
0.4
0.2
0
Pre-treatment
6hrs
24hrs
28hrs
697 control

Figure 57 Flow cytometry of acetylated H3 and H4 in panobinostat treated patients

Flow cytometric data and Western blot analysis of Acetylated Histone H3 and Acetylated Histone H4 at designated time points following exposure to panobinostat. This representative data confirms that panobinostat induces maximal acetylation of Histone H3 (A) and Histone H4 (B) at six hours post panobinostat dose. Western Blot analysis of protein lysates confirms maximal acetylation of Histone H4 at 6 hours post panobinostat dose. (C) represents the Western blot from which the quantitative data (D) is derived.

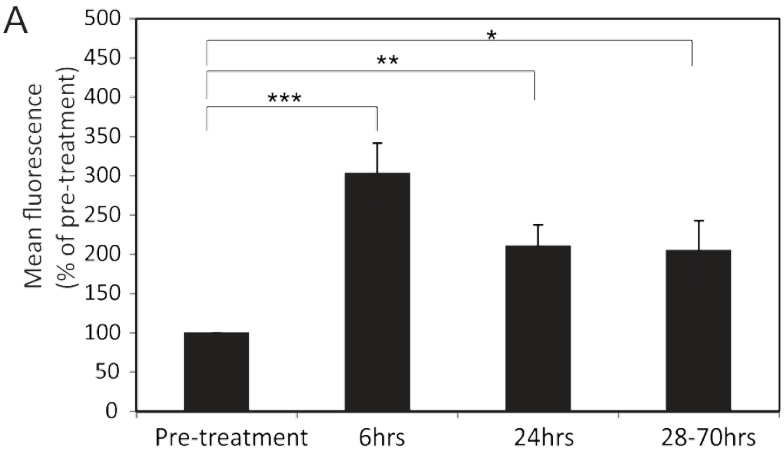
A
Mean fluorescence (% of pre-treatment)
500
450
400
350
300
250
200
150
100
50
0
*
**
***
Pre-treatment
6hrs
24hrs
28-70hrs

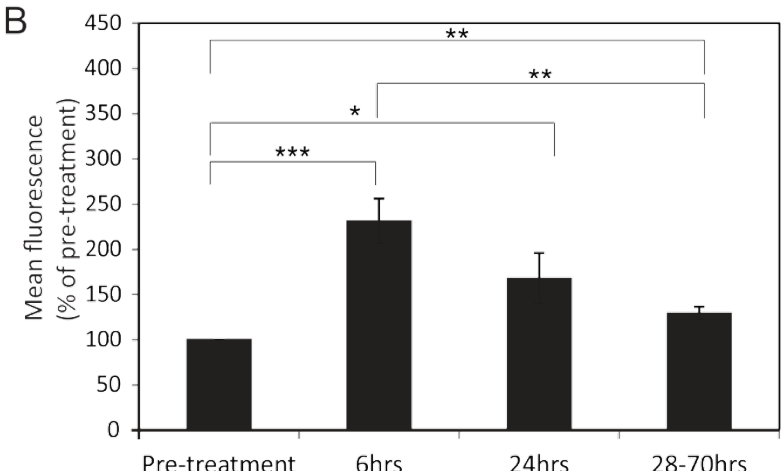
B
Mean fluorescence (% of pre-treatment)
450
400
350
300
250
200
150
100
50
0
**
**
*
***
Pre-treatment
6hrs
24hrs
28-70hrs

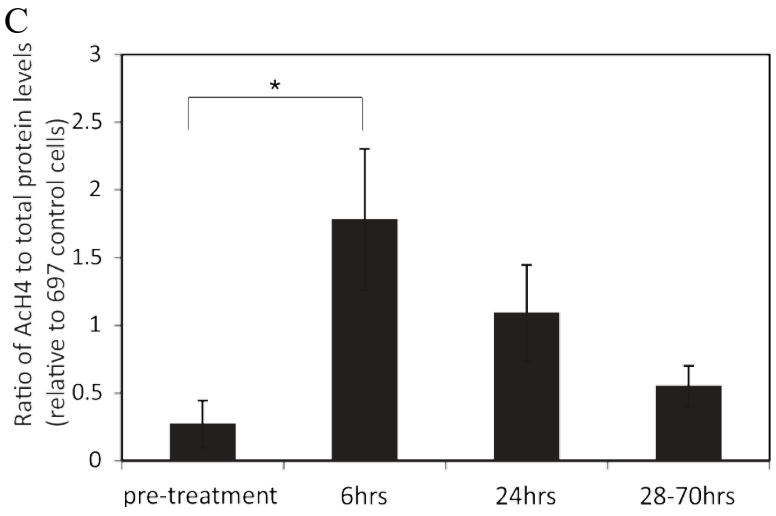
C
Ratio of AcH4 to total protein levels (relative to 697 control cells)
3
2.5
2
1.5
1
0.5
0
*
pre-treatment
6hrs
24hrs
28-70hrs

Figure 58 Quantitative analysis of pooled acetylated H3 and H4 data

Pooled flow cytometric data and Western blot analysis of Acetylated Histone H3 and Acetylated Histone H4, at designated time points following exposure to panobinostat. Panobinostat induces significant Acetylation of (A) Histone H3 and Histone (B) H4 at six hours post panobinostat dose. (C) Pooled Western Blot analysis of protein lysates confirm significant acetylation of Histone H4 at 6 hours post panobinostat dose. *p≤ 0.05 ** p ≤ 0.01 ***P ≤ 0.001

5.2.8. **Death Report**

All evaluable patients had disease progression whilst on study. Their deaths were not related to panobinostat. The three patients that were not evaluable for toxicities were removed from the study due to disease progression (Table 13).

Patient ID	Death Date	Reason	If death was attributable to treatment
JCH02	13/1/2011	Disease Progression	No
MON09	20/4/2013	Disease Progression	No
RCH04	5/5/2011	Disease Progression	No
RCH05	14/9/2011	Disease Progression	No
SCH03	28/3/2011	Disease Progression	No
SCH06	9/2/2012	Disease Progression	No

Table 13 Deaths of patients on study

Patient deaths on study.

5.2.9. **Delinquency Status**

Number of delinquencies affecting the assessment of DLT: 0

5.3.**Discussion**

Overall a panobinostat dose of 15mg/m^2 was well tolerated which compares to an adult MTD of 20mg/m^2. Only one DLT was observed in the six patients treated (M. Anne et al., 2013; Sharma et al., 2013). Because the I.V formulation of panobinostat was discontinued we were not able to continue dose escalations and establish a formal MTD.

The major dose limiting toxicity of panobinostat was transient, reversible myelosuppression, in particular thrombocytopenia, which is dose independent (M. Anne et al., 2013; Sharma et al., 2013). Other AE observed were similar to previously identified rates (M. Anne et al., 2013; Sharma et al., 2013). The pain reported by 50% of patients was thought to be more likely due to tumour progression than an AE related to the panobinostat.

QTcF prolongation, an AE seen in previous adult early phase studies of panobinostat, was observed. This prolongation may be dosing schedule dependent, seen most often with continuous I.V dosing (M. Anne et al., 2013). When using a weekly dosing schedule no cardiac DLT's occurred at doses of 10 mg/m^2 and 15 mg/m^2 (Sharma et al., 2013). We observed Grade II QTcF change in two patients (33%). One other cardiac DLT, T wave changes in inferior leads, was also reported at the 15mg/m^2 dosing level. This resolved at a reduced dose of 10mg/m^2 and the patient was able to continue on study.

PK analysis, which was performed on all nine patients enrolled, was consistent with previously published adult data. Although direct comparison is difficult due to the different study populations, PK data in paediatric population is vital for future drug development (Giles et al., 2006; Prince et al., 2007).

To date, histone acetylation status has only been established as a pharmacodynamic marker of biological activity for HDACi in pre-clinical models (Graham et al., 2006;

Marquard et al., 2008). Accordingly, qualitative and quantitative assessment of histone acetylation was obtained on circulating PMNC collected at the designated study time points. Flow cytometry and WB analysis of these patient samples demonstrated that panobinostat induced maximal acetylation of Histone H3 ($p<0.05$) and Histone H4 ($p<0.01$) at six hours post panobinostat dosing. This early and prolonged acetylation is what would be expected given the PK results, with a T_{max} of 0.83 hours and a $T_{1/2}$ of 7.3 hours. This is also consistent with other published data (Prince et al., 2007). What is most important, is that an adequate pharmacodynamic effect was observed at a dosing level of 15mg/m^2. Of the two biological markers investigated, Histone H4 was the more sensitive of the two when considering the ICC data (Figure 58).

In conclusion, panobinostat was well tolerated in the paediatric population at an almost equivalent MTD to that used in adults. A dose of 15mg/m^2 was associated with significant biological activity. The lack of response seen in this highly pre-treated group of patients suggest that future studies. should be considered as part of combination therapy.

6 Conclusions

This thesis focused on a form of embryonal childhood cancer, neuroblastoma, that still has relatively poor outcomes compared to other childhood solid tumours. In the evolving era of personalised medicine there are many biological pathways that have been identified that contribute to the cancer process and therefore may be attractive therapeutic targets. The focus of this project was the PI3K/AKT/mTOR pathway as well as epigenetic modulation via histone deacetylases. Specifically, inhibitors of these intracellular pathways were investigated in both NBL cell lines and the recently developed TH-*MYCN* NBL mouse model.

When this project started there were limited animal model systems available for translational studies in NBL. To this day the TH-*MYCN* model used in this thesis remains the most widely used pre-clinical mouse model for NBL (Ornell & Coburn, 2019). As this thesis progressed, and as more intricate dissection of anti-tumour mechanisms were required, it became apparent that a mouse system that could be manipulated was essential. Such a NBL murine system was simply not available at the time. In addition to this, seeing as the mechanisms of action of the inhibitors being studied involved processes such as angiogenesis and senescence, the importance of tumour microenvironment in the outcomes of these experiments became paramount. Indeed, it is the tumour microenvironment that hosts a heterogeneous population of tumour and non-tumour cells, including those of the immune system, that all contribute to, support and influence multiple cell signalling pathways including those being explored in this thesis (Nolan et al., 2020).

One of the most important outcomes of this project was the development of an orthotopic NBL mouse model with an intact immune system. NHO1A cell lines derived from the TH-*MYCN* mouse model were genetically manipulated and transplanted into immune-competent wild type littermates. By maintaining a functioning immune system important tumour microenvironment factors that influence both tumour formation and response to therapies are replicated. In particular, in the era of immunotherapies for cancer that include anti-GD2 for NBL, a

functional immune system is essential. From a translational medicine standpoint, this orthotopic model may be an essential tool going forward in the study of NBL.

Another unique aspect of this project was the validation of small animal imaging modalities such as ultrasound and FDG-PET to monitor treatment responses in the mouse models studied. Both quantitative and functional imaging modalities are used when evaluating treatment responses in humans and are considered a routine and essential tool in cancer therapy. Each modality provides very different, yet complimentary, tumour response information. In particular FDG-PET scans have been validated in many paediatric cancers and are accurate enough in staging that they have eliminated the need for other invasive staging procedures such as bone marrow aspirates. Because of this they are now considered standard of care in most solid tumours. It only makes sense that we use similar techniques when assessing treatment response in pre-clinical models.

Despite previous research confirming the importance of the PI3K/AKT/mTOR pathway in human NBL patients, the opportunity arose to confirm these findings in a small local cohort of patients. This select group of high risk NBL patients, that had relapsed and therefore demonstrated highly resistant disease, had evidence of PI3K/AKT/mTOR pathway activation both in their primary tumour samples and also, in the case of one patient, in their relapsed tumour samples. High risk NBL patients were chosen as the outcomes for patients with low and intermediate risk disease are excellent and it is not these patient groups that we need to focus this research on. Although it was a small sample size, these studies were consistent with previous research identifying the PI3K/AKT/mTOR pathway as a potential therapeutic target in both newly diagnosed and relapsed high risk NBL, thereby validating the pre-clinical studies described next (Johnsen et al., 2008; Sartelet et al., 2008).

When interrogating the PI3K/AKT/mTOR pathway it was apparent that the nature of the inhibitor used influenced the resulting treatment phenotype seen in the animal system. Temsirolimus, an exclusive mTORC1 inhibitor, primarily had an anti-

angiogenic effect with no clear evidence of apoptosis. As has been previously been published, it also induced cellular senescence (Wall et al., 2013). This effect on tumour angiogenesis produced a significant treatment benefit in the TH-*MYCN* mouse model with little or no benefit seen in NBL cell lines. The fact that temsirolimus had little or no effect on NBL cell lines, despite confirming the drug was inhibiting its biological target, is consistent with an experimental system where tumour viability and supply of essential nutrients functions independently of a vascular supply, as is the case *in-vitro*.

Experiments in chicken embryos have confirmed that both PI3K and AKT signalling are required for normal embryonal angiogenesis (Jiang, Zheng, Aoki, & Vogt, 2000). It has also been repeatedly established that the PI3K/AKT/mTOR pathway independently upregulates angiogenesis via mTORC1 (Karar & Maity, 2011) which increases levels of HIF-1α. In fact, mTORC1 inhibition may contribute to tumour angiogenesis and viability firstly by reducing tumour angiogenesis, secondly by normalising the tumour vasculature and thirdly by promoting the formation of thrombosis in tumour vessels (D.-M. Anne, Marc, Nicolas, & Olivier, 2012). Despite the fact that all three components of the PI3K/AKT/mTOR signalling pathway have been implicated in tumour angiogenesis, these results demonstrate that mTORC1 inhibition alone is enough to produce a significant treatment effect. This has been seen in other human cancers; however, single agent therapy has yet to provide a sustained effect in any patient population (Faes, Santoro, Demartines, & Dormond, 2017). Further studies of such therapies may need to be considered in the context of combination therapies.

In contrast to temsirolimus, PF-502 treatment was associated with significant apoptosis in combination with a significant anti-angiogenic effect, as seen with temsirolimus. Both phenotypes were essential to the anti-tumour activity and combined in an additive fashion to improve the significant treatment outcomes seen in PF-502 treated mice. Having said this, the survival benefit of PF-502 treated mice

did not exceed that seen in temsirolimus treated mice. What was observed was significant hepatoxicity in the PF-502 treated mice. Similar toxicities have been seen in early phase human trials using combined PI3K/mTORC1 inhibitors resulting in the discontinuation of many of these compounds (J. Yang et al., 2019). Further interrogation of the exact mode of action that contributed to the differences seen could form the scope of future research. This could include further validation of the BCL2 overexpressing mouse model and the generation of a model that would help further investigate the importance of vascularisation.

This result potentially helps narrow down which part of the PI3K/AKT/mTOR pathway is mostly responsible for contributing to apoptosis. Given mTORC1 inhibition alone did not result in significant apoptosis, it is reasonable to assume that upstream players such as AKT or PI3K itself may play a more important role. There is evidence to support that inhibition of PI3K alone results in apoptosis. This can either be dependent or independent of AKT (Franke, Hornik, Segev, Shostak, & Sugimoto, 2003). This could certainly be a focus of future research using dedicated inhibitors of these upstream members of the pathway.

The role of AKT in apoptosis has been previously discussed (1.10.1.3.4). Activated AKT phosphorylates and inhibits the pro-apoptotic Bcl-2 family members primarily by phosphorylation of FOXO's (X. Zhang et al., 2011). Although AKT is the primary mediator of PI3K signalling (F. Chang et al., 2003), PI3K can act independently of AKT via SGK1 (Orlacchio et al., 2017). In particular, SGK1 can mediate apoptosis via membrane androgen receptors (mAR) (G. Liu et al., 2015). PI3K inhibitors have been shown to induce rapid apoptosis via inhibition of RAS-ERK signalling (Will et al., 2014). However, the RAS-ERK pathway does converge on AKT meaning AKT signalling may still play an important part in this process.

These studies have confirmed that the PI3K/AKT/mTOR pathway is a valid therapeutic target in NBL. Therapies that target this pathway could be investigated alongside current treatment modalities. Current therapy for high-risk NBL is already

associated with significant short-term and long-term toxicities. Patients are exposed to highly toxic induction therapy, invasive surgery, even more toxic consolidation therapy, radiation therapy and then maintenance immune therapy with retinoic acid. Children undergoing such treatment regimens spend significant amounts of time in hospital for the treatment itself as well as the side-effects. When undertaking pre-clinical studies in any cancer treatment it is essential to have foresight and plan at what stage in current treatment protocols these new agents can be incorporated. Pre-clinical mouse models provide valuable information on drug efficacy, including mode of action and toxicity data. As previously stated, temsirolimus was well tolerated by the mice whereas PF-502 was associated with significant hepatic toxicity. Hepatic toxicity has been identified as a significant side effect of combined PI3K/mTOR inhibitors in early phase clinical trials and would only further contribute to the toxicities seen in this fragile patient group. In this context it is important to evolve our therapeutic strategies and tailor them to what stages of a patient's treatment protocol they might best be incorporated. At present, the maintenance phase of treatment for NBL is perhaps the best phase where a new treatment could be added to what is already an intense treatment. At present, anti-GD2 therapy has been added to the already established differentiation therapy of retinoic acid. Retinoic acid therapy comes with significant toxicities and has a limited therapeutic benefit (Reynolds et al., 2003). Given the early promise of histone deacetylase inhibitors as promoting tumour differentiation, it was logical to explore this option as an alternative differentiation treatment for high-risk NBL (Cain et al., 2013; Muscat et al., 2016).

When an aggressive form of murine neuroblastoma was treated with continuous, low dose, panobinostat there was an initial dramatic tumour response. The initial rapid response was most likely due to the well documented apoptosis phenotype associated with HDAC inhibitor use. When panobinostat was ceased after three weeks of treatment, all the mice that had no measurable disease burden on serial imaging eventually relapsed with NBL that was similar to their original disease. When treated for nine weeks, 90% of mice remained in remission and the small

amount of residual tissue had immunohistochemistry characteristics consistent with differentiation. This significant survival benefit was a unique result for this aggressive mouse model of NBL. Interestingly, the cellular processes associated with both apoptosis and differentiation were upregulated as early as 24 hours after starting panobinostat dosing. In mice treated for three weeks the differentiation must not have reached a terminal stage thereby allowing 100% of those mice to relapse upon removal of drug. This suggests that the time of exposure is essential when trying to achieve terminal differentiation.

A Phase I study in the use of panobinostat in children with refractory solid tumours has provided essential pharmacokinetic and toxicity data for future early phase studies using this compound in the paediatric setting. It has also validated the use of specific and validated drug biomarkers as surrogate indicators of pharmacodynamic drug activity in early phase clinical trials.

The future directions from this combined research would ideally be translating it into an early phase clinical trial in paediatric patients. This has in fact been achieved and the NORTH study (ACTRN12618000321246) is currently open and recruiting in most paediatric cancer centres in Australia. It has been funded by a successful NHMRC grant.

7 Bibliography

Abdelmonsif, D. A., Sultan, A. S., El-Hadidy, W. F., & Abdallah, D. M. (2018). Targeting AMPK, mTOR and beta-Catenin by Combined Metformin and Aspirin Therapy in HCC: An Appraisal in Egyptian HCC Patients. *Mol Diagn Ther, 22*(1), 115-127. doi:10.1007/s40291-017-0307-7

Abraham, A. G., & O'Neill, E. (2014). PI3K/Akt-mediated regulation of p53 in cancer. *Biochem Soc Trans, 42*(4), 798-803. doi:10.1042/bst20140070

Adams, C. M., Hiebert, S. W., & Eischen, C. M. (2016). Myc Induces miRNA-Mediated Apoptosis in Response to HDAC Inhibition in Hematologic Malignancies. *Cancer Research, 76*(3), 736-748. doi:10.1158/0008-5472.Can-15-1751

Adams, J. M., & Cory, S. (2007). The Bcl-2-regulated apoptosis switch: mechanism and therapeutic potential. *Curr Opin Immunol, 19*(5), 488-496. doi:10.1016/j.coi.2007.05.004

Adams, J. M., Harris, A. W., Pinkert, C. A., Corcoran, L. M., Alexander, W. S., Cory, S., . . . Brinster, R. L. (1985). The c-myc oncogene driven by immunoglobulin enhancers induces lymphoid malignancy in transgenic mice. *Nature, 318*, 533. doi:10.1038/318533a0

Adamson, P. C., Houghton, P. J., Perilongo, G., & Pritchard-Jones, K. (2014). Drug discovery in paediatric oncology: roadblocks to progress. *Nat Rev Clin Oncol, 11*(12), 732-739. doi:10.1038/nrclinonc.2014.149

Adhikary, S., & Eilers, M. (2005). Transcriptional regulation and transformation by Myc proteins. *Nat Rev Mol Cell Biol, 6*(8), 635-645. doi:10.1038/nrm1703

Afshar, M., Pascoe, J., Whitmarsh, S., James, N., & Porfiri, E. (2015). Temsirolimus for patients with metastatic renal cell carcinoma: outcomes in patients receiving

temsirolimus within a compassionate use program in a tertiary referral center. *Drug Design, Development and Therapy, 9*, 13-19. doi:10.2147/DDDT.S73686

Agarwal, M. L., Agarwal, A., Taylor, W. R., & Stark, G. R. (1995). p53 controls both the G2/M and the G1 cell cycle checkpoints and mediates reversible growth arrest in human fibroblasts. *Proc Natl Acad Sci U S A, 92*(18), 8493-8497.

Alaminos, M., Mora, J., Cheung, N. K., Smith, A., Qin, J., Chen, L., & Gerald, W. L. (2003). Genome-wide analysis of gene expression associated with MYCN in human neuroblastoma. *Cancer Research, 63*(15), 4538-4546.

Algar, E., Brickell, S., Deeble, G., Amor, D., & Smith, P. (2000). Analysis of CDKN1C in Beckwith Wiedemann syndrome. *Hum Mutat, 15*(6), 497-508. doi:10.1002/1098-1004(200006)15:6<497::Aid-humu2>3.0.Co;2-f

Aljubran, A. H., Griffin, A., Pintilie, M., & Blackstein, M. (2009). Osteosarcoma in adolescents and adults: survival analysis with and without lung metastases. *Ann Oncol, 20*(6), 1136-1141. doi:10.1093/annonc/mdn731

Alland, L., Muhle, R., Hou Jr, H., Potes, J., Chin, L., Schreiber-Agus, N., & DePinho, R. A. (1997). Role for N-CoR and histone deacetylase in Sin3-mediated transcriptional repression. *Nature, 387*, 49. doi:10.1038/387049a0

Allfrey, V. G., Faulkner, R., & Mirsky, A. E. (1964). ACETYLATION AND METHYLATION OF HISTONES AND THEIR POSSIBLE ROLE IN THE REGULATION OF RNA SYNTHESIS. *Proc Natl Acad Sci U S A, 51*, 786-794.

Anders, S., Pyl, P. T., & Huber, W. (2015). HTSeq--a Python framework to work with high-throughput sequencing data. *Bioinformatics, 31*(2), 166-169. doi:10.1093/bioinformatics/btu638

Andreu-Vieyra, C. V., & Berenson, J. R. (2014). The potential of panobinostat as a treatment option in patients with relapsed and refractory multiple myeloma. *Therapeutic Advances in Hematology, 5*(6), 197-210. doi:10.1177/2040620714552614

Anne, D.-M., Marc, D., Nicolas, D., & Olivier, D. (2012). mTOR Inhibition and the Tumor Vasculature. *Current Angiogenesis (Discontinued), 1*(1), 11-19. doi:http://dx.doi.org/10.2174/2211552811201010011

Anne, M., Sammartino, D., Barginear, M. F., & Budman, D. (2013). Profile of panobinostat and its potential for treatment in solid tumors: an update. *Onco Targets Ther, 6*, 1613-1624. doi:10.2147/ott.S30773

Ansell, S. M., Inwards, D. J., Rowland, K. M., Jr., Flynn, P. J., Morton, R. F., Moore, D. F., Jr., . . . Witzig, T. E. (2008). Low-dose, single-agent temsirolimus for relapsed mantle cell lymphoma: a phase 2 trial in the North Central Cancer Treatment Group. *Cancer, 113*(3), 508-514. doi:10.1002/cncr.23580

Antonello, Z. A., & Nucera, C. (2014). Orthotopic mouse models for the preclinical and translational study of targeted therapies against metastatic human thyroid carcinoma with BRAF(V600E) or wild-type BRAF. *Oncogene, 33*(47), 5397-5404. doi:10.1038/onc.2013.544

Arauchi, A., Yang, C. H., Cho, S., Jarboe, E. A., Peterson, C. M., Bae, Y. H., . . . Janat-Amsbury, M. M. (2015). An immunocompetent, orthotopic mouse model of epithelial ovarian cancer utilizing tissue engineered tumor cell sheets. *Tissue Eng Part C Methods, 21*(1), 23-34. doi:10.1089/ten.TEC.2014.0040

Arencibia, J. M., Pastor-Flores, D., Bauer, A. F., Schulze, J. O., & Biondi, R. M. (2013). AGC protein kinases: from structural mechanism of regulation to allosteric drug

development for the treatment of human diseases. *Biochim Biophys Acta, 1834*(7), 1302-1321. doi:10.1016/j.bbapap.2013.03.010

Arvanitis, C., & Felsher, D. W. (2006). Conditional transgenic models define how MYC initiates and maintains tumorigenesis. *Semin Cancer Biol, 16*(4), 313-317. doi:10.1016/j.semcancer.2006.07.012

Ashraf, K., Shaikh, F., Gibson, P., Baruchel, S., & Irwin, M. S. (2013). Treatment with topotecan plus cyclophosphamide in children with first relapse of neuroblastoma. *Pediatr Blood Cancer, 60*(10), 1636-1641. doi:10.1002/pbc.24587

Avanzino, B. C., Fuchs, G., & Fraser, C. S. (2017). Cellular cap-binding protein, eIF4E, promotes picornavirus genome restructuring and translation. *Proceedings of the National Academy of Sciences, 114*(36), 9611.

Aveic, S., & Tonini, G. P. (2016). Resistance to receptor tyrosine kinase inhibitors in solid tumors: can we improve the cancer fighting strategy by blocking autophagy? *Cancer Cell International, 16*, 62. doi:10.1186/s12935-016-0341-2

Baade, P. D., Youlden, D. R., Valery, P. C., Hassall, T., Ward, L., Green, A. C., & Aitken, J. F. (2010). Trends in incidence of childhood cancer in Australia, 1983–2006. *British Journal of Cancer, 102*(3), 620-626. doi:10.1038/sj.bjc.6605503

Babiss, L. E., & Friedman, J. M. (1990). Regulation of N-myc gene expression: use of an adenovirus vector to demonstrate posttranscriptional control. *Molecular and Cellular Biology, 10*(12), 6700-6708. doi:10.1128/mcb.10.12.6700

Badura, S., Tesanovic, T., Pfeifer, H., Wystub, S., Nijmeijer, B. A., Liebermann, M., . . . Ottmann, O. G. (2013). Differential Effects of Selective Inhibitors Targeting the PI3K/AKT/mTOR Pathway in Acute Lymphoblastic Leukemia. *PLoS ONE, 8*(11), e80070. doi:10.1371/journal.pone.0080070

Bagatell, R., London, W. B., Wagner, L. M., Voss, S. D., Stewart, C. F., Maris, J. M., . . . Cohn, S. L. (2011). Phase II study of irinotecan and temozolomide in children with relapsed or refractory neuroblastoma: a Children's Oncology Group study. *J Clin Oncol, 29*(2), 208-213. doi:10.1200/jco.2010.31.7107

Bagatell, R., Norris, R., Ingle, A. M., Ahern, C., Voss, S., Fox, E., . . . Blaney, S. (2014). Phase 1 trial of temsirolimus in combination with irinotecan and temozolomide in children, adolescents and young adults with relapsed or refractory solid tumors: a Children's Oncology Group Study. *Pediatr Blood Cancer, 61*(5), 833-839. doi:10.1002/pbc.24874

Baker, S. J., Ellison, D. W., & Gutmann, D. H. (2016). Pediatric gliomas as neurodevelopmental disorders. *Glia, 64*(6), 879-895. doi:10.1002/glia.22945

Balla, T., Szentpetery, Z., & Kim, Y. J. (2009). PHOSPHOINOSITIDE SIGNALING: NEW TOOLS AND INSIGHTS. *Physiology (Bethesda, Md.), 24*, 231-244. doi:10.1152/physiol.00014.2009

Bar-Shavit, R., Maoz, M., Kancharla, A., Nag, J. K., Agranovich, D., Grisaru-Granovsky, S., & Uziely, B. (2016). G Protein-Coupled Receptors in Cancer. *Int J Mol Sci, 17*(8), 1320. doi:10.3390/ijms17081320

Barneda-Zahonero, B., Collazo, O., Azagra, A., Fernandez-Duran, I., Serra-Musach, J., Islam, A. B., . . . Parra, M. (2015). The transcriptional repressor HDAC7 promotes apoptosis and c-Myc downregulation in particular types of leukemia and lymphoma. *Cell Death Dis, 6*, e1635. doi:10.1038/cddis.2014.594

Basta, N. O., Halliday, G. C., Makin, G., Birch, J., Feltbower, R., Bown, N., . . . McNally, R. J. (2016). Factors associated with recurrence and survival length following relapse in patients with neuroblastoma. *Br J Cancer, 115*(9), 1048-1057. doi:10.1038/bjc.2016.302

Bauer, S., Hilger, R. A., Muhlenberg, T., Grabellus, F., Nagarajah, J., Hoiczyk, M., . . . Pink, D. (2014). Phase I study of panobinostat and imatinib in patients with treatment-refractory metastatic gastrointestinal stromal tumors. *Br J Cancer, 110*(5), 1155-1162. doi:10.1038/bjc.2013.826

Bazzaro, M., Lin, Z., Santillan, A., Lee, M. K., Wang, M. C., Chan, K. C., . . . Roden, R. B. (2008). Ubiquitin proteasome system stress underlies synergistic killing of ovarian cancer cells by bortezomib and a novel HDAC6 inhibitor. *Clin Cancer Res, 14*(22), 7340-7347. doi:10.1158/1078-0432.Ccr-08-0642

Beltran, H. (2014). The N-myc Oncogene: Maximizing its Targets, Regulation, and Therapeutic Potential. *Mol Cancer Res, 12*(6), 815-822. doi:10.1158/1541-7786.Mcr-13-0536

Ben-Sahra, I., & Manning, B. D. (2017). mTORC1 signaling and the metabolic control of cell growth. *Curr Opin Cell Biol, 45*, 72-82. doi:10.1016/j.ceb.2017.02.012

Benayoun, B. A., Caburet, S., & Veitia, R. A. (2011). Forkhead transcription factors: key players in health and disease. *Trends in Genetics, 27*(6), 224-232. doi:https://doi.org/10.1016/j.tig.2011.03.003

Bender, A., Opel, D., Naumann, I., Kappler, R., Friedman, L., von Schweinitz, D., . . . Fulda, S. (2011). PI3K inhibitors prime neuroblastoma cells for chemotherapy by shifting the balance towards pro-apoptotic Bcl-2 proteins and enhanced mitochondrial apoptosis. *Oncogene, 30*(4), 494-503. doi:10.1038/onc.2010.429

Bensimon, A., Aebersold, R., & Shiloh, Y. (2011). Beyond ATM: The protein kinase landscape of the DNA damage response. *FEBS Letters, 585*(11), 1625-1639. doi:https://doi.org/10.1016/j.febslet.2011.05.013

Bent, E. H., Gilbert, L. A., & Hemann, M. T. (2016). A senescence secretory switch mediated by PI3K/AKT/mTOR activation controls chemoprotective endothelial

secretory responses. *Genes & Development, 30*(16), 1811-1821. doi:10.1101/gad.284851.116

Bergmann, E., Wanzel, M., Weber, A., Shin, I., Christiansen, H., & Eilers, M. (2001). Expression of P27(KIP1) is prognostic and independent of MYCN amplification in human neuroblastoma. *Int J Cancer, 95*(3), 176-183.

Berm, E. J. J., Looff, M. d., Wilffert, B., Boersma, C., Annemans, L., Vegter, S., . . . Postma, M. J. (2016). Economic Evaluations of Pharmacogenetic and Pharmacogenomic Screening Tests: A Systematic Review. Second Update of the Literature. *PLoS ONE, 11*(1), e0146262. doi:10.1371/journal.pone.0146262

Bernhart, E., Stuendl, N., Kaltenegger, H., Windpassinger, C., Donohue, N., Leithner, A., & Lohberger, B. (2017). Histone deacetylase inhibitors vorinostat and panobinostat induce G1 cell cycle arrest and apoptosis in multidrug resistant sarcoma cell lines. *Oncotarget, 8*(44), 77254-77267. doi:10.18632/oncotarget.20460

Berthold, F., Ernst, A., Hero, B., Klingebiel, T., Kremens, B., Schilling, F. H., & Simon, T. (2018). Long-term outcomes of the GPOH NB97 trial for children with high-risk neuroblastoma comparing high-dose chemotherapy with autologous stem cell transplantation and oral chemotherapy as consolidation. *British Journal of Cancer, 119*(3), 282-290. doi:10.1038/s41416-018-0169-8

Bidou, L., Bugaud, O., Belakhov, V., Baasov, T., & Namy, O. (2017). Characterization of new-generation aminoglycoside promoting premature termination codon readthrough in cancer cells. *RNA Biol, 14*(3), 378-388. doi:10.1080/15476286.2017.1285480

Biegel, J. A., Kalpana, G., Knudsen, E. S., Packer, R. J., Roberts, C. W., Thiele, C. J., . . . Smith, M. (2002). The role of INI1 and the SWI/SNF complex in the development of

rhabdoid tumors: meeting summary from the workshop on childhood atypical teratoid/rhabdoid tumors. *Cancer Research, 62*(1), 323-328.

Blois, J., Smith, A., & Josephson, L. (2011). The slow cell death response when screening chemotherapeutic agents. *Cancer chemotherapy and pharmacology, 68*(3), 795-803. doi:10.1007/s00280-010-1549-9

Blunt, M. D., Carter, M. J., Larrayoz, M., Smith, L. D., Aguilar-Hernandez, M., Cox, K. L., . . . Steele, A. J. (2015). The PI3K/mTOR inhibitor PF-04691502 induces apoptosis and inhibits microenvironmental signaling in CLL and the Emicro-TCL1 mouse model. *Blood, 125*(26), 4032-4041. doi:10.1182/blood-2014-11-610329

Bolden, J. E., Shi, W., Jankowski, K., Kan, C. Y., Cluse, L., Martin, B. P., . . . Johnstone, R. W. (2013). HDAC inhibitors induce tumor-cell-selective pro-apoptotic transcriptional responses. *Cell Death Dis, 4*, e519. doi:10.1038/cddis.2013.9

Boller, D., Schramm, A., Doepfner, K. T., Shalaby, T., von Bueren, A. O., Eggert, A., . . . Arcaro, A. (2008). Targeting the phosphoinositide 3-kinase isoform p110delta impairs growth and survival in neuroblastoma cells. *Clin Cancer Res, 14*(4), 1172-1181. doi:10.1158/1078-0432.Ccr-07-0737

Boon, K., Caron, H. N., van Asperen, R., Valentijn, L., Hermus, M. C., van Sluis, P., . . . Versteeg, R. (2001). N-myc enhances the expression of a large set of genes functioning in ribosome biogenesis and protein synthesis. *Embo j, 20*(6), 1383-1393. doi:10.1093/emboj/20.6.1383

Bos, J. L. (1989). ras oncogenes in human cancer: a review. *Cancer Research, 49*(17), 4682-4689.

Bots, M., Verbrugge, I., Martin, B. P., Salmon, J. M., Ghisi, M., Baker, A., . . . Johnstone, R. W. (2014). Differentiation therapy for the treatment of t(8;21) acute myeloid

leukemia using histone deacetylase inhibitors. *Blood, 123*(9), 1341-1352. doi:10.1182/blood-2013-03-488114

Bouvard, C., Lim, S. M., Ludka, J., Yazdani, N., Woods, A. K., Chatterjee, A. K., . . . Zhu, S. (2017). Small molecule selectively suppresses MYC transcription in cancer cells. *Proceedings of the National Academy of Sciences, 114*(13), 3497.

Bozulic, L., & Hemmings, B. A. (2009). PIKKing on PKB: regulation of PKB activity by phosphorylation. *Curr Opin Cell Biol, 21*(2), 256-261. doi:https://doi.org/10.1016/j.ceb.2009.02.002

Braekeveldt, N., & Bexell, D. (2018). Patient-derived xenografts as preclinical neuroblastoma models. *Cell Tissue Res, 372*(2), 233-243. doi:10.1007/s00441-017-2687-8

Britten, C. D., Adjei, A. A., Millham, R., Houk, B. E., Borzillo, G., Pierce, K., . . . LoRusso, P. M. (2014). Phase I study of PF-04691502, a small-molecule, oral, dual inhibitor of PI3K and mTOR, in patients with advanced cancer. *Investigational New Drugs, 32*(3), 510-517. doi:10.1007/s10637-013-0062-5

Brockmann, M., Poon, E., Berry, T., Carstensen, A., Deubzer, H. E., Rycak, L., . . . Eilers, M. (2013). Small molecule inhibitors of aurora-a induce proteasomal degradation of N-myc in childhood neuroblastoma. *Cancer cell, 24*(1), 75-89. doi:10.1016/j.ccr.2013.05.005

Brodeur, G. M. (2003). Neuroblastoma: biological insights into a clinical enigma. *Nat Rev Cancer, 3*(3), 203-216. doi:10.1038/nrc1014

Brodeur, G. M. (2018). Spontaneous regression of neuroblastoma. *Cell Tissue Res, 372*(2), 277-286. doi:10.1007/s00441-017-2761-2

Brodeur, G. M., & Bagatell, R. (2014). Mechanisms of neuroblastoma regression. *Nat Rev Clin Oncol, 11*(12), 704-713. doi:10.1038/nrclinonc.2014.168

Brodeur, G. M., Pritchard, J., Berthold, F., Carlsen, N. L., Castel, V., Castelberry, R. P., . . . et al. (1993). Revisions of the international criteria for neuroblastoma diagnosis, staging, and response to treatment. *J Clin Oncol, 11*(8), 1466-1477. doi:10.1200/jco.1993.11.8.1466

Brodeur, G. M., Seeger, R. C., Schwab, M., Varmus, H. E., & Bishop, J. M. (1984). Amplification of N-myc in untreated human neuroblastomas correlates with advanced disease stage. *Science, 224*(4653), 1121-1124.

Brown, J. S., & Banerji, U. (2017). Maximising the potential of AKT inhibitors as anti-cancer treatments. *Pharmacology & therapeutics, 172*, 101-115. doi:https://doi.org/10.1016/j.pharmthera.2016.12.001

Bruhn, M. A., Pearson, R. B., Hannan, R. D., & Sheppard, K. E. (2013). AKT-independent PI3-K signaling in cancer - emerging role for SGK3. *Cancer Manag Res, 5*, 281-292. doi:10.2147/cmar.S35178

Bruns, A. F., Yuldasheva, N., Latham, A. M., Bao, L., Pellet-Many, C., Frankel, P., . . . Ponnambalam, S. (2012). A Heat-Shock Protein Axis Regulates VEGFR2 Proteolysis, Blood Vessel Development and Repair. *PLoS ONE, 7*(11), e48539. doi:10.1371/journal.pone.0048539

Buchkovich, N. J., Yu, Y., Zampieri, C. A., & Alwine, J. C. (2008). The TORrid affairs of viruses: effects of mammalian DNA viruses on the PI3K–Akt–mTOR signalling pathway. *Nature Reviews Microbiology, 6*, 266. doi:10.1038/nrmicro1855

Bug, G., Burchert, A., Wagner, E. M., Kröger, N., Berg, T., Güller, S., . . . Ottmann, O. G. (2017). Phase I/II study of the deacetylase inhibitor panobinostat after allogeneic

stem cell transplantation in patients with high-risk MDS or AML (PANOBEST trial). *Leukemia, 31*(11), 2523-2525. doi:10.1038/leu.2017.242

Buglio, D., Khaskhely, N. M., Voo, K. S., Martinez-Valdez, H., Liu, Y. J., & Younes, A. (2011). HDAC11 plays an essential role in regulating OX40 ligand expression in Hodgkin lymphoma. *Blood, 117*(10), 2910-2917. doi:10.1182/blood-2010-08-303701

Buti, S., Leonetti, A., Dallatomasina, A., & Bersanelli, M. (2016). Everolimus in the management of metastatic renal cell carcinoma: an evidence-based review of its place in therapy. *Core Evidence, 11*, 23-36. doi:10.2147/CE.S98687

Bywater, M. J., Poortinga, G., Sanij, E., Hein, N., Peck, A., Cullinane, C., . . . Hannan, R. D. (2012). Inhibition of RNA Polymerase I as a Therapeutic Strategy to Promote Cancer-Specific Activation of p53. *Cancer cell, 22*(1), 51-65. doi:10.1016/j.ccr.2012.05.019

Cain, J. E., McCaw, A., Jayasekara, W. S., Rossello, F. J., Marini, K. D., Irving, A. T., . . . Watkins, D. N. (2013). Sustained Low-Dose Treatment with the Histone Deacetylase Inhibitor LBH589 Induces Terminal Differentiation of Osteosarcoma Cells. *Sarcoma, 2013*, 608964. doi:10.1155/2013/608964

Calero, R., Morchon, E., Johnsen, J. I., & Serrano, R. (2014). Sunitinib Suppress Neuroblastoma Growth through Degradation of MYCN and Inhibition of Angiogenesis. *PLoS ONE, 9*(4), e95628. doi:10.1371/journal.pone.0095628

Calleja, V., Alcor, D., Laguerre, M., Park, J., Vojnovic, B., Hemmings, B. A., . . . Larijani, B. (2007). Intramolecular and intermolecular interactions of protein kinase B define its activation in vivo. *PLoS Biol, 5*(4), e95. doi:10.1371/journal.pbio.0050095

Campaner, S., & Amati, B. (2012). Two sides of the Myc-induced DNA damage response: From tumor suppression to tumor maintenance. *Cell division, 7*, 6. doi:10.1186/1747-1028-7-6

Campbell, G. R., Bruckman, R. S., Chu, Y. L., & Spector, S. A. (2015). Autophagy induction by histone deacetylase inhibitors inhibits HIV type 1. *J Biol Chem, 290*(8), 5028-5040. doi:10.1074/jbc.M114.605428

Cannon, M., Philpott, N. J., & Cesarman, E. (2003). The Kaposi's Sarcoma-Associated Herpesvirus G Protein-Coupled Receptor Has Broad Signaling Effects in Primary Effusion Lymphoma Cells. *J Virol, 77*(1), 57.

Cargnello, M., & Roux, P. P. (2011). Activation and Function of the MAPKs and Their Substrates, the MAPK-Activated Protein Kinases. *Microbiology and Molecular Biology Reviews : MMBR, 75*(1), 50-83. doi:10.1128/MMBR.00031-10

Carlo, M. I., Molina, A. M., Lakhman, Y., Patil, S., Woo, K., DeLuca, J., . . . Voss, M. H. (2016). A Phase Ib Study of BEZ235, a Dual Inhibitor of Phosphatidylinositol 3-Kinase (PI3K) and Mammalian Target of Rapamycin (mTOR), in Patients With Advanced Renal Cell Carcinoma. *Oncologist, 21*(7), 787-788. doi:10.1634/theoncologist.2016-0145

Carroll, B., Nelson, G., Rabanal-Ruiz, Y., Kucheryavenko, O., Dunhill-Turner, N. A., Chesterman, C. C., . . . Korolchuk, V. I. (2017). Persistent mTORC1 signaling in cell senescence results from defects in amino acid and growth factor sensing. *The Journal of Cell Biology*.

Carroll, J. S., Swarbrick, A., Musgrove, E. A., & Sutherland, R. L. (2002). Mechanisms of growth arrest by c-myc antisense oligonucleotides in MCF-7 breast cancer cells: implications for the antiproliferative effects of antiestrogens. *Cancer Research, 62*(11), 3126-3131.

Carter, D. R., Murray, J., Cheung, B. B., Gamble, L., Koach, J., Tsang, J., . . . Marshall, G. M. (2015). Therapeutic targeting of the MYC signal by inhibition of histone chaperone FACT in neuroblastoma. *Sci Transl Med, 7*(312), 312ra176. doi:10.1126/scitranslmed.aab1803

Carter, S. K. (2000). Clinical strategy for the development of angiogenesis inhibitors. *Oncologist, 5 Suppl 1*, 51-54.

Casey, M. J., & Stewart, R. A. (2018). Zebrafish as a model to study neuroblastoma development. *Cell Tissue Res, 372*(2), 223-232. doi:10.1007/s00441-017-2702-0

Castellano, E., & Downward, J. (2011). RAS Interaction with PI3K: More Than Just Another Effector Pathway. *Genes Cancer, 2*(3), 261-274. doi:10.1177/1947601911408079

Castellano, E., Molina-Arcas, M., Krygowska, A. A., East, P., Warne, P., Nicol, A., & Downward, J. (2016). RAS signalling through PI3-Kinase controls cell migration via modulation of Reelin expression. *Nature communications, 7*, 11245. doi:10.1038/ncomms11245 https://www.nature.com/articles/ncomms11245#supplementary-information

Cauchy, P., James, S. R., Zacarias-Cabeza, J., Ptasinska, A., Imperato, M. R., Assi, S. A., . . . Cockerill, P. N. (2015). Chronic FLT3-ITD Signaling in Acute Myeloid Leukemia Is Connected to a Specific Chromatin Signature. *Cell Rep, 12*(5), 821-836. doi:10.1016/j.celrep.2015.06.069

Chaillou, T., Kirby, T. J., & McCarthy, J. J. (2014). Ribosome biogenesis: emerging evidence for a central role in the regulation of skeletal muscle mass. *Journal of cellular physiology, 229*(11), 1584-1594. doi:10.1002/jcp.24604

Chakrabarti, A., Oehme, I., Witt, O., Oliveira, G., Sippl, W., Romier, C., . . . Jung, M. (2015). HDAC8: a multifaceted target for therapeutic interventions. *Trends in Pharmacological Sciences, 36*(7), 481-492. doi:10.1016/j.tips.2015.04.013

Chalhoub, N., & Baker, S. J. (2009). PTEN and the PI3-Kinase Pathway in Cancer. *Annual Review Of Pathology, 4*, 127-150. doi:10.1146/annurev.pathol.4.110807.092311

Chalmers, Z. R., Connelly, C. F., Fabrizio, D., Gay, L., Ali, S. M., Ennis, R., . . . Frampton, G. M. (2017). Analysis of 100,000 human cancer genomes reveals the landscape of tumor mutational burden. *Genome Medicine, 9*(1), 34. doi:10.1186/s13073-017-0424-2

Chamberlain, J. (1994). Screening for neuroblastoma: a review of the evidence. *J Med Screen, 1*(3), 169-175. doi:10.1177/096914139400100307

Chang, F., Lee, J. T., Navolanic, P. M., Steelman, L. S., Shelton, J. G., Blalock, W. L., . . . McCubrey, J. A. (2003). Involvement of PI3K/Akt pathway in cell cycle progression, apoptosis, and neoplastic transformation: a target for cancer chemotherapy. *Leukemia, 17*(3), 590-603. doi:10.1038/sj.leu.2402824

Chang, P. C. Y., Wang, N.-L., Liu, H.-C., Liang, D.-C., Yeh, T.-C., Hou, J.-Y., & Sheu, J.-C. (2018). Low-stage pediatric neuroblastoma: A 20-year single institution review. *Journal of Cancer Research and Practice, 5*(1), 9-12. doi:https://doi.org/10.1016/j.jcrpr.2017.11.003

Chang, S., McKinsey, T. A., Zhang, C. L., Richardson, J. A., Hill, J. A., & Olson, E. N. (2004). Histone deacetylases 5 and 9 govern responsiveness of the heart to a subset of stress signals and play redundant roles in heart development. *Molecular & Cellular Biology, 24*(19), 8467-8476.

Chang, S., Young, B. D., Li, S., Qi, X., Richardson, J. A., & Olson, E. N. (2006). Histone deacetylase 7 maintains vascular integrity by repressing matrix metalloproteinase 10. *Cell, 126*(2), 321-334.

Chanthery, Y. H., Gustafson, W. C., Itsara, M., Persson, A., Hackett, C. S., Grimmer, M., . . . Weiss, W. A. (2012). Paracrine Signaling Through MYCN Enhances Tumor-Vascular Interactions in Neuroblastoma. *Sci Transl Med, 4*(115), 115ra113-115ra113. doi:10.1126/scitranslmed.3002977

Chauvin, C., Koka, V., Nouschi, A., Mieulet, V., Hoareau-Aveilla, C., Dreazen, A., . . . Pende, M. (2014). Ribosomal protein S6 kinase activity controls the ribosome biogenesis transcriptional program. *Oncogene, 33*(4), 474-483. doi:10.1038/onc.2012.606

Chen, A., Huang, X., Xue, Z., Cao, D., Huang, K., Chen, J., . . . Gao, Y. (2015). The Role of p21 in Apoptosis, Proliferation, Cell Cycle Arrest, and Antioxidant Activity in UVB-Irradiated Human HaCaT Keratinocytes. *Medical Science Monitor Basic Research, 21*, 86-95. doi:10.12659/MSMBR.893608

Chen, D., Mao, C., Zhou, Y., Su, Y., Liu, S., & Qi, W. Q. (2016). PF-04691502, a dual PI3K/mTOR inhibitor has potent pre-clinical activity by inducing apoptosis and G1 cell cycle arrest in aggressive B-cell non-Hodgkin lymphomas. *Int J Oncol, 48*(1), 253-260. doi:10.3892/ijo.2015.3231

Chen, H., Liu, H., & Qing, G. (2018). Targeting oncogenic Myc as a strategy for cancer treatment. *Signal Transduction and Targeted Therapy, 3*(1), 5. doi:10.1038/s41392-018-0008-7

Chen, L., Iraci, N., Gherardi, S., Gamble, L. D., Wood, K. M., Perini, G., . . . Tweddle, D. A. (2010). p53 is a direct transcriptional target of MYCN in neuroblastoma. *Cancer Research, 70*(4), 1377-1388. doi:10.1158/0008-5472.Can-09-2598

Chen, L., Yang, L., Yao, L., Kuang, X.-Y., Zuo, W.-J., Li, S., . . . Shao, Z.-M. (2018). Characterization of PIK3CA and PIK3R1 somatic mutations in Chinese breast cancer patients. *Nature communications, 9*(1), 1357. doi:10.1038/s41467-018-03867-9

Chen, X., Pappo, A., & Dyer, M. A. (2015). Pediatric solid tumor genomics and developmental pliancy. *Oncogene, 34*(41), 5207-5215. doi:10.1038/onc.2014.474

Chen, Y., Bathula, S. R., Yang, Q., & Huang, L. (2010). Targeted Nanoparticles Deliver siRNA to Melanoma. *Journal of Investigative Dermatology, 130*(12), 2790-2798. doi:https://doi.org/10.1038/jid.2010.222

Cheng, A. J., Cheng, N. C., Ford, J., Smith, J., Murray, J. E., Flemming, C., . . . Haber, M. (2007). Cell lines from MYCN transgenic murine tumours reflect the molecular and biological characteristics of human neuroblastoma. *European journal of cancer (Oxford, England : 1990), 43*(9), 1467-1475. doi:10.1016/j.ejca.2007.03.008

Cheng, H., Li, C., Bailey, S., Baxi, S. M., Goulet, L., Guo, L., . . . Zientek, M. (2013). Discovery of the Highly Potent PI3K/mTOR Dual Inhibitor. *ACS Medicinal Chemistry Letters, 4*(1), 91-97. doi:10.1021/ml300309h

Chesler, L., Goldenberg, D. D., Collins, R., Grimmer, M., Kim, G. E., Tihan, T., . . . Weiss, W. A. (2008). Chemotherapy-Induced Apoptosis in a Transgenic Model of Neuroblastoma Proceeds Through p53 Induction. *Neoplasia (New York, N.Y.), 10*(11), 1268-1274.

Chesler, L., Schlieve, C., Goldenberg, D. D., Kenney, A., Kim, G., McMillan, A., . . . Weiss, W. A. (2006). Inhibition of phosphatidylinositol 3-kinase destabilizes Mycn protein and blocks malignant progression in neuroblastoma. *Cancer Research, 66*(16), 8139-8146. doi:10.1158/0008-5472.Can-05-2769

Cheung, C. C., Martin, B. R., & Asa, S. L. (2013). Defining diagnostic tissue in the era of personalized medicine. *CMAJ : Canadian Medical Association Journal, 185*(2), 135-139. doi:10.1503/cmaj.120565

Cheung, L. W. T., Hennessy, B. T., Li, J., Yu, S., Myers, A. P., Djordjevic, B., . . . Mills, G. B. (2011). High Frequency of PIK3R1 and PIK3R2 Mutations in Endometrial Cancer Elucidates a Novel Mechanism for Regulation of PTEN Protein Stability. *Cancer Discovery, 1*(2), 170-185. doi:10.1158/2159-8290.CD-11-0039

Cheung, L. W. T., & Mills, G. B. (2016). Targeting therapeutic liabilities engendered by PIK3R1 mutations for cancer treatment. *Pharmacogenomics, 17*(3), 297-307. doi:10.2217/pgs.15.174

Childs, B. G., Baker, D. J., Kirkland, J. L., Campisi, J., & van Deursen, J. M. (2014). Senescence and apoptosis: dueling or complementary cell fates? *EMBO Rep, 15*(11), 1139-1153. doi:10.15252/embr.201439245

Ciarcia, R., Damiano, S., Montagnaro, S., Pagnini, U., Ruocco, A., Caparrotti, G., . . . Giordano, A. (2013). Combined effects of PI3K and SRC kinase inhibitors with imatinib on intracellular calcium levels, autophagy, and apoptosis in CML-PBL cells. *Cell Cycle, 12*(17), 2839-2848. doi:10.4161/cc.25920

Clawson, G. A. (2016). Histone deacetylase inhibitors as cancer therapeutics. *Ann Transl Med, 4*(15), 287. doi:10.21037/atm.2016.07.22

Coffer, P. J., & Woodgett, J. R. (1991). Molecular cloning and characterisation of a novel putative protein-serine kinase related to the cAMP-dependent and protein kinase C families. *Eur J Biochem, 201*(2), 475-481.

Coffey, D. C., Kutko, M. C., Glick, R. D., Butler, L. M., Heller, G., Rifkind, R. A., . . . La Quaglia, M. P. (2001). The histone deacetylase inhibitor, CBHA, inhibits growth of

human neuroblastoma xenografts in vivo, alone and synergistically with all-trans retinoic acid. *Cancer Research, 61*(9), 3591-3594.

Coffey, D. C., Kutko, M. C., Glick, R. D., Swendeman, S. L., Butler, L., Rifkind, R., . . . LaQuaglia, M. P. (2000). Histone deacetylase inhibitors and retinoic acids inhibit growth of human neuroblastoma in vitro. *Med Pediatr Oncol, 35*(6), 577-581.

Cohen, A. F., Burggraaf, J., van Gerven, J. M. A., Moerland, M., & Groeneveld, G. J. (2015). The Use of Biomarkers in Human Pharmacology (Phase I) Studies. *Annual Review of Pharmacology and Toxicology, 55*(1), 55-74. doi:10.1146/annurev-pharmtox-011613-135918

Cohen, P. (2002). Protein kinases--the major drug targets of the twenty-first century? *Nature Reviews. Drug Discovery, 1*(4), 309-315. doi:10.1038/nrd773

Cohn, S. L., Pearson, A. D. J., London, W. B., Monclair, T., Ambros, P. F., Brodeur, G. M., . . . Matthay, K. K. (2009). The International Neuroblastoma Risk Group (INRG) Classification System: An INRG Task Force Report. *Journal of Clinical Oncology, 27*(2), 289-297. doi:10.1200/JCO.2008.16.6785

Cole, M. D., & Cowling, V. H. (2008). Transcription-independent functions of MYC: regulation of translation and DNA replication. *Nat Rev Mol Cell Biol, 9*(10), 810-815. doi:10.1038/nrm2467

Collado, M., Medema, R. H., Garcia-Cao, I., Dubuisson, M. L., Barradas, M., Glassford, J., . . . Lam, E. W. (2000). Inhibition of the phosphoinositide 3-kinase pathway induces a senescence-like arrest mediated by p27Kip1. *J Biol Chem, 275*(29), 21960-21968. doi:10.1074/jbc.M000759200

Collins, A. T., Berry, P. A., Hyde, C., Stower, M. J., & Maitland, N. J. (2005). Prospective identification of tumorigenic prostate cancer stem cells. *Cancer Research, 65*(23), 10946-10951. doi:10.1158/0008-5472.Can-05-2018

Coppé, J.-P., Desprez, P.-Y., Krtolica, A., & Campisi, J. (2010). The Senescence-Associated Secretory Phenotype: The Dark Side of Tumor Suppression. *Annual Review Of Pathology, 5*, 99-118. doi:10.1146/annurev-pathol-121808-102144

Corallo, D., Candiani, S., Ori, M., Aveic, S., & Tonini, G. P. (2016). The zebrafish as a model for studying neuroblastoma. *Cancer Cell International, 16*, 82. doi:10.1186/s12935-016-0360-z

Cosker, K. E., Shadan, S., van Diepen, M., Morgan, C., Li, M., Allen-Baume, V., . . . Eickholt, B. J. (2008). Regulation of PI3K signalling by the phosphatidylinositol transfer protein PITPalpha during axonal extension in hippocampal neurons. *J Cell Sci, 121*(Pt 6), 796-803. doi:10.1242/jcs.019166

Cotterman, R., Jin, V. X., Krig, S. R., Lemen, J. M., Wey, A., Farnham, P. J., & Knoepfler, P. S. (2008). N-Myc regulates a widespread euchromatic program in the human genome partially independent of its role as a classical transcription factor. *Cancer Research, 68*(23), 9654-9662. doi:10.1158/0008-5472.CAN-08-1961

Coughlan, D., Gianferante, M., Lynch, C. F., Stevens, J. L., & Harlan, L. C. (2017). Treatment and survival of childhood neuroblastoma: Evidence from a population-based study in the United States. *Pediatr Hematol Oncol, 34*(5), 320-330. doi:10.1080/08880018.2017.1373315

Courtney, K. D., Corcoran, R. B., & Engelman, J. A. (2010). The PI3K Pathway As Drug Target in Human Cancer. *Journal of Clinical Oncology, 28*(6), 1075-1083. doi:10.1200/JCO.2009.25.3641

Couzin-Frankel, J. (2011). Personalized medicine. Pushing the envelope in neuroblastoma therapy. *Science, 333*(6049), 1569-1571. doi:10.1126/science.333.6049.1569

Cowling, V. H., & Cole, M. D. (2006). Mechanism of transcriptional activation by the Myc oncoproteins. *Semin Cancer Biol, 16*(4), 242-252. doi:10.1016/j.semcancer.2006.08.001

Cui, F., Fan, R., Chen, Q., He, Y., Song, M., Shang, Z., . . . Zhou, P. K. (2015). The involvement of c-Myc in the DNA double-strand break repair via regulating radiation-induced phosphorylation of ATM and DNA-PKcs activity. *Mol Cell Biochem, 406*(1-2), 43-51. doi:10.1007/s11010-015-2422-2

Cullinane, C., Dorow, D. S., Kansara, M., Conus, N., Binns, D., Hicks, R. J., . . . Thomas, D. M. (2005). An in vivo tumor model exploiting metabolic response as a biomarker for targeted drug development. *Cancer Research, 65*(21), 9633-9636. doi:10.1158/0008-5472.Can-05-2285

Cunha, L., Horvath, I., Ferreira, S., Lemos, J., Costa, P., Vieira, D., . . . Metello, L. F. (2014). Preclinical imaging: an essential ally in modern biosciences. *Mol Diagn Ther, 18*(2), 153-173. doi:10.1007/s40291-013-0062-3

Czabotar, P. E., Lessene, G., Strasser, A., & Adams, J. M. (2013). Control of apoptosis by the BCL-2 protein family: implications for physiology and therapy. *Nature Reviews Molecular Cell Biology, 15*, 49. doi:10.1038/nrm3722

Dai, Y., & Faller, D. V. (2008). Transcription Regulation by Class III Histone Deacetylases (HDACs)-Sirtuins. *Transl Oncogenomics, 3*, 53-65.

Dalla-Favera, R., Bregni, M., Erikson, J., Patterson, D., Gallo, R. C., & Croce, C. M. (1982). Human c-myc onc gene is located on the region of chromosome 8 that is translocated in Burkitt lymphoma cells. *Proc Natl Acad Sci U S A, 79*(24), 7824-7827.

Dam, V., Morgan, B. T., Mazanek, P., & Hogarty, M. D. (2006). Mutations in PIK3CA are infrequent in neuroblastoma. *BMC Cancer, 6*, 177. doi:10.1186/1471-2407-6-177

Dang, C. V. (2012). MYC on the Path to Cancer. *Cell, 149*(1), 22-35. doi:10.1016/j.cell.2012.03.003

Datta, S. R., Dudek, H., Tao, X., Masters, S., Fu, H., Gotoh, Y., & Greenberg, M. E. (1997). Akt phosphorylation of BAD couples survival signals to the cell-intrinsic death machinery. *Cell, 91*(2), 231-241.

Davar, D., Beumer, J. H., Hamieh, L., & Tawbi, H. (2012). Role of PARP Inhibitors in Cancer Biology and Therapy. *Current medicinal chemistry, 19*(23), 3907-3921.

David, M., Hodak, E., & Lowe, N. J. (1988). Adverse effects of retinoids. *Med Toxicol Adverse Drug Exp, 3*(4), 273-288. doi:10.1007/bf03259940

Davie, J. R. (1998). Covalent modifications of histones: expression from chromatin templates. *Current Opinion in Genetics & Development, 8*(2), 173-178.

Davis, A. J., So, S., & Chen, D. J. (2010). Dynamics of the PI3K-like protein kinase members ATM and DNA-PKcs at DNA double strand breaks. *Cell Cycle, 9*(13), 2529-2536. doi:10.4161/cc.9.13.12148

De Ioris, M. A., Crocoli, A., Contoli, B., Garganese, M. C., Natali, G., Tomà, P., . . . Inserra, A. (2015). Local control in metastatic neuroblastoma in children over 1 year of age. *BMC Cancer, 15*, 79. doi:10.1186/s12885-015-1082-7

De, P., Carlson, J., leyland-jones, B., & Dey, N. (2016). *PI3K-AKT-mTOR Pathway Cooperates with the DNA Damage Repair Pathway: Carcinogenesis in Triple-Negative Breast Cancers and Beyond*.

de Pretis, S., Kress, T. R., Morelli, M. J., Sabò, A., Locarno, C., Verrecchia, A., . . . Pelizzola, M. (2017). Integrative analysis of RNA polymerase II and transcriptional dynamics upon MYC activation. *Genome Research, 27*(10), 1658-1664. doi:10.1101/gr.226035.117

Deau, M.-C., Heurtier, L., Frange, P., Suarez, F., Bole-Feysot, C., Nitschke, P., . . . Kracker, S. (2014). A human immunodeficiency caused by mutations in the PIK3R1 gene. *The Journal of Clinical Investigation, 124*(9), 3923-3928. doi:10.1172/JCI75746

Del Bufalo, D., Ciuffreda, L., Trisciuoglio, D., Desideri, M., Cognetti, F., Zupi, G., & Milella, M. (2006). Antiangiogenic potential of the Mammalian target of rapamycin inhibitor temsirolimus. *Cancer Research, 66*(11), 5549-5554. doi:10.1158/0008-5472.Can-05-2825

Dela Cruz, F. S. (2013). Cancer stem cells in pediatric sarcomas. *Front Oncol, 3*, 168. doi:10.3389/fonc.2013.00168

Devlin, J. R., Hannan, K. M., Hein, N., Cullinane, C., Kusnadi, E., Ng, P. Y., . . . Pearson, R. B. (2016). Combination Therapy Targeting Ribosome Biogenesis and mRNA Translation Synergistically Extends Survival in MYC-Driven Lymphoma. *Cancer Discov, 6*(1), 59-70. doi:10.1158/2159-8290.Cd-14-0673

Deyell, R. J., & Attiyeh, E. F. (2011). Advances in the understanding of constitutional and somatic genomic alterations in neuroblastoma. *Cancer Genet, 204*(3), 113-121. doi:10.1016/j.cancergen.2011.03.001

Dienstmann, R., Rodon, J., Serra, V., & Tabernero, J. (2014). Picking the Point of Inhibition: A Comparative Review of PI3K/AKT/mTOR Pathway Inhibitors. *Mol Cancer Ther, 13*(5), 1021.

Dirks, P. B. (2010). Brain tumor stem cells: the cancer stem cell hypothesis writ large. *Molecular Oncology, 4*(5), 420-430. doi:10.1016/j.molonc.2010.08.001

Dokmanovic, M., Clarke, C., & Marks, P. A. (2007). Histone deacetylase inhibitors: overview and perspectives. *Mol Cancer Res, 5*(10), 981-989. doi:10.1158/1541-7786.Mcr-07-0324

Dong, Y., Tu, R., Liu, H., & Qing, G. (2020). Regulation of cancer cell metabolism: oncogenic MYC in the driver's seat. *Signal Transduction and Targeted Therapy, 5*(1), 124. doi:10.1038/s41392-020-00235-2

Dong, Z., Yang, Y., Liu, S., Lu, J., Huang, B., & Zhang, Y. (2018). HDAC inhibitor PAC-320 induces G2/M cell cycle arrest and apoptosis in human prostate cancer. *Oncotarget, 9*(1), 512-523. doi:10.18632/oncotarget.23070

Douarre, C., Gomez, D., Morjani, H., Zahm, J. M., O'Donohue M, F., Eddabra, L., . . . Trentesaux, C. (2005). Overexpression of Bcl-2 is associated with apoptotic resistance to the G-quadruplex ligand 12459 but is not sufficient to confer resistance to long-term senescence. *Nucleic Acids Res, 33*(7), 2192-2203. doi:10.1093/nar/gki514

Ducker, G. S., Atreya, C. E., Simko, J. P., Hom, Y. K., Matli, M. R., Benes, C. H., . . . Warren, R. S. (2013). Incomplete inhibition of phosphorylation of 4E-BP1 as a mechanism of primary resistance to ATP-competitive mTOR inhibitors. *Oncogene, 33*, 1590. doi:10.1038/onc.2013.92 https://www.nature.com/articles/onc201392#supplementary-information

Duffy, D. J., Krstic, A., Schwarzl, T., Higgins, D. G., & Kolch, W. (2014). GSK3 inhibitors regulate MYCN mRNA levels and reduce neuroblastoma cell viability through multiple mechanisms, including p53 and Wnt signaling. *Mol Cancer Ther, 13*(2), 454-467. doi:10.1158/1535-7163.Mct-13-0560-t

Easton, J. C., Gomez, S., Asdahl, P. H., Conner, J. M., Fynn, A. B., Ruiz, C., & Ojha, R. P. (2016). Survival of high-risk pediatric neuroblastoma patients in a developing country. *Pediatric transplantation, 20*(6), 825-830. doi:10.1111/petr.12731

Eberhardy, S. R., & Farnham, P. J. (2002). Myc recruits P-TEFb to mediate the final step in the transcriptional activation of the cad promoter. *J Biol Chem, 277*(42), 40156-40162. doi:10.1074/jbc.M207441200

Ebi, H., Costa, C., Faber, A. C., Nishtala, M., Kotani, H., Juric, D., . . . Engelman, J. A. (2013). PI3K regulates MEK/ERK signaling in breast cancer via the Rac-GEF, P-Rex1. *Proc Natl Acad Sci U S A, 110*(52), 21124-21129. doi:10.1073/pnas.1314124110

Ecker, J., Oehme, I., Mazitschek, R., Korshunov, A., Kool, M., Hielscher, T., . . . Milde, T. (2015). Targeting class I histone deacetylase 2 in MYC amplified group 3 medulloblastoma. *Acta Neuropathologica Communications, 3*, 22. doi:10.1186/s40478-015-0201-7

Eckschlager, T., Plch, J., Stiborova, M., & Hrabeta, J. (2017). Histone Deacetylase Inhibitors as Anticancer Drugs. *Int J Mol Sci, 18*(7). doi:10.3390/ijms18071414

Ehninger, A., Boch, T., Uckelmann, H., Essers, M. A., Mudder, K., Sleckman, B. P., & Trumpp, A. (2014). Posttranscriptional regulation of c-Myc expression in adult murine HSCs during homeostasis and interferon-alpha-induced stress response. *Blood, 123*(25), 3909-3913. doi:10.1182/blood-2013-10-531038

El-Andaloussi, S., Johansson, H., Magnusdottir, A., Järver, P., Lundberg, P., & Langel, Ü. (2005). TP10, a delivery vector for decoy oligonucleotides targeting the Myc protein. *Journal of Controlled Release, 110*(1), 189-201. doi:https://doi.org/10.1016/j.jconrel.2005.09.012

Eleveld, T. F., Oldridge, D. A., Bernard, V., Koster, J., Colmet Daage, L., Diskin, S. J., . . . Maris, J. M. (2015). Relapsed neuroblastomas show frequent RAS-MAPK pathway mutations. *Nat Genet, 47*(8), 864-871. doi:10.1038/ng.3333

Elkholi, R., Floros, K. V., & Chipuk, J. E. (2011). The Role of BH3-Only Proteins in Tumor Cell Development, Signaling, and Treatment. *Genes Cancer, 2*(5), 523-537. doi:10.1177/1947601911417177

Ellis, L., Hammers, H., & Pili, R. (2009). Targeting tumor angiogenesis with histone deacetylase inhibitors. *Cancer Letters, 280*(2), 145-153. doi:10.1016/j.canlet.2008.11.012

Ellison, D. W., Dalton, J., Kocak, M., Nicholson, S. L., Fraga, C., Neale, G., . . . Gilbertson, R. J. (2011). Medulloblastoma: clinicopathological correlates of SHH, WNT, and non-SHH/WNT molecular subgroups. *Acta neuropathologica, 121*(3), 381-396. doi:10.1007/s00401-011-0800-8

Elmore, S. (2007). Apoptosis: A Review of Programmed Cell Death. *Toxicologic pathology, 35*(4), 495-516. doi:10.1080/01926230701320337

Embi, N., Rylatt, D. B., & Cohen, P. (1980). Glycogen synthase kinase-3 from rabbit skeletal muscle. Separation from cyclic-AMP-dependent protein kinase and phosphorylase kinase. *Eur J Biochem, 107*(2), 519-527.

Engelman, J. A., Luo, J., & Cantley, L. C. (2006). The evolution of phosphatidylinositol 3-kinases as regulators of growth and metabolism. *Nature Reviews Genetics, 7*(8), 606-619. doi:10.1038/nrg1879

Esposito, M. R., Aveic, S., Seydel, A., & Tonini, G. P. (2017). Neuroblastoma treatment in the post-genomic era. *Journal of Biomedical Science, 24*(1), 14. doi:10.1186/s12929-017-0319-y

Ewald, J. A., Desotelle, J. A., Wilding, G., & Jarrard, D. F. (2010). Therapy-Induced Senescence in Cancer. *JNCI Journal of the National Cancer Institute, 102*(20), 1536-1546. doi:10.1093/jnci/djq364

Faes, S., & Dormond, O. (2015). PI3K and AKT: Unfaithful Partners in Cancer. *Int J Mol Sci, 16*(9), 21138-21152. doi:10.3390/ijms160921138

Faes, S., Santoro, T., Demartines, N., & Dormond, O. (2017). Evolving Significance and Future Relevance of Anti-Angiogenic Activity of mTOR Inhibitors in Cancer Therapy. *Cancers, 9*(11), 152. doi:10.3390/cancers9110152

Fagone, P., Donia, M., Mangano, K., Quattrocchi, C., Mammana, S., Coco, M., . . . Nicoletti, F. (2013). Comparative study of rapamycin and temsirolimus demonstrates superimposable anti-tumour potency on prostate cancer cells. *Basic Clin Pharmacol Toxicol, 112*(1), 63-69. doi:10.1111/j.1742-7843.2012.00923.x

Falasca, M., & Maffucci, T. (2012). Regulation and cellular functions of class II phosphoinositide 3-kinases. *Biochem J, 443*(3), 587-601. doi:10.1042/bj20120008

Falkenburger, B. H., Jensen, J. B., Dickson, E. J., Suh, B.-C., & Hille, B. (2010). Phosphoinositides: lipid regulators of membrane proteins. *The Journal of Physiology, 588*(Pt 17), 3179-3185. doi:10.1113/jphysiol.2010.192153

Fang, D., Nguyen, T. K., Leishear, K., Finko, R., Kulp, A. N., Hotz, S., . . . Herlyn, M. (2005). A tumorigenic subpopulation with stem cell properties in melanomas. *Cancer Research, 65*(20), 9328-9337. doi:10.1158/0008-5472.Can-05-1343

Fang, D. D., Zhang, C. C., Gu, Y., Jani, J. P., Cao, J., Tsaparikos, K., . . . Vanarsdale, T. (2013). Antitumor Efficacy of the Dual PI3K/mTOR Inhibitor PF-04691502 in a Human Xenograft Tumor Model Derived from Colorectal Cancer Stem Cells Harboring a PIK3CA Mutation. *PLoS ONE, 8*(6), e67258. doi:10.1371/journal.pone.0067258

Fantin, V. R., & Richon, V. M. (2007). Mechanisms of resistance to histone deacetylase inhibitors and their therapeutic implications. *Clin Cancer Res, 13*(24), 7237-7242. doi:10.1158/1078-0432.Ccr-07-2114

Farrell, A. S., & Sears, R. C. (2014). MYC Degradation. *Cold Spring Harbor Perspectives in Medicine, 4*(3), a014365. doi:10.1101/cshperspect.a014365

Fawzy, M., El-Beltagy, M., Shafei, M. E., Zaghloul, M. S., Kinaai, N. A., Refaat, A., & Azmy, S. (2015). Intraspinal neuroblastoma: Treatment options and neurological outcome of spinal cord compression. *Oncol Lett, 9*(2), 907-911. doi:10.3892/ol.2014.2795

Fei, H. R., Tian, H., Zhou, X. L., Yang, M. F., Sun, B. L., Yang, X. Y., . . . Wang, F. Z. (2016). Inhibition of autophagy enhances effects of PF-04691502 on apoptosis and DNA damage of lung cancer cells. *Int J Biochem Cell Biol, 78*, 52-62. doi:10.1016/j.biocel.2016.06.023

Feiler, T., Gaitskell, K., Maughan, T., & Hordern, J. (2017). Personalised Medicine: The Promise, the Hype and the Pitfalls. *The New Bioethics, 23*(1), 1-12. doi:10.1080/20502877.2017.1314895

Felsher, D. W., & Bishop, J. M. (1999). Reversible tumorigenesis by MYC in hematopoietic lineages. *Mol Cell, 4*(2), 199-207. doi:10.1016/s1097-2765(00)80367-6

Fernández-Medarde, A., & Santos, E. (2011). Ras in Cancer and Developmental Diseases. *Genes Cancer, 2*(3), 344-358. doi:10.1177/1947601911411084

Fletcher, S., & Prochownik, E. V. (2015). Small-Molecule Inhibitors of the Myc Oncoprotein. *Biochim Biophys Acta, 1849*(5), 525-543. doi:10.1016/j.bbagrm.2014.03.005

Fleurence, J., Fougeray, S., Bahri, M., Cochonneau, D., Clémenceau, B., Paris, F., . . . Birklé, S. (2017). Targeting O-Acetyl-GD2 Ganglioside for Cancer Immunotherapy. *Journal of Immunology Research, 2017*, 5604891. doi:10.1155/2017/5604891

Forrest, S. J., Geoerger, B., & Janeway, K. A. (2018). Precision medicine in pediatric oncology. *Current Opinion in Pediatrics, 30*(1), 17-24. doi:10.1097/MOP.0000000000000570

Fouladi, M., Park, J. R., Stewart, C. F., Gilbertson, R. J., Schaiquevich, P., Sun, J., . . . Adamson, P. C. (2010). Pediatric phase I trial and pharmacokinetic study of vorinostat: a Children's Oncology Group phase I consortium report. *J Clin Oncol, 28*(22), 3623-3629. doi:10.1200/jco.2009.25.9119

Franke, T. F., Hornik, C. P., Segev, L., Shostak, G. A., & Sugimoto, C. (2003). PI3K/Akt and apoptosis: size matters. *Oncogene, 22*(56), 8983-8998. doi:10.1038/sj.onc.1207115

Fransson, S., Abel, F., Kogner, P., Martinsson, T., & Ejeskar, K. (2013). Stage-dependent expression of PI3K/Aktpathway genes in neuroblastoma. *Int J Oncol, 42*(2), 609-616. doi:10.3892/ijo.2012.1732

Franz, D. N., & Capal, J. K. (2017). mTOR inhibitors in the pharmacologic management of tuberous sclerosis complex and their potential role in other rare neurodevelopmental disorders. *Orphanet Journal of Rare Diseases, 12*, 51. doi:10.1186/s13023-017-0596-2

Friedman, G. K., & Gillespie, G. Y. (2011). Cancer Stem Cells and Pediatric Solid Tumors. *Cancers, 3*(1), 298-318. doi:10.3390/cancers3010298

Fruman, D. A., Chiu, H., Hopkins, B. D., Bagrodia, S., Cantley, L. C., & Abraham, R. T. (2017). The PI3K Pathway in Human Disease. *Cell, 170*(4), 605-635. doi:10.1016/j.cell.2017.07.029

Fruman, D. A., & Rommel, C. (2014). PI3K and Cancer: Lessons, Challenges and Opportunities. *Nature Reviews. Drug Discovery, 13*(2), 140-156. doi:10.1038/nrd4204

Frumm, S. M., Fan, Z. P., Ross, K. N., Duvall, J. R., Gupta, S., VerPlank, L., . . . Stegmaier, K. (2013). Selective HDAC1/HDAC2 inhibitors induce neuroblastoma differentiation. *Chem Biol, 20*(5), 713-725. doi:10.1016/j.chembiol.2013.03.020

Fulda, S. (2009). The PI3K/Akt/mTOR pathway as therapeutic target in neuroblastoma. *Curr Cancer Drug Targets, 9*(6), 729-737.

Fulda, S. (2013). Modulation of mitochondrial apoptosis by PI3K inhibitors. *Mitochondrion, 13*(3), 195-198. doi:10.1016/j.mito.2012.05.001

Fulda, S., & Debatin, K. M. (2006). Extrinsic versus intrinsic apoptosis pathways in anticancer chemotherapy. *Oncogene, 25*, 4798. doi:10.1038/sj.onc.1209608

Gabay, M., Li, Y., & Felsher, D. W. (2014). MYC Activation Is a Hallmark of Cancer Initiation and Maintenance. *Cold Spring Harbor Perspectives in Medicine, 4*(6), a014241. doi:10.1101/cshperspect.a014241

Gallia, G. L., Rand, V., Siu, I. M., Eberhart, C. G., James, C. D., Marie, S. K., . . . Riggins, G. J. (2006). PIK3CA gene mutations in pediatric and adult glioblastoma multiforme. *Mol Cancer Res, 4*(10), 709-714. doi:10.1158/1541-7786.Mcr-06-0172

Gamble, L. D., Kees, U. R., Tweddle, D. A., & Lunec, J. (2012). MYCN sensitizes neuroblastoma to the MDM2-p53 antagonists Nutlin-3 and MI-63. *Oncogene, 31*(6), 752-763. doi:10.1038/onc.2011.270

Ganeshan, V. R., & Schor, N. F. (2011). Pharmacological Management of High-risk Neuroblastoma in Children. *Paediatric drugs, 13*(4), 245-255. doi:10.2165/11591630-000000000-00000

Gao, T., Furnari, F., & Newton, A. C. (2005). PHLPP: a phosphatase that directly dephosphorylates Akt, promotes apoptosis, and suppresses tumor growth. *Mol Cell, 18*(1), 13-24. doi:10.1016/j.molcel.2005.03.008

Garcia-Sanz, P., Quintanilla, A., Lafita, M. C., Moreno-Bueno, G., Garcia-Gutierrez, L., Tabor, V., . . . Leon, J. (2014). Sin3b Interacts with Myc and Decreases Myc Levels. *Journal of Biological Chemistry*. doi:10.1074/jbc.M113.538744

Garewal, H. S., Ahmann, F. R., Schifman, R. B., & Celniker, A. (1986). ATP assay: ability to distinguish cytostatic from cytocidal anticancer drug effects. *Journal of the National Cancer Institute, 77*(5), 1039-1045.

Gartel, A. L., Ye, X., Goufman, E., Shianov, P., Hay, N., Najmabadi, F., & Tyner, A. L. (2001). Myc represses the p21((WAF1/CIP1)) promoter and interacts with Sp1/Sp3. *Proc Natl Acad Sci U S A, 98*(8), 4510-4515. doi:10.1073/pnas.081074898

Gavan, S. P., Thompson, A. J., & Payne, K. (2018). The economic case for precision medicine. *Expert Review of Precision Medicine and Drug Development, 3*(1), 1-9. doi:10.1080/23808993.2018.1421858

Gentilella, A., Kozma, S. C., & Thomas, G. (2015). A liaison between mTOR signaling, ribosome biogenesis and cancer(). *Biochim Biophys Acta, 1849*(7), 812-820. doi:10.1016/j.bbagrm.2015.02.005

Geoerger, B., Kieran, M. W., Grupp, S., Perek, D., Clancy, J., Krygowski, M., . . . Spunt, S. L. (2012). Phase II trial of temsirolimus in children with high-grade glioma, neuroblastoma and rhabdomyosarcoma(). *European journal of cancer (Oxford, England : 1990), 48*(2), 253-262. doi:10.1016/j.ejca.2011.09.021

Georgantzi, K., Sköldenberg, E. G., Stridsberg, M., Kogner, P., Jakobson, Å., Janson, E. T., & Christofferson, R. H. B. (2018). Chromogranin A and neuron-specific enolase in neuroblastoma: Correlation to stage and prognostic factors. *Pediatr Hematol Oncol*, 1-10. doi:10.1080/08880018.2018.1464087

Giles, F., Fischer, T., Cortes, J., Garcia-Manero, G., Beck, J., Ravandi, F., . . . Bhalla, K. (2006). A phase I study of intravenous LBH589, a novel cinnamic hydroxamic acid

analogue histone deacetylase inhibitor, in patients with refractory hematologic malignancies. *Clin Cancer Res, 12*(15), 4628-4635. doi:10.1158/1078-0432.Ccr-06-0511

Gilley, J., Coffer, P. J., & Ham, J. (2003). FOXO transcription factors directly activate bim gene expression and promote apoptosis in sympathetic neurons. *J Cell Biol, 162*(4), 613-622. doi:10.1083/jcb.200303026

Gingras, A.-C., Gygi, S. P., Raught, B., Polakiewicz, R. D., Abraham, R. T., Hoekstra, M. F., . . . Sonenberg, N. (1999). Regulation of 4E-BP1 phosphorylation: a novel two-step mechanism. *Genes & Development, 13*(11), 1422-1437.

Ginn, K. F., & Gajjar, A. (2012). Atypical Teratoid Rhabdoid Tumor: Current Therapy and Future Directions. *Front Oncol, 2*, 114. doi:10.3389/fonc.2012.00114

Glaysher, S., Bolton, L. M., Johnson, P., Atkey, N., Dyson, M., Torrance, C., & Cree, I. A. (2013). Targeting EGFR and PI3K pathways in ovarian cancer. *British Journal of Cancer, 109*(7), 1786-1794. doi:10.1038/bjc.2013.529

Glick, R. D., Swendeman, S. L., Coffey, D. C., Rifkind, R. A., Marks, P. A., Richon, V. M., & La Quaglia, M. P. (1999). Hybrid polar histone deacetylase inhibitor induces apoptosis and CD95/CD95 ligand expression in human neuroblastoma. *Cancer Research, 59*(17), 4392-4399.

Glozak, M. A., & Seto, E. (2007). Histone deacetylases and cancer. *Oncogene, 26*, 5420. doi:10.1038/sj.onc.1210610

Goberdhan, D. C. I., & Wilson, C. (2003). PTEN: tumour suppressor, multifunctional growth regulator and more. *Hum Mol Genet, 12*(suppl_2), R239-R248. doi:10.1093/hmg/ddg288

Goel, H. L., & Mercurio, A. M. (2013). VEGF targets the tumour cell. *Nat Rev Cancer, 13*(12), 871-882. doi:10.1038/nrc3627

Goldberg, J. M., Glade-Bender, J., Sulis, M. L., Gardner, R. A., Pollard, J. A., Aquino, V., . . . Barredo, J. C. (2014). A Phase I Dose Finding Study of Panobinostat in Children with Hematologic Malignancies: Initial Report of TACL Study T2009-012 in Children with Acute Leukemia. *Blood, 124*(21), 3705-3705.

Gomez-Roman, N., Felton-Edkins, Z. A., Kenneth, N. S., Goodfellow, S. J., Athineos, D., Zhang, J., . . . White, R. J. (2006). Activation by c-Myc of transcription by RNA polymerases I, II and III. *Biochem Soc Symp*(73), 141-154.

Goodman, L. A., Liu, B. C., Thiele, C. J., Schmidt, M. L., Cohn, S. L., Yamashiro, J. M., . . . Wada, R. K. (1997). Modulation of N-myc expression alters the invasiveness of neuroblastoma. *Clin Exp Metastasis, 15*(2), 130-139.

Gottesman, M. M. (2002). Mechanisms of cancer drug resistance. *Annu Rev Med, 53*, 615-627. doi:10.1146/annurev.med.53.082901.103929

Gottlieb, T. M., Leal, J. F., Seger, R., Taya, Y., & Oren, M. (2002). Cross-talk between Akt, p53 and Mdm2: possible implications for the regulation of apoptosis. *Oncogene, 21*(8), 1299-1303. doi:10.1038/sj.onc.1205181

Graham, C., Tucker, C., Creech, J., Favours, E., Billups, C. A., Liu, T., . . . Houghton, P. J. (2006). Evaluation of the antitumor efficacy, pharmacokinetics, and pharmacodynamics of the histone deacetylase inhibitor depsipeptide in childhood cancer models in vivo. *Clin Cancer Res, 12*(1), 223-234. doi:10.1158/1078-0432.Ccr-05-1225

Grana, T. M., Rusyn, E. V., Zhou, H., Sartor, C. I., & Cox, A. D. (2002). Ras Mediates Radioresistance through Both Phosphatidylinositol 3-Kinase-dependent and Raf-

dependent but Mitogen-activated Protein Kinase/Extracellular Signal-regulated Kinase Kinase-independent Signaling Pathways. *Cancer Research, 62*(14), 4142.

Grandori, C., Cowley, S. M., James, L. P., & Eisenman, R. N. (2000). The Myc/Max/Mad network and the transcriptional control of cell behavior. *Annu Rev Cell Dev Biol, 16*, 653-699. doi:10.1146/annurev.cellbio.16.1.653

Gregory, M. A., Qi, Y., & Hann, S. R. (2003). Phosphorylation by glycogen synthase kinase-3 controls c-myc proteolysis and subnuclear localization. *J Biol Chem, 278*(51), 51606-51612. doi:10.1074/jbc.M310722200

Grinberg, A. V., Hu, C.-D., & Kerppola, T. K. (2004). Visualization of Myc/Max/Mad Family Dimers and the Competition for Dimerization in Living Cells. *Molecular and Cellular Biology, 24*(10), 4294-4308. doi:10.1128/mcb.24.10.4294-4308.2004

Gröbner, S. N., Worst, B. C., Weischenfeldt, J., Buchhalter, I., Kleinheinz, K., Rudneva, V. A., . . . Pfister, S. M. (2018). The landscape of genomic alterations across childhood cancers. *Nature, 555*, 321. doi:10.1038/nature25480 https://www.nature.com/articles/nature25480#supplementary-information

Groselj, B., Sharma, N. L., Hamdy, F. C., Kerr, M., & Kiltie, A. E. (2013). Histone deacetylase inhibitors as radiosensitisers: effects on DNA damage signalling and repair. *British Journal of Cancer, 108*(4), 748-754. doi:10.1038/bjc.2013.21

Gueugnon, F., Cartron, P.-F., Charrier, C., Bertrand, P., Fonteneau, J.-F., Gregoire, M., & Blanquart, C. (2014). New histone deacetylase inhibitors improve cisplatin antitumor properties against thoracic cancer cells. *Oncotarget, 5*(12), 4504-4515.

Gustafson, W. C., & Weiss, W. A. (2010). Myc proteins as therapeutic targets. *Oncogene, 29*(9), 1249-1259. doi:10.1038/onc.2009.512

Haberland, M., Montgomery, R. L., & Olson, E. N. (2009). The many roles of histone deacetylases in development and physiology: implications for disease and therapy. *Nature Reviews Genetics, 10*(1), 32-42. doi:https://dx.doi.org/10.1038/nrg2485

Han, S. S., Yun, H., Son, D. J., Tompkins, V. S., Peng, L., Chung, S. T., . . . Janz, S. (2010). NF-kappaB/STAT3/PI3K signaling crosstalk in iMyc E mu B lymphoma. *Mol Cancer, 9*, 97. doi:10.1186/1476-4598-9-97

Hannan, R. D., Drygin, D., & Pearson, R. B. (2013). Targeting RNA polymerase I transcription and the nucleolus for cancer therapy. *Expert Opin Ther Targets, 17*(8), 873-878. doi:10.1517/14728222.2013.818658

Hara, K., Yonezawa, K., Kozlowski, M. T., Sugimoto, T., Andrabi, K., Weng, Q.-P., . . . Avruch, J. (1997). Regulation of eIF-4E BP1 Phosphorylation by mTOR. *Journal of Biological Chemistry, 272*(42), 26457-26463. doi:10.1074/jbc.272.42.26457

Hart, J. R., & Vogt, P. K. (2011). Phosphorylation of AKT: a Mutational Analysis. *Oncotarget, 2*(6), 467-476.

Hatz, M. H., Schremser, K., & Rogowski, W. H. (2014). Is individualized medicine more cost-effective? A systematic review. *Pharmacoeconomics, 32*(5), 443-455. doi:10.1007/s40273-014-0143-0

He, G., Siddik, Z. H., Huang, Z., Wang, R., Koomen, J., Kobayashi, R., . . . Kuang, J. (2005). Induction of p21 by p53 following DNA damage inhibits both Cdk4 and Cdk2 activities. *Oncogene, 24*(18), 2929-2943. doi:10.1038/sj.onc.1208474

Heck, J. E., Ritz, B., Hung, R. J., Hashibe, M., & Boffetta, P. (2009). The epidemiology of neuroblastoma: a review. *Paediatr Perinat Epidemiol, 23*(2), 125-143. doi:10.1111/j.1365-3016.2008.00983.x

Hein, N., Cameron, D. P., Hannan, K. M., Nguyen, N.-Y. N., Fong, C. Y., Sornkom, J., . . . Hannan, R. D. (2017). Inhibition of Pol I transcription treats murine and human AML by targeting the leukemia-initiating cell population. *Blood, 129*(21), 2882-2895. doi:10.1182/blood-2016-05-718171

Heras-Sandoval, D., Pérez-Rojas, J. M., Hernández-Damián, J., & Pedraza-Chaverri, J. (2014). The role of PI3K/AKT/mTOR pathway in the modulation of autophagy and the clearance of protein aggregates in neurodegeneration. *Cellular Signalling, 26*(12), 2694-2701. doi:https://doi.org/10.1016/j.cellsig.2014.08.019

Hermida, M. A., Dinesh Kumar, J., & Leslie, N. R. (2017). GSK3 and its interactions with the PI3K/AKT/mTOR signalling network. *Adv Biol Regul, 65*, 5-15. doi:10.1016/j.jbior.2017.06.003

Herzog, A., Bian, Y., Vander Broek, R., Hall, B., Coupar, J., Cheng, H., . . . Van Waes, C. (2013). PI3K/mTOR inhibitor PF-04691502 antitumor activity is enhanced with induction of wild-type TP53 in human xenograft and murine knockout models of head and neck cancer. *Clin Cancer Res, 19*(14), 3808-3819. doi:10.1158/1078-0432.Ccr-12-2716

Hess, G., Herbrecht, R., Romaguera, J., Verhoef, G., Crump, M., Gisselbrecht, C., . . . Coiffier, B. (2009). Phase III study to evaluate temsirolimus compared with investigator's choice therapy for the treatment of relapsed or refractory mantle cell lymphoma. *J Clin Oncol, 27*(23), 3822-3829. doi:10.1200/jco.2008.20.7977

Heudel, P. E., Fabbro, M., Roemer-Becuwe, C., Kaminsky, M. C., Arnaud, A., Joly, F., . . . Ray-Coquard, I. (2017). Phase II study of the PI3K inhibitor BKM120 in patients with advanced or recurrent endometrial carcinoma: a stratified type I-type II study from the GINECO group. *Br J Cancer, 116*(3), 303-309. doi:10.1038/bjc.2016.430

Hidalgo, M., Amant, F., Biankin, A. V., Budinská, E., Byrne, A. T., Caldas, C., . . . Villanueva, A. (2014). Patient-derived xenograft models: an emerging platform for translational cancer research. *Cancer Discov, 4*(9), 998-1013. doi:10.1158/2159-8290.Cd-14-0001

Ho, J. S. L., Ma, W., Mao, D. Y. L., & Benchimol, S. (2005). p53-Dependent Transcriptional Repression of c-myc Is Required for G(1) Cell Cycle Arrest. *Molecular and Cellular Biology, 25*(17), 7423-7431. doi:10.1128/MCB.25.17.7423-7431.2005

Hogarty, M. D., Norris, M. D., Davis, K., Liu, X., Evageliou, N. F., Hayes, C. S., . . . Haber, M. (2008). ODC1 is a critical determinant of MYCN oncogenesis and a therapeutic target in neuroblastoma. *Cancer Research, 68*(23), 9735-9745. doi:10.1158/0008-5472.Can-07-6866

Hong, B., Wang, H., Deng, K., Wang, W., Dai, H., Yan Lui, V. W., & Lin, W. (2017). Combination treatment of RAD001 and BEZ235 exhibits synergistic antitumor activity via down-regulation of p-4E-BP1/Mcl-1 in small cell lung cancer. *Oncotarget, 8*(63), 106486-106498. doi:10.18632/oncotarget.18984

Hong, S., Derfoul, A., Pereira-Mouries, L., & Hall, D. J. (2009). A novel domain in histone deacetylase 1 and 2 mediates repression of cartilage-specific genes in human chondrocytes. *FASEB Journal, 23*(10), 3539-3552. doi:https://dx.doi.org/10.1096/fj.09-133215

Hortobagyi, G. N. (2015). Everolimus Plus Exemestane for the Treatment of Advanced Breast Cancer: A Review of Subanalyses from BOLERO-2(). *Neoplasia (New York, N.Y.), 17*(3), 279-288. doi:10.1016/j.neo.2015.01.005

Hotchkiss, R. S., Swanson, P. E., Knudson, C. M., Chang, K. C., Cobb, J. P., Osborne, D. F., . . . Karl, I. E. (1999). Overexpression of Bcl-2 in Transgenic Mice Decreases

Apoptosis and Improves Survival in Sepsis. *The Journal of Immunology, 162*(7), 4148.

Howell, J. J., Hellberg, K., Turner, M., Talbott, G., Kolar, M. J., Ross, D. S., . . . Manning, B. D. (2017). Metformin Inhibits Hepatic mTORC1 Signaling via Dose-Dependent Mechanisms Involving AMPK and the TSC Complex. *Cell Metabolism, 25*(2), 463-471. doi:10.1016/j.cmet.2016.12.009

Howell, J. J., & Manning, B. D. (2011). mTOR couples cellular nutrient sensing to organismal metabolic homeostasis. *Trends in endocrinology and metabolism: TEM, 22*(3), 94-102. doi:10.1016/j.tem.2010.12.003

Hoyer, C., Gass, N., Weber-Fahr, W., & Sartorius, A. (2014). Advantages and challenges of small animal magnetic resonance imaging as a translational tool. *Neuropsychobiology, 69*(4), 187-201. doi:10.1159/000360859

Hsu, K.-C., Liu, C.-Y., Lin, T. E., Hsieh, J.-H., Sung, T.-Y., Tseng, H.-J., . . . Huang, W.-J. (2017). Novel Class IIa-Selective Histone Deacetylase Inhibitors Discovered Using an in Silico Virtual Screening Approach. *Scientific Reports, 7*(1), 3228. doi:10.1038/s41598-017-03417-1

Hsuan, J., & Cockcroft, S. (2001). The PITP family of phosphatidylinositol transfer proteins. *Genome Biology, 2*(9), reviews3011.3011-reviews3011.3018.

Hudes, G., Carducci, M., Tomczak, P., Dutcher, J., Figlin, R., Kapoor, A., . . . Motzer, R. J. (2007). Temsirolimus, interferon alfa, or both for advanced renal-cell carcinoma. *N Engl J Med, 356*(22), 2271-2281. doi:10.1056/NEJMoa066838

Hui, R. C. Y., Gomes, A. R., Constantinidou, D., Costa, J. R., Karadedou, C. T., Fernandez de Mattos, S., . . . Lam, E. W. F. (2008). The Forkhead Transcription Factor FOXO3a Increases Phosphoinositide-3 Kinase/Akt Activity in Drug-Resistant Leukemic Cells

through Induction of PIK3CA Expression. *Molecular and Cellular Biology, 28*(19), 5886.

Hummel, T. R., Wagner, L., Ahern, C., Fouladi, M., Reid, J. M., McGovern, R. M., . . . Blaney, S. M. (2013). A Pediatric Phase 1 Trial Of Vorinostat And Temozolomide In Relapsed Or Refractory Primary Brain Or Spinal Cord Tumors: A Children's Oncology Group Phase 1 Consortium Study. *Pediatric blood & cancer, 60*(9), 1452-1457. doi:10.1002/pbc.24541

Humphrey, G. W., Wang, Y. H., Hirai, T., Padmanabhan, R., Panchision, D. M., Newell, L. F., . . . Howard, B. H. (2008). Complementary roles for histone deacetylases 1, 2, and 3 in differentiation of pluripotent stem cells. *Differentiation, 76*(4), 348-356. doi:10.1111/j.1432-0436.2007.00232.x

Hussain, A. R., Ahmed, S. O., Ahmed, M., Khan, O. S., Al AbdulMohsen, S., Platanias, L. C., . . . Uddin, S. (2012). Cross-Talk between NFkB and the PI3-Kinase/AKT Pathway Can Be Targeted in Primary Effusion Lymphoma (PEL) Cell Lines for Efficient Apoptosis. *PLoS ONE, 7*(6), e39945. doi:10.1371/journal.pone.0039945

Imperial, R., Toor, O. M., Hussain, A., Subramanian, J., & Masood, A. (2017). Comprehensive pancancer genomic analysis reveals (RTK)-RAS-RAF-MEK as a key dysregulated pathway in cancer: Its clinical implications. *Semin Cancer Biol*. doi:10.1016/j.semcancer.2017.11.016

Inoue, A., Yoshida, N., Omoto, Y., Oguchi, S., Yamori, T., Kiyama, R., & Hayashi, S. (2002). Development of cDNA microarray for expression profiling of estrogen-responsive genes. *J Mol Endocrinol, 29*(2), 175-192.

Isaevska, E., Manasievska, M., Alessi, D., Mosso, M. L., Magnani, C., Sacerdote, C., . . . Maule, M. (2017). Cancer incidence rates and trends among children and

adolescents in Piedmont, 1967–2011. *PLoS ONE, 12*(7), e0181805. doi:10.1371/journal.pone.0181805

Ito, H., Ichiyanagi, O., Naito, S., Bilim, V. N., Tomita, Y., Kato, T., . . . Tsuchiya, N. (2016). GSK-3 directly regulates phospho-4EBP1 in renal cell carcinoma cell-line: an intrinsic subcellular mechanism for resistance to mTORC1 inhibition. *BMC Cancer, 16*, 393. doi:10.1186/s12885-016-2418-7

Jaber, N., & Zong, W. X. (2013). Class III PI3K Vps34: essential roles in autophagy, endocytosis, and heart and liver function. *Ann N Y Acad Sci, 1280*, 48-51. doi:10.1111/nyas.12026

Jackstadt, R., & Hermeking, H. (2015). MicroRNAs as regulators and mediators of c-MYC function. *Biochimica et Biophysica Acta (BBA) - Gene Regulatory Mechanisms, 1849*(5), 544-553. doi:https://doi.org/10.1016/j.bbagrm.2014.04.003

Jakobovits, A., Schwab, M., Bishop, J. M., & Martin, G. R. (1985). Expression of N-myc in teratocarcinoma stem cells and mouse embryos. *Nature, 318*(6042), 188-191.

James, M. J., & Zomerdijk, J. C. (2004). Phosphatidylinositol 3-kinase and mTOR signaling pathways regulate RNA polymerase I transcription in response to IGF-1 and nutrients. *J Biol Chem, 279*(10), 8911-8918. doi:10.1074/jbc.M307735200

Janku, F., Yap, T. A., & Meric-Bernstam, F. (2018). Targeting the PI3K pathway in cancer: are we making headway? *Nat Rev Clin Oncol, 15*(5), 273-291. doi:10.1038/nrclinonc.2018.28

Jean, S., & Kiger, A. A. (2014). Classes of phosphoinositide 3-kinases at a glance. *Journal of Cell Science, 127*(5), 923-928. doi:10.1242/jcs.093773

Jiang, B.-H., Zheng, J. Z., Aoki, M., & Vogt, P. K. (2000). Phosphatidylinositol 3-kinase signaling mediates angiogenesis and expression of vascular endothelial growth

factor in endothelial cells. *Proceedings of the National Academy of Sciences, 97*(4), 1749. doi:10.1073/pnas.040560897

Jin, P., Wong, C. C., Mei, S., He, X., Qian, Y., & Sun, L. (2016). MK-2206 co-treatment with 5-fluorouracil or doxorubicin enhances chemosensitivity and apoptosis in gastric cancer by attenuation of Akt phosphorylation. *OncoTargets and therapy, 9*, 4387-4396. doi:10.2147/OTT.S106303

Jin, Z., Jiang, W., Jiao, F., Guo, Z., Hu, H., Wang, L., & Wang, L. (2014). Decreased expression of histone deacetylase 10 predicts poor prognosis of gastric cancer patients. *Int J Clin Exp Pathol, 7*(9), 5872-5879.

Johnsen, J. I., Segerstrom, L., Orrego, A., Elfman, L., Henriksson, M., Kagedal, B., . . . Kogner, P. (2008). Inhibitors of mammalian target of rapamycin downregulate MYCN protein expression and inhibit neuroblastoma growth in vitro and in vivo. *Oncogene, 27*(20), 2910-2922. doi:10.1038/sj.onc.1210938

Johnstone, R. W. (2002). Histone-deacetylase inhibitors: novel drugs for the treatment of cancer. *Nature Reviews. Drug Discovery, 1*(4), 287-299.

Jokinen, E., & Koivunen, J. P. (2015). MEK and PI3K inhibition in solid tumors: rationale and evidence to date. *Therapeutic Advances in Medical Oncology, 7*(3), 170-180. doi:10.1177/1758834015571111

Jones, D. T., Jäger, N., Kool, M., Zichner, T., Hutter, B., Sultan, M., . . . Lichter, P. (2012). Dissecting the genomic complexity underlying medulloblastoma. *Nature, 488*(7409), 100-105. doi:10.1038/nature11284

Jones, S. F., Bendell, J. C., Infante, J. R., Spigel, D. R., Thompson, D. S., Yardley, D. A., . . . Burris, H. A., 3rd. (2011). A phase I study of panobinostat in combination with gemcitabine in the treatment of solid tumors. *Clin Adv Hematol Oncol, 9*(3), 225-230.

Jung, M., Russell, A. J., Liu, B., George, J., Liu, P. Y., Liu, T., . . . Henderson, M. J. (2017). A Myc Activity Signature Predicts Poor Clinical Outcomes in Myc-Associated Cancers. *Cancer Research, 77*(4), 971-981. doi:10.1158/0008-5472.Can-15-2906

Justice, M. J., & Dhillon, P. (2016). Using the mouse to model human disease: increasing validity and reproducibility. *Disease Models & Mechanisms, 9*(2), 101. doi:10.1242/dmm.024547

Juvekar, A., Hu, H., Yadegarynia, S., Lyssiotis, C. A., Ullas, S., Lien, E. C., . . . Wulf, G. M. (2016). Phosphoinositide 3-kinase inhibitors induce DNA damage through nucleoside depletion. *Proceedings of the National Academy of Sciences, 113*(30), E4338.

Kaiser, F. J., Ansari, M., Braunholz, D., Concepcion Gil-Rodriguez, M., Decroos, C., Wilde, J. J., . . . Deardorff, M. A. (2014). Loss-of-function HDAC8 mutations cause a phenotypic spectrum of Cornelia de Lange syndrome-like features, ocular hypertelorism, large fontanelle and X-linked inheritance. *Hum Mol Genet, 23*(11), 2888-2900. doi:10.1093/hmg/ddu002

Kalkat, M., De Melo, J., Hickman, K. A., Lourenco, C., Redel, C., Resetca, D., . . . Penn, L. Z. (2017). MYC Deregulation in Primary Human Cancers. *Genes, 8*(6), 151. doi:10.3390/genes8060151

Kang, C., & Elledge, S. J. (2016). How autophagy both activates and inhibits cellular senescence. *Autophagy, 12*(5), 898-899. doi:10.1080/15548627.2015.1121361

Kang, J., Rychahou, P. G., Ishola, T. A., Mourot, J. M., Evers, B. M., & Chung, D. H. (2008). N-myc is a novel regulator of PI3K-mediated VEGF expression in neuroblastoma. *Oncogene, 27*(28), 3999-4007. doi:10.1038/onc.2008.15

Kao, G. D., McKenna, W. G., Guenther, M. G., Muschel, R. J., Lazar, M. A., & Yen, T. J. (2003). Histone deacetylase 4 interacts with 53BP1 to mediate the DNA damage

response. *The Journal of Cell Biology, 160*(7), 1017-1027. doi:10.1083/jcb.200209065

Karagianni, P., & Wong, J. (2007). HDAC3: taking the SMRT-N-CoRrect road to repression. *Oncogene, 26*(37), 5439-5449. doi:10.1038/sj.onc.1210612

Karar, J., & Maity, A. (2011). PI3K/AKT/mTOR Pathway in Angiogenesis. *Frontiers in Molecular Neuroscience, 4*, 51. doi:10.3389/fnmol.2011.00051

Karimian, A., Ahmadi, Y., & Yousefi, B. (2016). Multiple functions of p21 in cell cycle, apoptosis and transcriptional regulation after DNA damage. *DNA Repair (Amst), 42*, 63-71. doi:10.1016/j.dnarep.2016.04.008

Karlsson, A. K., & Saleh, S. N. (2017). Checkpoint inhibitors for malignant melanoma: a systematic review and meta-analysis. *Clinical, Cosmetic and Investigational Dermatology, 10*, 325-339. doi:10.2147/CCID.S120877

Kennedy, A. L., Adams, P. D., & Morton, J. P. (2011). Ras, PI3K/Akt and senescence: Paradoxes provide clues for pancreatic cancer therapy. *Small GTPases, 2*(5), 264-267. doi:10.4161/sgtp.2.5.17367

Kiechle, F. L., & Zhang, X. (2002). Apoptosis: biochemical aspects and clinical implications. *Clinica Chimica Acta, 326*(1), 27-45. doi:https://doi.org/10.1016/S0009-8981(02)00297-8

Kim, A. H., Khursigara, G., Sun, X., Franke, T. F., & Chao, M. V. (2001). Akt phosphorylates and negatively regulates apoptosis signal-regulating kinase 1. *Molecular & Cellular Biology, 21*(3), 893-901. doi:10.1128/mcb.21.3.893-901.2001

Kim, H. J., Lee, S., Chun, K. H., Jeon, J. Y., Han, S. J., Kim, D. J., . . . Lee, K. W. (2018). Metformin reduces the risk of cancer in patients with type 2 diabetes: An analysis

based on the Korean National Diabetes Program Cohort. *Medicine, 97*(8), e0036. doi:10.1097/MD.0000000000010036

Kim, M. S., Kwon, H. J., Lee, Y. M., Baek, J. H., Jang, J. E., Lee, S. W., . . . Kim, K. W. (2001). Histone deacetylases induce angiogenesis by negative regulation of tumor suppressor genes. *Nat Med, 7*(4), 437-443. doi:10.1038/86507

Kim, Y. B., Ki, S. W., Yoshida, M., & Horinouchi, S. (2000). Mechanism of cell cycle arrest caused by histone deacetylase inhibitors in human carcinoma cells. *J Antibiot (Tokyo), 53*(10), 1191-1200.

King, D., Yeomanson, D., & Bryant, H. E. (2015). PI3King the lock: targeting the PI3K/Akt/mTOR pathway as a novel therapeutic strategy in neuroblastoma. *J Pediatr Hematol Oncol, 37*(4), 245-251. doi:10.1097/mph.0000000000000329

Klapproth, K., & Wirth, T. (2010). Advances in the understanding of MYC-induced lymphomagenesis. *British Journal of Haematology, 149*(4), 484-497. doi:10.1111/j.1365-2141.2010.08159.x

Kline, N. E., & Sevier, N. (2003). Solid tumors in children. *J Pediatr Nurs, 18*(2), 96-102. doi:10.1053/jpdn.2003.12

Koh, C. M., Sabò, A., & Guccione, E. (2016). Targeting MYC in cancer therapy: RNA processing offers new opportunities. *Bioessays, 38*(3), 266-275. doi:10.1002/bies.201500134

Kohl, N. E., Kanda, N., Schreck, R. R., Bruns, G., Latt, S. A., Gilbert, F., & Alt, F. W. (1983). Transposition and amplification of oncogene-related sequences in human neuroblastomas. *Cell, 35*(2 Pt 1), 359-367.

Kong, G., Hofman, M. S., Murray, W. K., Wilson, S., Wood, P., Downie, P., . . . Hicks, R. J. (2016). Initial Experience With Gallium-68 DOTA-Octreotate PET/CT and Peptide

Receptor Radionuclide Therapy for Pediatric Patients With Refractory Metastatic Neuroblastoma. *J Pediatr Hematol Oncol, 38*(2), 87-96. doi:10.1097/mph.0000000000000411

Konstantinidou, G., Bey, E. A., Rabellino, A., Schuster, K., Maira, M. S., Gazdar, A. F., . . . Scaglioni, P. P. (2009). Dual phosphoinositide 3-kinase/mammalian target of rapamycin blockade is an effective radiosensitizing strategy for the treatment of non-small cell lung cancer harboring K-RAS mutations. *Cancer Research, 69*(19), 7644-7652. doi:10.1158/0008-5472.Can-09-0823

Kostopoulou, O. N., Holzhauser, S., Lange, B. K. A., Ohmayer, A., Andonova, T., Bersani, C., . . . Dalianis, T. (2019). Analyses of FGFR3 and PIK3CA mutations in neuroblastomas and the effects of the corresponding inhibitors on neuroblastoma cell lines. *Int J Oncol, 55*(6), 1372-1384. doi:10.3892/ijo.2019.4896

Kouzarides, T. (1999). Histone acetylases and deacetylases in cell proliferation. *Current Opinion in Genetics & Development, 9*(1), 40-48.

Krepelova, A., Neri, F., Maldotti, M., Rapelli, S., & Oliviero, S. (2014). Myc and Max Genome-Wide Binding Sites Analysis Links the Myc Regulatory Network with the Polycomb and the Core Pluripotency Networks in Mouse Embryonic Stem Cells. *PLoS ONE, 9*(2), e88933. doi:10.1371/journal.pone.0088933

Kumar, R., Dhull, V., Sharma, P., Agarwala, S., Bakhshi, S., Bal, C., . . . Malhotra, A. (2013). Utility of 18F-FDG PET-CT in pediatric neuroblastoma: Comparison with 131I-MIBG scintigraphy. *Journal of Nuclear Medicine, 54*(supplement 2), 199-199.

Kunnimalaiyaan, S., Schwartz, V. K., Jackson, I. A., Clark Gamblin, T., & Kunnimalaiyaan, M. (2018). Antiproliferative and apoptotic effect of LY2090314, a GSK-3 inhibitor, in neuroblastoma in vitro. *BMC Cancer, 18*, 560. doi:10.1186/s12885-018-4474-7

Kwon, Y., Kim, J. W., Jeoung, J. A., Kim, M.-S., & Kang, C. (2017). Autophagy Is Pro-Senescence When Seen in Close-Up, but Anti-Senescence in Long-Shot. *Molecules and Cells, 40*(9), 607-612. doi:10.14348/molcells.2017.0151

Lang, W. H., & Sandoval, J. A. (2014). Detection of PI3K inhibition in human neuroblastoma using multiplex luminex bead immunoassay: a targeted approach for pathway analysis. *J Biomol Screen, 19*(9), 1235-1245. doi:10.1177/1087057114545650

Langenau, D. M., Jette, C., Berghmans, S., Palomero, T., Kanki, J. P., Kutok, J. L., & Look, A. T. (2005). Suppression of apoptosis by bcl-2 overexpression in lymphoid cells of transgenic zebrafish. *Blood, 105*(8), 3278-3285. doi:10.1182/blood-2004-08-3073

Larsen, J. T., Shanafelt, T. D., Leis, J. F., LaPlant, B., Call, T., Pettinger, A., . . . Ding, W. (2017). Akt inhibitor MK-2206 in combination with bendamustine and rituximab in relapsed or refractory chronic lymphocytic leukemia: Results from the N1087 alliance study. *Am J Hematol, 92*(8), 759-763. doi:10.1002/ajh.24762

Lasky, J. L., 3rd, Choe, M., & Nakano, I. (2009). Cancer stem cells in pediatric brain tumors. *Curr Stem Cell Res Ther, 4*(4), 298-305. doi:10.2174/157488809789649278

Laubach, J. P., Moreau, P., San-Miguel, J. F., & Richardson, P. G. (2015). Panobinostat for the Treatment of Multiple Myeloma. *Clin Cancer Res, 21*(21), 4767-4773. doi:10.1158/1078-0432.Ccr-15-0530

Law, C. W., Chen, Y., Shi, W., & Smyth, G. K. (2014). voom: Precision weights unlock linear model analysis tools for RNA-seq read counts. *Genome Biol, 15*(2), R29. doi:10.1186/gb-2014-15-2-r29

Lawlor, M. A., & Alessi, D. R. (2001). PKB/Akt. *Journal of Cell Science, 114*(16), 2903.

Le Rhun, E., Bertrand, N., Dumont, A., Tresch, E., Le Deley, M.-C., Mailliez, A., . . . Bonneterre, J. (2017). Identification of single nucleotide polymorphisms of the PI3K-AKT-mTOR pathway as a risk factor of central nervous system metastasis in metastatic breast cancer. *European Journal of Cancer, 87*, 189-198. doi:https://doi.org/10.1016/j.ejca.2017.10.006

Le Tourneau, C., Faivre, S., Serova, M., & Raymond, E. (2008). mTORC1 inhibitors: is temsirolimus in renal cancer telling us how they really work? *British Journal of Cancer, 99*(8), 1197-1203. doi:10.1038/sj.bjc.6604636

Lee, S., Qiao, J., Paul, P., O'Connor, K. L., Evers, B. M., & Chung, D. H. (2012). FAK is a Critical Regulator of Neuroblastoma Liver Metastasis. *Oncotarget, 3*(12), 1576-1587.

Leibowitz, B., & Yu, J. (2010). Mitochondrial signaling in cell death via the Bcl-2 family. *Cancer Biol Ther, 9*(6), 417-422.

Leon, J., Ferrandiz, N., Acosta, J. C., & Delgado, M. D. (2009). Inhibition of cell differentiation: a critical mechanism for MYC-mediated carcinogenesis? *Cell Cycle, 8*(8), 1148-1157. doi:10.4161/cc.8.8.8126

Leoni, V., & Biondi, A. (2015). Tyrosine kinase inhibitors in BCR-ABL positive acute lymphoblastic leukemia. *Haematologica, 100*(3), 295-299. doi:10.3324/haematol.2015.124016

Leroux, A. E., Schulze, J. O., & Biondi, R. M. (2018). AGC kinases, mechanisms of regulation and innovative drug development. *Semin Cancer Biol, 48*, 1-17. doi:https://doi.org/10.1016/j.semcancer.2017.05.011

Lertkiatmongkol, P., Liao, D., Mei, H., Hu, Y., & Newman, P. J. (2016). Endothelial functions of PECAM-1 (CD31). *Current opinion in hematology, 23*(3), 253-259. doi:10.1097/MOH.0000000000000239

Levens, D. (2008). How the c-myc Promoter Works and Why It Sometimes Does Not. *Journal of the National Cancer Institute. Monographs*(39), 41-43. doi:10.1093/jncimonographs/lgn004

Li, J., Dang, Y., Gao, J., Li, Y., Zou, J., & Shen, L. (2015). PI3K/AKT/mTOR pathway is activated after imatinib secondary resistance in gastrointestinal stromal tumors (GISTs). *Med Oncol, 32*(4), 111. doi:10.1007/s12032-015-0554-6

Li, J., & Kurokawa, M. (2015). Regulation of MDM2 Stability After DNA Damage. *J Cell Physiol, 230*(10), 2318-2327. doi:10.1002/jcp.24994

Li, P., Zhou, L., Zhao, T., Liu, X., Zhang, P., Liu, Y., . . . Li, Q. (2017). Caspase-9: structure, mechanisms and clinical application. *Oncotarget, 8*(14), 23996-24008. doi:10.18632/oncotarget.15098

Li, Q., Wu, Y., Fang, S., Wang, L., Qi, H., Zhang, Y., . . . Li, W. (2015). BCR/ABL oncogene-induced PI3K signaling pathway leads to chronic myeloid leukemia pathogenesis by impairing immuno-modulatory function of hemangioblasts. *Cancer Gene Ther, 22*(5), 227-237. doi:10.1038/cgt.2014.65

Li, X., Ashana, A. O., Moretti, V. M., & Lackman, R. D. (2011). The relation of tumour necrosis and survival in patients with osteosarcoma. *International Orthopaedics, 35*(12), 1847-1853. doi:10.1007/s00264-011-1209-7

Li, X., Dai, D., Chen, B., Tang, H., Xie, X., & Wei, W. (2018). Efficacy of PI3K/AKT/mTOR pathway inhibitors for the treatment of advanced solid cancers: A literature-based meta-analysis of 46 randomised control trials. *PLoS ONE, 13*(2), e0192464. doi:10.1371/journal.pone.0192464

Li, Y., Fu, S., Chen, H., Feng, Q., Gao, Y., Xue, H., . . . Xiao, S. (2014). Inhibition of endothelial Slit2/Robo1 signaling by thalidomide restrains angiogenesis by blocking

the PI3K/Akt pathway. *Dig Dis Sci, 59*(12), 2958-2966. doi:10.1007/s10620-014-3257-5

Li, Y., Shin, D., & Kwon, S. H. (2013). Histone deacetylase 6 plays a role as a distinct regulator of diverse cellular processes. *Febs j, 280*(3), 775-793. doi:10.1111/febs.12079

Li, Y., Zhang, P., Qiu, F., Chen, L., Miao, C., Li, J., . . . Ma, E. (2012). Inactivation of PI3K/Akt signaling mediates proliferation inhibition and G2/M phase arrest induced by andrographolide in human glioblastoma cells. *Life Sciences, 90*(25), 962-967. doi:https://doi.org/10.1016/j.lfs.2012.04.044

Liegl, R., Koenig, S., Siedlecki, J., Haritoglou, C., Kampik, A., & Kernt, M. (2014). *Temsirolimus Inhibits Proliferation and Migration in Retinal Pigment Epithelial and Endothelial Cells via mTOR Inhibition and Decreases VEGF and PDGF Expression* (Vol. 9).

Lin, C.-J., Malina, A., & Pelletier, J. (2009). c-Myc and eIF4F Constitute a Feedforward Loop That Regulates Cell Growth: Implications for Anticancer Therapy. *Cancer Research, 69*(19), 7491.

Linseman, D. A., Butts, B. D., Precht, T. A., Phelps, R. A., Le, S. S., Laessig, T. A., . . . Heidenreich, K. A. (2004). Glycogen synthase kinase-3beta phosphorylates Bax and promotes its mitochondrial localization during neuronal apoptosis. *J Neurosci, 24*(44), 9993-10002. doi:10.1523/jneurosci.2057-04.2004

Liu, G., Honisch, S., Liu, G., Schmidt, S., Pantelakos, S., Alkahtani, S., . . . Stournaras, C. (2015). Inhibition of SGK1 enhances mAR-induced apoptosis in MCF-7 breast cancer cells. *Cancer Biol Ther, 16*(1), 52-59. doi:10.4161/15384047.2014.986982

Liu, J., Livingston, M. J., Dong, G., Tang, C., Su, Y., Wu, G., . . . Dong, Z. (2018). Histone deacetylase inhibitors protect against cisplatin-induced acute kidney injury by

activating autophagy in proximal tubular cells. *Cell Death & Disease, 9*(3), 322. doi:10.1038/s41419-018-0374-7

Liu, Q., Turner, K. M., Alfred Yung, W. K., Chen, K., & Zhang, W. (2014). Role of AKT signaling in DNA repair and clinical response to cancer therapy. *Neuro-Oncology, 16*(10), 1313-1323. doi:10.1093/neuonc/nou058

Liu, R., Li, X., Gao, W., Zhou, Y., Wey, S., Mitra, S. K., . . . Gill, P. S. (2013). Monoclonal antibody against cell surface GRP78 as a novel agent in suppressing PI3K/AKT signaling, tumor growth, and metastasis. *Clin Cancer Res, 19*(24), 6802-6811. doi:10.1158/1078-0432.Ccr-13-1106

Liu, T., Liu, P. Y., & Marshall, G. M. (2009). The critical role of the class III histone deacetylase SIRT1 in cancer. *Cancer Research, 69*(5), 1702-1705. doi:https://dx.doi.org/10.1158/0008-5472.CAN-08-3365

Liu, X., & Cohen, J. I. (2015). The Role of PI3K/Akt in Human Herpesvirus Infection: from the Bench to the Bedside. *Virology, 0*, 568-577. doi:10.1016/j.virol.2015.02.040

Liu, Y., Pandeswara, S., Dao, V., Padron, A., Drerup, J. M., Lao, S., . . . Curiel, T. J. (2017). Biphasic Rapamycin Effects in Lymphoma and Carcinoma Treatment. *Cancer Research, 77*(2), 520-531. doi:10.1158/0008-5472.Can-16-1140

Loh, A. H. P., Brennan, R. C., Lang, W. H., Hickey, R. J., Malkas, L. H., & Sandoval, J. A. (2013). Dissecting the PI3K Signaling Axis in Pediatric Solid Tumors: Novel Targets for Clinical Integration. *Front Oncol, 3*, 93. doi:10.3389/fonc.2013.00093

Lonergan, G. J., Schwab, C. M., Suarez, E. S., & Carlson, C. L. (2002). Neuroblastoma, ganglioneuroblastoma, and ganglioneuroma: radiologic-pathologic correlation. *Radiographics, 22*(4), 911-934. doi:10.1148/radiographics.22.4.g02jl15911

Lopez-Carballo, G., Moreno, L., Masia, S., Perez, P., & Barettino, D. (2002). Activation of the phosphatidylinositol 3-kinase/Akt signaling pathway by retinoic acid is required for neural differentiation of SH-SY5Y human neuroblastoma cells. *J Biol Chem, 277*(28), 25297-25304. doi:10.1074/jbc.M201869200

Lu, H., Xue, Y., Yu, G. K., Arias, C., Lin, J., Fong, S., . . . Zhou, Q. (2015). Compensatory induction of MYC expression by sustained CDK9 inhibition via a BRD4-dependent mechanism. *eLife, 4*, e06535. doi:10.7554/eLife.06535

Lu, Z., Boyapati, A., Kirschmeier, P., & Windsor, W. (2008). Pdk1 regulation of proliferation and survival in mapk pathway activated cancer cell lines. *Cancer Research, 68*(9 Supplement), 2735.

Luo, J., Nikolaev, A. Y., Imai, S., Chen, D., Su, F., Shiloh, A., . . . Gu, W. (2001). Negative control of p53 by Sir2alpha promotes cell survival under stress. *Cell, 107*(2), 137-148.

MacKeigan, J. P., & Krueger, D. A. (2015). Differentiating the mTOR inhibitors everolimus and sirolimus in the treatment of tuberous sclerosis complex. *Neuro-Oncology, 17*(12), 1550-1559. doi:10.1093/neuonc/nov152

Macy, M. E., Sawczyn, K. K., Garrington, T. P., Graham, D. K., & Gore, L. (2008). Novel Therapies for Pediatric Cancers. *Curr Oncol Rep, 10*(6), 477-490.

Madsen, R. R., Vanhaesebroeck, B., & Semple, R. K. (2018). Cancer-Associated PIK3CA Mutations in Overgrowth Disorders. *Trends in Molecular Medicine, 24*(10), 856-870. doi:10.1016/j.molmed.2018.08.003

Magnuson, B., Ekim, B., & Fingar, D. C. (2012). Regulation and function of ribosomal protein S6 kinase (S6K) within mTOR signalling networks. *Biochem J, 441*(1), 1-21. doi:10.1042/bj20110892

Maira, S. M., Stauffer, F., Brueggen, J., Furet, P., Schnell, C., Fritsch, C., . . . Garcia-Echeverria, C. (2008). Identification and characterization of NVP-BEZ235, a new orally available dual phosphatidylinositol 3-kinase/mammalian target of rapamycin inhibitor with potent in vivo antitumor activity. *Mol Cancer Ther, 7*(7), 1851-1863. doi:10.1158/1535-7163.Mct-08-0017

Malek, M., Kielkowska, A., Chessa, T., Anderson, K. E., Barneda, D., Pir, P., . . . Stephens, L. R. (2017). PTEN Regulates PI(3,4)P2 Signaling Downstream of Class I PI3K. *Mol Cell, 68*(3), 566-580.e510. doi:10.1016/j.molcel.2017.09.024

Mandoli, A., Singh, A. A., Jansen, P. W., Wierenga, A. T., Riahi, H., Franci, G., . . . Martens, J. H. (2014). CBFB-MYH11/RUNX1 together with a compendium of hematopoietic regulators, chromatin modifiers and basal transcription factors occupies self-renewal genes in inv(16) acute myeloid leukemia. *Leukemia, 28*(4), 770-778. doi:10.1038/leu.2013.257

Mannick, J. B., Morris, M., Hockey, H.-U. P., Roma, G., Beibel, M., Kulmatycki, K., . . . Klickstein, L. B. (2018). TORC1 inhibition enhances immune function and reduces infections in the elderly. *Sci Transl Med, 10*(449).

Manning, B. D., & Toker, A. (2017). AKT/PKB Signaling: Navigating the Network. *Cell, 169*(3), 381-405. doi:https://doi.org/10.1016/j.cell.2017.04.001

Maréchal, A., & Zou, L. (2013). DNA Damage Sensing by the ATM and ATR Kinases. *Cold Spring Harbor Perspectives in Biology, 5*(9), a012716. doi:10.1101/cshperspect.a012716

Maris, J. M. (2010). Recent Advances in Neuroblastoma. *New England Journal of Medicine, 362*(23), 2202-2211. doi:10.1056/NEJMra0804577

Maris, J. M., Hogarty, M. D., Bagatell, R., & Cohn, S. L. (2007). Neuroblastoma. *Lancet, 369*(9579), 2106-2120. doi:10.1016/s0140-6736(07)60983-0

Markaki, E. A., Stiakaki, E., Zafiropoulos, A., Arvanitis, D. A., Katzilakis, N., Dimitriou, H., . . . Kalmanti, M. (2006). Mutational analysis of the cell cycle inhibitor Kip1/p27 in childhood leukemia. *Pediatric blood & cancer, 47*(1), 14-21. doi:10.1002/pbc.20730

Marks, P., Rifkind, R. A., Richon, V. M., Breslow, R., Miller, T., & Kelly, W. K. (2001). Histone deacetylases and cancer: causes and therapies. *Nat Rev Cancer, 1*(3), 194-202. doi:10.1038/35106079

Marks, P. A., Richon, V. M., & Rifkind, R. A. (2000). Histone deacetylase inhibitors: inducers of differentiation or apoptosis of transformed cells. *Journal of the National Cancer Institute, 92*(15), 1210-1216.

Marks, P. A., & Xu, W. S. (2009). Histone deacetylase inhibitors: Potential in cancer therapy. *Journal of Cellular Biochemistry, 107*(4), 600-608. doi:https://dx.doi.org/10.1002/jcb.22185

Marquard, L., Petersen, K. D., Persson, M., Hoff, K. D., Jensen, P. B., & Sehested, M. (2008). Monitoring the effect of belinostat in solid tumors by H4 acetylation. *Apmis, 116*(5), 382-392. doi:10.1111/j.1600-0463.2008.00957.x

Marrano, P., Irwin, M. S., & Thorner, P. S. (2017). Heterogeneity of MYCN amplification in neuroblastoma at diagnosis, treatment, relapse, and metastasis. *Genes Chromosomes Cancer, 56*(1), 28-41. doi:10.1002/gcc.22398

Martin, G., Grant, A., & D'Agostino, M. (2012). Global health funding and economic development. *Globalization and Health, 8*, 8-8. doi:10.1186/1744-8603-8-8

Maruiwa, M., Nakamura, Y., Motomura, K., Murakami, T., Kojiro, M., Kato, M., . . . Hashimoto, T. (1988). Cornelia de Lange syndrome associated with Wilms' tumour and infantile haemangioendothelioma of the liver: report of two autopsy cases. *Virchows Archiv A, 413*(5), 463-468. doi:10.1007/bf00716995

Mateo, J., Olmos, D., Dumez, H., Poondru, S., Samberg, N. L., Barr, S., . . . Schöffski, P. (2016). A first in man, dose-finding study of the mTORC1/mTORC2 inhibitor OSI-027 in patients with advanced solid malignancies. *British Journal of Cancer, 114*, 889. doi:10.1038/bjc.2016.59
https://www.nature.com/articles/bjc201659#supplementary-information

Matsumura, I., Mizuki, M., & Kanakura, Y. (2008). Roles for deregulated receptor tyrosine kinases and their downstream signaling molecules in hematologic malignancies. *Cancer Sci, 99*(3), 479-485. doi:10.1111/j.1349-7006.2007.00717.x

Matthay, K. K., Maris, J. M., Schleiermacher, G., Nakagawara, A., Mackall, C. L., Diller, L., & Weiss, W. A. (2016). Neuroblastoma. *Nature Reviews Disease Primers, 2*, 16078. doi:10.1038/nrdp.2016.78

Matthay, K. K., Villablanca, J. G., Seeger, R. C., Stram, D. O., Harris, R. E., Ramsay, N. K., . . . Reynolds, C. P. (1999). Treatment of high-risk neuroblastoma with intensive chemotherapy, radiotherapy, autologous bone marrow transplantation, and 13-cis-retinoic acid. Children's Cancer Group. *N Engl J Med, 341*(16), 1165-1173. doi:10.1056/nejm199910143411601

Maurer, U., Preiss, F., Brauns-Schubert, P., Schlicher, L., & Charvet, C. (2014). GSK-3 – at the crossroads of cell death and survival. *Journal of Cell Science, 127*(7), 1369.

McClellan, K. A., Avard, D., Simard, J., & Knoppers, B. M. (2013). Personalized medicine and access to health care: potential for inequitable access? *European Journal of Human Genetics, 21*(2), 143-147. doi:10.1038/ejhg.2012.149

McKinnon, P. J. (2004). ATM and ataxia telangiectasia. *EMBO Reports, 5*(8), 772-776. doi:10.1038/sj.embor.7400210

Megison, M. L., Gillory, L. A., & Beierle, E. A. (2013). Cell Survival Signaling in Neuroblastoma. *Anti-cancer agents in medicinal chemistry, 13*(4), 563-575.

Megison, M. L., Stewart, J. E., Nabers, H. C., Gillory, L. A., & Beierle, E. A. (2013). FAK inhibition decreases cell invasion, migration and metastasis in MYCN amplified neuroblastoma. *Clin Exp Metastasis, 30*(5), 555-568. doi:10.1007/s10585-012-9560-7

Mei, H., Wang, Y., Lin, Z., & Tong, Q. (2013). The mTOR signaling pathway in pediatric neuroblastoma. *Pediatr Hematol Oncol, 30*(7), 605-615. doi:10.3109/08880018.2013.798058

Meric-Bernstam, F., & Gonzalez-Angulo, A. M. (2009). Targeting the mTOR signaling network for cancer therapy. *J Clin Oncol, 27*(13), 2278-2287. doi:10.1200/jco.2008.20.0766

Michlewski, G., & Cáceres, J. F. (2019). Post-transcriptional control of miRNA biogenesis. *Rna, 25*(1), 1-16. doi:10.1261/rna.068692.118

Milde, T., Oehme, I., Korshunov, A., Kopp-Schneider, A., Remke, M., Northcott, P., . . . Witt, O. (2010). HDAC5 and HDAC9 in medulloblastoma: novel markers for risk stratification and role in tumor cell growth. *Clin Cancer Res, 16*(12), 3240-3252. doi:10.1158/1078-0432.Ccr-10-0395

Miller, K. M., Tjeertes, J. V., Coates, J., Legube, G., Polo, S. E., Britton, S., & Jackson, S. P. (2010). Human HDAC1 and HDAC2 function in the DNA-damage response to promote DNA nonhomologous end-joining. *Nat Struct Mol Biol, 17*(9), 1144-1151. doi:10.1038/nsmb.1899

Mingeot-Leclercq, M.-P., Glupczynski, Y., & Tulkens, P. M. (1999). Aminoglycosides: Activity and Resistance. *Antimicrobial Agents and Chemotherapy, 43*(4), 727-737.

Miyazaki, T., Kato, H., Nakajima, M., Sohda, M., Fukai, Y., Masuda, N., . . . Kuwano, H. (2003). FAK overexpression is correlated with tumour invasiveness and lymph node

metastasis in oesophageal squamous cell carcinoma. *British Journal of Cancer, 89*, 140. doi:10.1038/sj.bjc.6601050

Mizuno, T., Fukuda, T., Christians, U., Perentesis, J. P., Fouladi, M., & Vinks, A. A. (2017). Population pharmacokinetics of temsirolimus and sirolimus in children with recurrent solid tumours: a report from the Children's Oncology Group. *Br J Clin Pharmacol, 83*(5), 1097-1107. doi:10.1111/bcp.13181

Mlakar, V., Jurkovic Mlakar, S., Lopez, G., Maris, J. M., Ansari, M., & Gumy-Pause, F. (2017). 11q deletion in neuroblastoma: a review of biological and clinical implications. *Molecular Cancer, 16*, 114. doi:10.1186/s12943-017-0686-8

Mody, R., Naranjo, A., Van Ryn, C., Yu, A. L., London, W. B., Shulkin, B. L., . . . Bagatell, R. (2017). Irinotecan-temozolomide with temsirolimus or dinutuximab in children with refractory or relapsed neuroblastoma (COG ANBL1221): an open-label, randomised, phase 2 trial. *Lancet Oncol, 18*(7), 946-957. doi:10.1016/s1470-2045(17)30355-8

Molenaar, J. J., Koster, J., Zwijnenburg, D. A., van Sluis, P., Valentijn, L. J., van der Ploeg, I., . . . Versteeg, R. (2012). Sequencing of neuroblastoma identifies chromothripsis and defects in neuritogenesis genes. *Nature, 483*(7391), 589-593. doi:10.1038/nature10910

Monclair, T., Brodeur, G. M., Ambros, P. F., Brisse, H. J., Cecchetto, G., Holmes, K., . . . Pearson, A. D. J. (2009). The International Neuroblastoma Risk Group (INRG) Staging System: An INRG Task Force Report. *Journal of Clinical Oncology, 27*(2), 298-303. doi:10.1200/JCO.2008.16.6876

Montgomery, R. L., Davis, C. A., Potthoff, M. J., Haberland, M., Fielitz, J., Qi, X., . . . Olson, E. N. (2007). Histone deacetylases 1 and 2 redundantly regulate cardiac morphogenesis, growth, and contractility. *Genes & Development, 21*(14), 1790-1802.

Moore, H. C., Wood, K. M., Jackson, M. S., Lastowska, M. A., Hall, D., Imrie, H., . . . Tweddle, D. A. (2008). Histological profile of tumours from MYCN transgenic mice. *J Clin Pathol, 61*(10), 1098-1103. doi:10.1136/jcp.2007.054627

Moore, N. F., Azarova, A. M., Bhatnagar, N., Ross, K. N., Drake, L. E., Frumm, S., . . . George, R. E. (2014). Molecular rationale for the use of PI3K/AKT/mTOR pathway inhibitors in combination with crizotinib in ALK-mutated neuroblastoma. *Oncotarget, 5*(18), 8737-8749. doi:10.18632/oncotarget.2372

Moreno, L., Rubie, H., Varo, A., Le Deley, M. C., Amoroso, L., Chevance, A., . . . Pearson, A. D. (2017). Outcome of children with relapsed or refractory neuroblastoma: A meta-analysis of ITCC/SIOPEN European phase II clinical trials. *Pediatr Blood Cancer, 64*(1), 25-31. doi:10.1002/pbc.26192

Moriya, M., Yamada, T., Tamura, M., Ishikawa, D., Hoda, M. A., Matsumoto, I., . . . Watanabe, G. (2014). Antitumor effect and antiangiogenic potential of the mTOR inhibitor temsirolimus against malignant pleural mesothelioma. *Oncol Rep, 31*(3), 1109-1115. doi:10.3892/or.2013.2948

Morris, M. J., & Monteggia, L. M. (2013). Unique functional roles for class I and class II histone deacetylases in central nervous system development and function. *International journal of developmental neuroscience : the official journal of the International Society for Developmental Neuroscience, 31*(6), 370-381. doi:10.1016/j.ijdevneu.2013.02.005

Moskowitz, A. J., & Horwitz, S. M. (2017). Targeting histone deacetylases in T-cell lymphoma. *Leuk Lymphoma, 58*(6), 1306-1319. doi:10.1080/10428194.2016.1247956

Mosse, Y. P., Laudenslager, M., Khazi, D., Carlisle, A. J., Winter, C. L., Rappaport, E., & Maris, J. M. (2004). Germline PHOX2B Mutation in Hereditary Neuroblastoma. *American Journal of Human Genetics, 75*(4), 727-730.

Mossë, Y. P., Laudenslager, M., Longo, L., Cole, K. A., Wood, A., Attiyeh, E. F., . . . Maris, J. M. (2008). Identification of ALK as the Major Familial Neuroblastoma Predisposition Gene. *Nature, 455*(7215), 930-935. doi:10.1038/nature07261

Mrakovcic, M., Kleinheinz, J., & Fröhlich, L. F. (2017). Histone Deacetylase Inhibitor-Induced Autophagy in Tumor Cells: Implications for p53. *Int J Mol Sci, 18*(9), 1883. doi:10.3390/ijms18091883

Mukherjee, B., Morgenbesser, S. D., & DePinho, R. A. (1992). Myc family oncoproteins function through a common pathway to transform normal cells in culture: cross-interference by Max and trans-acting dominant mutants. *Genes & Development, 6*(8), 1480-1492.

Mukohara, T. (2015). PI3K mutations in breast cancer: prognostic and therapeutic implications. *Breast Cancer : Targets and Therapy, 7*, 111-123. doi:10.2147/BCTT.S60696

Muppidi, J., Porter, M., & Siegel, R. M. (2004). Measurement of apoptosis and other forms of cell death. *Curr Protoc Immunol, Chapter 3*, Unit 3.17. doi:10.1002/0471142735.im0317s59

Murillo, M. M., Zelenay, S., Nye, E., Castellano, E., Lassailly, F., Stamp, G., & Downward, J. (2014). RAS interaction with PI3K p110α is required for tumor-induced angiogenesis. *The Journal of Clinical Investigation, 124*(8), 3601-3611. doi:10.1172/JCI74134

Murphy, M. F., Bithell, J. F., Stiller, C. A., Kendall, G. M., & O'Neill, K. A. (2013). Childhood and adult cancers: contrasts and commonalities. *Maturitas, 76*(1), 95-98. doi:10.1016/j.maturitas.2013.05.017

Muscat, A., Popovski, D., Jayasekara, W. S., Rossello, F. J., Ferguson, M., Marini, K. D., . . . Ashley, D. M. (2016). Low-Dose Histone Deacetylase Inhibitor Treatment Leads to Tumor Growth Arrest and Multi-Lineage Differentiation of Malignant Rhabdoid Tumors. *Clinical Cancer Research, 22*(14), 3560-3570.

Mutlu, M., Saatci, Ö., Ansari, S. A., Yurdusev, E., Shehwana, H., Konu, Ö., . . . Şahin, Ö. (2016). miR-564 acts as a dual inhibitor of PI3K and MAPK signaling networks and inhibits proliferation and invasion in breast cancer. *Scientific Reports, 6*, 32541. doi:10.1038/srep32541 https://www.nature.com/articles/srep32541#supplementary-information

Nag, S., Qin, J., Srivenugopal, K. S., Wang, M., & Zhang, R. (2013). The MDM2-p53 pathway revisited. *Journal of Biomedical Research, 27*(4), 254-271. doi:10.7555/JBR.27.20130030

Najafov, A., Shpiro, N., & Alessi, D. R. (2012). Akt is efficiently activated by PIF-pocket- and PtdIns(3,4,5)P3-dependent mechanisms leading to resistance to PDK1 inhibitors. *Biochem J, 448*(2), 285-295. doi:10.1042/bj20121287

Naughton, R., Quiney, C., Turner, S. D., & Cotter, T. G. (2009). Bcr-Abl-mediated redox regulation of the PI3K/AKT pathway. *Leukemia, 23*, 1432. doi:10.1038/leu.2009.49 https://www.nature.com/articles/leu200949#supplementary-information

Navid, F., Santana, V. M., & Barfield, R. C. (2010). Anti-GD2 Antibody Therapy for GD2-expressing Tumors. *Current cancer drug targets, 10*(2), 200-209.

Navrátilová, J., Karasová, M., Kohutková Lánová, M., Jiráková, L., Budková, Z., Pacherník, J., . . . Beneš, P. (2017). Selective elimination of neuroblastoma cells by

synergistic effect of Akt kinase inhibitor and tetrathiomolybdate. *Journal of Cellular and Molecular Medicine, 21*(9), 1859-1869. doi:10.1111/jcmm.13106

Netland, I. A., Førde, H. E., Sleire, L., Leiss, L., Rahman, M. A., Skeie, B. S., . . . Goplen, D. (2016). Treatment with the PI3K inhibitor buparlisib (NVP-BKM120) suppresses the growth of established patient-derived GBM xenografts and prolongs survival in nude rats. *Journal of Neuro-Oncology, 129*, 57-66. doi:10.1007/s11060-016-2158-1

New, M., Olzscha, H., & La Thangue, N. B. (2012). HDAC inhibitor-based therapies: can we interpret the code? *Molecular Oncology, 6*(6), 637-656. doi:https://dx.doi.org/10.1016/j.molonc.2012.09.003

Nijmeijer, S., Leurs, R., Smit, M. J., & Vischer, H. F. (2010). The Epstein-Barr Virus-encoded G Protein-coupled Receptor BILF1 Hetero-oligomerizes with Human CXCR4, Scavenges Gα(i) Proteins, and Constitutively Impairs CXCR4 Functioning. *J Biol Chem, 285*(38), 29632-29641. doi:10.1074/jbc.M110.115618

Nishioka, C., Ikezoe, T., Yang, J., Gery, S., Koeffler, H. P., & Yokoyama, A. (2009). Inhibition of mammalian target of rapamycin signaling potentiates the effects of all-trans retinoic acid to induce growth arrest and differentiation of human acute myelogenous leukemia cells. *Int J Cancer, 125*(7), 1710-1720. doi:10.1002/ijc.24472

Nitulescu, G. M., Margina, D., Juzenas, P., Peng, Q., Olaru, O. T., Saloustros, E., . . . Tsatsakis, A. M. (2016). Akt inhibitors in cancer treatment: The long journey from drug discovery to clinical use (Review). *International Journal of Oncology, 48*(3), 869-885. doi:10.3892/ijo.2015.3306

Noguchi, K., Kitanaka, C., Yamana, H., Kokubu, A., Mochizuki, T., & Kuchino, Y. (1999). Regulation of c-Myc through Phosphorylation at Ser-62 and Ser-71 by c-Jun N-Terminal Kinase. *Journal of Biological Chemistry, 274*(46), 32580-32587. doi:10.1074/jbc.274.46.32580

Nolan, J. C., Frawley, T., Tighe, J., Soh, H., Curtin, C., & Piskareva, O. (2020). Preclinical models for neuroblastoma: Advances and challenges. *Cancer Letters, 474*, 53-62. doi:https://doi.org/10.1016/j.canlet.2020.01.015

Northcott, P. A., Dubuc, A. M., Pfister, S., & Taylor, M. D. (2012). Molecular subgroups of medulloblastoma. *Expert review of neurotherapeutics, 12*(7), 871-884. doi:10.1586/ern.12.66

Novac, O., Guenier, A. S., & Pelletier, J. (2004). Inhibitors of protein synthesis identified by a high throughput multiplexed translation screen. *Nucleic Acids Research, 32*(3), 902-915. doi:10.1093/nar/gkh235

Nugent, A., & Proia, R. L. (2017). The role of G protein-coupled receptors in lymphoid malignancies. *Cellular Signalling, 39*, 95-107. doi:https://doi.org/10.1016/j.cellsig.2017.08.002

O'Connor, M. J. (2015). Targeting the DNA Damage Response in Cancer. *Mol Cell, 60*(4), 547-560. doi:10.1016/j.molcel.2015.10.040

Obaya, A. J., Kotenko, I., Cole, M. D., & Sedivy, J. M. (2002). The Proto-oncogene c-myc Acts through the Cyclin-dependent Kinase (Cdk) Inhibitor p27Kip1to Facilitate the Activation of Cdk4/6 and Early G1Phase Progression. *Journal of Biological Chemistry, 277*(34), 31263-31269. doi:10.1074/jbc.M202528200

Oehme, I., Deubzer, H. E., Wegener, D., Pickert, D., Linke, J. P., Hero, B., . . . Witt, O. (2009). Histone deacetylase 8 in neuroblastoma tumorigenesis. *Clin Cancer Res, 15*(1), 91-99. doi:10.1158/1078-0432.Ccr-08-0684

Oehme, I., Linke, J. P., Bock, B. C., Milde, T., Lodrini, M., Hartenstein, B., . . . Witt, O. (2013). Histone deacetylase 10 promotes autophagy-mediated cell survival. *Proc Natl Acad Sci U S A, 110*(28), E2592-2601. doi:10.1073/pnas.1300113110

Ogawara, Y., Kishishita, S., Obata, T., Isazawa, Y., Suzuki, T., Tanaka, K., . . . Gotoh, Y. (2002). Akt Enhances Mdm2-mediated Ubiquitination and Degradation of p53. *Journal of Biological Chemistry, 277*(24), 21843-21850. doi:10.1074/jbc.M109745200

Oh, W. J., & Jacinto, E. (2011). mTOR complex 2 signaling and functions. *Cell Cycle, 10*(14), 2305-2316. doi:10.4161/cc.10.14.16586

Olsen, R. R., Otero, J. H., Garcia-Lopez, J., Wallace, K., Finkelstein, D., Rehg, J. E., . . . Freeman, K. W. (2017). MYCN induces neuroblastoma in primary neural crest cells. *Oncogene, 36*(35), 5075-5082. doi:10.1038/onc.2017.128

Olson, D. E., Udeshi, N. D., Wolfson, N. A., Pitcairn, C. A., Sullivan, E. D., Jaffe, J. D., . . . Holson, E. B. (2014). An Unbiased Approach To Identify Endogenous Substrates of "Histone" Deacetylase 8. *ACS Chemical Biology, 9*(10), 2210-2216. doi:10.1021/cb500492r

Onarheim, K. H., Iversen, J. H., & Bloom, D. E. (2016). Economic Benefits of Investing in Women's Health: A Systematic Review. *PLoS ONE, 11*(3), e0150120. doi:10.1371/journal.pone.0150120

Opel, D., Poremba, C., Simon, T., Debatin, K. M., & Fulda, S. (2007). Activation of Akt predicts poor outcome in neuroblastoma. *Cancer Research, 67*(2), 735-745. doi:10.1158/0008-5472.Can-06-2201

Orlacchio, A., Ranieri, M., Brave, M., Arciuch, V. A., Forde, T., De Martino, D., . . . Di Cristofano, A. (2017). SGK1 Is a Critical Component of an AKT-Independent Pathway Essential for PI3K-Mediated Tumor Development and Maintenance. *Cancer Research, 77*(24), 6914-6926. doi:10.1158/0008-5472.Can-17-2105

Ornell, K. J., & Coburn, J. M. (2019). Developing preclinical models of neuroblastoma: driving therapeutic testing. *BMC Biomedical Engineering, 1*(1), 33. doi:10.1186/s42490-019-0034-8

Osada, H., Tatematsu, Y., Saito, H., Yatabe, Y., Mitsudomi, T., & Takahashi, T. (2004). Reduced expression of class II histone deacetylase genes is associated with poor prognosis in lung cancer patients. *Int J Cancer, 112*(1), 26-32. doi:10.1002/ijc.20395

Oshiro, N., Yoshino, K., Hidayat, S., Tokunaga, C., Hara, K., Eguchi, S., . . . Yonezawa, K. (2004). Dissociation of raptor from mTOR is a mechanism of rapamycin-induced inhibition of mTOR function. *Genes Cells, 9*(4), 359-366. doi:10.1111/j.1356-9597.2004.00727.x

Ottmann, O. G., & Pfeifer, H. (2009). Management of Philadelphia chromosome-positive acute lymphoblastic leukemia (Ph+ ALL). *Hematology Am Soc Hematol Educ Program*, 371-381. doi:10.1182/asheducation-2009.1.371

Otto, T., Horn, S., Brockmann, M., Eilers, U., Schuttrumpf, L., Popov, N., . . . Eilers, M. (2009). Stabilization of N-Myc is a critical function of Aurora A in human neuroblastoma. *Cancer cell, 15*(1), 67-78. doi:10.1016/j.ccr.2008.12.005

Park, J. H., Jung, K. H., Kim, S. J., Fang, Z., Yan, H. H., Son, M. K., . . . Hong, S.-S. (2017). Radiosensitization of the PI3K inhibitor HS-173 through reduction of DNA damage repair in pancreatic cancer. *Oncotarget, 8*(68), 112893-112906. doi:10.18632/oncotarget.22850

Park, J. H., Kim, S. H., Choi, M. C., Lee, J., Oh, D. Y., Im, S. A., . . . Kim, T. Y. (2008). Class II histone deacetylases play pivotal roles in heat shock protein 90-mediated proteasomal degradation of vascular endothelial growth factor receptors. *Biochem Biophys Res Commun, 368*(2), 318-322. doi:10.1016/j.bbrc.2008.01.056

Park, J. R., Bagatell, R., Cohn, S. L., Pearson, A. D., Villablanca, J. G., Berthold, F., . . . Valteau-Couanet, D. (2017). Revisions to the International Neuroblastoma Response Criteria: A Consensus Statement From the National Cancer Institute Clinical Trials Planning Meeting. *J Clin Oncol, 35*(22), 2580-2587. doi:10.1200/jco.2016.72.0177

Park, J. R., Villablanca, J. G., London, W. B., Gerbing, R. B., Haas-Kogan, D., Stanton Adkins, E., . . . Matthay, K. K. (2009). Outcome of High-Risk Stage 3 Neuroblastoma with Myeloablative Therapy and 13-cis-Retinoic Acid: A Report from the Children's Oncology Group. *Pediatric blood & cancer, 52*(1), 44-50. doi:10.1002/pbc.21784

Parmar, R., Wadia, F., Yassa, R., & Zenios, M. (2013). Neuroblastoma: a rare cause of a limping child. How to avoid a delayed diagnosis? *J Pediatr Orthop, 33*(4), e45-51. doi:10.1097/BPO.0b013e318279c636

Pesola, F., Ferlay, J., & Sasieni, P. (2017). Cancer incidence in English children, adolescents and young people: past trends and projections to 2030. *British Journal of Cancer, 117*(12), 1865-1873. doi:10.1038/bjc.2017.341

Pession, A., Tonelli, R., Fronza, R., Sciamanna, E., Corradini, R., Sforza, S., . . . Paolucci, G. (2004). Targeted inhibition of NMYC by peptide nucleic acid in N-myc amplified human neuroblastoma cells: cell-cycle inhibition with induction of neuronal cell differentiation and apoptosis. *Int J Oncol, 24*(2), 265-272.

Petrij, F., Giles, R. H., Dauwerse, H. G., Saris, J. J., Hennekam, R. C., Masuno, M., . . . et al. (1995). Rubinstein-Taybi syndrome caused by mutations in the transcriptional co-activator CBP. *Nature, 376*(6538), 348-351.

Phesse, T. J., Myant, K. B., Cole, A. M., Ridgway, R. A., Pearson, H., Muncan, V., . . . Sansom, O. J. (2014). Endogenous c-Myc is essential for p53-induced apoptosis in response to DNA damage in vivo. *Cell Death And Differentiation, 21*, 956. doi:10.1038/cdd.2014.15

https://www.nature.com/articles/cdd201415#supplementary-information

Pierce, J. L., Frazier, A. L., & Amatruda, J. F. (2018). Pediatric Germ Cell Tumors: A Developmental Perspective. *Adv Urol, 2018*, 9059382. doi:10.1155/2018/9059382

Poortinga, G., Hannan, K. M., Snelling, H., Walkley, C. R., Jenkins, A., Sharkey, K., . . . Hannan, R. D. (2004). MAD1 and c-MYC regulate UBF and rDNA transcription during granulocyte differentiation. *The EMBO Journal, 23*(16), 3325-3335. doi:10.1038/sj.emboj.7600335

Poortinga, G., Quinn, L. M., & Hannan, R. D. (2015). Targeting RNA polymerase I to treat MYC-driven cancer. *Oncogene, 34*(4), 403-412. doi:10.1038/onc.2014.13

Poortinga, G., Wall, M., Sanij, E., Siwicki, K., Ellul, J., Brown, D., . . . McArthur, G. A. (2011). c-MYC coordinately regulates ribosomal gene chromatin remodeling and Pol I availability during granulocyte differentiation. *Nucleic Acids Res, 39*(8), 3267-3281. doi:10.1093/nar/gkq1205

Popkie, A. P., Zeidner, L. C., Albrecht, A. M., D'Ippolito, A., Eckardt, S., Newsom, D. E., . . . Phiel, C. J. (2010). Phosphatidylinositol 3-Kinase (PI3K) Signaling via Glycogen Synthase Kinase-3 (Gsk-3) Regulates DNA Methylation of Imprinted Loci. *Journal of Biological Chemistry, 285*(53), 41337-41347. doi:10.1074/jbc.M110.170704

Porta, C., Paglino, C., & Mosca, A. (2014). Targeting PI3K/Akt/mTOR Signaling in Cancer. *Front Oncol, 4*, 64. doi:10.3389/fonc.2014.00064

Porter, A. G., & Janicke, R. U. (1999). Emerging roles of caspase-3 in apoptosis. *Cell Death Differ, 6*(2), 99-104. doi:10.1038/sj.cdd.4400476

Posternak, V., & Cole, M. D. (2016). Strategically targeting MYC in cancer. *F1000Res, 5*. doi:10.12688/f1000research.7879.1

Price, D. H. (2010). Regulation of RNA polymerase II elongation by c-Myc. *Cell, 141*(3), 399-400. doi:10.1016/j.cell.2010.04.016

Prince, H. M., George, D., Patnaik, A., Mita, M., Dugan, M., Butterfoss, D., . . . Beck, J. (2007). Phase I study of oral LBH589, a novel deacetylase (DAC) inhibitor in advanced solid tumors and non-hodgkin's lymphoma. *Journal of Clinical Oncology, 25*(18_suppl), 3500-3500. doi:10.1200/jco.2007.25.18_suppl.3500

Prior, I. A., Lewis, P. D., & Mattos, C. (2012). A comprehensive survey of Ras mutations in cancer. *Cancer Research, 72*(10), 2457-2467. doi:10.1158/0008-5472.CAN-11-2612

Psathas, J. N., & Thomas-Tikhonenko, A. (2014). MYC and the Art of MicroRNA Maintenance. *Cold Spring Harbor Perspectives in Medicine, 4*(8), 10.1101/cshperspect.a014175 a014175. doi:10.1101/cshperspect.a014175

Pugh, T. J., Morozova, O., Attiyeh, E. F., Asgharzadeh, S., Wei, J. S., Auclair, D., . . . Maris, J. M. (2013). The genetic landscape of high-risk neuroblastoma. *Nature genetics, 45*(3), 279-284. doi:10.1038/ng.2529

Qiao, J., Lee, S., Paul, P., Qiao, L., Taylor, C. J., Schlegel, C., . . . Chung, D. H. (2013). Akt2 Regulates Metastatic Potential in Neuroblastoma. *PLoS ONE, 8*(2), e56382. doi:10.1371/journal.pone.0056382

Qin, X., Jiang, B., & Zhang, Y. (2016). 4E-BP1, a multifactor regulated multifunctional protein. *Cell Cycle, 15*(6), 781-786. doi:10.1080/15384101.2016.1151581

Quentmeier, H., Eberth, S., Romani, J., Zaborski, M., & Drexler, H. G. (2011). BCR-ABL1-independent PI3Kinase activation causing imatinib-resistance. *Journal of Hematology & Oncology, 4*(1), 6. doi:10.1186/1756-8722-4-6

Quin, J., Chan, K. T., Devlin, J. R., Cameron, D. P., Diesch, J., Cullinane, C., . . . Hannan, R. D. (2016). Inhibition of RNA polymerase I transcription initiation by CX-5461 activates non-canonical ATM/ATR signaling. *Oncotarget, 7*(31), 49800-49818. doi:10.18632/oncotarget.10452

Rabanal-Ruiz, Y., Otten, E. G., & Korolchuk, V. I. (2017). mTORC1 as the main gateway to autophagy. *Essays Biochem, 61*(6), 565-584. doi:10.1042/ebc20170027

Radhakrishnan, R., Li, Y., Xiang, S., Yuan, F., Yuan, Z., Telles, E., . . . Seto, E. (2015). Histone deacetylase 10 regulates DNA mismatch repair and may involve the deacetylation of MutS homolog 2. *J Biol Chem, 290*(37), 22795-22804. doi:10.1074/jbc.M114.612945

Raha, D., Wang, Z., Moqtaderi, Z., Wu, L., Zhong, G., Gerstein, M., . . . Snyder, M. (2010). Close association of RNA polymerase II and many transcription factors with Pol III genes. *Proceedings of the National Academy of Sciences, 107*(8), 3639.

Rahal, Z., Abdulhai, F., Kadara, H., & Saab, R. (2018). Genomics of adult and pediatric solid tumors. *American journal of cancer research, 8*(8), 1356-1386.

Rahl, P. B., Lin, C. Y., Seila, A. C., Flynn, R. A., McCuine, S., Burge, C. B., . . . Young, R. A. (2010). c-Myc Regulates Transcriptional Pause Release. *Cell, 141*(3), 432-445. doi:https://doi.org/10.1016/j.cell.2010.03.030

Rahl, P. B., & Young, R. A. (2014). MYC and Transcription Elongation. *Cold Spring Harbor Perspectives in Medicine, 4*(1), a020990. doi:10.1101/cshperspect.a020990

Ramaswamy, V., Remke, M., Bouffet, E., Bailey, S., Clifford, S. C., Doz, F., . . . Pomeroy, S. L. (2016). Risk stratification of childhood medulloblastoma in the molecular era: the current consensus. *Acta Neuropathol, 131*(6), 821-831. doi:10.1007/s00401-016-1569-6

Rasmuson, A., Segerstrom, L., Nethander, M., Finnman, J., Elfman, L. H., Javanmardi, N., . . . Kogner, P. (2012). Tumor development, growth characteristics and spectrum of genetic aberrations in the TH-MYCN mouse model of neuroblastoma. *PLoS ONE, 7*(12), e51297. doi:10.1371/journal.pone.0051297

Rettig, I., Koeneke, E., Trippel, F., Mueller, W. C., Burhenne, J., Kopp-Schneider, A., . . . Oehme, I. (2015). Selective inhibition of HDAC8 decreases neuroblastoma growth in vitro and in vivo and enhances retinoic acid-mediated differentiation. *Cell Death Dis, 6*, e1657. doi:10.1038/cddis.2015.24

Reynolds, C. P., Matthay, K. K., Villablanca, J. G., & Maurer, B. J. (2003). Retinoid therapy of high-risk neuroblastoma. *Cancer Letters, 197*(1-2), 185-192.

Rickman, D. S., Schulte, J. H., & Eilers, M. (2018). The Expanding World of N-MYC–Driven Tumors. *Cancer Discovery, 8*(2), 150.

Ridinger, J., Koeneke, E., Kolbinger, F. R., Koerholz, K., Mahboobi, S., Hellweg, L., . . . Oehme, I. (2018). Dual role of HDAC10 in lysosomal exocytosis and DNA repair promotes neuroblastoma chemoresistance. *Scientific Reports, 8*(1), 10039. doi:10.1038/s41598-018-28265-5

Rigby, L., Muscat, A., Ashley, D., & Algar, E. (2012). Methods for the analysis of histone H3 and H4 acetylation in blood. *Epigenetics: Official Journal of the DNA Methylation Society, 7*(8), 875-882. doi:10.4161/epi.20983

Rini, B. I. (2008). Temsirolimus, an Inhibitor of Mammalian Target of Rapamycin. *Clinical Cancer Research, 14*(5), 1286.

Rini, B. I., & Atkins, M. B. (2009). Resistance to targeted therapy in renal-cell carcinoma. *Lancet Oncol, 10*(10), 992-1000. doi:10.1016/s1470-2045(09)70240-2

Rini, B. I., Bellmunt, J., Clancy, J., Wang, K., Niethammer, A. G., Hariharan, S., & Escudier, B. (2014). Randomized phase III trial of temsirolimus and bevacizumab versus interferon alfa and bevacizumab in metastatic renal cell carcinoma: INTORACT trial. *J Clin Oncol, 32*(8), 752-759. doi:10.1200/jco.2013.50.5305

Robert, C., & Rassool, F. V. (2012). HDAC inhibitors: roles of DNA damage and repair. *Adv Cancer Res, 116*, 87-129. doi:10.1016/b978-0-12-394387-3.00003-3

Rodier, F., & Campisi, J. (2011). Four faces of cellular senescence. *The Journal of Cell Biology, 192*(4), 547.

Rogers, H. A., Estranero, J., Gudka, K., & Grundy, R. G. (2017). The therapeutic potential of targeting the PI3K pathway in pediatric brain tumors. *Oncotarget, 8*(2), 2083-2095. doi:10.18632/oncotarget.13781

Rogers, H. A., Sousa, S., Salto, C., Arenas, E., Coyle, B., & Grundy, R. G. (2012). WNT/β-catenin pathway activation in Myc immortalised cerebellar progenitor cells inhibits neuronal differentiation and generates tumours resembling medulloblastoma. *British Journal of Cancer, 107*(7), 1144-1152. doi:10.1038/bjc.2012.377

Rokita, J. L., Rathi, K. S., Cardenas, M. F., Upton, K. A., Jayaseelan, J., Cross, K. L., . . . Maris, J. M. (2019). Genomic Profiling of Childhood Tumor Patient-Derived Xenograft Models to Enable Rational Clinical Trial Design. *Cell Rep, 29*(6), 1675-1689.e1679. doi:10.1016/j.celrep.2019.09.071

Rolli-Derkinderen, M., Machavoine, F., Baraban, J. M., Grolleau, A., Beretta, L., & Dy, M. (2003). ERK and p38 Inhibit the Expression of 4E-BP1 Repressor of Translation through Induction of Egr-1. *Journal of Biological Chemistry, 278*(21), 18859-18867. doi:10.1074/jbc.M211696200

Ronzoni, S., Faretta, M., Ballarini, M., Pelicci, P., & Minucci, S. (2005). New method to detect histone acetylation levels by flow cytometry. *Cytometry A, 66*(1), 52-61. doi:10.1002/cyto.a.20151

Ropero, S., & Esteller, M. (2007). The role of histone deacetylases (HDACs) in human cancer. *Molecular Oncology, 1*(1), 19-25. doi:https://dx.doi.org/10.1016/j.molonc.2007.01.001

Roussel, M. F., & Robinson, G. W. (2013). Role of MYC in Medulloblastoma. *Cold Spring Harbor Perspectives in Medicine, 3*(11), a014308. doi:10.1101/cshperspect.a014308

Roy, A. L., Carruthers, C., Gutjahr, T., & Roeder, R. G. (1993). Direct role for Myc in transcription initiation mediated by interactions with TFII-I. *Nature, 365*(6444), 359-361. doi:10.1038/365359a0

Rozengurt, E., Soares, H. P., & Sinnet-Smith, J. (2014). Suppression of feedback loops mediated by PI3K/mTOR induces multiple over-activation of compensatory pathways: an unintended consequence leading to drug resistance. *Mol Cancer Ther, 13*(11), 2477-2488. doi:10.1158/1535-7163.MCT-14-0330

Rubie, H., Hartmann, O., Michon, J., Frappaz, D., Coze, C., Chastagner, P., . . . Sommelet, D. (1997). N-Myc gene amplification is a major prognostic factor in localized neuroblastoma: results of the French NBL 90 study. Neuroblastoma Study Group of the Societe Francaise d'Oncologie Pediatrique. *J Clin Oncol, 15*(3), 1171-1182. doi:10.1200/jco.1997.15.3.1171

Rudnick, E., Khakoo, Y., Antunes, N. L., Seeger, R. C., Brodeur, G. M., Shimada, H., . . . Matthay, K. K. (2001). Opsoclonus-myoclonus-ataxia syndrome in neuroblastoma: clinical outcome and antineuronal antibodies-a report from the Children's Cancer Group Study. *Med Pediatr Oncol, 36*(6), 612-622. doi:10.1002/mpo.1138

Rundle, S., Bradbury, A., Drew, Y., & Curtin, N. J. (2017). Targeting the ATR-CHK1 Axis in Cancer Therapy. *Cancers, 9*(5), 41. doi:10.3390/cancers9050041

Rundlett, S. E., Carmen, A. A., Kobayashi, R., Bavykin, S., Turner, B. M., & Grunstein, M. (1996). HDA1 and RPD3 are members of distinct yeast histone deacetylase complexes that regulate silencing and transcription. *Proc Natl Acad Sci U S A, 93*(25), 14503-14508.

Ruvinsky, I., Sharon, N., Lerer, T., Cohen, H., Stolovich-Rain, M., Nir, T., . . . Meyuhas, O. (2005). Ribosomal protein S6 phosphorylation is a determinant of cell size and glucose homeostasis. *Genes & Development, 19*(18), 2199-2211. doi:10.1101/gad.351605

Sabatini, D. M. (2017). Twenty-five years of mTOR: Uncovering the link from nutrients to growth. *Proceedings of the National Academy of Sciences, 114*(45), 11818.

Sabers, C. J., Martin, M. M., Brunn, G. J., Williams, J. M., Dumont, F. J., Wiederrecht, G., & Abraham, R. T. (1995). Isolation of a protein target of the FKBP12-rapamycin complex in mammalian cells. *J Biol Chem, 270*(2), 815-822.

Sabò, A., Kress, T. R., Pelizzola, M., de Pretis, S., Gorski, M. M., Tesi, A., . . . Amati, B. (2014). Selective transcriptional regulation by Myc in cellular growth control and lymphomagenesis. *Nature, 511*, 488. doi:10.1038/nature13537 https://www.nature.com/articles/nature13537#supplementary-information

Sait, S., & Modak, S. (2017). Anti-GD2 immunotherapy for neuroblastoma. *Expert Rev Anticancer Ther, 17*(10), 889-904. doi:10.1080/14737140.2017.1364995

Saletta, F., Seng, M. S., & Lau, L. M. S. (2014). Advances in paediatric cancer treatment. *Translational Pediatrics, 3*(2), 156-182. doi:10.3978/j.issn.2224-4336.2014.02.01

Salian-Mehta, S., Xu, M., McKinsey, T. A., Tobet, S., & Wierman, M. E. (2015). Novel Interaction of Class IIb Histone Deacetylase 6 (HDAC6) with Class IIa HDAC9 Controls Gonadotropin Releasing Hormone (GnRH) Neuronal Cell Survival and Movement. *J Biol Chem, 290*(22), 14045-14056. doi:10.1074/jbc.M115.640482

Samuels, Y., & Waldman, T. (2010). Oncogenic Mutations of PIK3CA in Human Cancers. *Curr Top Microbiol Immunol, 347*, 21-41. doi:10.1007/82_2010_68

Sander, S., Calado, D. P., Srinivasan, L., Köchert, K., Zhang, B., Rosolowski, M., . . . Rajewsky, K. (2012). Synergy between PI3K Signaling and MYC in Burkitt Lymphomagenesis. *Cancer cell, 22*(2), 167-179. doi:10.1016/j.ccr.2012.06.012

Sarbassov, D. D., Ali, S. M., Sengupta, S., Sheen, J. H., Hsu, P. P., Bagley, A. F., . . . Sabatini, D. M. (2006). Prolonged rapamycin treatment inhibits mTORC2 assembly and Akt/PKB. *Mol Cell, 22*(2), 159-168. doi:10.1016/j.molcel.2006.03.029

Sarbassov, D. D., Guertin, D. A., Ali, S. M., & Sabatini, D. M. (2005). Phosphorylation and regulation of Akt/PKB by the rictor-mTOR complex. *Science, 307*(5712), 1098-1101. doi:10.1126/science.1106148

Sarker, D., Ang, J. E., Baird, R., Kristeleit, R., Shah, K., Moreno, V., . . . de Bono, J. S. (2015). First-in-human Phase I study of Pictilisib (GDC-0941), a potent pan-class I phosphatidylinositol-3-kinase (PI3K) inhibitor, in patients with advanced solid tumors. *Clin Cancer Res, 21*(1), 77-86. doi:10.1158/1078-0432.CCR-14-0947

Sartelet, H., Oligny, L. L., & Vassal, G. (2008). AKT pathway in neuroblastoma and its therapeutic implication. *Expert Rev Anticancer Ther, 8*(5), 757-769. doi:10.1586/14737140.8.5.757

Savelieva, M., Woo, M. M., Schran, H., Mu, S., Nedelman, J., & Capdeville, R. (2015). Population pharmacokinetics of intravenous and oral panobinostat in patients with

hematologic and solid tumors. *Eur J Clin Pharmacol, 71*(6), 663-672. doi:10.1007/s00228-015-1846-7

Saxton, R. A., & Sabatini, D. M. (2017). mTOR Signaling in Growth, Metabolism, and Disease. *Cell, 168*(6), 960-976. doi:10.1016/j.cell.2017.02.004

Schenone, S., Brullo, C., Musumeci, F., Radi, M., & Botta, M. (2011). ATP-competitive inhibitors of mTOR: an update. *Curr Med Chem, 18*(20), 2995-3014.

Schleiermacher, G., Rubie, H., Hartmann, O., Bergeron, C., Chastagner, P., Mechinaud, F., & Michon, J. (2003). Treatment of stage 4s neuroblastoma--report of 10 years' experience of the French Society of Paediatric Oncology (SFOP). *Br J Cancer, 89*(3), 470-476. doi:10.1038/sj.bjc.6601154

Schmidt, E. V. (1999). The role of c-myc in cellular growth control. *Oncogene, 18*(19), 2988-2996. doi:10.1038/sj.onc.1202751

Schneikert, J., & Behrens, J. (2007). The canonical Wnt signalling pathway and its APC partner in colon cancer development. *Gut, 56*(3), 417-425. doi:10.1136/gut.2006.093310

Schulte, J. H., Schulte, S., Heukamp, L. C., Astrahantseff, K., Stephan, H., Fischer, M., . . . Eggert, A. (2013). Targeted Therapy for Neuroblastoma: ALK Inhibitors. *Klin Padiatr, 225*(6), 303-308. doi:10.1055/s-0033-1357132

Schwab, M., Alitalo, K., Klempnauer, K.-H., Varmus, H. E., Bishop, J. M., Gilbert, F., . . . Trent, J. (1983). Amplified DNA with limited homology to myc cellular oncogene is shared by human neuroblastoma cell lines and a neuroblastoma tumour. *Nature, 305*, 245. doi:10.1038/305245a0

Segerstrom, L., Baryawno, N., Sveinbjornsson, B., Wickstrom, M., Elfman, L., Kogner, P., & Johnsen, J. I. (2011). Effects of small molecule inhibitors of PI3K/Akt/mTOR

signaling on neuroblastoma growth in vitro and in vivo. *Int J Cancer, 129*(12), 2958-2965. doi:10.1002/ijc.26268

Seo, H. R., Kim, J., Bae, S., Soh, J.-W., & Lee, Y.-S. (2008). Cdk5-mediated Phosphorylation of c-Myc on Ser-62 Is Essential in Transcriptional Activation of Cyclin B1 by Cyclin G1. *J Biol Chem, 283*(23), 15601-15610. doi:10.1074/jbc.M800987200

Seront, E., Rottey, S., Filleul, B., Glorieux, P., Goeminne, J. C., Verschaeve, V., . . . Machiels, J. P. (2016). Phase II study of dual phosphoinositol-3-kinase (PI3K) and mammalian target of rapamycin (mTOR) inhibitor BEZ235 in patients with locally advanced or metastatic transitional cell carcinoma. *BJU Int, 118*(3), 408-415. doi:10.1111/bju.13415

Seto, B. (2012). Rapamycin and mTOR: a serendipitous discovery and implications for breast cancer. *Clinical and Translational Medicine, 1*, 29-29. doi:10.1186/2001-1326-1-29

Shahbazi, J., Liu, P. Y., Atmadibrata, B., Bradner, J. E., Marshall, G. M., Lock, R. B., & Liu, T. (2016). The Bromodomain Inhibitor JQ1 and the Histone Deacetylase Inhibitor Panobinostat Synergistically Reduce N-Myc Expression and Induce Anticancer Effects. *Clin Cancer Res, 22*(10), 2534-2544. doi:10.1158/1078-0432.Ccr-15-1666

Shaimerdenova, M., Karapina, O., Mektepbayeva, D., Alibek, K., & Akilbekova, D. (2017). The effects of antiviral treatment on breast cancer cell line. *Infectious Agents and Cancer, 12*, 18. doi:10.1186/s13027-017-0128-7

Sharma, S., Beck, J., Mita, M., Paul, S., Woo, M. M., Squier, M., . . . Prince, H. M. (2013). A phase I dose-escalation study of intravenous panobinostat in patients with

lymphoma and solid tumors. *Invest New Drugs, 31*(4), 974-985. doi:10.1007/s10637-013-9930-2

She, Q.-B., Halilovic, E., Ye, Q., Zhen, W., Shirasawa, S., Sasazuki, T., . . . Rosen, N. (2010). 4E-BP1 Is A Key Effector of the Oncogenic Activation of the AKT and ERK Signaling Pathways That Integrates Their Function in Tumors. *Cancer cell, 18*(1), 39-51. doi:10.1016/j.ccr.2010.05.023

Sheiness, D., Fanshier, L., & Bishop, J. M. (1978). Identification of nucleotide sequences which may encode the oncogenic capacity of avian retrovirus MC29. *J Virol, 28*(2), 600-610.

Shih, W. L., Fang, C. T., & Chen, P. J. (2014). Anti-viral treatment and cancer control. *Recent Results Cancer Res, 193*, 269-290. doi:10.1007/978-3-642-38965-8_14

Shimada, H., Ambros, I. M., Dehner, L. P., Hata, J., Joshi, V. V., Roald, B., . . . Castleberry, R. P. (1999). The International Neuroblastoma Pathology Classification (the Shimada system). *Cancer, 86*(2), 364-372.

Shortt, J., Martin, B. P., Newbold, A., Hannan, K. M., Devlin, J. R., Baker, A. J., . . . Johnstone, R. W. (2013). Combined inhibition of PI3K-related DNA damage response kinases and mTORC1 induces apoptosis in MYC-driven B-cell lymphomas. *Blood, 121*(15), 2964-2974. doi:10.1182/blood-2012-08-446096

Shostak, A., Ruppert, B., Ha, N., Bruns, P., Toprak, U. H., Eils, R., . . . Brunner, M. (2016). MYC/MIZ1-dependent gene repression inversely coordinates the circadian clock with cell cycle and proliferation. *Nature communications, 7*, 11807. doi:10.1038/ncomms11807

Showkat, M., Beigh, M. A., & Andrabi, K. I. (2014). mTOR Signaling in Protein Translation Regulation: Implications in Cancer Genesis and Therapeutic Interventions. *Mol Biol Int, 2014*, 686984. doi:10.1155/2014/686984

Shukla, N., Ameur, N., Yilmaz, I., Nafa, K., Lau, C.-Y., Marchetti, A., . . . Ladanyi, M. (2012). ONCOGENE MUTATION PROFILING OF PEDIATRIC SOLID TUMORS REVEALS SIGNIFICANT SUBSETS OF EMBRYONAL RHABDOMYOSARCOMA AND NEUROBLASTOMA WITH MUTATED GENES IN GROWTH SIGNALING PATHWAYS. *Clinical Cancer Research, 18*(3), 748-757. doi:10.1158/1078-0432.CCR-11-2056

Sikalidis, A., M Mazor, K., Kang, M., Liu, H., & Stipanuk, M. (2013). *Total 4EBP1 Is Elevated in Liver of Rats in Response to Low Sulfur Amino Acid Intake* (Vol. 2013).

Singh, B. N., Zhang, G., Hwa, Y. L., Li, J., Dowdy, S. C., & Jiang, S. W. (2010). Nonhistone protein acetylation as cancer therapy targets. *Expert Rev Anticancer Ther, 10*(6), 935-954. doi:10.1586/era.10.62

Singh, S. K., Clarke, I. D., Terasaki, M., Bonn, V. E., Hawkins, C., Squire, J., & Dirks, P. B. (2003). Identification of a cancer stem cell in human brain tumors. *Cancer Research, 63*(18), 5821-5828.

Sjostrom, S. K., Finn, G., Hahn, W. C., Rowitch, D. H., & Kenney, A. M. (2005). The Cdk1 Complex Plays a Prime Role in Regulating N-Myc Phosphorylation and Turnover in Neural Precursors. *Developmental Cell, 9*(3), 327-338. doi:https://doi.org/10.1016/j.devcel.2005.07.014

Smith, S. J., Diehl, N., Leavitt, J. A., & Mohney, B. G. (2010). Incidence of Pediatric Horner Syndrome and the Risk of Neuroblastoma: A Population-Based Study. *Archives of ophthalmology, 128*(3), 324-329. doi:10.1001/archophthalmol.2010.6

Smyth, M. J., Ngiow, S. F., Ribas, A., & Teng, M. W. (2016). Combination cancer immunotherapies tailored to the tumour microenvironment. *Nat Rev Clin Oncol, 13*(3), 143-158. doi:10.1038/nrclinonc.2015.209

Song, M. S., Salmena, L., & Pandolfi, P. P. (2012). The functions and regulation of the PTEN tumour suppressor. *Nature Reviews Molecular Cell Biology, 13*, 283. doi:10.1038/nrm3330 https://www.nature.com/articles/nrm3330#supplementary-information

Soto-Gamez, A., & Demaria, M. (2017). Therapeutic interventions for aging: the case of cellular senescence. *Drug Discovery Today, 22*(5), 786-795. doi:https://doi.org/10.1016/j.drudis.2017.01.004

Spitzenberg, V., Konig, C., Ulm, S., Marone, R., Ropke, L., Muller, J. P., . . . Wetzker, R. (2010). Targeting PI3K in neuroblastoma. *J Cancer Res Clin Oncol, 136*(12), 1881-1890. doi:10.1007/s00432-010-0847-2

Srinivas, N. R. (2017). Clinical pharmacokinetics of panobinostat, a novel histone deacetylase (HDAC) inhibitor: review and perspectives. *Xenobiotica, 47*(4), 354-368. doi:10.1080/00498254.2016.1184356

Staal, S. P. (1987). Molecular cloning of the akt oncogene and its human homologues AKT1 and AKT2: amplification of AKT1 in a primary human gastric adenocarcinoma. *Proc Natl Acad Sci U S A, 84*(14), 5034-5037.

Stanton, B. R., Perkins, A. S., Tessarollo, L., Sassoon, D. A., & Parada, L. F. (1992). Loss of N-myc function results in embryonic lethality and failure of the epithelial component of the embryo to develop. *Genes & Development, 6*(12a), 2235-2247.

Stronach, E. A., Chen, M., Maginn, E. N., Agarwal, R., Mills, G. B., Wasan, H., & Gabra, H. (2011). DNA-PK Mediates AKT Activation and Apoptosis Inhibition in Clinically Acquired Platinum Resistance. *Neoplasia (New York, N.Y.), 13*(11), 1069-1080.

Subocz, E., Hałka, J., & Dziuk, M. (2017). The role of FDG-PET in Hodgkin lymphoma. *Contemporary Oncology, 21*(2), 104-114. doi:10.5114/wo.2017.68618

Subramanian, A., Tamayo, P., Mootha, V. K., Mukherjee, S., Ebert, B. L., Gillette, M. A., . . . Mesirov, J. P. (2005). Gene set enrichment analysis: a knowledge-based approach for interpreting genome-wide expression profiles. *Proc Natl Acad Sci U S A, 102*(43), 15545-15550. doi:10.1073/pnas.0506580102

Sugimoto, Y., Whitman, M., Cantley, L. C., & Erikson, R. L. (1984). Evidence that the Rous sarcoma virus transforming gene product phosphorylates phosphatidylinositol and diacylglycerol. *Proc Natl Acad Sci U S A, 81*(7), 2117-2121.

Sun, X., Wei, L., Chen, Q., & Terek, R. M. (2009). HDAC4 represses vascular endothelial growth factor expression in chondrosarcoma by modulating RUNX2 activity. *J Biol Chem, 284*(33), 21881-21890. doi:10.1074/jbc.M109.019091

Sun, Y., Liu, P. Y., Scarlett, C. J., Malyukova, A., Liu, B., Marshall, G. M., . . . Liu, T. (2014). Histone deacetylase 5 blocks neuroblastoma cell differentiation by interacting with N-Myc. *Oncogene, 33*(23), 2987-2994. doi:10.1038/onc.2013.253

Sung, K. W. (2012). Treatment of high-risk neuroblastoma. *Korean Journal of Pediatrics, 55*(4), 115-120. doi:10.3345/kjp.2012.55.4.115

Swanton, E., Savory, P., Cosulich, S., Clarke, P., & Woodman, P. (1999). Bcl-2 regulates a caspase-3/caspase-2 apoptotic cascade in cytosolic extracts. *Oncogene, 18*, 1781. doi:10.1038/sj.onc.1202490

Szarewski, A. (2012). HPV vaccination and cervical cancer. *Curr Oncol Rep, 14*(6), 559-567. doi:10.1007/s11912-012-0259-3

Tahergorabi, Z., & Khazaei, M. (2012). A Review on Angiogenesis and Its Assays. *Iranian Journal of Basic Medical Sciences, 15*(6), 1110-1126.

Takahashi, Y., & Fukusato, T. (2014). Histopathology of nonalcoholic fatty liver disease/nonalcoholic steatohepatitis. *World Journal of Gastroenterology : WJG, 20*(42), 15539-15548. doi:10.3748/wjg.v20.i42.15539

Takahashi-Yanaga, F., & Sasaguri, T. (2008). GSK-3beta regulates cyclin D1 expression: a new target for chemotherapy. *Cell Signal, 20*(4), 581-589. doi:10.1016/j.cellsig.2007.10.018

Tan, M. H., Mester, J. L., Ngeow, J., Rybicki, L. A., Orloff, M. S., & Eng, C. (2012). Lifetime cancer risks in individuals with germline PTEN mutations. *Clin Cancer Res, 18*(2), 400-407. doi:10.1158/1078-0432.Ccr-11-2283

Tanaka, K., Babic, I., Nathanson, D., Akhavan, D., Guo, D., Gini, B., . . . Mischel, P. S. (2011). Oncogenic EGFR signaling activates an mTORC2-NF-kappaB pathway that promotes chemotherapy resistance. *Cancer Discov, 1*(6), 524-538. doi:10.1158/2159-8290.Cd-11-0124

Tang, Y., Boucher, J. M., & Liaw, L. (2012). Histone deacetylase activity selectively regulates notch-mediated smooth muscle differentiation in human vascular cells. *J Am Heart Assoc, 1*(3), e000901. doi:10.1161/jaha.112.000901

Teachey, D. T., Obzut, D. A., Cooperman, J., Fang, J., Carroll, M., Choi, J. K., . . . Grupp, S. A. (2006). The mTOR inhibitor CCI-779 induces apoptosis and inhibits growth in preclinical models of primary adult human ALL. *Blood, 107*(3), 1149.

Tee, A. R. (2018). The Target of Rapamycin and Mechanisms of Cell Growth. *Int J Mol Sci, 19*(3). doi:10.3390/ijms19030880

Terranova-Barberio, M., Thomas, S., Ali, N., Pawlowska, N., Park, J., Krings, G., . . . Munster, P. N. (2017). HDAC inhibition potentiates immunotherapy in triple negative breast cancer. *Oncotarget, 8*(69), 114156-114172. doi:10.18632/oncotarget.23169

Thapa, N., & Anderson, R. A. (2012). PIP2 signaling, an integrator of cell polarity and vesicle trafficking in directionally migrating cells. *Cell Adhesion & Migration, 6*(5), 409-412. doi:10.4161/cam.21192

The Cancer Genome Atlas Research, N., McLendon, R., Friedman, A., Bigner, D., Van Meir, E. G., Brat, D. J., . . . Thomson, E. (2008). Comprehensive genomic characterization defines human glioblastoma genes and core pathways. *Nature, 455*, 1061. doi:10.1038/nature07385 https://www.nature.com/articles/nature07385#supplementary-information

Thurn, K. T., Thomas, S., Raha, P., Qureshi, I., & Munster, P. N. (2013). Histone deacetylase regulation of ATM-mediated DNA damage signaling. *Mol Cancer Ther, 12*(10), 2078-2087. doi:10.1158/1535-7163.Mct-12-1242

Toker, A. (2000). Protein Kinases as Mediators of Phosphoinositide 3-Kinase Signaling. *Molecular Pharmacology, 57*(4), 652.

Tong, Q. S., Zheng, L. D., Tang, S. T., Ruan, Q. L., Liu, Y., Li, S. W., . . . Cai, J. B. (2008). Expression and clinical significance of stem cell marker CD133 in human neuroblastoma. *World J Pediatr, 4*(1), 58-62. doi:10.1007/s12519-008-0012-z

Tosh, D., & Slack, J. M. (2002). How cells change their phenotype. *Nat Rev Mol Cell Biol, 3*(3), 187-194. doi:10.1038/nrm761

Tsang, C. K., Liu, H., & Zheng, X. F. S. (2010). mTOR binds to the promoters of RNA polymerase I- and III-transcribed genes. *Cell Cycle, 9*(5), 953-957.

Tsubono, Y., & Hisamichi, S. (2004). A Halt to Neuroblastoma Screening in Japan. *New England Journal of Medicine, 350*(19), 2010-2011. doi:10.1056/nejm200405063501922

Tsui, P. C., Lee, Y.-F., Liu, Z. W. Y., Ip, L. R. H., Piao, W., Chiang, A. K. S., & Lui, V. W. Y. (2017). An update on genomic-guided therapies for pediatric solid tumors. *Future Oncology, 13*(15), 1345-1358. doi:10.2217/fon-2017-0003

Tulla, M., Berthold, F., Graf, N., Rutkowski, S., von Schweinitz, D., Spix, C., & Kaatsch, P. (2015). Incidence, Trends, and Survival of Children With Embryonal Tumors. *Pediatrics, 136*(3), e623.

Tyler, W. A., Gangoli, N., Gokina, P., Kim, H. A., Covey, M., Levison, S. W., & Wood, T. L. (2009). Activation of the Mammalian Target of Rapamycin (mTOR) is Essential for Oligodendrocyte Differentiation. *J Neurosci, 29*(19), 6367-6378. doi:10.1523/JNEUROSCI.0234-09.2009

Van Arendonk, K. J., & Chung, D. H. (2019). Neuroblastoma: Tumor Biology and Its Implications for Staging and Treatment. *Children (Basel), 6*(1). doi:10.3390/children6010012

van Bokhoven, H., Celli, J., van Reeuwijk, J., Rinne, T., Glaudemans, B., van Beusekom, E., . . . Brunner, H. G. (2005). MYCN haploinsufficiency is associated with reduced brain size and intestinal atresias in Feingold syndrome. *Nat Genet, 37*(5), 465-467. doi:10.1038/ng1546

van Riggelen, J., Müller, J., Otto, T., Beuger, V., Yetil, A., Choi, P. S., . . . Eilers, M. (2010). The interaction between Myc and Miz1 is required to antagonize TGFβ-dependent autocrine signaling during lymphoma formation and maintenance. *Genes & Development, 24*(12), 1281-1294. doi:10.1101/gad.585710

Van Veggel, M., Westerman, E., & Hamberg, P. (2018). Clinical Pharmacokinetics and Pharmacodynamics of Panobinostat. *Clin Pharmacokinet, 57*(1), 21-29. doi:10.1007/s40262-017-0565-x

Vandamme, T. F. (2014). Use of rodents as models of human diseases. *Journal of pharmacy & bioallied sciences, 6*(1), 2-9. doi:10.4103/0975-7406.124301

Vaughan, L., Clarke, P. A., Barker, K., Chanthery, Y., Gustafson, C. W., Tucker, E., . . . Chesler, L. (2016). Inhibition of mTOR-kinase destabilizes MYCN and is a potential therapy for MYCN-dependent tumors. *Oncotarget, 7*(36), 57525-57544. doi:10.18632/oncotarget.10544

Vega, R. B., Matsuda, K., Oh, J., Barbosa, A. C., Yang, X., Meadows, E., . . . Olson, E. N. (2004). Histone deacetylase 4 controls chondrocyte hypertrophy during skeletogenesis. *Cell, 119*(4), 555-566.

Verdin, E., Dequiedt, F., & Kasler, H. G. (2003). Class II histone deacetylases: versatile regulators. *Trends Genet, 19*(5), 286-293. doi:10.1016/s0168-9525(03)00073-8

Vervoorts, J., Lüscher-Firzlaff, J., & Lüscher, B. (2006). The Ins and Outs of MYC Regulation by Posttranslational Mechanisms. *Journal of Biological Chemistry, 281*(46), 34725-34729. doi:10.1074/jbc.R600017200

Vezina, C., Kudelski, A., & Sehgal, S. N. (1975). Rapamycin (AY-22,989), a new antifungal antibiotic. I. Taxonomy of the producing streptomycete and isolation of the active principle. *J Antibiot (Tokyo), 28*(10), 721-726.

Vogelstein, B., Papadopoulos, N., Velculescu, V. E., Zhou, S., Diaz, L. A., Jr., & Kinzler, K. W. (2013). Cancer genome landscapes. *Science, 339*(6127), 1546-1558. doi:10.1126/science.1235122

von Eyss, B., & Eilers, M. (2011). Addicted to Myc--but why? *Genes & Development, 25*(9), 895-897. doi:10.1101/gad.2053311

Voss, M. H., Molina, A. M., & Motzer, R. J. (2011). mTOR Inhibitors in Advanced Renal Cell Carcinoma. *Hematology/oncology clinics of North America, 25*(4), 835-852. doi:10.1016/j.hoc.2011.04.008

Waaijer, S. J. H., Kok, I. C., Eisses, B., Schroder, C. P., Jalving, M., Brouwers, A. H., . . . de Vries, E. G. E. (2018). Molecular Imaging in Cancer Drug Development. *J Nucl Med, 59*(5), 726-732. doi:10.2967/jnumed.116.188045

Wainwright, L. J., Lasorella, A., & Iavarone, A. (2001). Distinct mechanisms of cell cycle arrest control the decision between differentiation and senescence in human neuroblastoma cells. *Proceedings of the National Academy of Sciences, 98*(16), 9396.

Waldeck, K., Cullinane, C., Ardley, K., Shortt, J., Martin, B., Tothill, R. W., . . . Wood, P. J. (2016). Long term, continuous exposure to panobinostat induces terminal differentiation and long term survival in the TH-MYCN neuroblastoma mouse model. *International Journal of Cancer, 139*(1), 194-204.

Waligora, M., Bala, M. M., Koperny, M., Wasylewski, M. T., Strzebonska, K., Jaeschke, R. R., . . . Kimmelman, J. (2018). Risk and surrogate benefit for pediatric Phase I trials in oncology: A systematic review with meta-analysis. *PLoS Med, 15*(2), e1002505. doi:10.1371/journal.pmed.1002505

Wall, M., Poortinga, G., Stanley, K. L., Lindemann, R. K., Bots, M., Chan, C. J., . . . McArthur, G. A. (2013). The mTORC1 inhibitor everolimus prevents and treats Emu-Myc lymphoma by restoring oncogene-induced senescence. *Cancer Discov, 3*(1), 82-95. doi:10.1158/2159-8290.Cd-12-0404

Walsh, D., Mathews, M. B., & Mohr, I. (2013). Tinkering with Translation: Protein Synthesis in Virus-Infected Cells. *Cold Spring Harbor Perspectives in Biology, 5*(1), a012351. doi:10.1101/cshperspect.a012351

Wan, X., Shen, N., Mendoza, A., Khanna, C., & Helman, L. J. (2006). CCI-779 Inhibits Rhabdomyosarcoma Xenograft Growth by an Antiangiogenic Mechanism Linked to the Targeting of mTOR/Hif-1α/VEGF Signaling. *Neoplasia (New York, N.Y.), 8*(5), 394-401.

Wang, D., Gao, L., Liu, X., Yuan, C., & Wang, G. (2017). Improved antitumor effect of ionizing radiation in combination with rapamycin for treating nasopharyngeal carcinoma. *Oncol Lett, 14*(1), 1105-1108. doi:10.3892/ol.2017.6208

Wang, F.-Z., Peng-Jiao, Yang, N.-N., Chuang-Yuan, Zhao, Y.-L., Liu, Q.-Q., . . . Zhang, J.-G. (2013). *PF-04691502 triggers cell cycle arrest, apoptosis and inhibits the angiogenesis in hepatocellular carcinoma cells* (Vol. 220).

Wang, L., Shi, W.-Y., Wu, Z.-Y., Varna, M., Wang, A.-H., Zhou, L., . . . Janin, A. (2010). Cytostatic and anti-angiogenic effects of temsirolimus in refractory mantle cell lymphoma. *Journal of Hematology & Oncology, 3*(1), 30. doi:10.1186/1756-8722-3-30

Wang, R., Xia, L., Gabrilove, J., Waxman, S., & Jing, Y. (2013). Down-regulation of Mcl-1 through GSK-3β activation contributes to arsenic trioxide-induced apoptosis in acute myeloid leukemia cells. *Leukemia, 27*(2), 315-324. doi:10.1038/leu.2012.180

Wang, W., Ren, F., Wu, Q., Jiang, D., Li, H., & Shi, H. (2014). MicroRNA-497 suppresses angiogenesis by targeting vascular endothelial growth factor A through the PI3K/AKT and MAPK/ERK pathways in ovarian cancer. *Oncol Rep, 32*(5), 2127-2133. doi:10.3892/or.2014.3439

Wang, X., & Proud, C. G. (2015). mTORC2 is a tyrosine kinase. *Cell Research, 26*, 1. doi:10.1038/cr.2015.134

Wang, X., Zhao, X., Gao, P., & Wu, M. (2013). c-Myc modulates microRNA processing via the transcriptional regulation of Drosha. *Scientific Reports, 3*, 1942. doi:10.1038/srep01942 https://www.nature.com/articles/srep01942#supplementary-information

Wang, Z., Lyu, J., Wang, F., Miao, C., Nan, Z., Zhang, J., . . . Ge, W. (2018). The histone deacetylase HDAC1 positively regulates Notch signaling during Drosophila wing development. *Biol Open, 7*(2). doi:10.1242/bio.029637

Weber, A. M., & Ryan, A. J. (2015). ATM and ATR as therapeutic targets in cancer. *Pharmacology & therapeutics, 149*, 124-138. doi:https://doi.org/10.1016/j.pharmthera.2014.12.001

Wei, L., Zhu, S., Wang, J., & Liu, J. (2012). Activation of the Phosphatidylinositol 3-Kinase/Akt Signaling Pathway during Porcine Circovirus Type 2 Infection Facilitates Cell Survival and Viral Replication. *J Virol, 86*(24), 13589-13597. doi:10.1128/JVI.01697-12

Weichhart, T. (2018). mTOR as Regulator of Lifespan, Aging, and Cellular Senescence: A Mini-Review. *Gerontology, 64*(2), 127-134. doi:10.1159/000484629

Weidle, U. H., & Grossmann, A. (2000). Inhibition of histone deacetylases: a new strategy to target epigenetic modifications for anticancer treatment. *Anticancer research, 20*(3A), 1471-1485.

Weinstein, I. B. (2002). Cancer. Addiction to oncogenes--the Achilles heal of cancer. *Science, 297*(5578), 63-64. doi:10.1126/science.1073096

Weiss, W. A., Aldape, K., Mohapatra, G., Feuerstein, B. G., & Bishop, J. M. (1997). Targeted expression of MYCN causes neuroblastoma in transgenic mice. *The EMBO Journal, 16*(11), 2985-2995. doi:10.1093/emboj/16.11.2985

West, A. C., Mattarollo, S. R., Shortt, J., Cluse, L. A., Christiansen, A. J., Smyth, M. J., & Johnstone, R. W. (2013). An intact immune system is required for the anticancer activities of histone deacetylase inhibitors. *Cancer Research, 73*(24), 7265-7276. doi:10.1158/0008-5472.Can-13-0890

Wherry, E. J., & Kurachi, M. (2015). Molecular and cellular insights into T cell exhaustion. *Nat Rev Immunol, 15*(8), 486-499. doi:10.1038/nri3862

Whitman, M., Kaplan, D. R., Schaffhausen, B., Cantley, L., & Roberts, T. M. (1985). Association of phosphatidylinositol kinase activity with polyoma middle-T competent for transformation. *Nature, 315*, 239. doi:10.1038/315239a0

Whittle, S. B., Smith, V., Doherty, E., Zhao, S., McCarty, S., & Zage, P. E. (2017). Overview and recent advances in the treatment of neuroblastoma. *Expert Rev Anticancer Ther, 17*(4), 369-386. doi:10.1080/14737140.2017.1285230

Wiese, K. E., Walz, S., von Eyss, B., Wolf, E., Athineos, D., Sansom, O., & Eilers, M. (2013). The Role of MIZ-1 in MYC-Dependent Tumorigenesis. *Cold Spring Harbor Perspectives in Medicine, 3*(12), a014290. doi:10.1101/cshperspect.a014290

Will, M., Qin, A. C., Toy, W., Yao, Z., Rodrik-Outmezguine, V., Schneider, C., . . . Rosen, N. (2014). Rapid induction of apoptosis by PI3K inhibitors is dependent upon their transient inhibition of RAS-ERK signaling. *Cancer Discov, 4*(3), 334-347. doi:10.1158/2159-8290.Cd-13-0611

Willers, H., Azzoli, C. G., Santivasi, W. L., & Xia, F. (2013). Basic mechanisms of therapeutic resistance to radiation and chemotherapy in lung cancer. *Cancer J, 19*(3), 200-207. doi:10.1097/PPO.0b013e318292e4e3

William, D., Mullins, C. S., Schneider, B., Orthmann, A., Lamp, N., Krohn, M., . . . Linnebacher, M. (2017). Optimized creation of glioblastoma patient derived

xenografts for use in preclinical studies. *Journal of Translational Medicine, 15*, 27. doi:10.1186/s12967-017-1128-5

Wilson, L. M. K., & Draper, G. J. (1974). Neuroblastoma, Its Natural History and Prognosis: A Study of 487 Cases. *British Medical Journal, 3*(5926), 301-307.

Wisinski, K. B., Tevaarwerk, A. J., Burkard, M. E., Rampurwala, M., Eickhoff, J., Bell, M. C., . . . Liu, G. (2016). Phase I Study of an AKT Inhibitor (MK-2206) Combined with Lapatinib in Adult Solid Tumors Followed by Dose Expansion in Advanced HER2+ Breast Cancer. *Clin Cancer Res, 22*(11), 2659-2667. doi:10.1158/1078-0432.Ccr-15-2365

Witt, O., Deubzer, H. E., Milde, T., & Oehme, I. (2009). HDAC family: What are the cancer relevant targets? *Cancer Letters, 277*(1), 8-21. doi:https://dx.doi.org/10.1016/j.canlet.2008.08.016

Wood, P. J., Strong, R., McArthur, G. A., Michael, M., Algar, E., Muscat, A., . . . Ashley, D. M. (2018). A phase I study of panobinostat in pediatric patients with refractory solid tumors, including CNS tumors. *Cancer Chemother Pharmacol, 82*(3), 493-503. doi:10.1007/s00280-018-3634-4

Woods, D., & Turchi, J. J. (2013). Chemotherapy induced DNA damage response: convergence of drugs and pathways. *Cancer Biol Ther, 14*(5), 379-389. doi:10.4161/cbt.23761

Worsley, C. M., Mayne, E. S., & Veale, R. B. (2016). Clone wars: the evolution of therapeutic resistance in cancer. *Evolution, Medicine, and Public Health, 2016*(1), 180-181. doi:10.1093/emph/eow015

Worst, B. C., van Tilburg, C. M., Balasubramanian, G. P., Fiesel, P., Witt, R., Freitag, A., . . . Witt, O. (2016). Next-generation personalised medicine for high-risk paediatric

cancer patients – The INFORM pilot study. *European Journal of Cancer, 65*, 91-101. doi:https://doi.org/10.1016/j.ejca.2016.06.009

Wright, J. H. (1910). NEUROCYTOMA OR NEUROBLASTOMA, A KIND OF TUMOR NOT GENERALLY RECOGNIZED. *The Journal of Experimental Medicine, 12*(4), 556-561.

Xiang, T., Ohashi, A., Huang, Y., Pandita, T. K., Ludwig, T., Powell, S. N., & Yang, Q. (2008). Negative Regulation of AKT Activation by BRCA1. *Cancer Research, 68*(24), 10040-10044. doi:10.1158/0008-5472.Can-08-3009

Xin, P., Li, C., Zheng, Y., Peng, Q., Xiao, H., Huang, Y., & Zhu, X. (2017). Efficacy of the dual PI3K and mTOR inhibitor NVP-BEZ235 in combination with imatinib mesylate against chronic myelogenous leukemia cell lines. *Drug Des Devel Ther, 11*, 1115-1126. doi:10.2147/dddt.S132092

Xu, H., Di Antonio, M., McKinney, S., Mathew, V., Ho, B., O'Neil, N. J., . . . Aparicio, S. (2017). CX-5461 is a DNA G-quadruplex stabilizer with selective lethality in BRCA1/2 deficient tumours. *Nature communications, 8*, 14432. doi:10.1038/ncomms14432 https://www.nature.com/articles/ncomms14432#supplementary-information

Xu, L., Morgenbesser, S. D., & DePinho, R. A. (1991). Complex transcriptional regulation of myc family gene expression in the developing mouse brain and liver. *Molecular and Cellular Biology, 11*(12), 6007-6015. doi:10.1128/mcb.11.12.6007

Yada, E., Wada, S., Yoshida, S., & Sasada, T. (2018). Use of patient-derived xenograft mouse models in cancer research and treatment. *Future Science OA, 4*(3), FSO271. doi:10.4155/fsoa-2017-0136

Yamaguchi, T., Cubizolles, F., Zhang, Y., Reichert, N., Kohler, H., Seiser, C., & Matthias, P. (2010). Histone deacetylases 1 and 2 act in concert to promote the G1-to-S progression. *Genes & Development, 24*(5), 455-469. doi:10.1101/gad.552310

Yan, Y., Gong, P., Jin, W., Xu, J., Wu, X., Xu, T., . . . Gao, Y. (2012). The cell-specific upregulation of bone morphogenetic protein-10 (BMP-10) in a model of rat cortical brain injury. *J Mol Histol, 43*(5), 543-552. doi:10.1007/s10735-012-9431-1

Yang, G., Murashige, Danielle S., Humphrey, Sean J., & James, David E. (2015). A Positive Feedback Loop between Akt and mTORC2 via SIN1 Phosphorylation. *Cell Rep, 12*(6), 937-943. doi:https://doi.org/10.1016/j.celrep.2015.07.016

Yang, J., Nie, J., Ma, X., Wei, Y., Peng, Y., & Wei, X. (2019). Targeting PI3K in cancer: mechanisms and advances in clinical trials. *Molecular Cancer, 18*(1), 26. doi:10.1186/s12943-019-0954-x

Yang, X.-J., & Grégoire, S. (2005). Class II Histone Deacetylases: from Sequence to Function, Regulation, and Clinical Implication. *Molecular and Cellular Biology, 25*(8), 2873-2884. doi:10.1128/mcb.25.8.2873-2884.2005

Yanginlar, C., & Logie, C. (2018). HDAC11 is a regulator of diverse immune functions. *Biochimica et Biophysica Acta (BBA) - Gene Regulatory Mechanisms, 1861*(1), 54-59. doi:https://doi.org/10.1016/j.bbagrm.2017.12.002

Yao, R., Lecomte, R., & Crawford, E. S. (2012). Small-animal PET: what is it, and why do we need it? *J Nucl Med Technol, 40*(3), 157-165. doi:10.2967/jnmt.111.098632

Yao, X., Zhang, J. R., Huang, H. R., Dai, L. C., Liu, Q. J., & Zhang, M. (2010). Histone deacetylase inhibitor promotes differentiation of embryonic stem cells into neural cells in adherent monoculture. *Chin Med J (Engl), 123*(6), 734-738.

Yao, Z. G., Li, W. H., Hua, F., Cheng, H. X., Zhao, M. Q., Sun, X. C., . . . Li, J. M. (2017). LBH589 Inhibits Glioblastoma Growth and Angiogenesis Through Suppression of HIF-1alpha Expression. *J Neuropathol Exp Neurol, 76*(12), 1000-1007. doi:10.1093/jnen/nlx088

Yatscoff, R. W., LeGatt, D. F., & Kneteman, N. M. (1993). Therapeutic monitoring of rapamycin: a new immunosuppressive drug. *Ther Drug Monit, 15*(6), 478-482.

Yazbeck, V. Y., Georgakis, G. V., Li, Y., Iwado, E., Kondo, S., & Younes, A. (2006). Molecular Mechanisms of the mTOR Inhibitor Temsirolimus (CCI-779) Antiproliferative Effects in Mantle Cell Lymphoma: Induction of Cell Cycle Arrest, Autophagy, and Synergy with Vorinostat (SAHA). *Blood, 108*(11), 2493.

Yee, A. J., & Raje, N. S. (2018). Panobinostat and Multiple Myeloma in 2018. *Oncologist, 23*(5), 516-517. doi:10.1634/theoncologist.2017-0644

Yee, L. M., Lively, T. G., & McShane, L. M. (2018). Biomarkers in early-phase trials: fundamental issues. *Bioanalysis, 10*(12), 933-944. doi:10.4155/bio-2018-0006

Yu, A. L., Gilman, A. L., Ozkaynak, M. F., London, W. B., Kreissman, S. G., Chen, H. X., . . . Sondel, P. M. (2010). Anti-GD2 Antibody with GM-CSF, Interleukin-2, and Isotretinoin for Neuroblastoma. *New England Journal of Medicine, 363*(14), 1324-1334. doi:10.1056/NEJMoa0911123

Yu, Z., Xie, G., Zhou, G., Cheng, Y., Zhang, G., Yao, G., . . . Zhao, G. (2015). NVP-BEZ235, a novel dual PI3K-mTOR inhibitor displays anti-glioma activity and reduces chemoresistance to temozolomide in human glioma cells. *Cancer Letters, 367*(1), 58-68. doi:10.1016/j.canlet.2015.07.007

Yuan, J., Mehta, P. P., Yin, M. J., Sun, S., Zou, A., Chen, J., . . . Bagrodia, S. (2011). PF-04691502, a potent and selective oral inhibitor of PI3K and mTOR kinases with

antitumor activity. *Mol Cancer Ther, 10*(11), 2189-2199. doi:10.1158/1535-7163.Mct-11-0185

Yuan, T. L., & Cantley, L. C. (2008). PI3K pathway alterations in cancer: variations on a theme. *Oncogene, 27*(41), 5497-5510. doi:10.1038/onc.2008.245

Yuki, Y., Imoto, I., Imaizumi, M., Hibi, S., Kaneko, Y., Amagasa, T., & Inazawa, J. (2004). Identification of a novel fusion gene in a pre-B acute lymphoblastic leukemia with t(1;19)(q23;p13). *Cancer Sci, 95*(6), 503-507.

Zachari, M., & Ganley, I. G. (2017). The mammalian ULK1 complex and autophagy initiation. *Essays Biochem, 61*(6), 585-596. doi:10.1042/ebc20170021

Zage, P. E., Subramonian, D., Mo, Q., & Huang, S. (2017). Effects of the multikinase inhibitor regorafenib in neuroblastoma. *Journal of Clinical Oncology, 35*(15_suppl), 10553-10553. doi:10.1200/JCO.2017.35.15_suppl.10553

Zeller, K. I., Jegga, A. G., Aronow, B. J., O'Donnell, K. A., & Dang, C. V. (2003). An integrated database of genes responsive to the Myc oncogenic transcription factor: identification of direct genomic targets. *Genome Biology, 4*(10), R69-R69.

Zeng, H., & Chi, H. (2017). mTOR signaling in the differentiation and function of regulatory and effector T cells. *Curr Opin Immunol, 46*, 103-111. doi:10.1016/j.coi.2017.04.005

Zenonos, K., & Kyprianou, K. (2013). RAS signaling pathways, mutations and their role in colorectal cancer. *World Journal of Gastrointestinal Oncology, 5*(5), 97-101. doi:10.4251/wjgo.v5.i5.97

Zhang, H., Berel, D., Wang, Y., Li, P., Bhowmick, N. A., Figlin, R. A., & Kim, H. L. (2013). A comparison of Ku0063794, a dual mTORC1 and mTORC2 inhibitor, and

temsirolimus in preclinical renal cell carcinoma models. *PLoS ONE, 8*(1), e54918. doi:10.1371/journal.pone.0054918

Zhang, H., Dou, J., Yu, Y., Zhao, Y., Fan, Y., Cheng, J., . . . Yang, J. (2015). mTOR ATP-competitive inhibitor INK128 inhibits neuroblastoma growth via blocking mTORC signaling. *Apoptosis : an international journal on programmed cell death, 20*(1), 50-62. doi:10.1007/s10495-014-1066-0

Zhang, J., & Zhong, Q. (2014). Histone deacetylase inhibitors and cell death. *Cell Mol Life Sci, 71*(20), 3885-3901. doi:10.1007/s00018-014-1656-6

Zhang, S., Li, Y., Wu, Y., Shi, K., Bing, L., & Hao, J. (2012). Wnt/beta-catenin signaling pathway upregulates c-Myc expression to promote cell proliferation of P19 teratocarcinoma cells. *Anat Rec (Hoboken), 295*(12), 2104-2113. doi:10.1002/ar.22592

Zhang, X., Lu, X., Akhter, S., Georgescu, M. M., & Legerski, R. J. (2016). FANCI is a negative regulator of Akt activation. *Cell Cycle, 15*(8), 1134-1143. doi:10.1080/15384101.2016.1158375

Zhang, X., Tang, N., Hadden, T. J., & Rishi, A. K. (2011). Akt, FoxO and regulation of apoptosis. *Biochim Biophys Acta, 1813*(11), 1978-1986. doi:10.1016/j.bbamcr.2011.03.010

Zhang, Y., Xiong, Y., & Yarbrough, W. G. (1998). ARF promotes MDM2 degradation and stabilizes p53: ARF-INK4a locus deletion impairs both the Rb and p53 tumor suppression pathways. *Cell, 92*(6), 725-734.

Zhong, H., Chiles, K., Feldser, D., Laughner, E., Hanrahan, C., Georgescu, M. M., . . . Semenza, G. L. (2000). Modulation of hypoxia-inducible factor 1alpha expression by the epidermal growth factor/phosphatidylinositol 3-kinase/PTEN/AKT/FRAP

pathway in human prostate cancer cells: implications for tumor angiogenesis and therapeutics. *Cancer Research, 60*(6), 1541-1545.

Zhou, H., Luo, Y., & Huang, S. (2010). Updates of mTOR inhibitors. *Anti-cancer agents in medicinal chemistry, 10*(7), 571-581.

Zimmerman, M. W., Liu, Y., He, S., Durbin, A. D., Abraham, B. J., Easton, J., . . . Look, A. T. (2018). MYC Drives a Subset of High-Risk Pediatric Neuroblastomas and Is Activated through Mechanisms Including Enhancer Hijacking and Focal Enhancer Amplification. *Cancer Discov, 8*(3), 320-335. doi:10.1158/2159-8290.Cd-17-0993

Zlotorynski, E. (2017). The cancer link(RNA) between PIP3 and AKT. *Nature Reviews Molecular Cell Biology, 18*, 212. doi:10.1038/nrm.2017.18

Zuberi, A., & Lutz, C. (2017). Mouse Models for Drug Discovery. Can New Tools and Technology Improve Translational Power? *ILAR Journal, 57*(2), 178-185. doi:10.1093/ilar/ilw021